SAN ONOFRE NUCLEAR GENERATING STATION (SONGS)

SONGS MEAN SEA LEVEL RISE IMPACT ASSESSMENT

Technical Report For

Provision 14 In Lease No. Prc 6785.1

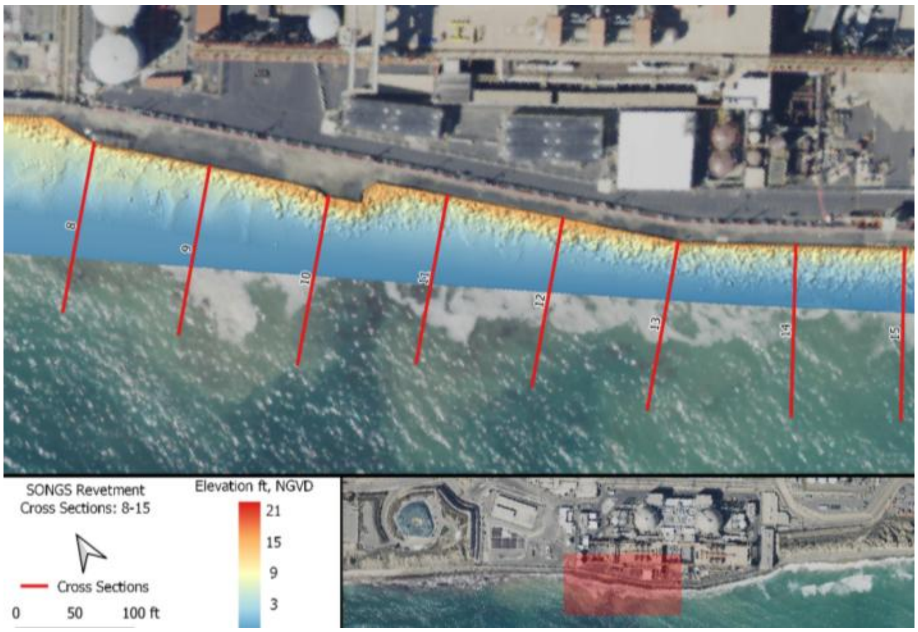

by

Hany Elwany, Ph.D.
Reinhard E. Flick, Ph.D.
Frederico Scarelli, Ph.D.

for

Southern California Edison
2244 Walnut Grove Avenue
Rosemead, CA 91770

Coastal Environments, Inc.
2166 Avenida de la Playa, Suite E
La Jolla, CA 92037

CE Reference No. 20-08
30 March 2020

TABLE OF CONTENTS

LIST OF APPENDICES

LIST OF TABLES

LIST OF FIGURES

LIST OF PHOTOGRAPHS

EXECUTIVE SUMMARY

This report is being written to comply with California State Lands Commission Special Provision 14, for standards addressing sea level rise that may be required or adopted by local, state, or federal agencies related to the Lease Premises. The report presents the current information about sea level rise projections from the state and federal agency guidelines; assessments for San Onofre beach and the San Onofre Nuclear Generating Station (SONGS) revetment walkway and seawall; and the impacts of Mean Sea Level Rise (MSLR) on SONGS, including the premises located east of the seawall, such as the Independent Spent Fuel Storage Installation (ISFSI) and its Security Building, and the adaption capacity of the Lease Premises and facilities therein. The report presents:

a. Sea level rise and beach profile assessments, site photographs taken in 2019 of shoreline facilities such as riprap, pedestrian walkways, and seawalls, and descriptions of repair and maintenance operations of shoreline facilities. The sea level rise vulnerability information considered the Medium-High Risk Aversion (0.5% probability) projection scenarios from the most recent state guidance (issued by the Ocean Protection Council [OPC] every five years), as well as the extreme H++ projection scenario, in combination with the annual and 20-year events, as well as extreme high tide heights ("King Tides"). Pertinent information may be sourced from Southern California Edison (SCE) or any other research conducted within the region that is relevant to conditions at the Lease Provision 14(a).

b. Quarterly groundwater elevation data collected from onsite monitoring wells relevant to conditions at Lease Provision 14 (b).

Chapter 1 presents the overall structure of this report and provides a summary of the major information presented in this study with emphasis on the main points outlined in Special Provision 14.

Projections of future MSLR are evolving continuously as the understanding of key climate change processes improves (Chapter 2). In Sections 2.1.1 to 2.1.3, we summarize the state agencies' updated guidelines and previous relevant studies. In Section 2.1.4, we discuss sea level extremes and provide OPC MSLR projections (2018) for 2030, 2040, and 2050.

The beach prevents toe scouring that can undermine the revetment and cause rock units to settle. When the beach is narrow, or water level unusually high, or both, waves breaking on the revetment can cause dislocation of individual rocks, which contributes to revetment instability. Section 3.7 gives a summary of San Onofre Beach assessments based on SCE's beach monitoring program at San Onofre Beach from 1964 to the present, with gaps presented in Appendix E. Selected photographs of the beach taken in 2017, 2018, and 2019 are also presented in Appendix E. These insights will be valuable as sea level rise accelerates in the future. Elwany et al. (2017) have addressed the impacts of sea level rise on San Onofre Beach.

The assessment of the SONGS revetment is reviewed in Chapter 3. Revetment maintenance carried out in 2018 and 2019 are summarized in Section 3.1.1. In Section 3.2 and Appendices A, B, and C, we gauge the current revetment condition and describe the characteristics of the riprap, namely rock, and dimension and weight distributions, based on two site inspections carried out in February and March 2020. We evaluate the revetment stability based upon these observations and standard coastal engineering criteria (Sections 3.3 to 3.6).

Our study finds that the revetment, in its present condition, is likely to tolerate wave forces with acceptable rock movement that will not affect the integrity of the revetment as a whole. The study found that as designed and with regular maintenance, the revetment will withstand wave forces over the next 30 years (Section 3.8). The revetment, retaining wall, and walkway also provide additional protection to the SONGS seawall. Appendix C presents aerial photographs of the revetment for the period from 2003 to 2018. Photographs taken during the 18 February 2020 site visit are shown in Appendix D.

Section 3.9 addresses the maintenance and adaptive capacity of the Lease Premises. The major threats to revetment stability in the future include wave storms, or clusters of wave storms, such as those that occurred in 1981 to 1983. In this respect, the revetment's adaptive capacity to MSLR is high in the sense that its current stable condition along with occasional maintenance will allow it to continue functioning as intended.

Impacts of groundwater on the ISFSI based on quarterly measurements of the groundwater from 8 coastal wells out of 16 total wells are presented in Appendix F. The OPC (2018) 67% low risk aversion, medium-high (0.5%) and H++ SLR scenarios for groundwater elevation for 2050 are 3.92, 4.62 and 5.28 ft, NGVD (Section 3.9) and are 2.05, 1.35 and 0.55 ft lower than the bottom of the ISFSI support foundation, respectively. The ISFSI support foundation is 3 ft thick.

The analysis of vulnerability of the revetment to wave runup and overtopping of the revetment is presented in Chapter 4. This study considers the Medium-High Risk Aversion projection (0.5%) and extreme H++ projection scenarios from the most recent state guidance issued by the OPC (2018) in combination with the annual, 2-, 5-, 10-, 25-, 50-, and 100-year wave return period wave and high water events, which include storm surges and King Tides. Our conclusions are stated in Chapter 5.

SAN ONOFRE NUCLEAR GENERATING STATION (SONGS)

SONGS MEAN SEA LEVEL RISE IMPACT ASSESSMENT

Technical Report For

Provision 14 In Lease No. Prc 6785.1

1.0 INTRODUCTION

This report has been compiled per Lease Provision 14 in the California State Lands Commission Lease No. PRC 6785.1 for the use, maintenance, and decommissioning of exiting offshore improvements associated with the San Onofre Nuclear Generating Station (SONGS). Lease Provision 14 requires, as part of compliance with applicable provisions or standards addressing sea level rise that may be required or adopted by local, state, or federal agencies related to and affecting the lease premises, that the Lessee provide an annual summary, including information related to sea level rise vulnerability, structural integrity, and adaptation capacity of the Lease Premises and the facilities therein.

The information in this report will include sea level rise discussion and beach profile assessments, annual site photographs of shoreline facilities (i.e., riprap, pedestrian walkway, and seawall), and description of repair and maintenance operations for shoreline facilities. Sea level rise vulnerability information considers the Medium-High Risk Aversion (0.5 % probability) projection scenarios from the most recent state guidance (issued by the Ocean Protection Council [OPC] every five years), as well as the extreme H++ projection scenario, in combination with the annual, 20-year, and 100-year storm events, as well as extreme high tide heights (“King Tides”). Pertinent information may be sourced from Southern California Edison (SCE), likewise the quarterly groundwater elevation data collected from onsite monitoring wells, or any other research conducted within the region that is relevant to conditions at the Lease Provision 14(b).

In Chapter 2 of this report, we summarize the present knowledge of mean sea level rise (MSLR) using state and federal agency guidelines. These guidelines are evolving constantly in response to the rapid pace of data acquisition and scientific understanding of MSLR, especially concerning the long-term consequences of accelerating ice sheet melt in Greenland and Antarctica. We presented agency guidance current as of 2018 and the associated MSLR projections to determine impacts on the SONGS shoreline and cliffs, and the likelihood of wave overtopping of the seawall in Elwany et al. 2016 and 2017.

The SONGS revetment provides protection to the SONGS seawall and is essential to maintaining the walkway that enables safe lateral access for beach users. The revetment shelters the walkway from most wave runup and overtopping, thus preventing or reducing negative impact to lateral beach access due to flooding and other hazards from high water levels and waves. The presence of the revetment and walkway fronting the seawall eliminate wave impacts on seawall.

The assessment of the SONGS revetment is reviewed in Chapter 3. In Chapter 3, we determine the current revetment and walkway exposure and vulnerability to waves and high water level events by gauging their present condition. We describe the characteristics of the riprap, namely rock, and dimension and weight distributions, based on two site inspections in February and March 2020. We evaluate its stability based upon these observations and standard coastal engineering criteria. The importance of the presence of sand beach offshore of the revetment is discussed in Section 3.7, along with the recent characteristics of the beach nearby SONGS and observed short- and long-term erosion and accretion patterns based on the ongoing beach profile surveys carried out in 2017, 2018, and 2019 (CE, 2020).

Additionally, in Section 3.9, we discussed the adaptation capacity of the Lease Premises and the facilities and present adaptive management plan to maintain the facilities such as revetment, walkway and seawall, Independent Spent Fuel Storage Installation (ISFSI), and its Security Building in good condition during the lease agreement.

MSLR will likely increase both the wave forces on the rocks (due to greater water depth and wave height fronting the revetment), and sand scour undermining that could lower and destabilize the revetment (due to beach retreat). This study considers the Medium-High Risk Aversion projection (0.5%) scenarios from the most recent state guidance issued by the OPC (2018), as well as the extreme H++ projection scenario, in combination with the annual, 2-, 5-, 10-, 25-, 50-, and 100-year return period wave and high water events, which include king tides. The vulnerability of revetment to wave runup and overtopping analysis of the revetment is presented in Chapter 4.

Our study finds that the revetment, in its present condition, is likely to tolerate wave forces with acceptable rock movement that will not affect the integrity of the revetment as a whole. The study found that as designed with regular maintenance, the revetment will withstand wave forces over the next 30 years.

The walkway behind the revetment at elevation 14 ft (NGVD) is relatively low and likely will be overtopped under large wave conditions, especially if these occur during extreme high water levels. However, the impact of wave runup and overtopping on the walkway itself or public access is limited and temporary, since the beach will not be accessible during such conditions, and flood water has adequate drainage from the site and off the public walkway. Our major conclusions are stated in Chapter 5.

Chapter 6 provides a references list, followed by six Appendices labeled alphabetically from A to F. Appendices A, B, C, and D provide information regarding the 5 March 2000 survey carried out at the SONGS revetment, including location of the transects, and the profiles analyzed along the riprap, as well as the photographs taken during the survey. Appendix E presents our assessment of the San Onofre Beach and the results of the beach profile surveys carried out at San Onofre Beach from 2017 through 2019. Appendix F is written in compliance with provision 14b. This Chapter discusses the groundwater elevations measured quarterly in 2019 and the sea level rise impacts on the ISFSI up to 2050. The 2019 quarterly groundwater elevation monitoring program was carried out by SCE.

2.0 MEAN SEA LEVEL RISE IMPACT ASSESSMENT

2.1 MEAN SEA LEVEL RISE GUIDANCE

Projections of future MSLR are evolving continuously as understanding of key climate change processes improves. Of special concern are the possible ranges and rates of glacial ice loss in Greenland and Antarctica (e.g., DeConto and Pollard 2016). Future MSLR is highly uncertain, especially after about 2050, for several reasons. The largest unknown is what approaches, if any, humans will employ to decrease the rates and ultimate amounts of greenhouse gas (GHG) emissions. Second, the climate sensitivity, or amount and rate of warming for a given increase in GHGs is not precisely known. Third, polar ice response to warming is not yet accurately predictable.

2.1.1 State Agency Advances

State agencies responsible for coastal activities update their MSLR guidance and related requirements periodically as sea level science improves. Over the past several years, four key reports have been issued that summarize the relevant scientific findings that underlie and define current State of California climate change policy, including MSLR. These reports are:

1. *Rising Seas in California, An Update on Sea Level Rise Science* (California Ocean Protection Council and Ocean Science Trust-Science Advisory Team, Griggs et al. 2017).

2. *California's Fourth Climate Change Assessment*, *Statewide Summary Report* (California Governor's Office of Planning and Research, Scripps Institution of Oceanography, California Energy Commission, and California Public Utilities Commission, Bedsworth et al. 2018).

3. *State of California Sea Level Rise Guidance, 2018 Update* (California Natural Resources Agency Ocean Protection Council, OPC 2018).

4. *California Coastal Commission Sea Level Rise Policy Guidance* (California Coastal Commission, [CCC] 2015, updated 2018).

Griggs et al. (2017) reviewed the science of MSLR, especially regarding advances in understanding polar ice loss. *"This document, requested by the California Ocean Protection Council and guided by a set of questions from the state Sea Level Rise Policy Advisory Committee, provides a synthesis of the state of the science on sea level rise. It provides the scientific foundation for the pending update to the guidance document."* This was one of the first documents to associate probabilities with future MSLR projections in California. Tables are included specifying likelihood ranges for various scenarios to 2100 at Crescent City, San Francisco, and La Jolla.

California's Fourth Climate Change Assessment (Bedsworth et al. 2018) has a much broader focus that includes essentially all aspects of climate change relevant to California, both inland and coastal, including sea level. The statewide summary report is supplemented by nine regional reports emphasizing relevant factors at a more local level. In addition, it is supported by 44 technical reports and seven external scientific contributions providing the technical details. Sea level rise, flooding, and erosion projections for the state are summarized. The Statewide Summary Report (Bedsworth et al. 2018) contains probabilistic MSLR projections for La Jolla (as representative for California) to 2100 for the high and medium-high (respectively) Intergovernmental Panel on Climate Change (IPCC) "Representative Concentration Pathways" (RCP) 8.5 and RCP 4.5 scenarios. The RCP 8.5 MSLR trajectory exceeds 9 ft by 2100, and is the same magnitude as the extreme H++ trajectory presented in the OPC (2018) and CCC (2015, updated 2018) reports that define California MSLR policy. As considerable uncertainty remains, *"…the Fourth Assessment projections are meant for research purposes, while the OPC projections are meant for regulatory and planning purposes."*

OPC (2018) expanded the geographic detail and temporal extent of Griggs et al. (2017) by including probabilistic MSLR projections at 12 California locations with long-term tide records through 2150.[1] The report states, *"The purpose of this Guidance is to assist decision makers at state and local levels in planning for, and making decisions about, sea level rise and related coastal hazards in light of the current state of the science."* In addition to establishing *"the best available science,"* the report also aims to help "…*agencies to incorporate and adapt to the latest sea level rise projections and related hazard information in different types of decisions across California;"* and to, "*Articulate OPC's preferred coastal adaptation planning approaches in the context of existing law, expressed policy preferences by the Governor and the Legislature, and OPC's goal to foster consistency across coastal and ocean government agencies."* This last aim strongly implies that OPC (2018) should be broadly adopted and followed in California, suggesting that it supplants the previous CCC guidance (CCC 2015), which was promptly updated in 2018 to reflect the contents of OPC (2018).

2.1.2 Previous Studies

Studies and guidance documents prior to 2017 are summarized in Elwany et al. (2016, 2017). We note here that California MSLR guidance prior to 2017 consisted of a selection of scenarios ranging from low to high, respectively corresponding to matching emissions or temperature trajectories (e.g., IPCC AR5, 2013) but with no likelihood-of-occurrence estimates. The prior round of MSLR estimates were largely based on the National Research Council (NRC) report (NRC 2012) focused on Washington, Oregon, and California. As now, estimates had large ranges owing to uncertainty in actual future emissions. In southern California, MSLR projections relative to year 2000 ranged from 0.15-0.98 ft (0.05-0.30 m) by 2030, 0.42-2.0 ft (0.13-0.61 m)

[1] The stations are: Crescent City, North Spit Humboldt Bay, Arena Cove, Point Reyes, San Francisco, Monterey, Port San Luis, Santa Barbara, Santa Monica, Los Angeles, La Jolla, and San Diego Bay.

by 2050, and 1.4-5.5 ft (0.44-1.7 m) by 2100. The possibility that greatly accelerated ice loss could push the upper limit much higher was acknowledged.

Elwany et al. 2016, 2017 evaluated the coastal processes important to determining the end-state associated with deconstruction of SONGS by considering four MSLR scenarios that reach 3.3, 4.7, 5.5, and 6.6 ft (1.0, 1.42, 1.67, and 2.0 m) by 2100 relative to 2000. These scenarios were (respectively) named DoD 1.0, CCC 1.67, RCP '4.5', and DoD 2.0 according to their origins. Projections of MSLR to 2050 ranged from about 1-2 ft (0.3-0.6 m), as specified in Table 2-1. Elwany et al. (2016, 2017) was based on the CCC (2015) guidance document before it was updated in 2018, and other work including a Navy study (Chadwick et al. 2014) funded by the Strategic Environmental Research and Development Program (SERDP) to determine future land loss from MSLR at Marine Corps Base Camp Pendleton and Naval Station San Diego, and Hall et al. (2016).

2.1.3 Ocean Protection Council (2018) Mean Sea Level Rise Guidance

Table 2-2 lists more recent MSLR projections for La Jolla to 2050 that appear in the latest guidance in the *State of California Sea Level Rise Guidance, 2018 Update* (OPC 2018). The columns in Tables 2-1 and 2- 2 are aligned to stress their similarities, and to highlight the new (Table 2-2) extreme H++ trajectory that reaches about 10 ft (3 m) by 2100, and which covers the unquantifiable, but highly unlikely, rapid demise of the West Antarctic Ice Sheet (WAIS) H++ projects 2.8 ft (0.9 m) MSLR by 2050.

The OPC (2018) MSLR projections in Table 2-2 have the probability range estimates associated with them. These originated from IPCC AR5 (2013) by calculating probabilities of RCP scenarios. Each RCP has a numerical designation condensing a host of factors into a final radiation imbalance in Watts/m^2 by 2100. The full range was RCP2.6-RCP8.5. Thus "RCP4.2" represents a (moderate) GHG trajectory that results in a net heating of the earth by 4.2 Watts/m^2 by 2100. The probability estimates use the framework of Kopp et al. (2014).

OPC (2018) focused on the highest (RCP8.5) and lowest (RCP2.6) pathways *"to bound a range of potential sea level futures based on GHG emissions trajectories."* RCP8.5 is often called the "business as usual" scenario that anticipates a doubling of annual carbon emissions between 2015 and 2050. Average global air temperatures could rise about 4°-5° C (7°-9° F) by 2100. On the other hand, RCP2.6 closely tracks the ambitious emissions reduction goals of the 2015 United Nations Framework Convention on Climate Change, also known as the "Paris Agreement." RCP 2.6 imagines a radical global decarbonization that reduces CO_2 emissions to net-zero by 2080 and limits atmospheric temperature increase to about 2° C (3.6° F).

It is important to note that from 2000-2050, only the "High" MSLR trajectory is considered in OPC (2018). This is based on two factors: first, there are no ambitious global GHG emissions reduction plans presently apparent, and second, even if emissions immediately dropped to net-zero, warming and MSLR would continue for at least several more decades owing to climate inertia. In effect, both the High and Low trajectories produce near-identical projections between 2000 and 2050, and only begin to differ after mid-century.

Table 2-2 shows four columns (Columns 2-5) headed with percentage probability numbers, and one (Column 6) indicated as H++. Column 2 titled "50%" indicates the median projected MSLR each year (Column 1) relative to 2000. That means, for example, there is a 50-50, or "even" chance that MSLR will be less than or greater than 0.9 ft by 2050. Columns 3-4 titled "> 67% <" bracket the 2/3 probability that MSLR will fall between these numbers. In other words, it is 2/3 likely that MSLR will reach from 0.7-1.2 ft by 2050. Columns 5 and 6, respectively, provide the MSLR that has a "1 in 20" and "1 in 200" chance of being exceeded. This means there is only a 1 in 200 (0.5%) chance that MSLR will reach or exceed 2 ft by 2050.

By comparing the corresponding columns of Tables 2-1 and 2-2, it is apparent that the range of the previous projections used in Elwany et al. (2016, 2017) and current scenarios from 2000-2050 are essentially the same, excepting H++.

The H++ scenario is included in OPC (2018) to account for the (currently) remote possibility that *"…rapid ice sheet loss on Antarctica could drive rates of sea level rise in California above 50 mm/year (2 inches/year) by the end of the century, leading to potential sea level rise exceeding 10 feet. This rate of sea level rise would be about 30-40 times faster than the sea level rise experienced over the last century."*

Figure 2-1 illustrates the OPC (2018) trajectories described above along with the actual average annual mean sea level (MSL) data measured at the La Jolla tide gauge (941 0230) located at the end of Scripps Institution of Oceanography pier. Data begin in 1925, but Figure 2-1 only spans 2000-2050. The observations were adjusted so that their average over the 19-year epoch (1991-2009) centered on year 2000 was zero to facilitate comparison with projections beginning in 2000 (see Flick et al. 2013 for adjustment rationale and procedure).

2.1.4 Sea Level Extremes

It remains crucial to recognize that water elevation at or around MSL generally does not present risks for flooding, erosion, or infrastructure damage. These almost always occur during times of extreme high water levels that, on the California coast, are driven mainly by coincidence of peak high tides and large storm waves. Maximum astronomical tide elevations reach about 7 ft (NAVD88 [North American Vertical Datum]) on the San Diego region coast. California tides show periods of variation from twice daily, twice monthly, twice annually, and every 4.4 and 18.6 years (Zetler and Flick 1985). Runup from storms varies greatly in magnitude depending on the height, direction, and period of offshore swell, the strength of local winds that drive short-period seas and other factors. For discussion of these relevant to conditions at SONGS, see Elwany et al. (2016, 2017).

Other factors that contribute to enhanced water levels include storm surges owing to high winds and low barometric pressure and El Niño warming events that bring higher than average ocean levels. Large storm surges in southern California typically range up to about 1 ft during storm peaks. El Niño warming can enhance coastal sea levels by about 0.5 ft for a year or more depending on its strength (Flick 2016).

Observed maximum monthly water levels are compiled and published by the National Oceanic and Atmospheric Administration's (NOAA) National Ocean Service (NOS) for all tide gauge stations they operate, including La Jolla, California, where measurements began in 1925. These observations are presented in Figures 2A and 2B. Figure 2A shows the data plotted relative to the NAVD88 datum, which is the official national standard supported by NOAA's National Geodetic Survey (NGS), and used by surveyors and engineers. By coincidence, NAVD88 in the San Diego area lies just above Mean Lower Low Water (MLLW), currently differing by only 0.19 ft. Figure 2B shows the same data plotted relative to the legacy datum of National Geodetic Vertical Datum (NGVD) (also called NGVD29 or MSL 29), which lay close to MSL in the past. While NGVD is no longer supported by NGS or routinely employed by surveyors and engineers, it is still beneficial because of its extensive and long use for coastal measurements and studies, including many at SONGS. NGVD lies 0.43 ft below current MSL (as defined by the 1983-2001 epoch).

It is apparent from Figures 2A and 2B, that monthly maxima are increasing as MSL rises, and this is expected to continue in the future. NOS also provides statistics of extreme sea levels based on the observations discussed. Their current estimates of "return period," or the probability of exceeding a given value in any year are summarized in Table 2-3 relative to NAVD88 and NGVD. Note the relatively small spread of less than 1 ft between the 1% (100-yr) and 99% (1-yr) extreme high water level events. This illustrates the dominant influence of the astronomical tide on extreme water levels along the California coast. The highest tide is about 7 ft above NAVD88, less than about 0.5 ft below the 100-yr return event. It also illustrates the exceedingly rare coincidence of peak high tides with extraordinary storm surges or other water level enhancing processes, such as El Niño, which can raise MSL up to about 1.5 ft over time scales of days to a year.[2]

These considerations are used in the following sections as a basis for determining the maximum water level trajectories and their consequences at SONGS in the future.

[2] See Flick (2016) for details exemplified by the 2015-16 El Niño winter.

Table 2-1. Elwany et al. (2016, 2017) SONGS MSLR Analysis (ft).

	DoD 1.0	CCC 1.67	RCP '4.5'	DoD 2.0
2000	0.0	0.0	0.0	0.0
2030	0.5	0.4	1.0	0.9
2040	0.7	0.7	1.5	1.4
2050	1.0	1.1	2.0	2.0

Table 2-2. Ocean Protection Council (2018) MSLR Guidance (ft).

	50%	> 67% <		5%	Medium-High Risk Aversion 0.5%	H++
2000	0.0	0.0	0.0	0.0	0.0	0.0
2030	0.5	0.4	0.6	0.7	0.9	1.1
2040	0.7	0.5	0.9	1.0	1.3	1.8
2050	0.9	0.7	1.2	1.4	2.0	2.8

Table 2-3. NOAA-NOS La Jolla Extreme Water Level Statistics (ft).

Percent/Yr	Return (Yrs)	NAVD88	NGVD
1%	100	7.43	5.32
10%	10	7.20	5.09
50%	2	6.94	4.82
99%	1	6.51	4.40

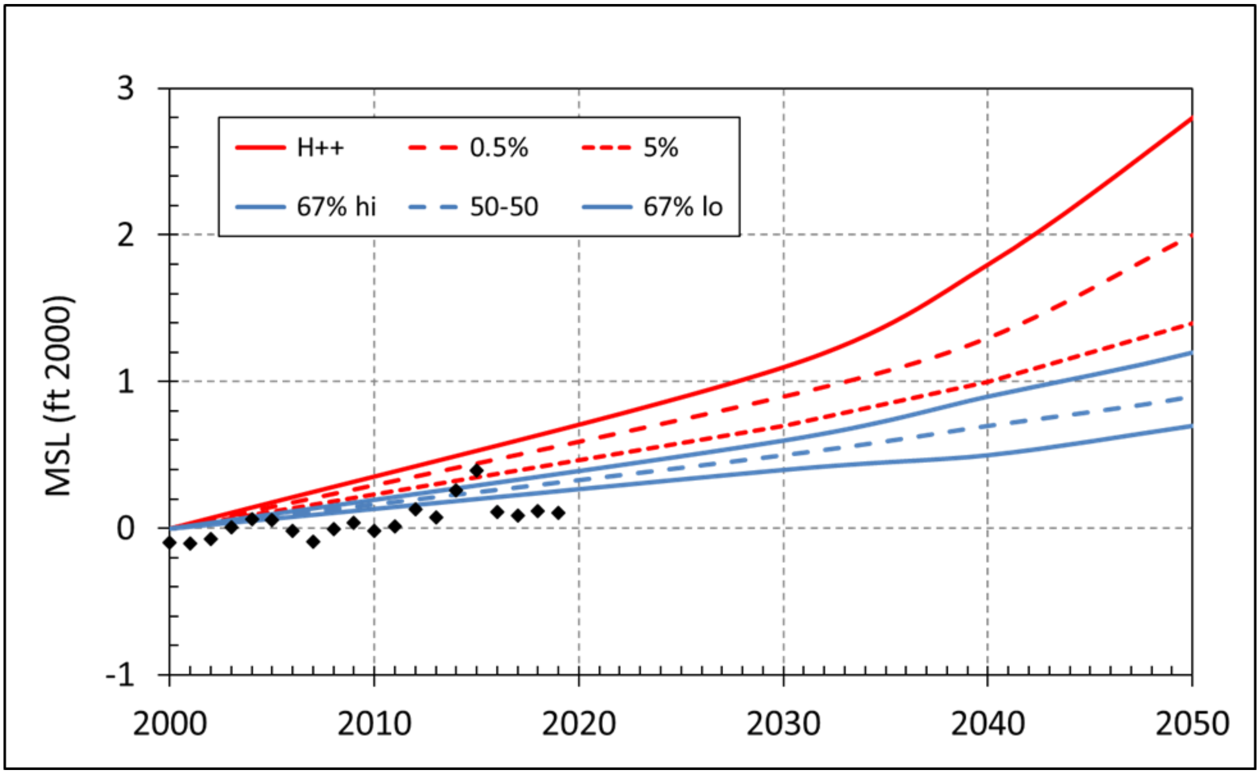

Figure 2-1. Annual average MSL measured at La Jolla, 2000-2019 (black symbols) adjusted to zero over 1991-2009 epoch centered on 2000. MSLR trajectories (colored lines, see legend) from OPC (2018) described in text. Maximum annual average height of 0.4 ft represents 2015 El Niño warming event.

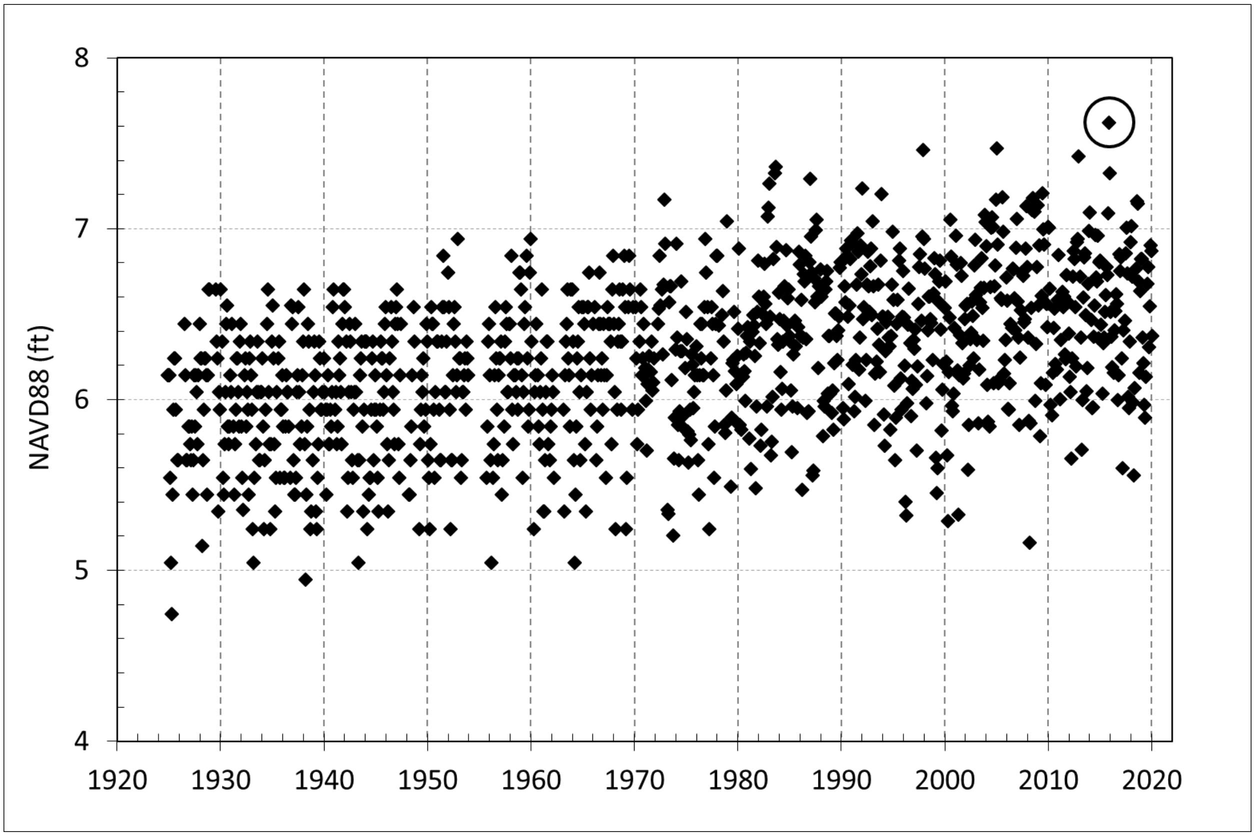

Figure 2-2A. Monthly maximum sea level measured at La Jolla, 1925-2019 (black symbols) relative to NAVD88 datum (see text). Maximum observed height of 7.62 ft (circled) occurred on 25 November 2015 during the 2015-16 El Niño warming event.

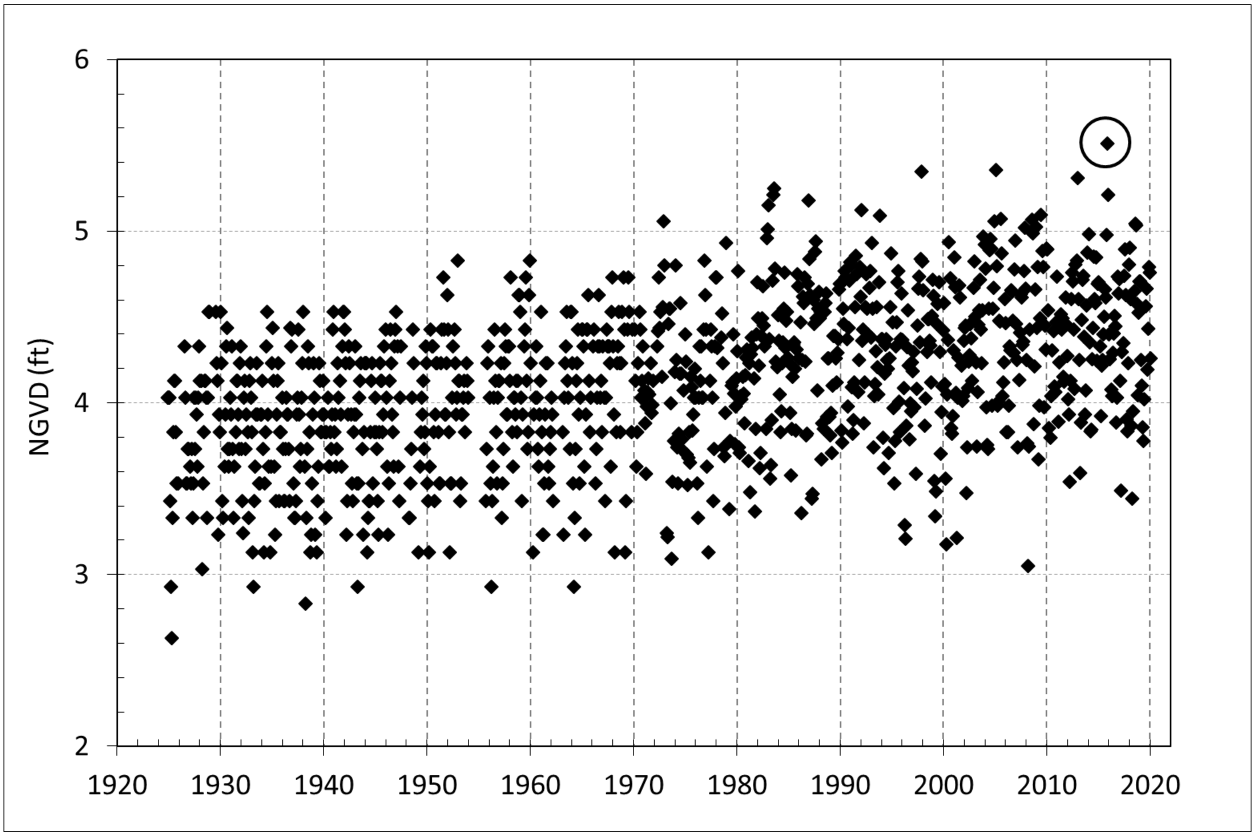

Figure 2-2B. Monthly maximum sea level measured at La Jolla, 1925-2019 (black symbols) relative to NGVD datum (see text). Maximum observed height of 5.51 ft (circled) occurred on 25 November 2015 during the 2015-16 El Niño warming event.

3.0 SONGS REVETMENT

3.1 DESCRIPTION OF THE SONGS REVETMENT

The SONGS revetment provides partial first-line protection to the SONGS seawall, it is essential to maintaining the walkway that enables safe lateral access for beach users. The revetment shelters the walkway from most wave runup and overtopping, thus preventing or reducing negative impact to lateral beach access due to flooding and other hazards from high water levels and waves.

Figure 3-1 is an air photograph showing the revetment, which extends along the entire length of SONGS on the beach fronting the walkway. Figure 3-2 is a close up of the revetment at its southern end. The revetment is about 2,200 ft long, extending from the north end of Unit 1 to the south end of Units 2 and 3. The revetment is constructed of multiple layers of placed riprap consisting of quarry rock “rubble.” A well-known desirable characteristic of placed rubble structures is their ability to adjust and resettle under wave attack. The advantage of using rock riprap is that it is highly durable and readily available in southern California. Further, because of their rough surface, rock revetments produce less wave runup and overtopping as opposed to smoothed-faced structures.

3.1.1 Revetment and Walkway Maintenance 2018-2019

The repairs for SONGS revetment fronting Units 2 and 3 were done in two phases. Phase 1 started on 7 May 2018 until 10 October 2018, and Phase 2 started on 15 October 2019 and finished on 16 December 2109.

During Phase 1, SCE: (1) placed imported riprap along 500 linear ft at the southern portion of the public access walkway (Figure 3-3); and (2) elevated the access ramp of the southern public walkway using imported cobbles and sand.

The elevating of the south public access ramp was needed to compensate for the sand lost caused by wave action which resulted approximately in a 10 ft lowering the beach at the south end of the walkway and scouring the riprap of the revetment protecting the sheet pile seawall. Consequently, the riprap has been undermined and eventually the revetment would no longer be effective.

During Phase 2, SCE: (1) placed additional 150 linear ft of imported riprap north of the previously placed riprap, for a total of 650 ft linear ft of revetment repair; and (2) added 70 ft of riprap in front of the sheet pile seawall closure section at the south of the public walkway and reinstalled the Vehicle Barrier System at the south end of the public walkway. Figure 3-4 shows the south end of walkway before and after the repair.

3.2 SITE VISITS

Two inspections of the revetment were made for this study. The first visit was on 18 February 2020, when we measured the length, width, and height of 80 revetment rocks selected randomly to determine the distribution of rock size and weight. The second visit was on 5 March 2020, when we carried out a laser scan survey to obtain data to construct a digital elevation model (DEM) of the revetment.

3.2.1 Rocks Measurements

The size of individual rocks is expressed by the dimensions of their three axes. The long axis, ‘a’, is the maximum length of the stone (Figure 3-5), the intermediate axis, ‘b’, is the maximum width perpendicular to the long axis, and the short axis, ‘c’, is the height of the stone perpendicular to the plane of the a-axis and b-axis. The size of an individual rock is usually expressed as its b-axis dimension, or alternatively by its calculated or actual weight. Rock weight estimates, which are needed to evaluate riprap stability, are discussed in Section 3.3 below. Histograms of the lengths, widths, and heights of the 80 sample rocks measured at SONGS are presented in Figure 3-6, and their cumulative distributions in percent are shown in Figure 3-7.

3.2.2 Revetment Laser Scanner Survey

A laser scanner survey was carried out using a Trimble SX10 scanning total station (Figure 3-8) for the purpose of creating a DEM to visualize the spatial characteristics of the revetment. Control points were established to aid in subsequent station setups. The revetment was scanned from the beach and the scanner location was determined from the control points. We opted not to scan from the walkway, as the walkway retaining wall blocked much of the view of the riprap. The system scanned a full 360 degrees in a vertical direction and slowly rotates horizontally to cover certain areas of the revetment at a high resolution. Scans were carried out roughly 100 ft (30 m) apart, repeating the procedure described above.

Tide was a limiting factor in obtaining complete coverage from the beach at the southern portion of the revetment. Therefore, some scans were carried out from the top of the revetment near the walkway to fill data gaps.

The survey on 5 March 2020 acquired over a 100,000 data points, assembled in a “point cloud.” The data set was pre-processed using “CloudCompare” software, which enables the outlier points, and those points likely reflected from the walkway wall, to be removed. The pre-processed data were then graphically presented to show the revetment and adjacent beach. For clarity, the revetment data were divided into three DEMs, labeled north, middle and south. The model results are presented in Appendix A.

An advantage of creating a DEM is that the model can be “sampled,” for example to show cross sections or contour maps, that would otherwise be difficult or impossible to derive in a reliable way. Twenty-one cross section transects were generated from the DEM at locations shown in Figure 3-9. Selected model results for the revetment are shown in Figure 3-10.

Representative cross sections are shown in Figure 3-11. All 21 transects are presented in Appendix B. Table 3-1 provides riprap height, walkway wall height, and the revetment slope β for each transect.

The DEM was also used to determine the height of the revetment along its upper edge adjacent to the walkway retaining wall (Figure 3-12). The height of this upper edge varies from about 8 ft to 12 ft (NGVD), a few feet lower than the upper edge of the retaining wall, which lies at about 14 ft.

3.3 RIPRAP ROCK UNIT WEIGHT

Riprap rock unit weights and their variation are essential to estimating the stability of a revetment. Individual rock weight is proportional to volume and specific weight (or density) of the stone. The estimation of weight is complicated by the fact that each rock unit is not a simple geometric form, such as a sphere or a rectangular shape, like a brick.

Individual rock weight, W(x), was estimated from Equation 3-1, which assumes each Rock(x) is equivalent to a sphere with diameter D(x) = b(x), the maximum width perpendicular to the long axis, as described in Section 3.2 above. Dimension 'b' is often referred to as rock "diameter." Then:

$$W\ x\ =\ \frac{\pi \gamma_s\ D(x)^{\ 3}}{6} \tag{3-1}$$

Where:

γ_s = Specific weight of revetment rock.

Table 3-2 gives the dimensions and weights of each sampled rock. The mean and standard deviation for the length, width, and weight of the rocks are presented in Table 3-3. Percent distribution of rock weights and the cumulative distribution of estimated rock weights are shown in Figure 3-13.

A key design parameter for any revetment is the median rock weight, designated W_{50}. Half of the rocks are heavier, and the other half are lighter than W_{50}. We estimated W_{50} in two different ways using standard coastal engineering practice (U.S. Army Corps of Engineers [USACE] 1994a, b). These gave nearly identical results.

First, we determined the individual rock weight estimates from each rock diameter, D(x), as described above in equation 3-1. The result was a W_{50} = 600 kg. Second, we calculated the median diameter of the 80 sampled rocks, D_{50}. The result was D_{50} = 2.5 ft. We then used this number in place of D(x) in Equation 3-1, which resulted in W_{50} = 580 kg.

3.4 DESIGN WATER LEVEL

Water surface elevation is dependent on tides, storm surge, and MSLR in response to climate change. These factors are discussed in Section 2.1.4, and the values of current extreme water levels are given in Table 2-3. Table 2-3 gives the NOAA estimates for the extreme water level for various return estimates. The 100-year return period for surface water elevation at La Jolla is 5.32 ft, NGVD (7.43 ft NAVD88) while the maximum observed water surface elevation of 5.5 ft occurred on 25 November 2015 during the 2015-16 El Niño warming event.

These estimations include astronomical tide, storm surge, and sea level fluctuations due to normal seasonal heating and cooling, as well as El Niño condition enhancements. They do not include wave setup caused by breaking waves, since tide gauges are located offshore of the surfzone, and their water level sampling system filters out relatively high frequency fluctuations such as wave surges. The design water level used for this study is the extreme thus far observed, 5.5 ft (1.7 m) NGVD, or 7.6 ft (2.3 m) NAVD88 (rounded to one significant figures).

3.5 DESIGN WAVE ESTIMATION

Wave runup can be the dominant contribution to high water levels on beaches, depending on the state of the tide, and the height, direction, and period of the waves, especially during storms. The wave record for San Onofre, estimated from measurements at SONGS and comparison to Oceanside wave array data between 1978 through 1994, was used to calculate wave height return periods for San Onofre (see Section 5.2 in Elwany et al. 2016).

The Seasonal Maxima Distribution Model (SMDM) developed by L. E. Borgman and published in USACOE (1988) was selected as the appropriate analysis method to estimate the design wave height at a range of return periods. Monthly wave maxima were extracted from the wave data and split into seasonal sets. The seasonal maximum wave-height distribution functions were calculated for each season and then multiplied together to produce the annual maximum distribution. This distribution function was used to estimate extreme wave-height return periods.

The design wave analysis shown in Figure 3-14 was used to identify the significant wave heights associated with 5-, 10-, 25-, 50-, and 100-year wave events at San Onofre. Wave spectra matching those wave heights were selectively extracted from the record. The wave spectra from these storms (Figure 3-15) were extracted from the Coastal Data Information Program (CDIP) database (https://cdip.ucsd.edu/) and used to estimate the peak period associated with wave-height return period. A typical wave storm on this southern California coast has a wave height of about 6.9 ft (2.1 m). Extreme-values for the 5-, 10-, 25-, 50-, and 100-year return period wave heights at San Onofre are given in Table 3-4.

The largest storm on record between 1980 and 2016 occurred on 18 January 1988. The deepwater wave height was 16 ft (4.9 m) with a period of 17 sec (as measured at the Oceanside buoy). The corresponding wave height at San Onofre was about 12.5 ft (3.8 m) approaching the shore from the west. Table 3-5 represents the highest significant wave heights at San Onofre in descending order estimated from the Oceanside measured wave data for summer, winter, and all data.

3.6 SONGS REVETMENT STABILITY ESTIMATION

As outlined above, the median rock weight W_{50} is a key parameter in assessing the stability of a revetment. Hudson's formula (Ahrens, 1981a,b ; USACOE 1984, 1994a,b; BCMELP, 2000) is the standard practice method used to estimate W_{50} necessary for revetment stability:

$$W_{50} = \frac{\gamma_r H^3}{K_D \left(\frac{\gamma_r}{\gamma_w} - 1\right)^3 \cot\alpha} \quad (3\text{-}2)$$

Where:

W_{50} = required median armor unit weight,
γ_r = specific weight of the rock unit, Kg/m^3,
H = wave height at the toe of the revetment,
K_D = stability coefficient,
γ_w = specific weight of water at the site.
α = revetment slope angle from horizontal

K_D values vary primarily with the shape of the rocks, roughness of their surface, sharpness of edges, and degree of interlocking, Typically K_D = 2.1. Wave height H at the structure is estimated by shoaling the design waves to the breaking point (H_b). If H_b is less than the wave height at toe H_{toe} of the revetment we use $H_{b,}$ otherwise H_{toe} is used.

The height of the wave at the toe of the revetment is depth limited. The extreme water depth at the toe of the SONGS revetment (Ds) is 5.5 ft + 2.29 = 7.79 ft, MLLW, where 5.5 ft, NGVD is extreme water level (Section 3.4) and the 2.29 is the difference in elevation between datums NGVD and MLLW.

The water depth at the toe of the structure (Ds) varies as the sea level rises. In 2050, the water depth at the toe of the structure is projected to be 9.79 ft, MLLW (OPC, 2018 Medium-High Scenario) and 10.59 ft, MLLW (OPC, 2018 H++ Scenario). A calculation of the wave height (H) was made from the equation H = 0.56 x Ds (Thornton and Guza 1982 and 1983).

Equation 3-2 is used to compute the W_{50} for stable revetment. Table 3-6 gives the values of W_{50} for the MSLR projections medium-high and H++ at 2020 and 2050.

3.7 ASSESSMENT OF SAN ONOFRE BEACH

The condition of the beach fronting SONGS is significant since it prevents or buffers wave attack of the revetment and retaining wall, which in turn protect the walkway required for lateral beach access. The stability of the SONGS revetment depends on the condition of the beach. Presence of a healthy beach causes waves to break farther seaward of the revetment, thus reducing wave run-up, splashing, and overtopping. The beach also prevents toe scouring that can undermine the revetment and cause rock units to settle. When the beach is narrow, or water level unusually high, or both, waves breaking on the revetment can cause dislocation of individual rocks, which contributes to revetment instability.

Recent beach conditions are defined by the 2017, 2018, and 2019 quarterly profile measurements (Appendix E), which characterize the beach configuration in autumn, winter, spring, and summer seasons. Comparisons with earlier beach profiles dating back as early as 1964 show long-term erosion or accretion tendencies. The main factors controlling erosion or accretion are waves and sand supply. Other contributing factors are the nearshore and offshore bathymetry of the region, particularly any wide, flat shelf areas, and the presence of reefs, all of which limit wave height. Structures, particularly the SONGS temporary laydown pads used for Unit 1 and Units 2 and 3 constructions, also influence beach width and stability. In the future, MSLR will cause beaches worldwide to migrate landward and upward. Depending on the state of the backshore, especially its erodibility, beaches may or may not continue to exist. The study documents the complex changes of beach conditions at SONGS and puts these into their Southern California context.

Two surveys each year include the offshore portion of the beach at SONGS. The results of each survey have been presented in reports by Coastal Environments (CE, 2017, 2018, 2019). Longer-term beach change patterns are characterized by comparing beach widths from these recent surveys to comparable measurements from 1985-1993 sponsored by SCE. The earliest directly comparable data were taken in May 1985, just after the sand release of the SONGS Units 2 and 3 laydown pad (Flick and Wanetick, 1989), and from 1990-1993 (Elwany et al., 1994), 2000 (CE, 2000), 2016 (Elwany et al., 2016), 2017, 2018, 2019 (CE, 2020).

In Section 2 of Appendix E, we present an overview of the data and how it was collected. In Section 3, we then discuss the characteristics of SONGS beach profiles and how these relate to typical Southern California beaches. Wave climate at San Onofre is presented in Section 4. Beach width changes and shoreline trends are discussed in Sections 5 and 6. In Section 7, we utilized the available historical information to better understand beach width fluctuations over a long time scale and shoreline changes at San Onofre. Our conclusions are detailed in Section 8.

For convenience, Figures 3-16 and 3-17, and Table 3-7 reproduced from Appendix E in this section to show the long-term changes of beach width.

The beach profile surveys and photography programs sponsored by SCE since 1964 have provided valuable information and understanding of the response at San Onofre to beach filling and the construction of stabilizing structures (Flick and Wanetick, 1989; Flick eta al., 2010). This insight will be valuable as sea level rise accelerates in the future. Elwany et al. (2017) addressed the impacts of sea level rise on San Onofre Beach.

3.8 EVALUATION CRITERIA

A “stable” rock revetment must perform satisfactorily in the sense that it functions as designed even though individual rocks may move such that portions or the entire revetment settles or changes slope. Such changes are expected in rock revetments, and as previously noted, are strength if accounted for in the original design, and if the revetment is maintained. In short, a revetment is functioning properly if it provides protection as designed, and is stable if no damage exceeds ordinary maintenance needs. At a minimum, the design must successfully withstand conditions that have a 50% probability of being exceeded during the revetment’s economic life.

Revetment failure can be caused by either large dislocation of individual rocks such that they become sufficiently separated to no longer function as a unit to dampen wave attack, or from extreme settlement where the height is no longer sufficient to prevent excessive overtopping. In addition, failure of the project during probable maximum conditions should not result in loss of life or unreasonable cost.

From our observations, the SONGS revetment is in good condition, rocks gradation is within acceptable limits, the rocks interlock with others, and there is currently no obvious significant damage. Additionally, a comparison between Transects 6, 15, and 18 with 2009 and 2016 surveys show that the revetment is keeping its shape (Figure 3-18). The noticeable differences in elevation between 2020 and 2009 (top figure) is likely due to the fact that during 2009, Transect 6 was covered by sand. The differences between 2020 and 2016 (bottom figure) are a result of the fact that additional rocks were added during routine maintenance at Transect 18 to elevate it.

The north portion of the revetment is currently covered by beach sand (Figure 3-19). Under large waves this sand will be removed, and the revetment exposed. The southern part of the revetment is subject to refracted waves that attack at an angle transporting sand to south, thus potentially scouring the revetment foundation and causing settlement (Figure 3-20).

Appendix C presents the aerial photographs of the revetment for the period from 2003 to 2018. Photographs taken during the 18 February 2020 site visit are shown in Appendix D.

3.9 MAINTENANCE AND ADAPTIVE CAPACITY

As described in Section 3.8, the SONGS revetment is currently in good condition. It is stable in the sense that it can likely provide its intended function of wave protection to the retaining wall and walkway through at least 2050. The major threats to revetment stability in the future include wave storms, or clusters of wave storms, such as those that occurred in 1981 to 1983. As described above, revetment damages depend on the height of waves, and the duration of wave attack. Large waves can cause dramatic narrowing and lowering of the beach fronting the revetment, leading to rock settlement and displacement, and wave runup, and overtopping.

The revetment is expected to occasionally sustain future damages of this sort, and therefore require occasional maintenance. It is not expected to collapse or fail in a way that will prevent its function if properly maintained. Such damages are expected in rock revetments as previously noted, and accounted for in the original design such that no damage exceeds ordinary maintenance needs. In this respect, the revetment's adaptive capacity to MSLR is high in the sense that its current stable condition along with occasional maintenance will allow it to continue functioning as intended.

For these reasons, it is important to monitor the cross-sections of the revetment at various locations either by systematic photographs (Appendix D) or surveys (Sections 3.2.1 and 3.2.2) and especially before and after large wave storms. It is also important to monitor the beach fronting the revetment and at the north and south of it as described in Section 3.7 and Appendix E.

The revetment, retaining wall, and walkway also provide additional protection to the main SONGS sea wall. It is crucial that the seawall remain in place at least until the deconstruction efforts of Units 2 and 3 are completed. The sea wall also provides critical protection for the ISFSI and its security building.

Impacts of ground water on the ISFSI based on quarterly measurements of the groundwater from 8 coastal wells out of 16 total wells are presented Appendix F. The OPC (2018) 0.5% (medium-high)and H++ SLR scenarios for ground water elevation for 2050 are 4.62 ft and 5.28 ft, NGVD and are 1.35 ft and 0.55 ft lower respectively than the bottom of the ISFSI support foundation which is 3 ft thick (Figure 3-21).

Continued maintenance of the SONGS revetment as necessary (Section 3.1.1), as is maintaining the main SONGS seawall. These both substantially decrease exposure and risk to SONGS from future MSLR, and therefore increase the resilience and adaptive capacity of all SONGS facilities and the Lease Premises in compliance with SCE lease agreement.

Figure 3-1. Photograph taken on 20 August 2018, showing the SONGS revetment. Notice the north part of the revetment is covered by beach sand.

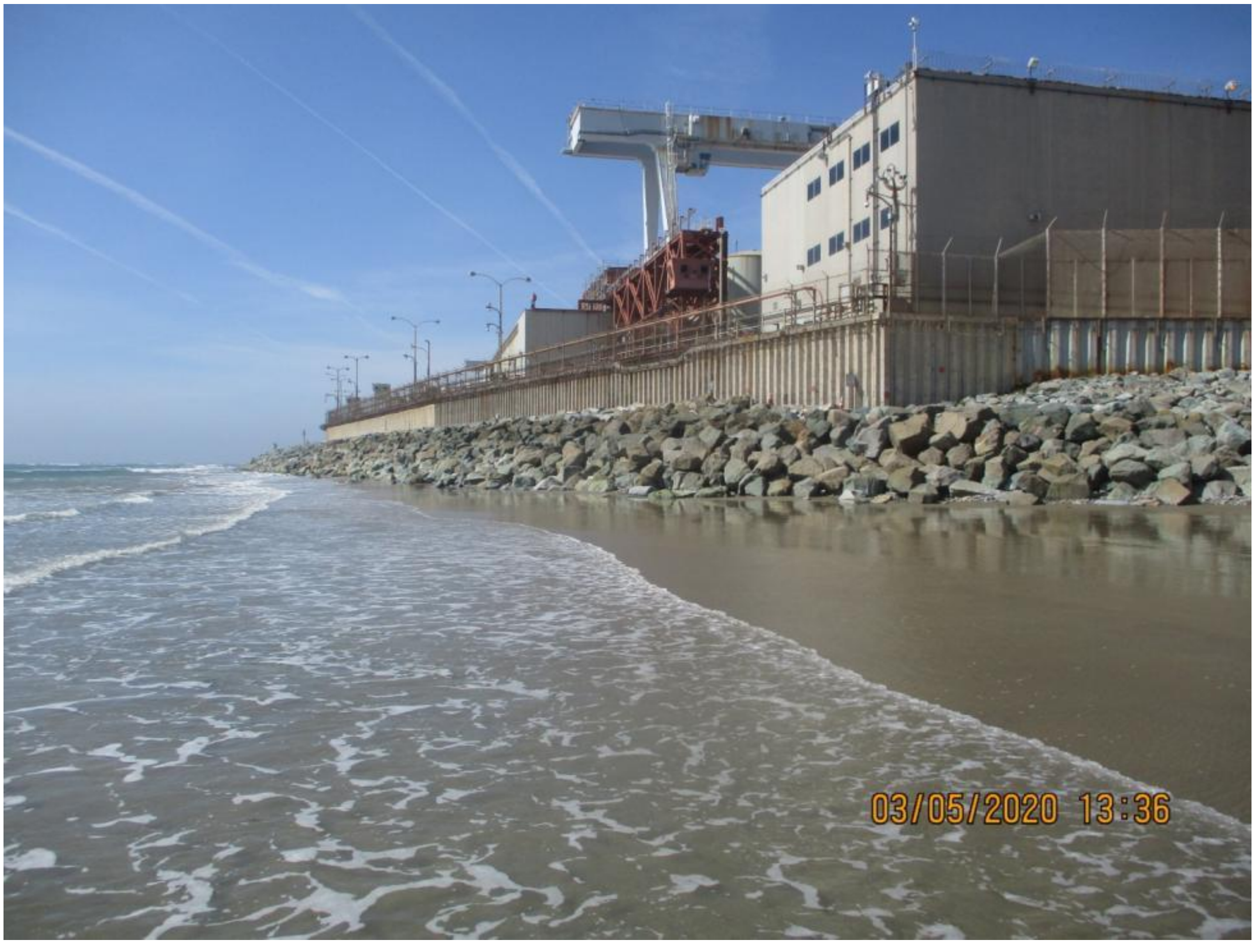

Figure 3-2. Close up of the revetment at its southern end.

Figure 3-3. Top photograph taken on 20 March 2018, before placement of riprap. Bottom photograph taken on 17 December 2019, after placement of riprap within gaps and depredated areas of the revetment. Direction of the photograph taken towards the south.

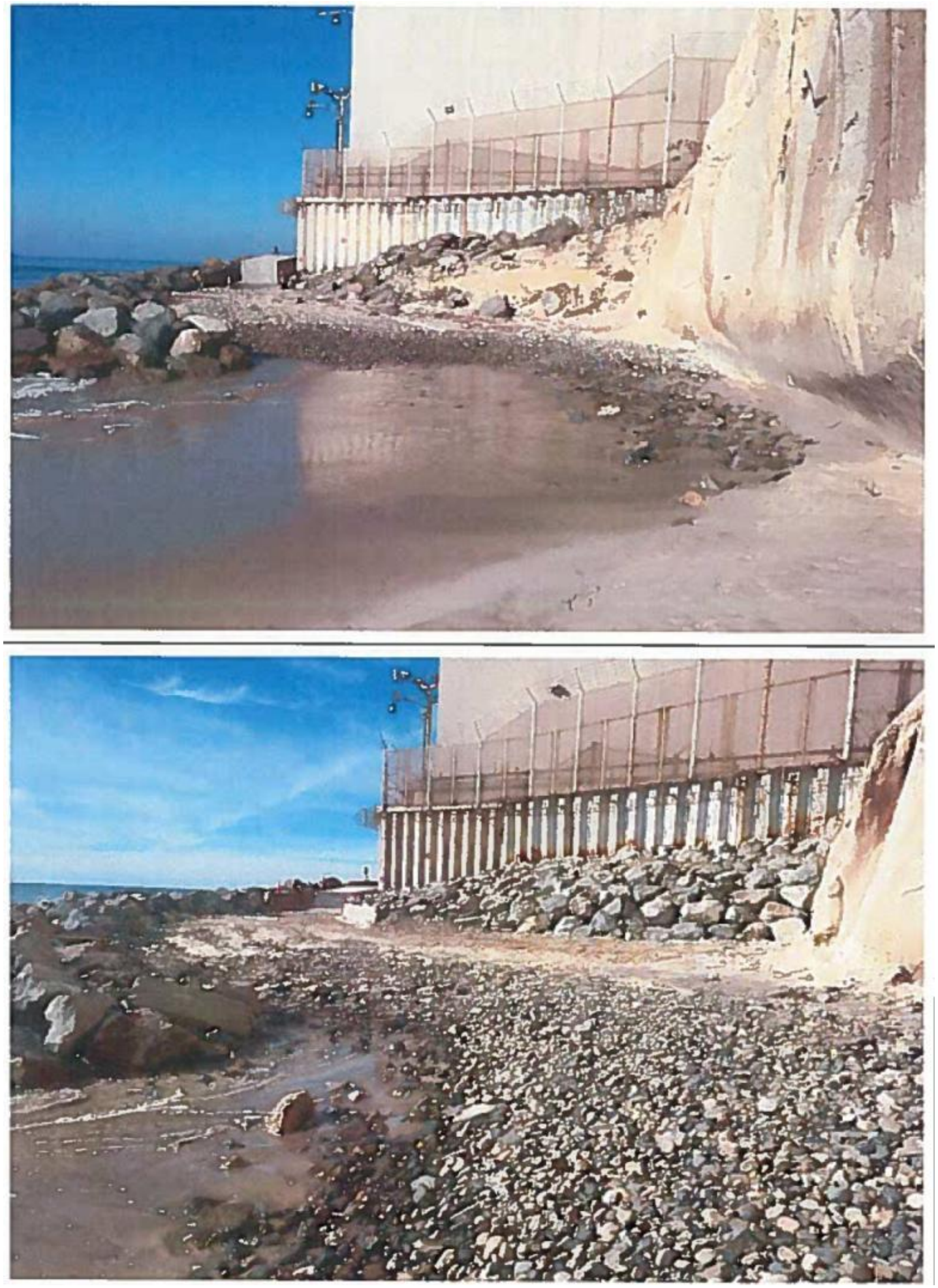

Figure 3-4. Top photograph taken on 15 October 2019, showing the sheet pile seawall before repairing the south end of the walkway. Bottom photograph taken on 17 December 2019, showing the sheet pile seawall after repairing the south end of the walkway.

Figure 3-5. Measurements of the long axis of the rock (length).

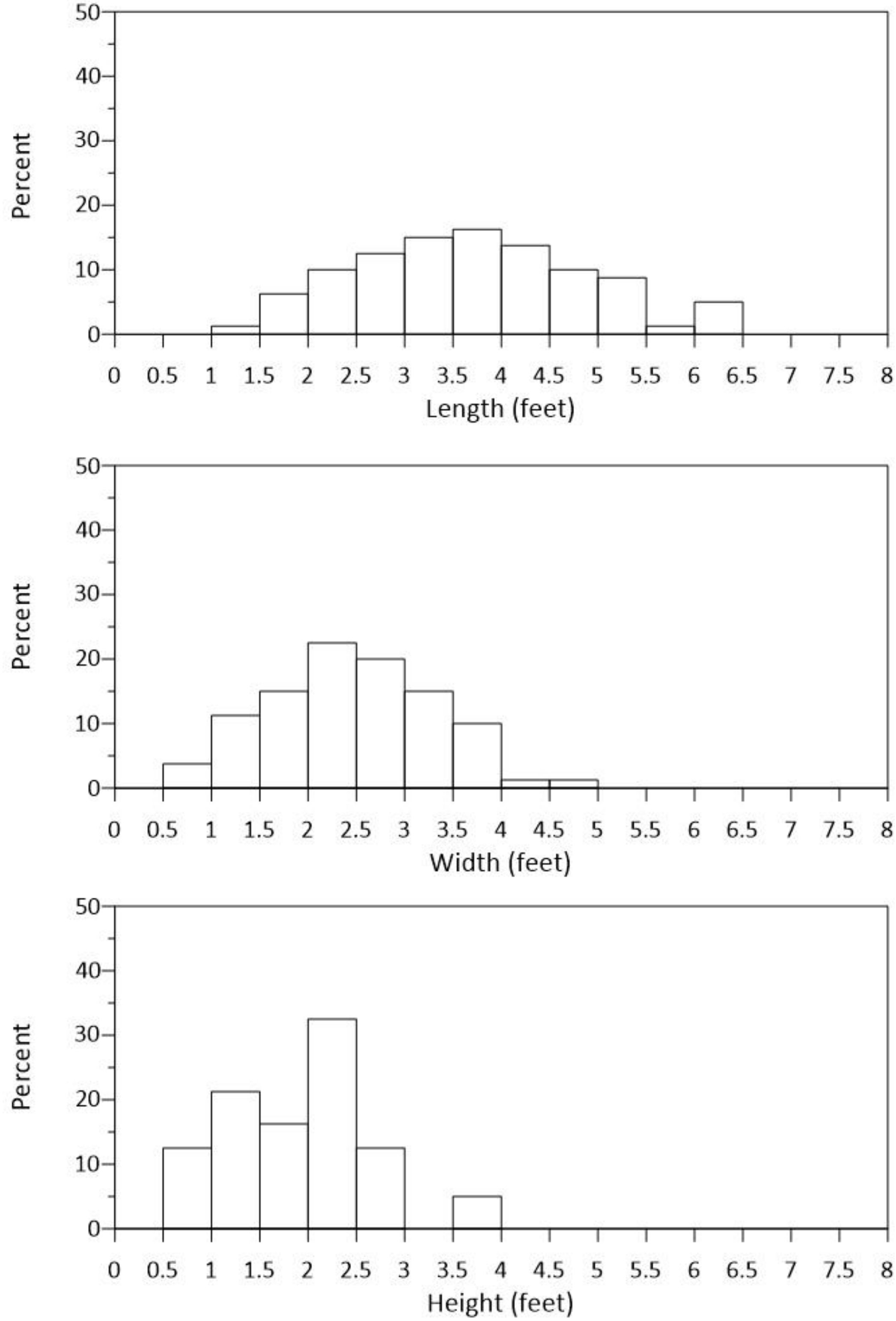

Figure 3-6. Histograms of rock length, width, and height.

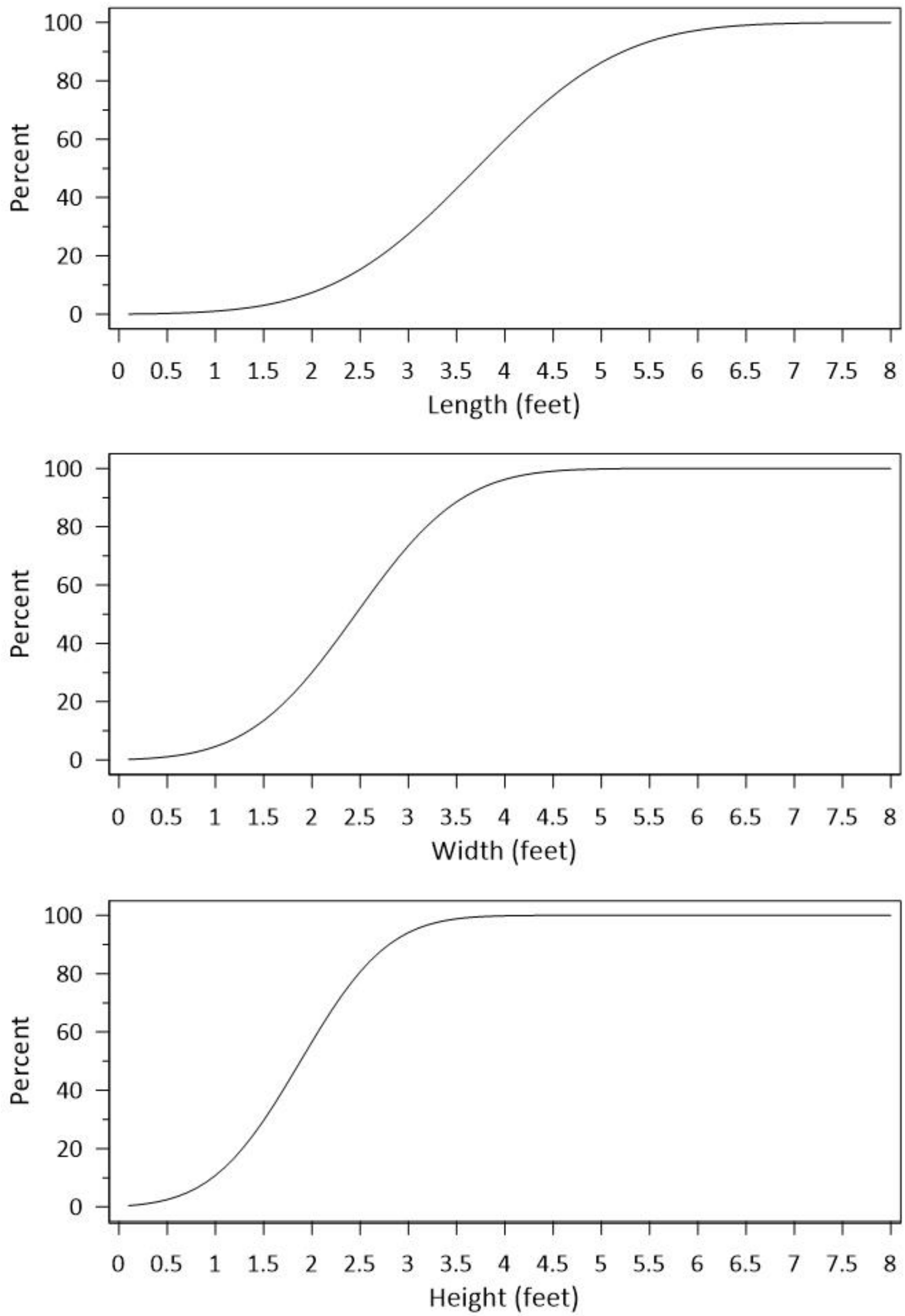

Figure 3-7. Cumulative distributions of rock length, width, and height.

Figure 3-8. Trimble SX10 scanning total station.

Figure 3-9. Location of 21 transects along the revetment, spaced 100 ft apart.

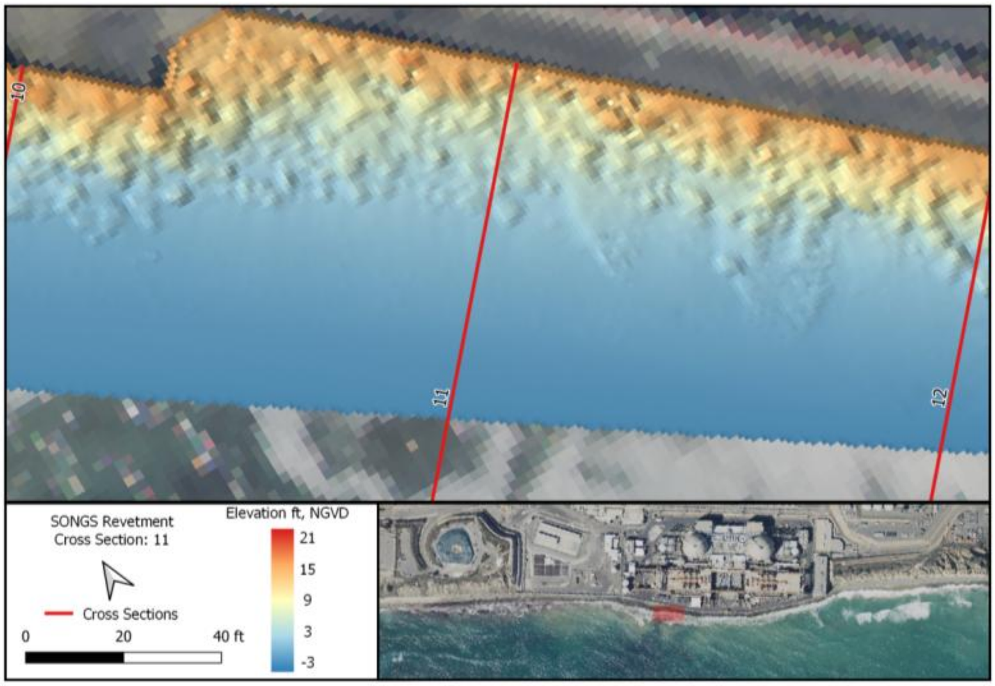

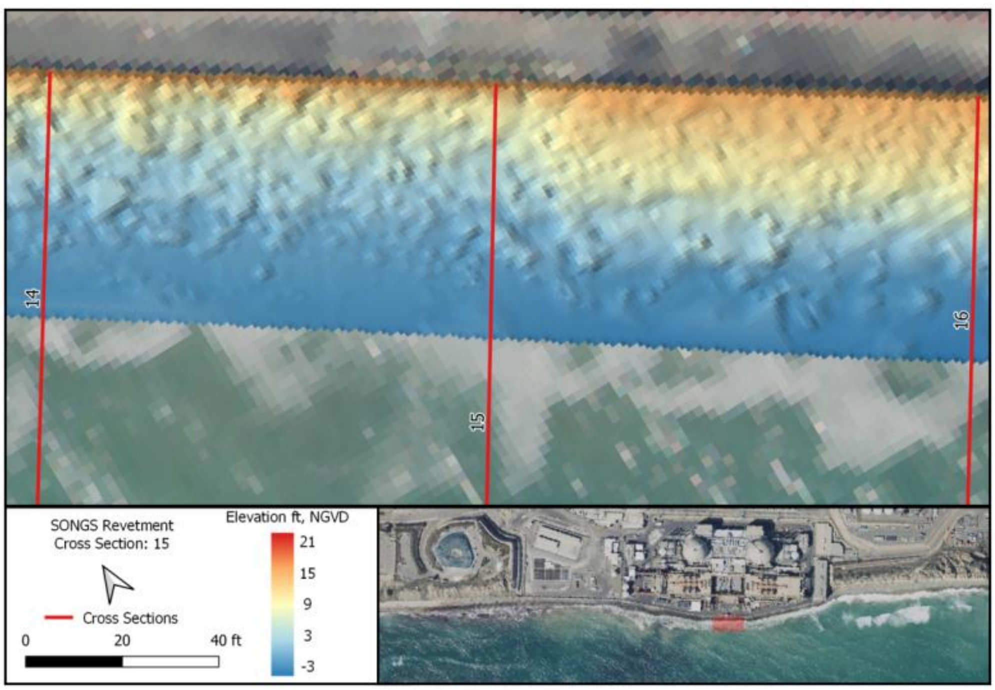

Figure 3-10. Elevation models of SONGS revetment from Laser Scanner.

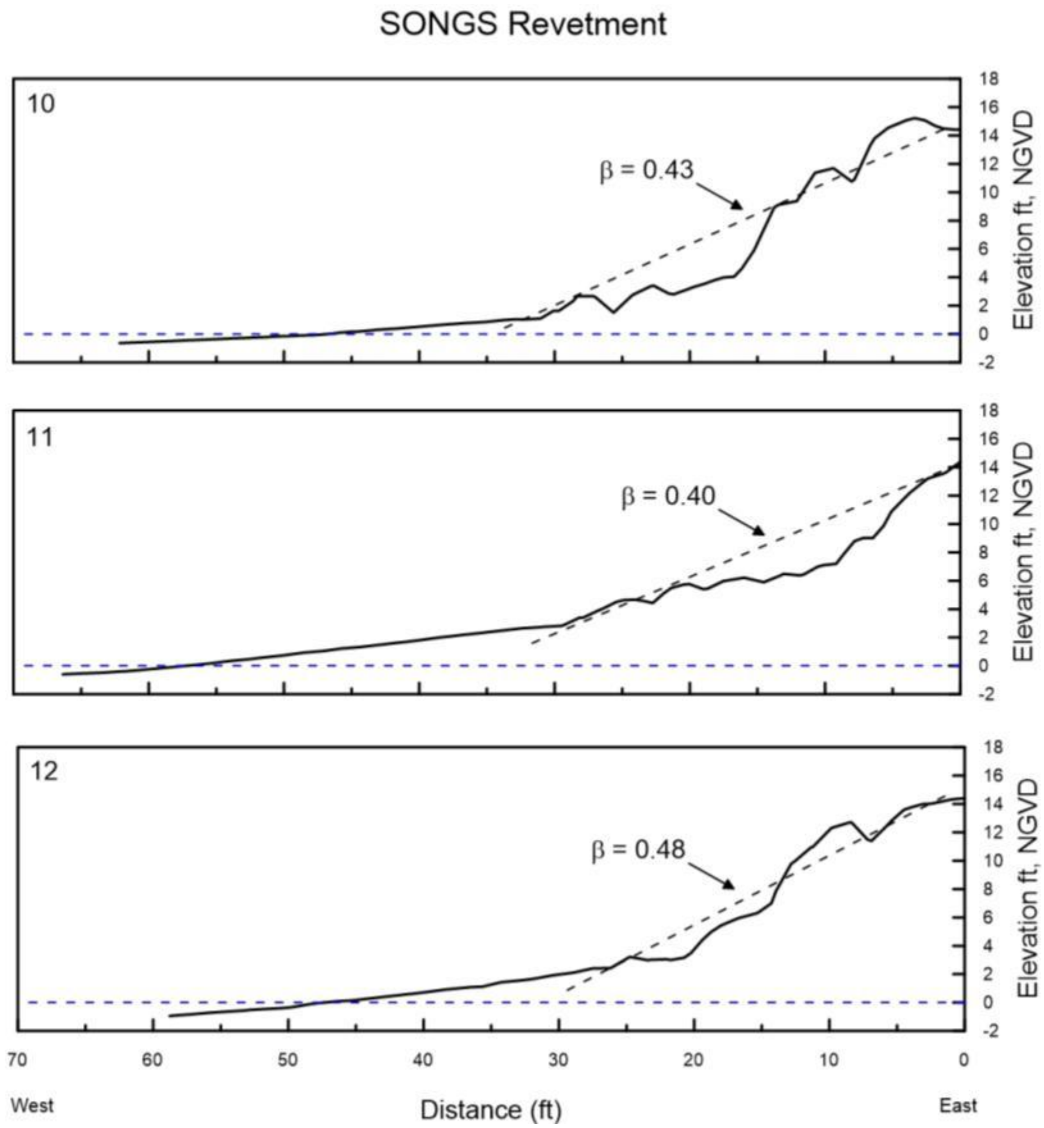

Figure 3-11. Typical revetment cross sections showing slope "β" at the indicated section.

Table 3-1. Riprap and walkway wall heights and revetment slope (β).

Transect #	Riprap Height ft, NGVD29	Wall Height ft, NGVD29	Slope (β)
1	12.89	16.79	0.58
2	12.27	14.27	0.66
3	12.15	14.27	0.64
4	9.22	14.32	0.26
5	9.44	14.27	0.35
6	10.13	14.2	0.43
7	12.48	14.34	0.67
8	9.55	14.39	0.20
9	10.59	14.29	0.38
10	15.12	14.39	0.43
11	13.69	14.34	0.40
12	13.63	14.39	0.48
13	12.37	14.39	0.42
14	12.34	14.37	0.38
15	10.34	14.34	0.39
16	14.24	14.21	0.42
17	12.98	14.27	0.38
18	13.58	14.22	0.39
19	14	14.31	0.40
20	13.49	14.32	0.37
21	14.4	14.32	0.35

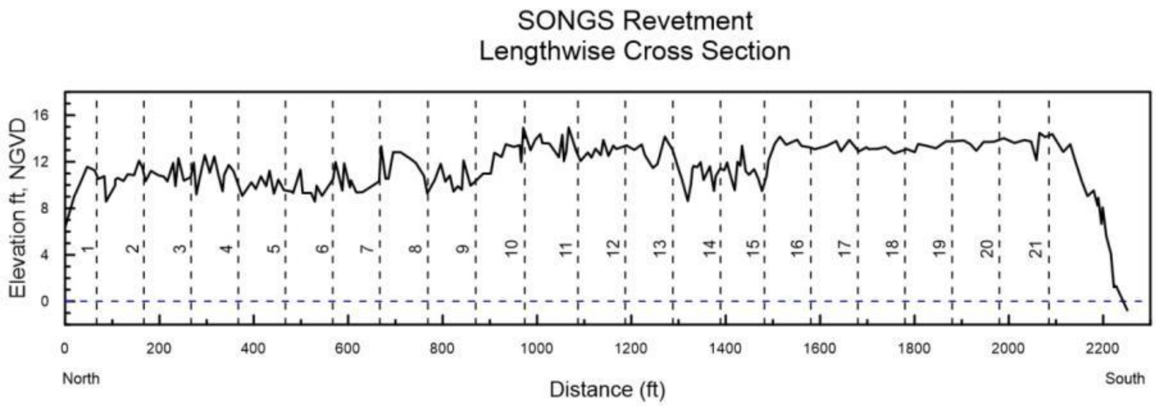

Figure 3-12. Elevation of the top of revetment for the 21 transects.

Table 3-2. Length, width, height, and estimated weight of the measured rocks.

Rock	Length (ft)	Width (ft)	Height (ft)	Weight (kg)
1	2.6	2.1	2	369
2	3.3	2.4	2.7	551
3	3.3	2.9	2.1	973
4	2	1.8	1.4	233
5	4.8	3.9	1.8	2,366
6	3.5	1.7	1.2	196
7	3.2	2.6	2.5	701
8	2.8	1.6	1	163
9	3.2	2.4	1.7	551
10	1.9	1	1	40
11	3.5	1.9	2	274
12	2	1.5	0.9	135
13	2.6	2.3	1.1	485
14	4.3	3.5	2.5	1,710
15	3.8	2.6	1.3	701
16	2.3	1.7	1	196
17	5.2	3	1.4	1,077
18	4.3	3.9	1.2	2,366
19	5.3	3.6	3	1,861
20	4.4	3.2	2.1	1,307
21	4.3	3.5	2.7	1,710
22	4.7	3	2.6	1,077
23	2.6	1.4	1.5	109
24	4.8	3.2	1.8	1,307
25	5.2	2.9	2.3	973
26	3.7	2.5	2.5	623
27	3.4	1.9	1.6	274
28	4.6	2.2	2.1	425
29	4	3.4	2.1	1,568
30	3.4	1.9	1.3	274
31	3.8	2.7	2.1	785
32	4.6	3.9	0.9	2,366
33	4.3	3.2	2.3	1,307
34	4.9	2.4	2.3	551
35	3.5	2.7	2.2	785
36	2.8	2.8	1.5	876
37	3	2.2	1.6	425
38	3.6	1.8	0.9	233
39	4.5	3.8	3.7	2,189
40	3.8	2.2	2	425
41	4.9	4.6	2.4	3,883
42	2.9	2.7	2.4	785

Rock	Length (ft)	Width (ft)	Height (ft)	Weight (kg)
43	3.6	2.1	2.1	369
44	4	2.4	2.6	551
45	4.3	2.7	3.6	785
46	3.8	2.2	3.6	425
47	4.1	3.3	2.1	1,433
48	3.6	2.5	1.5	623
49	3.9	2.4	1.2	551
50	6.3	3.4	2.3	1,568
51	5.1	2.9	2.2	973
52	2.2	1.5	1.1	135
53	2	1.2	0.9	69
54	2.3	1.6	1.6	163
55	4.4	2.7	2.1	785
56	3.3	2.6	1.2	701
57	2.4	2.1	1.1	369
58	2.5	2.1	2.1	369
59	5.5	3.7	2.7	2,020
60	3.4	1.9	2.2	274
61	4.2	1.7	1.9	196
62	2.9	1.4	2.1	109
63	5.4	4.2	2.8	2,955
64	2.9	1.9	2.3	274
65	5	3.2	1.6	1,307
66	5.8	3.3	2	1,433
67	6.1	3.4	3.7	1,568
68	6.4	4	2.8	2,553
69	4.2	3.7	2.9	2,020
70	6.3	3.2	2.2	1,307
71	3	1.1	2.2	53
72	3.4	2.2	1.3	425
73	2.2	1.1	1.3	53
74	1.3	1.1	0.6	53
75	1.6	1	0.8	40
76	3.8	2.7	2.7	785
77	5.4	2.4	2.1	551
78	2.3	1.2	0.7	69
79	2.1	0.7	1.4	14
80	3.8	2.9	2	973

Table 3-3. Mean and standard deviation for rocks parameters.

Rock Parameters	Length (ft)	Width (ft)	Height (ft)	Calculated weight (kg/m^3)
Mean	3.8	2.5	1.9	849
Minimum	1.3	0.7	0.6	14
Maximum	6.4	4.6	3.7	3,882
Std Dev	1.2	0.9	0.7	779

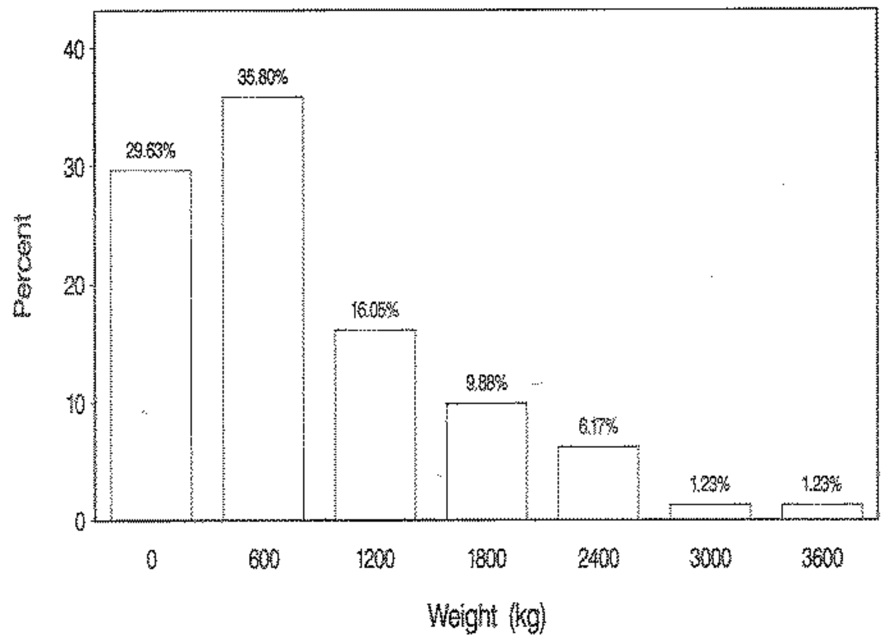

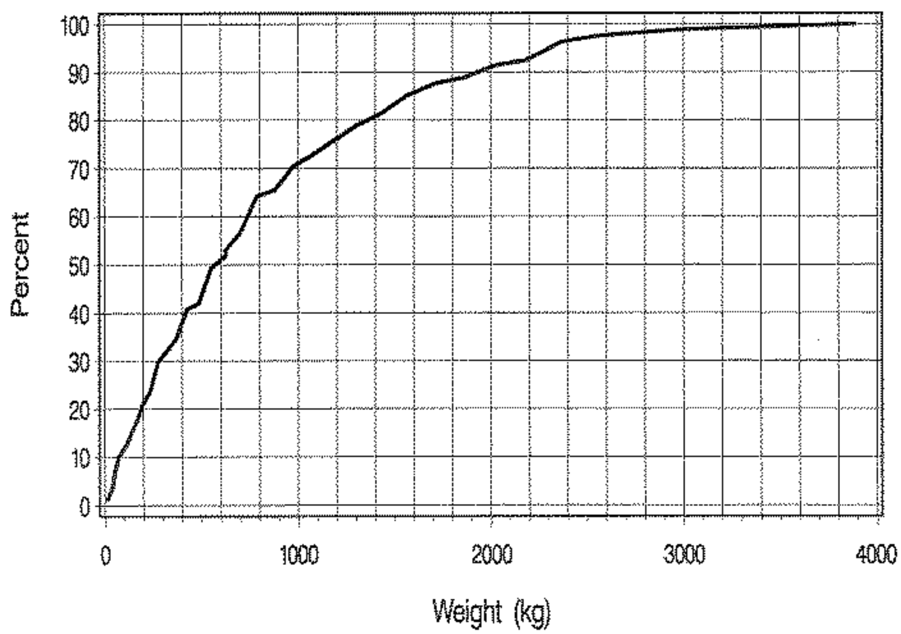

Figure 3-13. Weight distribution of SONGS revetment rocks.

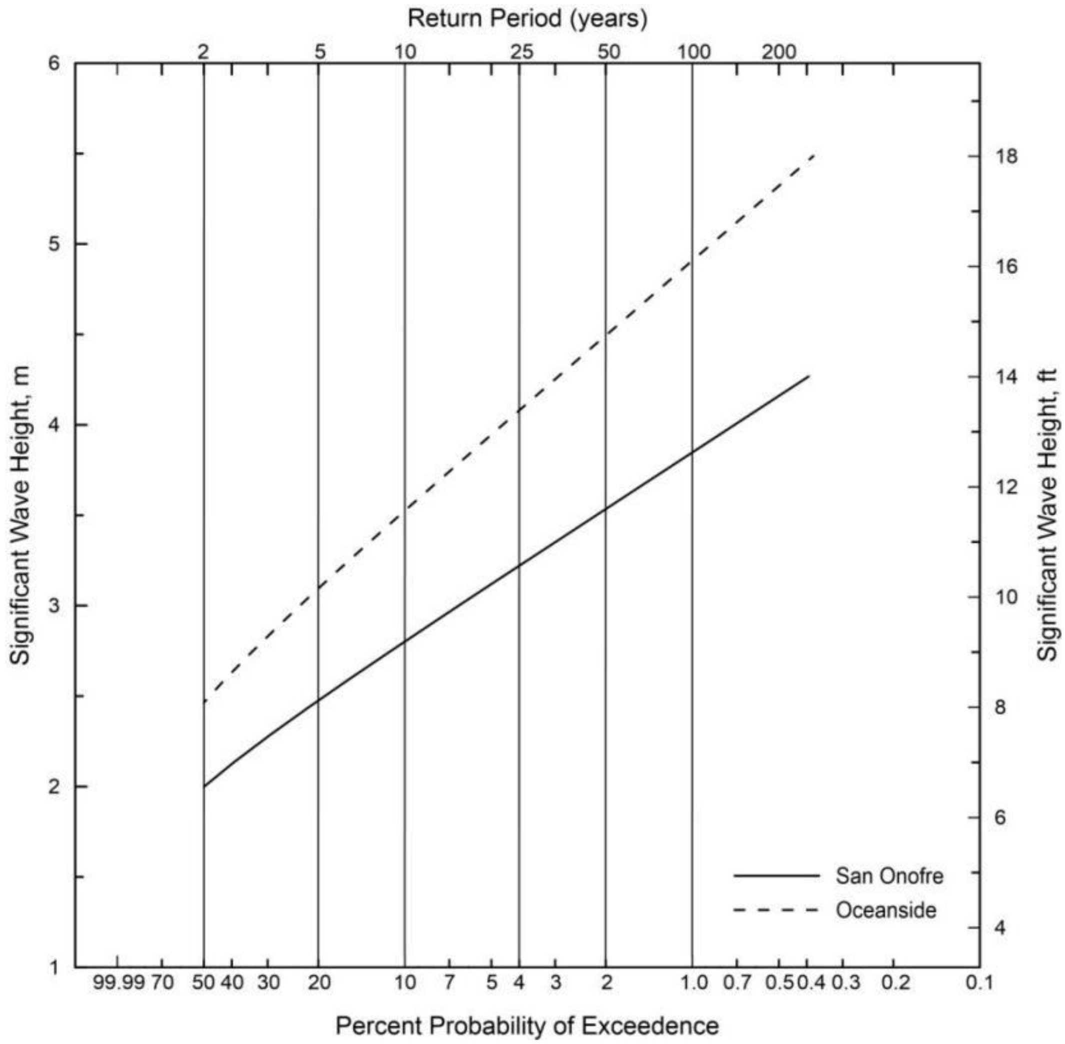

Figure 3-14. Design wave heights for various return periods at San Onofre.

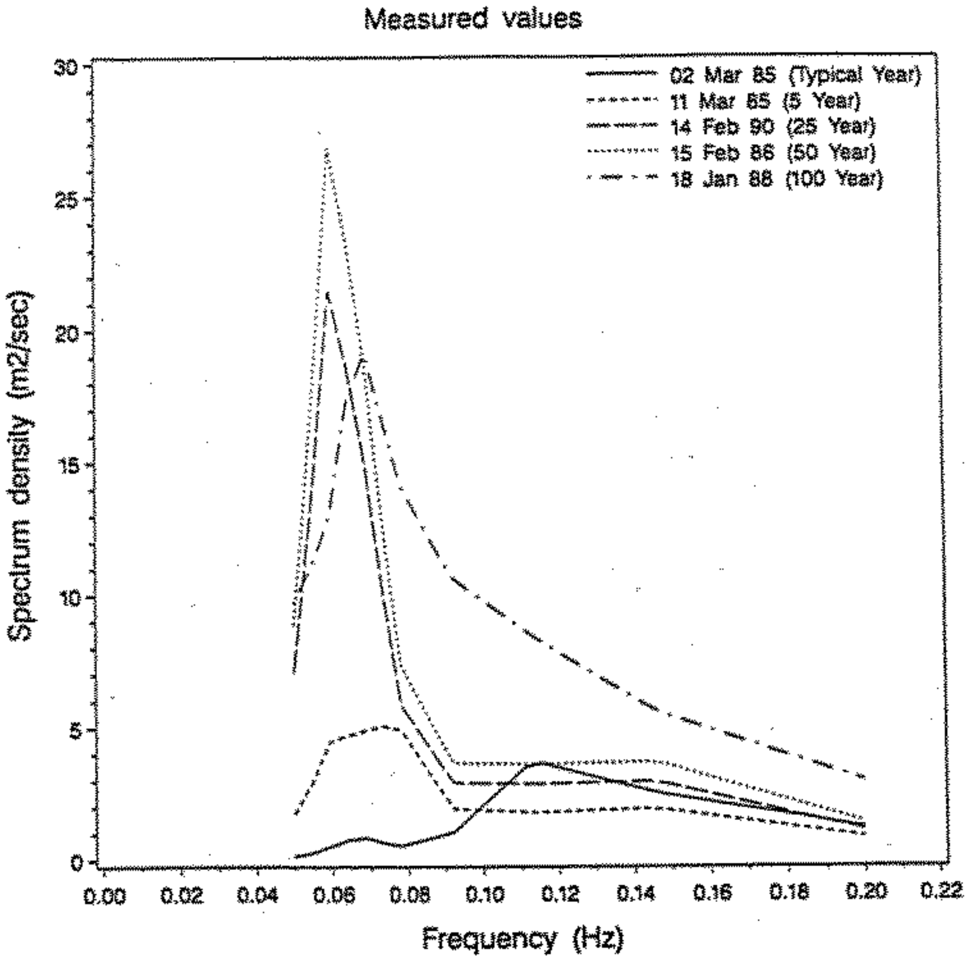

Figure 3-15. Measured spectrum density for various storms.

Table 3-4. Design wave characteristics at San Onofre.

Storm Return Period (yr)	Significant Wave Height, Hs (m)	Peak Period, Tp (sec)
2	2.0	9
5	2.4	12
10	2.8	12
25	3.2	17
50	3.5	17
100	3.8	16

Table 3-5. Largest 20 waves at San Onofre ranked in descending order (1976-1994).

Rank	Winter		Summer		All	
	Hs (m)	Tp (secs)	Hs (m)	Tp (secs)	Hs (m)	Tp (secs)
1	3.85	14.22	2.01	8.00	3.85	14.22
2	3.28	12.80	1.76	8.53	3.28	12.80
3	2.88	14.22	1.73	7.11	2.88	14.22
4	2.88	8.53	1.70	8.53	2.88	8.53
5	2.52	12.80	1.64	16.00	2.52	12.80
6	2.41	8.53	1.64	8.26	2.41	8.53
7	2.36	8.53	1.60	7.53	2.36	8.53
8	2.31	7.53	1.59	7.11	2.31	7.53
9	2.26	6.74	1.52	8.53	2.26	6.74
10	2.25	12.80	1.50	7.53	2.25	12.80
11	2.25	12.80	1.47	8.00	2.25	12.80
12	2.12	12.80	1.47	9.48	2.12	12.80
13	2.06	7.53	1.44	14.22	2.06	7.53
14	2.06	14.22	1.44	7.53	2.06	14.22
15	2.06	12.80	1.42	7.53	2.06	12.80
16	2.05	14.22	1.42	7.53	2.05	14.22
17	2.04	7.53	1.42	16.00	2.04	7.53
18	2.03	9.14	1.41	6.74	2.03	9.14
19	2.03	7.53	1.41	9.85	2.03	7.53
20	2.03	14.22	1.41	16.00	2.03	14.22

Table 3-6. Rock weights (W50) for 2020 and 2050.

Year	Water Depth Ds (ft)	H (ft)	H (m)	W50 (kg)
2020	7.79	4.4	1.33	276
2050 (P .05%)	9.79	5.5	1.67	548
2050 (H++)	10.59	5.9	1.8	685

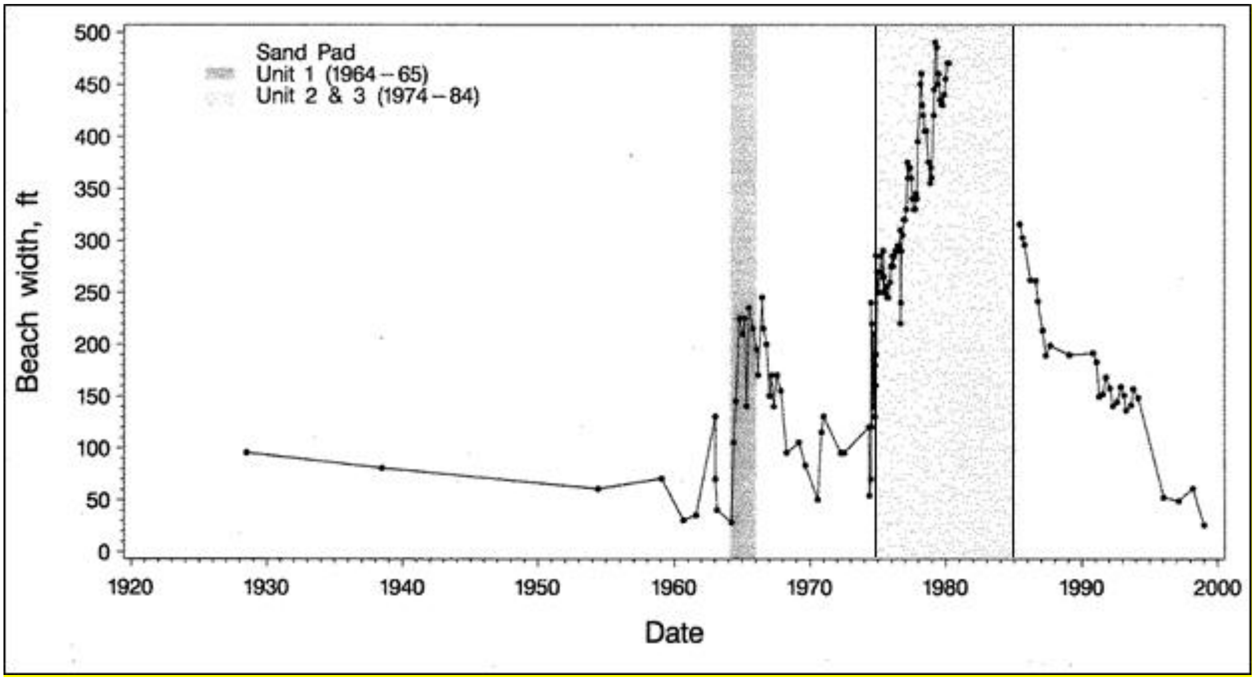

Figure 3-16. Historical beach width adjacent to Unit 1, 1928-2000. Vertical columns show periods when laydown pads were present. From Appendix E.

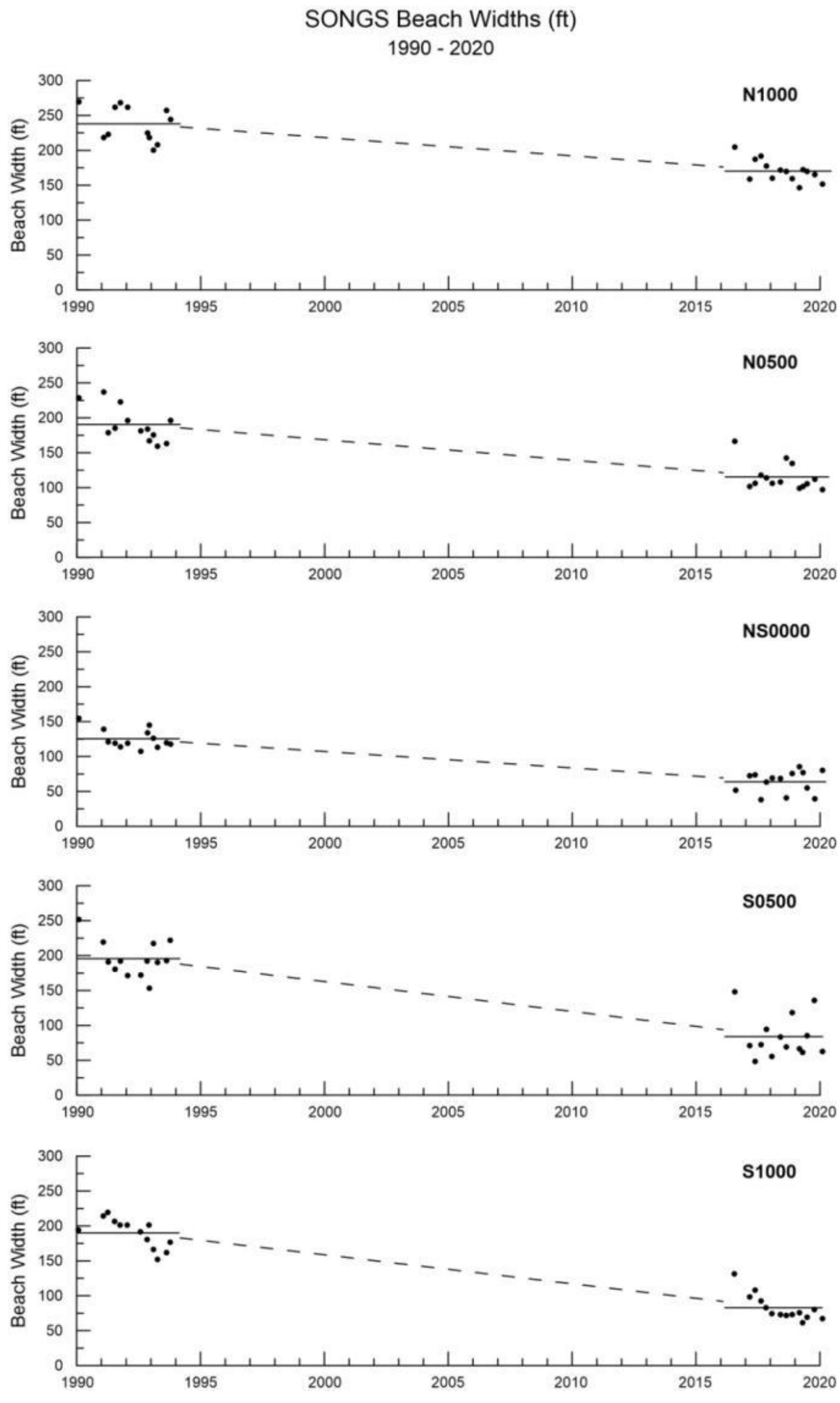

Figure 3-17. Beach width measured between 1991 through 1993 and between 2016 through 2019. Solid lines are the mean of beach width for the referenced periods and dotted lines cover the period where no long-term measurements were carried out. From Appendix E.

Table 3-7. Mean beach widths (ft) at San Onofre. From Appendix E.

Survey Period	Profiles				
	N1000[a]	N0500[a]	NS0000[b]	S0500[c]	S1000[c]
1990-1993	227.3	173.5	119.1	205.5	164.3
Aug 2000	275.8	183.2	106.6	362.8	220.86
July 2016	204.5	116.4	204.5	102.3	106.7
2017-2019	169.2	112.5	63.3	80.2	80.1

[a] Average beach profile width at North Beach in 1964 is 295 ft. from Figure 7-3.
[b] Average beach profile width Fronting SONGS in 1964 is 229 ft. from Figure 7-3.
[c] Average beach profile width at South Beach in 1964 is 196 ft. from Figure 7-3.

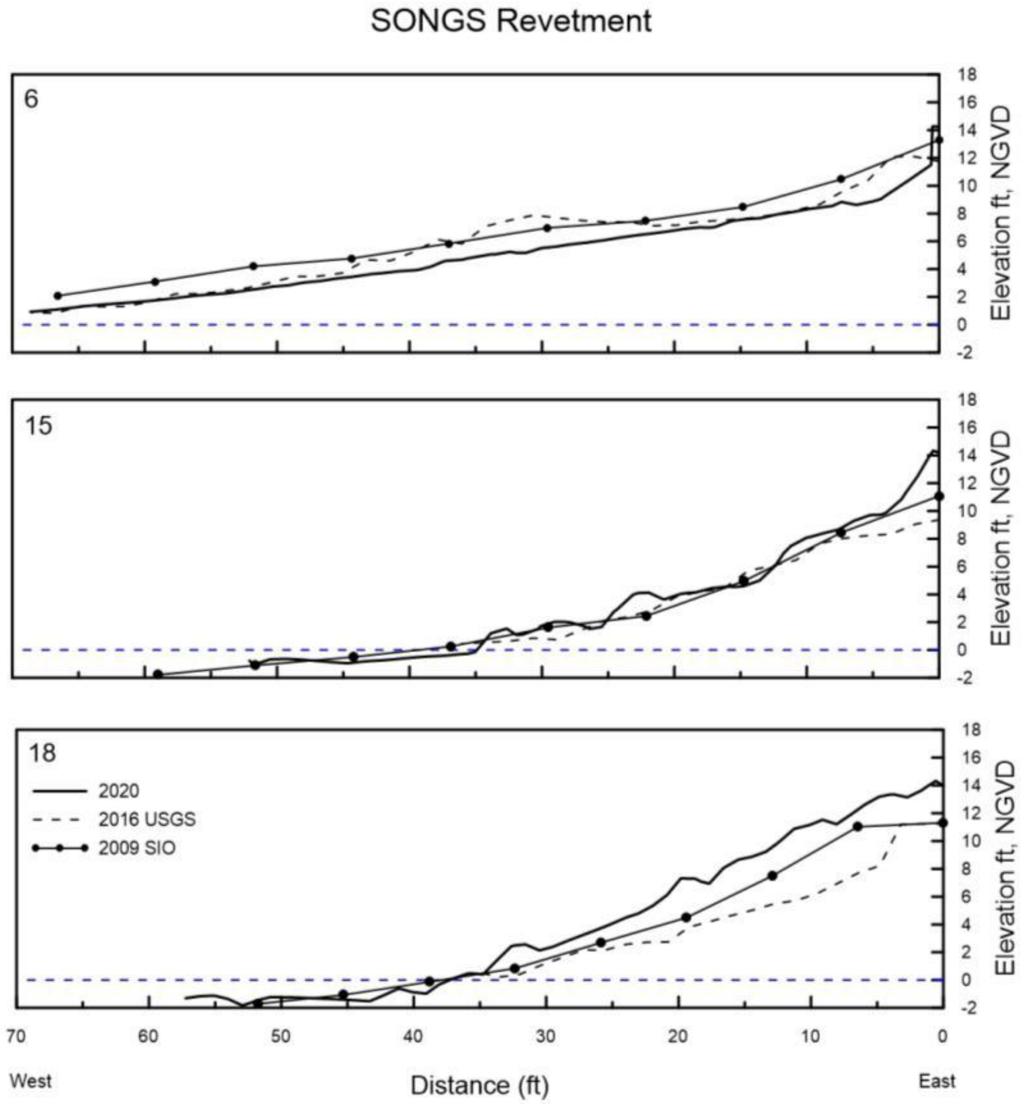

Figure 3-18. Comparison of 2020 laser scan transects 6, 15, and 18 and surveys carried in 2009 and 2016.

Figure 3-19. North portion of the revetment covered by beach sand.

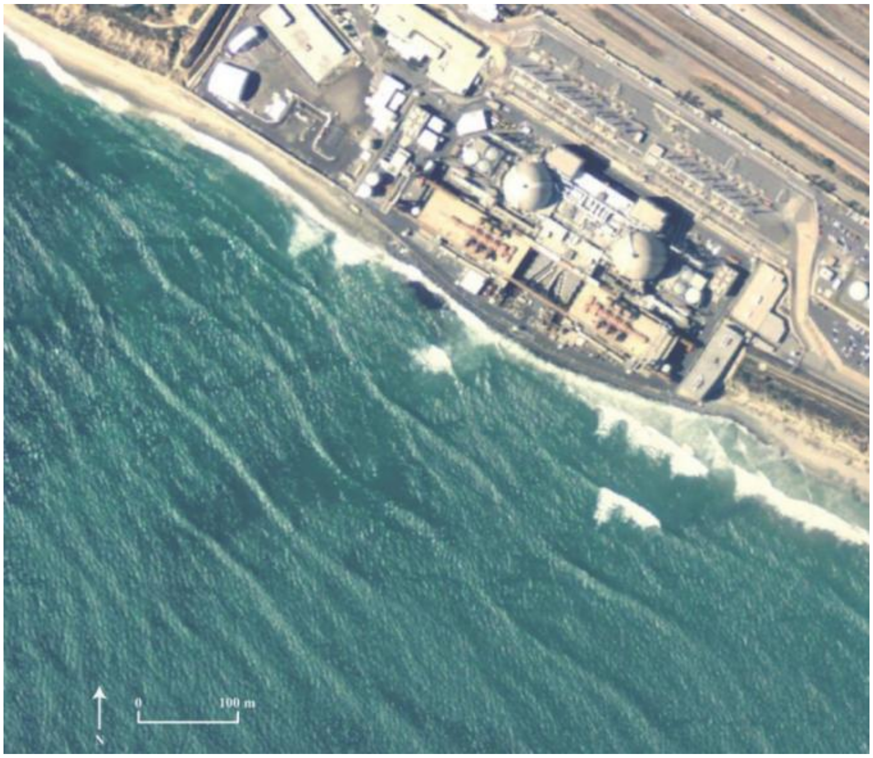

Figure 3-20. Waves attacking SONGS revetment at an angle and transporting sand south.

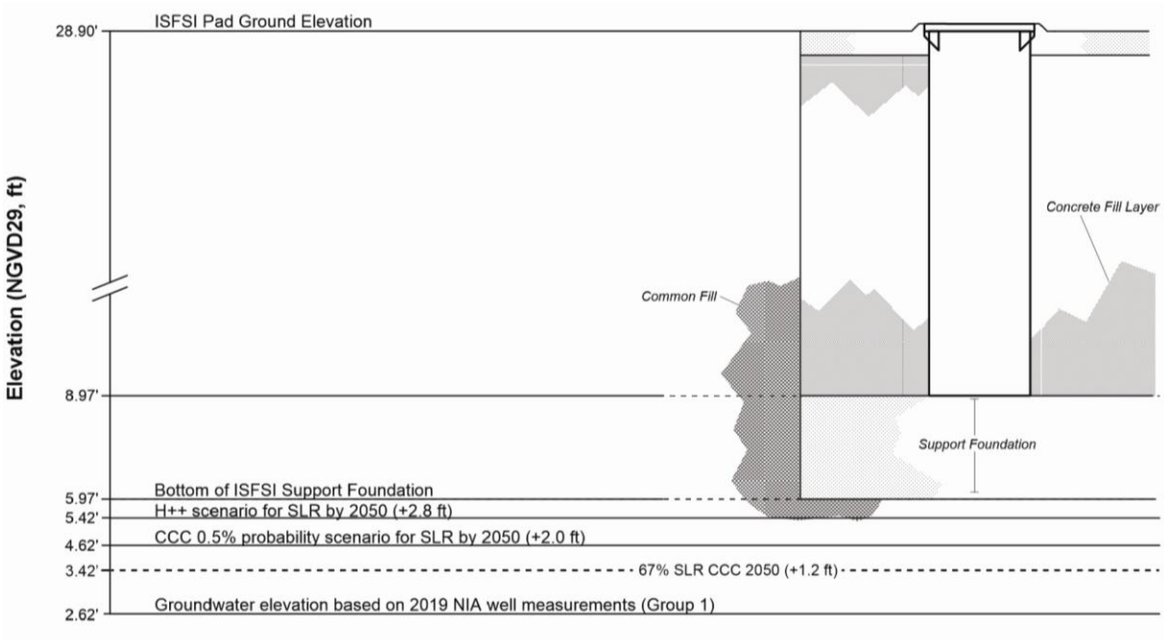

Figure 3-21. Groundwater elevations for 2019 and for the OPC projections in 2050. The CCC projections (2018) for sea level rise are based on OPC projections. From Appendix F.

4.0 RUNUP AND OVERTOPPING ANALYSIS

Wave runup is defined as the rush of water up a beach or coastal structure caused by, or associated with, wave-breaking. The runup elevation, designated *R* (Figure 4-1), is the maximum vertical height above still water level that the runup will reach. If the runup elevation is higher than the beach berm (or back of the beach) elevation, the excess is then representative of overtopping. Runup elevation is dependent on the incident wave characteristics, beach slope, and porosity, and if a structure is present, on that structure's shape, slope, roughness, permeability, and water depth at the toe. Runup analysis is important to assess possible flooding and damage to the SONGS revetment, retaining wall, and walkway. The amount of damage is dependent on the runup elevation and amount of overtopping, as well as on storm wave duration.

4.1 RANDOM WAVE METHOD

Wave runup (R) is composed of wave setup and swash runup. The swash runup is defined as a super elevation of the mean water level and fluctuation about that mean (S). *R* is given by the equation:

$$R = \acute{\eta} + S/2 \tag{4-1}$$

where ή is the setup and *S* is swash runup.

A large number of both small- and large-scale laboratory studies have been conducted to measure runup values for modeled beaches, sloped dikes, and seawalls (e.g., Hunt 1959; Van der Meer and Jenssen 1995; Hedges and Reis 1998). Based on laboratory experiments, Hunt (1959) proposed various formulas for estimating wave runup, *R*, on a smooth slope as a function of offshore wave height, *H*, and the Iribarren number, ζ, such that:

$$R=kH\zeta, \tag{4-2}$$

where *k* is a constant and ζ is the Iribarren number defined as:

$$\zeta = \frac{tan\beta}{\sqrt{Ho/Lo}} \tag{4-3}$$

where tan *β* is beach slope, *Ho* is deepwater wave height, and *Lo* is deepwater wavelength.

Fewer studies have centered on runup on beaches (Holland and Holman 1993; Raubenheimer et al. 1995; Ruggiero et al. 2004; Stockdon et al. 2006).

Stockdon et al. (2006) considered the contribution from both incident and infra gravity waves, using data from 10 field experiments with varying bathymetries and wave heights. They empirically estimated $R_{2\%}$ by:

$$R_2 = A \quad 0.35\,\beta_f \; H_0 L_0 \quad ^{1/2} + \frac{H_0 L_0 \quad 0.563\beta_r^2 + 0.004 \quad ^{1/2}}{2} \tag{4-4}$$

where β_f is the foreshore beach slope and H_o is the deepwater significant wave height, A is a coefficient equal to 1.1 as estimated by Stockdon, and $R_{2\%}$ is the 2% exceedance level of runup for each run. The units of the Equation 4-4 are in meters.

The SONGS revetment reduces wave runup by factor that varies from 0.5 to 0.6 (USACE 1994b, Table 7-2) due to slope roughness and permeability.

4.2 OVERTOPPING

The overtopping rate (Q) is defined as the volume of water that overtops a coastal structure or beach berm along the beach length per unit time and length. The units are volume per second per unit length (ft^3/sec-ft or m^3/sec-m). Overtopping empirical models are based on laboratory studies of structure overtopping. These models are used to test design specifications intended to limit the overtopping of levees and dikes, and they, therefore, give conservative values. A beach berm can act in the same manner as these structures in protecting the backshore development from wave attack and flooding.

Wave overtopping values depend on the ratio of freeboard height and wave runup height. Freeboard *Rc* is defined as the height of the berm crest above mean water level. In order for waves to overtop a berm, the runup heights must be greater than the freeboard height. Overtopping is dependent on the runup height and, therefore, dependent on incident wave height and period, and beach slope.

Hedges and Reis (1998) introduced a semi-empirical model (H&R model) based on an overtopping theory for regular waves developed by Kikkawa et al. (1968), which assumed that a seawall or beach berm acted as a weir whenever the incident water level exceeded the seawall level and the described instantaneous discharge by the weir formula. The H&R model extended the concept to random waves. Reis et al. (2008) compared the H&R model with three other methods used to estimate the overtopping rate for various structures subject to random wave action. The slopes of these structures varied from 1:1 to 1:20, and wave steepness varied from 0.01 to 0.3. The models were: (1) Owen model (Owen 1980); (2) Van der Meer Janssen model (Van der Meer and Janssen 1995); and (3) AMAZON Numerical Model (Hu 2000). The results showed good agreement between the H&R model and the data. There was general agreement between H&R and AMAZON models, while Owen's model systematically over-predicted the discharges. Van der Meer and Janssen's model gave similar results to the H&R model, except that they over-predicted discharges for some conditions which are outside the ranges of applicability.

The H&R model extending the concept to random waves can be written as:

$$\frac{Q}{\overline{gR3\max}} = A \quad 1 - \frac{Rc}{\gamma r Rmax} \quad B \qquad for 0 \le \frac{Rc}{\gamma r Rmax} < 1 \tag{4-5}$$

and

$$\frac{Q}{\sqrt{gR3\max}} = 0 \qquad for \qquad \frac{Rc}{\gamma r Rmax} \geq 1 \tag{4-6}$$

where g is gravitational acceleration, R_{max} is the maximum runup on smooth slope, and γr is reduction factor to account for rough slope. In this study, R_{max} is estimated by equation number 9 presented by Reis et al. (2008). Additionally, the coefficients of the HR model were given by Reis et al. (2008) as:

$$A = \begin{matrix} 0.0033 + 0.0025\ 1/\beta & for 0.08 \leq \beta \leq 1 \\ 0.0333 & for 0.05 \leq \beta < 0.083 \end{matrix} \tag{4-7}$$

$$B = \begin{matrix} 2.8 + 0.65\ 1/\beta & for 0.13 \leq \beta \leq 1 \\ 10.2 - 0.275\ 1/\beta & for 0.05 \leq \beta < 0.13 \end{matrix} \tag{4-8}$$

where β is the beach slope.

4.3 RESULTS

Figure 3-11 shows typical cross sections of the SONGS revetment. The locations of these profiles are shown in Figure 3-9. The slope (β) of the revetment varies from 0.40 to 0.48. The height of the walkway is about 14 ft (NGVD). The design water level is estimated as 5.5 ft (NGVD). Table 4-1 provides runup and overtopping results for all design wave and water level conditions, including MSLR under the medium-high scenario for 2020, 2030, 2040, and 2050. Table 4-2 shows these results for the extreme H++ MSLR projection. Tables 4-1 and 4-2 suggest that wave overtopping already occurs (in 2020) for storm wave conditions meeting or exceeding a 10-year return period, that is, waves with 10% probability of occurrence in a given year. This is consistent with observations.

As MSLR progresses, overtopping rates are expected to increase. For large storms, rates are projected to reach 0.5 ft^3/sec-ft by 2030, and 1-1.6 ft^3/sec-ft by 2050. There is a short segment in the walkway where the concrete wall is replaced by rails to provide a flow path for the saltwater cooling system during plant operations. This opening in the wall will increase the overtopping on the walkway (Figure 4-2). However, they do not represent a significant hazard to pedestrian since the walkway will be closed during storms, and there are no more discharges from the system.

4.4 PROBABILITY ANALYSIS

The probability associated with runup and overtopping are considered in quantitative terms. This risk is defined as the probability that a "T-year" return period event will occur at least once during a given "n-year" long time period. The runup results in Tables 4-1 and 4-2 can be used to estimate the risk for any selected "n-year" long time period. The results can also be used to estimate the probability of runup of a given size during a specified time period. The probability of a T-year runup in any one year is $P = 1/T$.

In other words, there is a one percent chance that the 100-year runup will occur during a given year. The probability is equal to the sum of the probabilities of having 1 runup, 2 runup, or *n* runup events occurring during *n* years of interest, or to 1 minus the probability of having no runups. The risk can be calculated from Equation 4-9:

$$P = 1 - (1 - 1/T)^n \qquad (4\text{-}9)$$

Equation 4-9 indicates that there is a 63% chance that the 100-year magnitude runup will occur at least once during any 100-year time interval. Similarly, Equation 4-9 can be used to calculate the risk associated with any T-year runup during any time period.

Figure 4-3 gives the probability of occurrence of T = 25-year, 50-year and 100-year runups in an n-year period based on Equation 4-9.

4.5 DISCUSSION

Observations suggest that over the last decade or longer, the SONGS revetment has adjusted to reach an equilibrium configuration. Under its current condition, the revetment is expected to withstand projected wave forces with acceptable minimum damages that will not impact the integrity of the revetment as a whole.

The walkway elevation at 14 ft (NGVD) is relatively low and will continue to be flooded under large wave conditions that overtop the revetment. However, it should be noted that the results of runup and overtopping presented in this study are conservative for the following reasons:

1. The results are based on extreme high water level of 5.5 ft (NGVD) that includes king tides, El Niño enhancements, and 1-ft storm surges. Observations suggest that it is exceedingly unlikely for large storm waves to occur precisely at the time of peak high (King) tides (e.g., Elwany and Flick, 1999; Flick 1998 and 2016; Young et al. 2018).

2. Figure 4-4 illustrates the joint probability distribution between significant wave height and water level between 1976-1994, a period characterized by large waves events occurring between 1981-1984. Figure 4-3 shows that the probability of 50-year and 100-year waves to occur in the next 30 years is 0.45 and 0.28, respectively. Multiplying these probabilities by the probability of larger waves occurring at high tides will lead to an extremely low probability of occurrence.

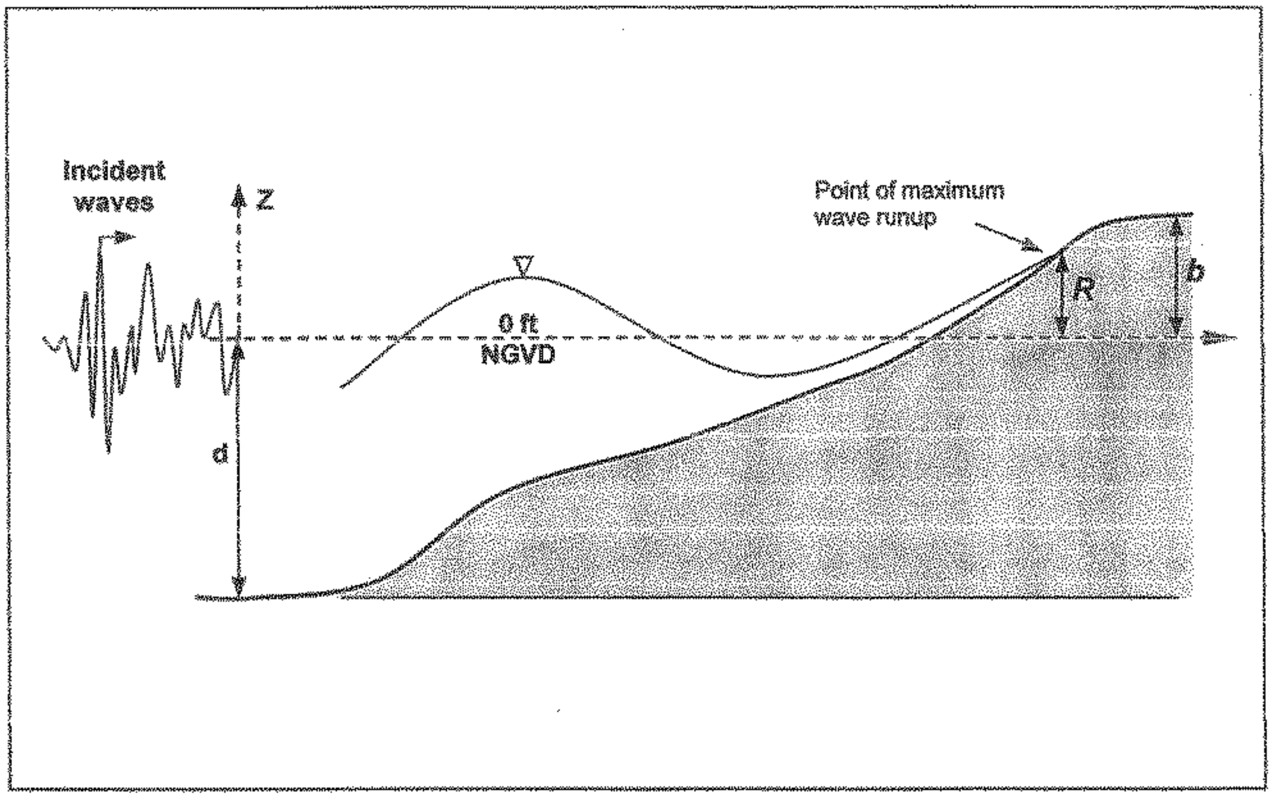

Figure 4-1. Wave runup on a slope. R is the runup elevation, b is the height of the beach berm. If R > b, then overtopping will occur.

Table 4-1. Runup and overtopping summary for Medium-High Risk Aversion.

Year	Return Period (yr)	HS (ft)	Tp (Sec)	Sea Level Rise (ft)	Runup (ft)	Runup Elevation (ft)	Overtopping Rate (ft^3/sec-ft)
2020	2	2	9	0	5.27	10.77	0.00
	5	2.4	12	0	7.23	12.73	0.00
	10	2.8	12	0	7.81	13.31	0.01
	25	3.2	17	0	10.58	16.08	0.18
	50	3.5	17	0	11.06	16.56	0.28
	100	3.8	16	0	11.09	16.59	0.32
2030	2	2	9	0.9	5.27	11.67	0.00
	5	2.4	12	0.9	7.23	13.63	0.01
	10	2.8	12	0.9	7.81	14.21	0.04
	25	3.2	17	0.9	10.58	16.98	0.34
	50	3.5	17	0.9	11.06	17.46	0.49
	100	3.8	16	0.9	11.09	17.49	0.56
2040	2	2	9	1.3	5.27	12.07	0.00
	5	2.4	12	1.3	7.23	14.03	0.02
	10	2.8	12	1.3	7.81	14.61	0.06
	25	3.2	17	1.3	10.58	17.38	0.44
	50	3.5	17	1.3	11.06	17.86	0.62
	100	3.8	16	1.3	11.09	17.89	0.71
2050	2	2	9	2	5.27	12.77	0.00
	5	2.4	12	2	7.23	14.73	0.05
	10	2.8	12	2	7.81	15.31	0.12
	25	3.2	17	2	10.58	18.08	0.69
	50	3.5	17	2	11.06	18.56	0.94
	100	3.8	16	2	11.09	18.59	1.05

Table 4-2. Runup and overtopping summary for Extreme Risk Aversion (H++).

Year	Return Period (yr)	HS (ft)	Tp (Sec)	Sea Level Rise (ft)	Runup (ft)	Runup Elevation (ft)	Overtopping Rate (ft^3/sec-ft)
2020	2	2	9	0	5.27	10.77	0.00
	5	2.4	12	0	7.23	12.73	0.00
	10	2.8	12	0	7.81	13.31	0.01
	25	3.2	17	0	10.58	16.08	0.18
	50	3.5	17	0	11.06	16.56	0.28
	100	3.8	16	0	11.09	16.59	0.32
2030	2	2	9	1.1	5.27	11.87	0.00
	5	2.4	12	1.1	7.23	13.83	0.02
	10	2.8	12	1.1	7.81	14.41	0.05
	25	3.2	17	1.1	10.58	17.18	0.39
	50	3.5	17	1.1	11.06	17.66	0.55
	100	3.8	16	1.1	11.09	17.69	0.63
2040	2	2	9	1.8	5.27	12.57	0.00
	5	2.4	12	1.8	7.23	14.53	0.04
	10	2.8	12	1.8	7.81	15.11	0.10
	25	3.2	17	1.8	10.58	17.88	0.61
	50	3.5	17	1.8	11.06	18.36	0.84
	100	3.8	16	1.8	11.09	18.39	0.94
2050	2	2	9	2.8	5.27	13.57	0.01
	5	2.4	12	2.8	7.23	15.53	0.12
	10	2.8	12	2.8	7.81	16.11	0.24
	25	3.2	17	2.8	10.58	18.88	1.12
	50	3.5	17	2.8	11.06	19.36	1.47
	100	3.8	16	2.8	11.09	19.39	1.62

Figure 4-2. Exposed area in the walkway wall.

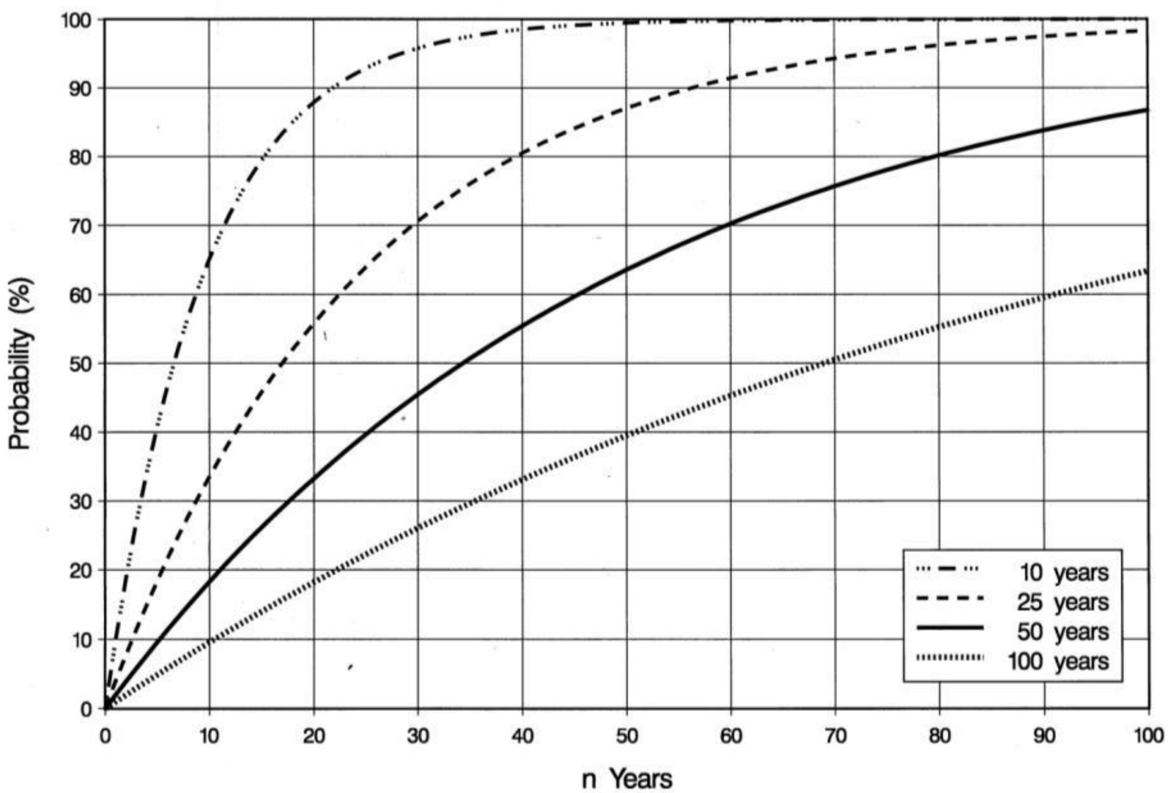

Figure 4-3. Probability of 10-, 25-, 50-, and 100-year waves return period to occur in the next 100 years.

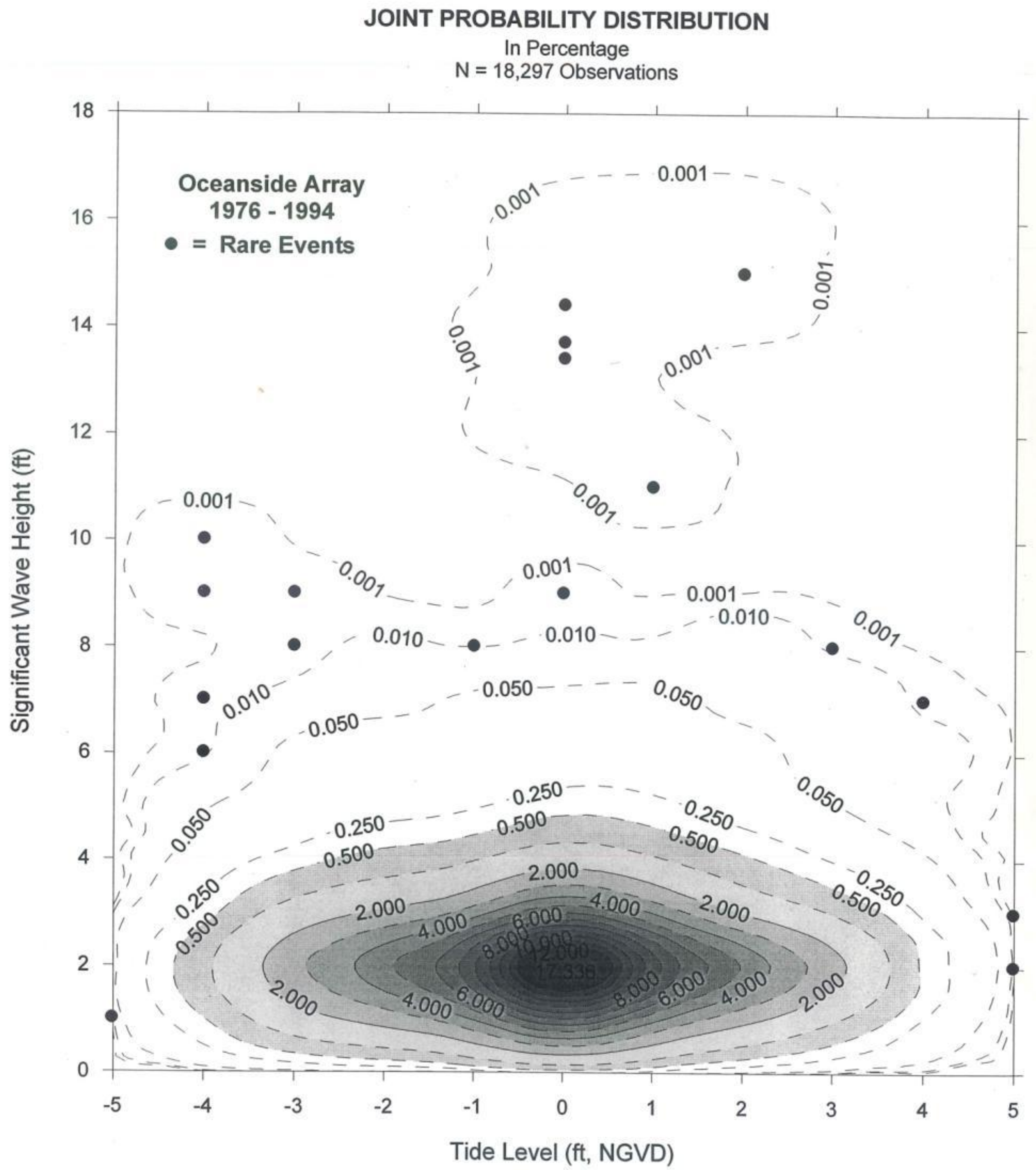

Figure 4-4. Joint Probability distribution between significant wave height and tide level. From Elwany and Flick (1999).

5.0 CONCLUSIONS

The objective of this report is to provide information related to sea level rise vulnerability, structural integrity, and adaptation capacity of the Lease Premises and the facilities therein. In particular, we summarize the present knowledge of MSLR using the latest state and federal agency guidelines, especially OPC (2018). We also evaluate the current SONGS revetment and walkway exposure and vulnerability to waves and high water level events by gauging their present condition. We review the revetment stability by comparing the weight of the rocks in it to the design weight needed to withstand wave forces for various design waves return periods.

The SONGS Revetment provides protection to walkway and SONGS seawall. The walkway enables safe lateral access for beach users, and the seawall provides protection for all the structures located east of it and for the ISFSI and ISFSI security building. Based on the quarterly groundwater monitoring program, according to the OPC SLR projections for Medium-High Risk Aversion and H++ scenarios, the undergroundwater elevation in 2050 will be, respectively, 1.35 ft and 0.55 ft lower than the bottom elevation of the ISFSI. The thickness of the ISFSI foundation is about 3 ft.

Our main conclusions are:

1. The updated OPC (2018) probability-based on MSLR scenario ranges from 2000 to 2050 are essentially the same as the previous projections presented in Elwany et al. (2016, 2017), except for a new extreme H++ trajectory, which has no probability assigned, except that it is deemed highly unlikely.

2. Observations suggest that the SONGS revetment is in good condition, with rock gradation within acceptable limits, the rocks interlock with others, and there is currently no obvious significant damage.

3. Revetment stability analysis indicates that the rocks are of sufficient size and weight to withstand at least the median expected combined design wave height and maximum sea level expected between now and 2050.

4. The Stability of SONGS revetment depends on the condition of the San Onofre Beach and the underlying geology. The presence of a sand beach provide protection to the revetment from toe scouring and cause the waves to break farther away from the revetment.

5. Beach Profiles surveys from 1964 to present, with gaps, document the complexity and the temporal changes of the beach widths and beach profiles at San Onofre Beach. Figures 3-16 and 3-17 and Table 3-7 describe the nature of the changes of San Onofre Beach width over decades.

6. The beach profile surveys, and photography programs sponsored by SCE since 1964 have provided valuable information and understanding of the response of the beach process at San Onofre to beach filling and the construction of stabilizing structures. This insight will be valuable as sea level rise accelerates in the future.

7. Wave overtopping and walkway flooding will occur when high wave events coincide with extreme water levels due to the relatively low elevation of the walkway at 14 ft, NGVD. However, occasional flooding is not likely to impact lateral public beach access since this will be limited during storms in any case. Furthermore, flood waters will drain from the walkway after each event.

8. Adapting sound monitoring and maintenance programs for the cross-sections of the revetment at various locations and especially before and after large wave storms along with monitoring San Onofre Beach, at north and south of SONGS, will maintain and increase the adaptive capacity of the Lease Premises and the facilities therein as stated in Section 3.9.

6.0 REFERENCES

Ahrens J. P., 1981a. *Irregular Wave Runup pn Smooth Slopes.* Coastal Engineering Technical Aid No. 81-17. USACE, 26 pp.

Ahrens J. P., 1981b. *Design of Riprap Revetments for Protection Against Wave Attack.* Technical Paper No. 81-5. USACE, 31 pp.

Bedsworth, L., D. Cayan, G. Franco, L. Fisher, and S. Ziaja, 2018. *Statewide Summary Report, California's Fourth Climate Change Assessment*, California Governor's Office of Planning and Research, Scripps Institution of Oceanography, California Energy Commission, and California Public Utilities Commission, Publication Number SUM-CCCA4-2018-013, 133 pp.

British Columbia Ministry of Environment, Lands and Parks (BCMELP), 2000. *Riprap Design and Construction Guide.* Public Safety Section Water Management Branch, 12 pp.

California Coastal Commission, 2015, updated 2018. *California Coastal Commission Sea Level Rise Policy Guidance, Interpretive Guidelines for Addressing Sea Level Rise in Local Coastal Programs and Coastal Development Permits,* California Coastal Commission, San Francisco, CA, 307 pp.

Chadwick, B., P. F. Wang, M. Brand, R. Flick, A. Young, W. O'Reilly, P. Bromirski, W. Crampton, R. Guza, J. Helly, T. Nishikawa, S. Boyce, M. Landon, M. Martinez, I. Canner, and B. Leslie, 2014. *A Methodology for Assessing the Impact of Sea Level Rise on Representative Military Installations in the Southwestern United States*, SPAWAR Systems Center Pacific, in Collaboration with TerraCosta Consulting Group, University of California San Diego, San Diego State University, U.S. Geological Survey, U.S. Army Corps of Engineers, and Moffatt & Nichol, Final Report submitted to the Strategic Environmental Research and Development Program (SERDP), 680 pp.

Coastal Environments, 2000. *SONGS Unit 1 Deconstruction Marine Impacts Study, Phase I.* Unpublished report submitted to Southern California Edison Company, 24 January 2000, CE Ref. No. 2000-03, 44 pp. plus 2 appendices.

Coastal Environments Inc., 2020.2017-2019 Beach Profile Surveys at San Onofre. Report Submitted to Southern California Edison, Rosemead, CA 91770, 9 March 2020, CE Ref No. 20-03. 41 pp. and 6 Appendices.

DeConto, R., and D. Pollard, 2016. Contribution of Antarctica to past and future sea level rise. *Nature* 531, 591-597.

Elwany, H, R Flick and S. Aijaz, 1994. 1993 Beach Profile Surveys at San Onofre, Final Report. Submitted to Southern California Edison, Rosemead, C A 91770, CE Ref. No. 94-07.32 pp. and 2 Appendices.

Elwany, H., and R. E. Flick, 1999. *Coastal and Oceanographic Conditions in the Vicinity of the Proposed Manchester Resort Development Oceanside, California.* Coastal Environments Reference No. 99-03, prepared for Manchester Resort, 1 Market Place, San Diego, CA, 61 pp. and 4 Appendices.

Elwany, H., R. E. Flick, and A.D. Young, 2016. *Coastal Analysis for End-State Planning of San Onofre Nuclear Generating Station, Phase 1*, Coastal Environments Reference No. 16-26, prepared for Southern California Edison Company, Rosemead, CA, 151 pp.

Elwany, H., R. E. Flick, and A.P. Young, 2017. *Coastal Processes Analysis at San Onofre Nuclear Generating Station, Phase 2,* Coastal Environments Reference No. 17-08, prepared for Southern California Edison, 160 pp.

Flick, R.E., and J.R. Wanetick, 1989. *San Onofre Beach Study*. Unpublished report submitted to Southern California Edison Co., Rosemead, CA, October 1989, SIO Ref. No 89-20. 26 pp. and 25 figures.

Flick, R. E., 1998. Comparison of California Tides, Storm Surges, and Sea Level During the El Niño Winters of 1982-83 and 1997-98, *Shore & Beach*, 66(3), 7-11.

Flick, R. E., 2016. California tides, sea level, and waves – Winter 2015-16, *Shore & Beach*, 84(2), 25-30.

Flick, R. E., K. Knuuti, and S. K. Gill, 2013. Matching Mean Sea Level Rise Projections to Local Elevation Datums, *J. Waterway, Port, Coastal and Ocean Eng*., Amer. Soc. Civil Engineers, 139(2), 142-146.

Griggs, G., J. Árvai, D. Cayan, R. DeConto, J. Fox, H. A. Fricker, R. E. Kopp, C. Tebaldi, and E. A. Whiteman, 2017. *Rising Seas in California, An Update on Sea Level Rise Science* (California Ocean Protection Council Science Advisory Team Working Group), 71 pp.

Hall, J. A., S. Gill, J. Obeysekera, W. Sweet, K. Knuuti, and J. Marburger, 2016. *Regional Sea Level Scenarios for Coastal Risk Management: Managing the Uncertainty of Future Sea Level Change and Extreme Water Levels for Department of Defense Coastal Sites Worldwide.* U.S. Department of Defense, Strategic Environmental Research and Development Program, 224 pp.

Hedges, T.S., Reis, M.T., 1998. *Random wave overtopping of simple seawalls: a new regression model*. Water, Maritime and Energy Journal, 130(1), pp. 1-10.

Holland, K. T., and R. A. Holman, 1993. *The statistical distribution of swash maxima on natural beaches*. J. Geophys. Res.,87, 10,271-10, 278.

Hu, K., 2000. High-Resolution Finite Volume Methods for Hydraulic Flow Modelling.

Manchester, U.K.: Centre for Mathematical Modelling and Flow Analysis, Manchester Metropolitan University, Doctoral thesis, 194 pp.

Hunt, I. A., 1959. *Design of Seawalls and Breakwaters*. J. Waterways and Harbors Div., ASCE, Vol. 85, No. WW3.

Intergovernmental Panel on Climate Change, 2013. *Climate Change 2013: The Physical Science Basis, Contribution of Working Group I to the Fifth Assessment Report of the Intergovernmental Panel on Climate Change*, Cambridge University Press, Cambridge, United Kingdom and New York, NY, 1535 pp.

Kikkawa, H., Shi-igai, H. and Kono, T., 1968. *Fundamental Study of Wave Over-Topping on Levees.* Journal of Coastal Engineering in Japan, 11, 107-115.

Kopp, R. E., R. M. Horton, C. M. Little, J. X. Mitrovica, M. Oppenheimer, D.J. Rasmussen, B. H. Strauss, and C. Tebaldi, 2014. Probabilistic 21st and 22nd century sea level projections at a global network of tide-gauge sites. *Earth's Future*, 2, 383-406.

National Research Council, 2012. *Sea Level Rise for the Coasts of California, Oregon, and Washington: Past, Present, and Future*, Committee on Sea Level Rise in California, Oregon, and Washington. National Academies Press, Washington, DC. 250 pp.

Ocean Protection Council, 2018. *State of California Sea Level Rise Guidance, 2018 Update* (California Natural Resources Agency Ocean Protection Council), 84 pp.

Owen, M.W., 1980. *Design of Seawalls Allowing for Wave Overtopping*. Report. EX 924, Hydraulics Research Station, Wallingford, UK.

Raubenheimer, B., R.T. Guza, Steve Elgar, and N. Kobayashi, 1995. *Swash on a gently sloping beach*, J. Geophys. Res., 100, 8751-8760.

Reis, M. T., Hu, K., Hedges, T. S., and Mase, H., 2008. *A comparison of empirical, semiempirical, and numerical wave overtopping models*. J. Coastal Res., 24(2A), 250–262.

Ruggiero, Peter & Holman, Robert & Beach, R., 2004. *Wave runup on a high-energy dissipative beach*. Journal of Geophysical Research C: Oceans. 109. 10.1029/2003JC002160.

Stockdon, H. F., Holman, R. A., Howd, P. A., and Sallenger, A. H., 2006. *Empirical parameterization of setup, swash, and runup,* Coastal Engineering, 53, 573–588.

Thornton, E. B. and Guza, R. T., 1982. *Energy Saturation and Phase Speeds Measured on a Natural Beach*. Journal of Geophysical Research, 87(C12), 9499-9508.

Thornton, E. B. and Guza, R. T., 1983. *Transformation of Wave Height Distribution*. Journal of Geophysical Research, 88 (C10), 5925-5938.

USACOE.1984. Shore Protection Manual. Waterways Experiment Station, Coastal Engineering Research Center, Vicksburg, MS, 2 vols.

USACOE, 1988. *Historic Wave and Sea Level Data Report: San Diego Region*. Coast of California Storm and Tidal Wave Study, Reference No. 88-6.

USACOE, 1994a. *Hydraulic Design of Flood Control Channels*. Department of the Army. CECW-EH-D, Engineer Manual 1110-2-1601.

USACOE, 1994b. *Shore Protection Manual, Volume II.* Department of the Army. Coastal Engineering Research Center.

USACE, 1995. *Design of Revetments, Seawalls and Bulkheads*. Department of the Army. Coastal Engineering Manual, Engineer Manual 1110-2-1614.

Van der Meer, J.W. and J.P.F.M. Janssen, 1995. *Wave runup and wave overtopping at dikes*. In: Wave Forces on Inclined and Vertical Wall Structures. ASCE. Ed. N. Kobayashi and Z. Demirbilek. Ch. 1, p. 1-27.

Young, A.P., R. E. Flick, T.W. Gallien, S. N. Giddings, R.T. Guza, M. Harvey, L. Lenain, B.C. Ludka, W. K. Melville, and W. C. O'Reilly, 2018. Southern California coastal response to the 2015-2016 El Niño, *J. Geophys. Res: Earth Surface,* 123.

Zetler, B.D. and R. E. Flick, 1985. Predicted Extreme High Tides for Mixed-Tide Regimes, *J. Phys. Oceanog*., 15(3), 357-359.

APPENDIX A

DEM AND CROSS SECTION LOCATIONS ALONG SONGS REVETMENT

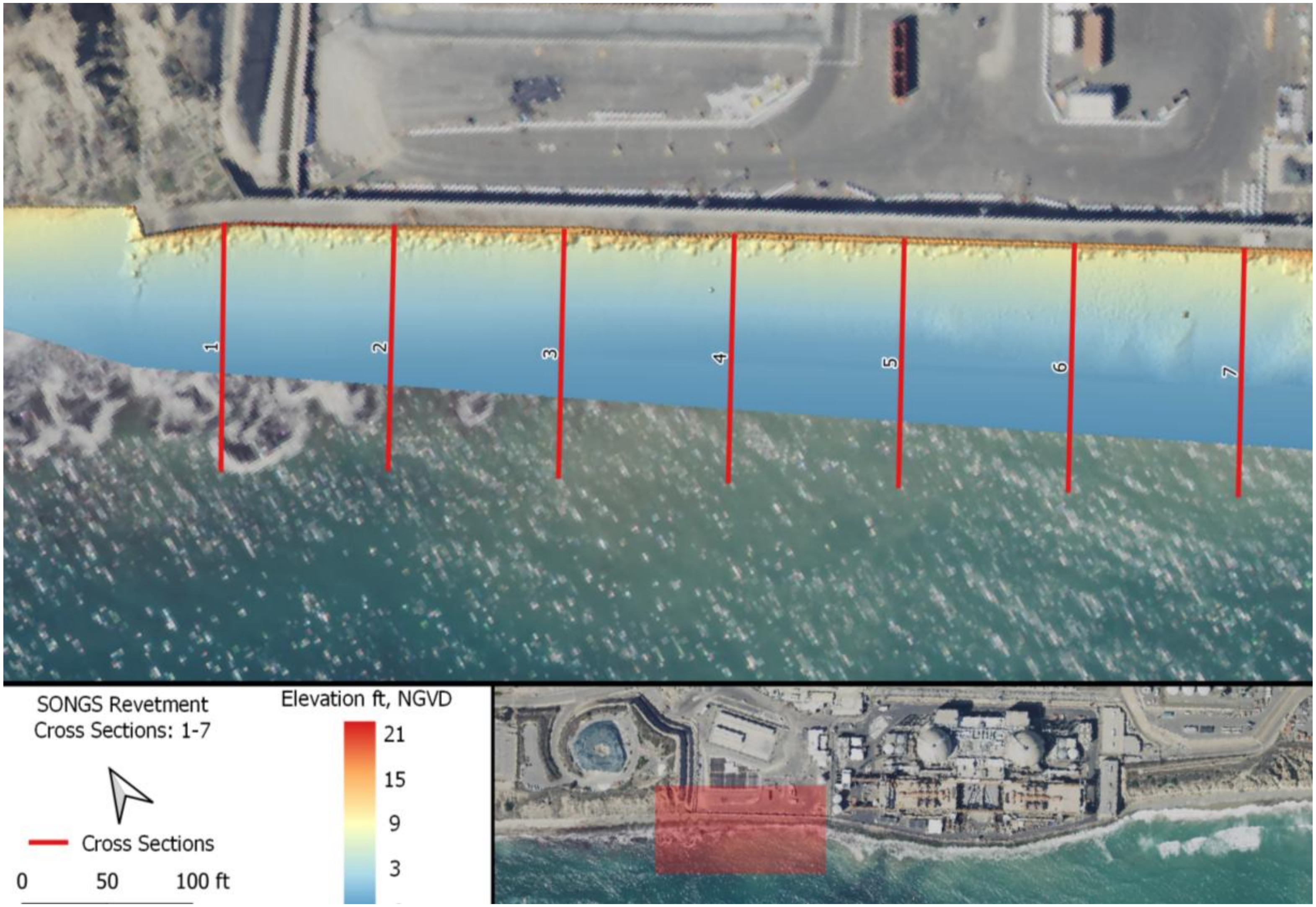

Figure A-1. Cross section ranges 1-7 overlapping the DEM at the northern end of the SONGS revetment on 5 March 2020.

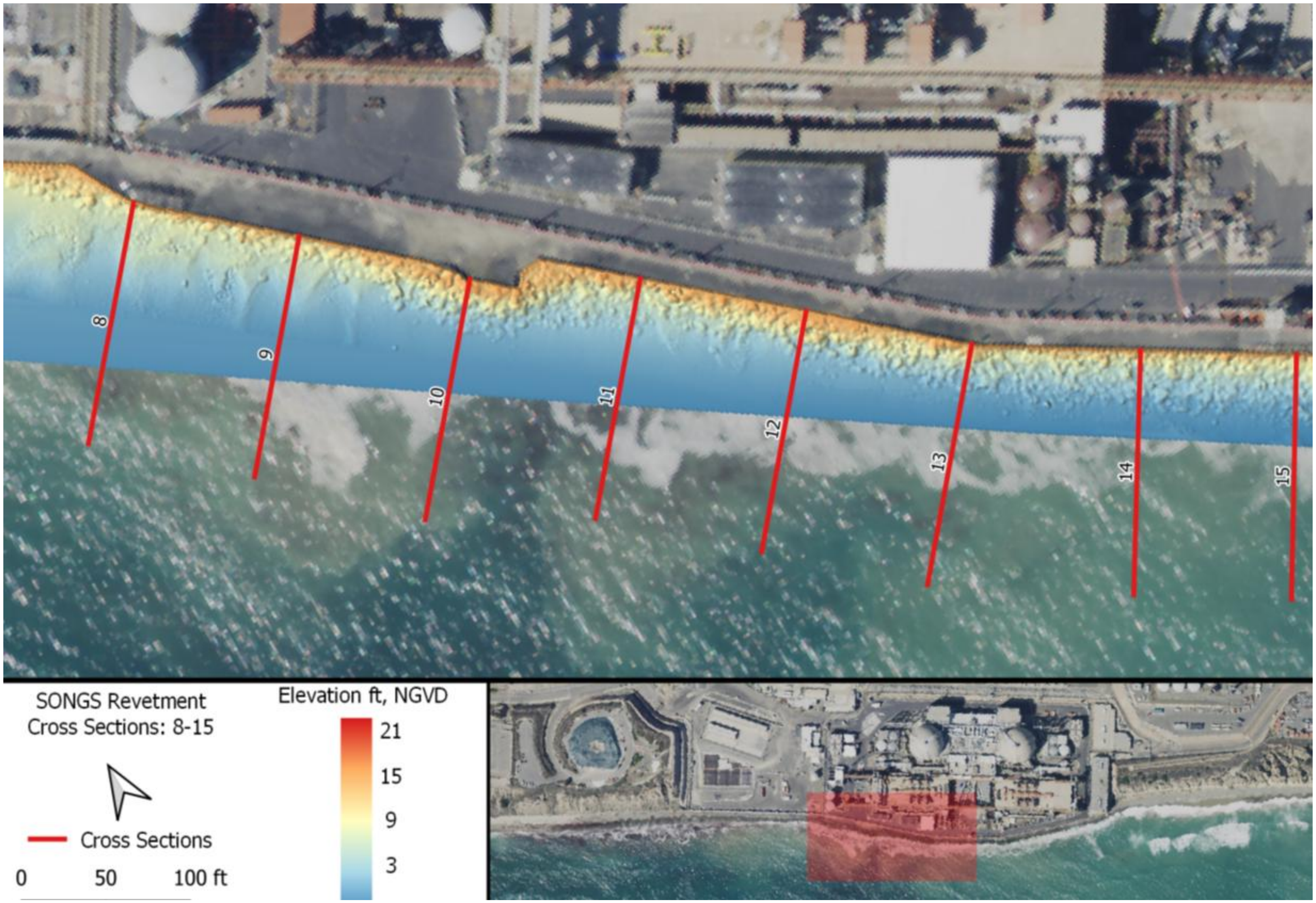

Figure A-2. Cross section ranges 8-15 overlapping the DEM at the middle of the SONGS revetment on 5 March 2020.

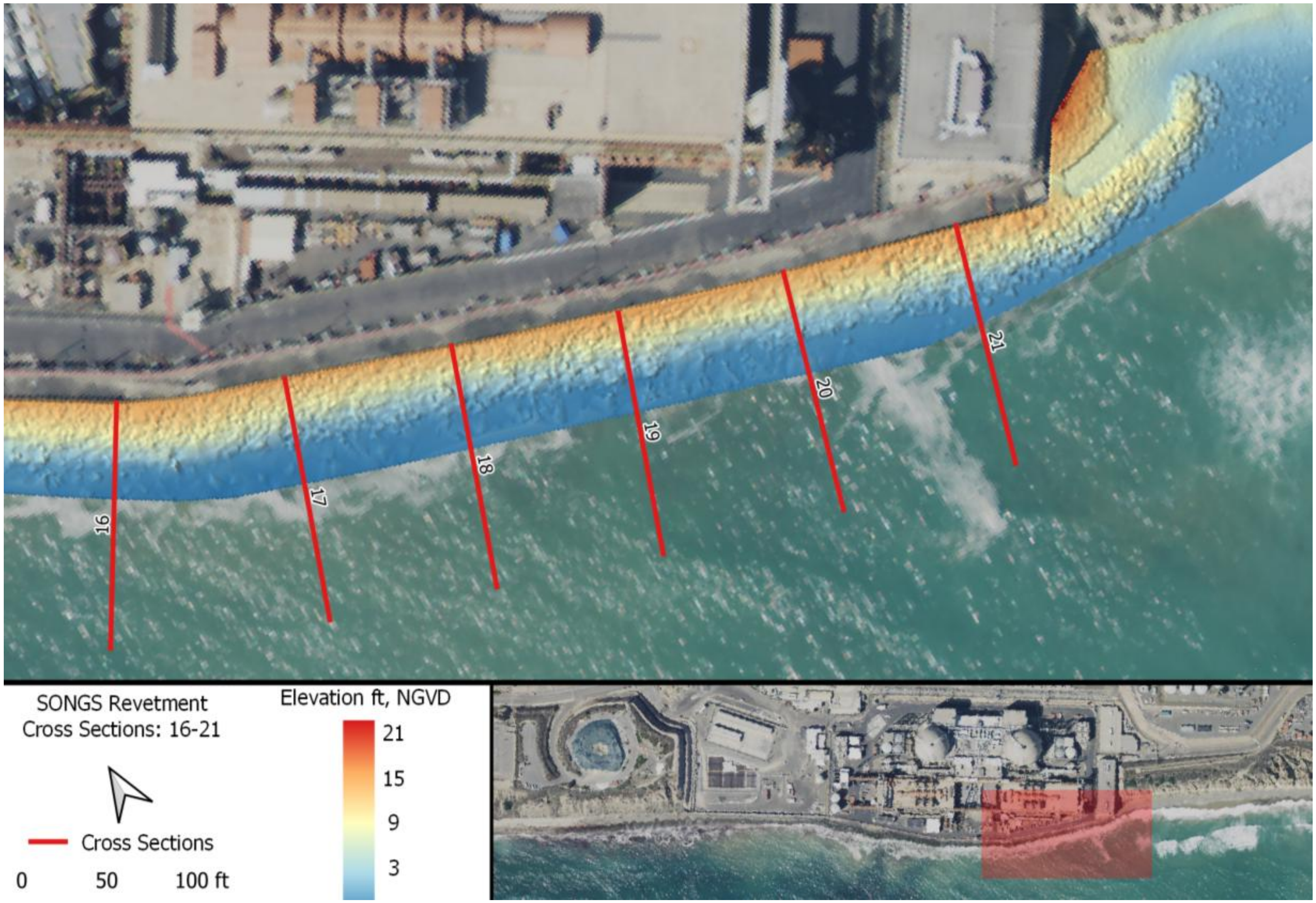

Figure A-3. Cross section ranges 16-21 overlapping the DEM at the southern end of the SONGS revetment on 5 March 2020.

APPENDIX B

CROSS SECTION ELEVATIONS OF SONGS REVETMENT

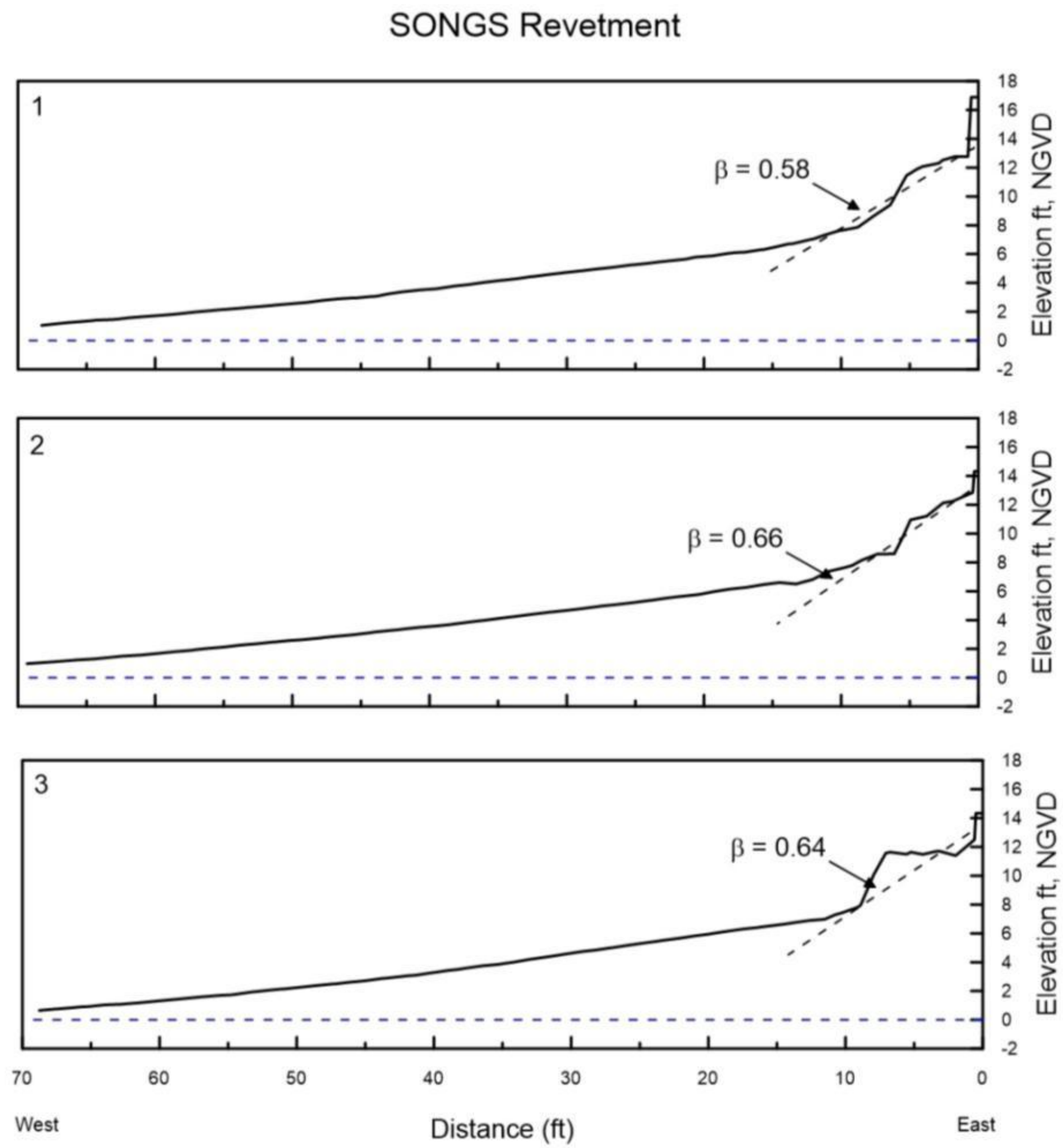

Figure B-1. Cross sections of SONGS revetment along ranges 1-3, surveyed on 5 March 2020. β represents the revetment slope.

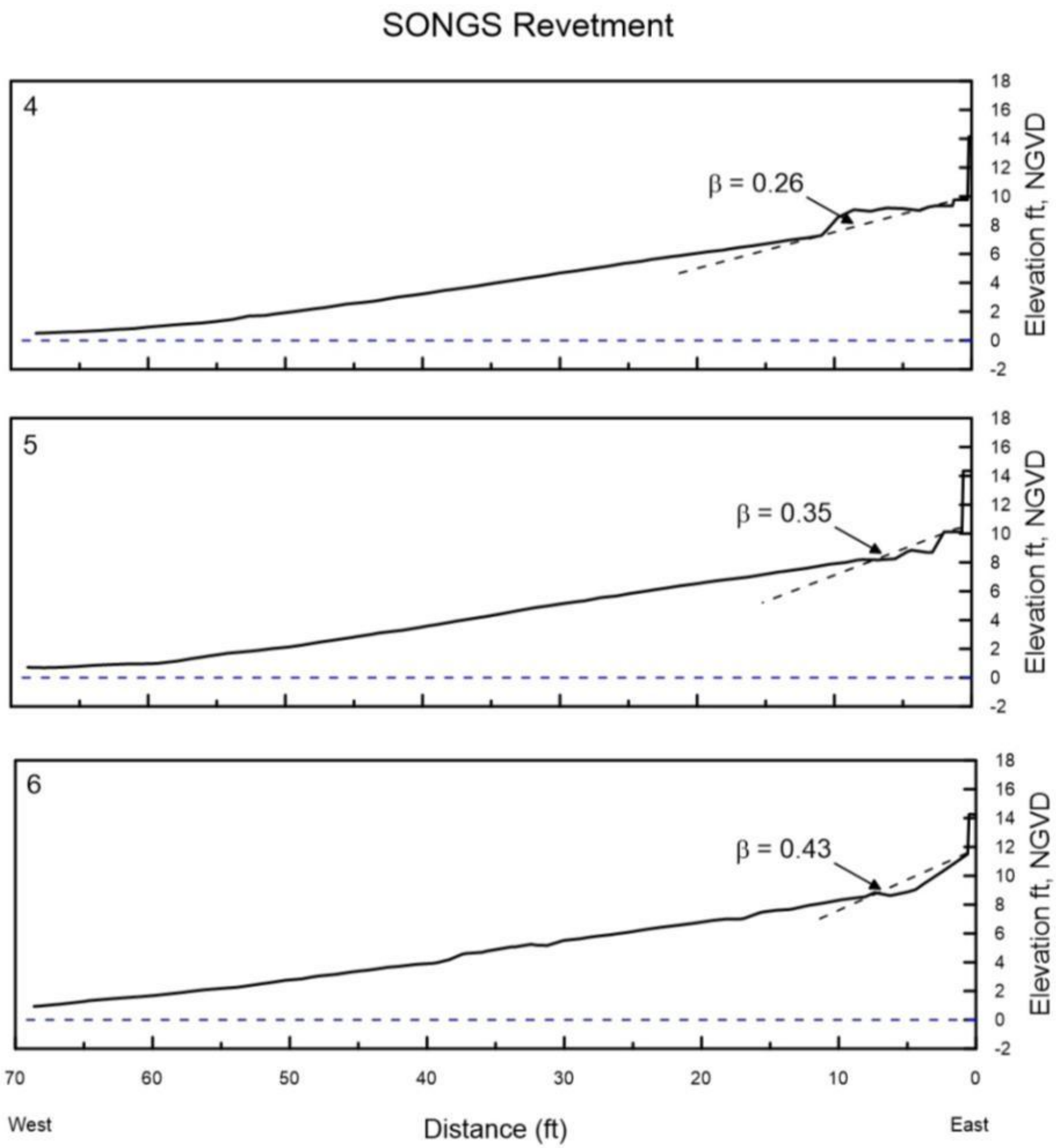

Figure B-2. Cross sections of SONGS revetment along ranges 4-6, surveyed on 5 March 2020. β represents the revetment slope.

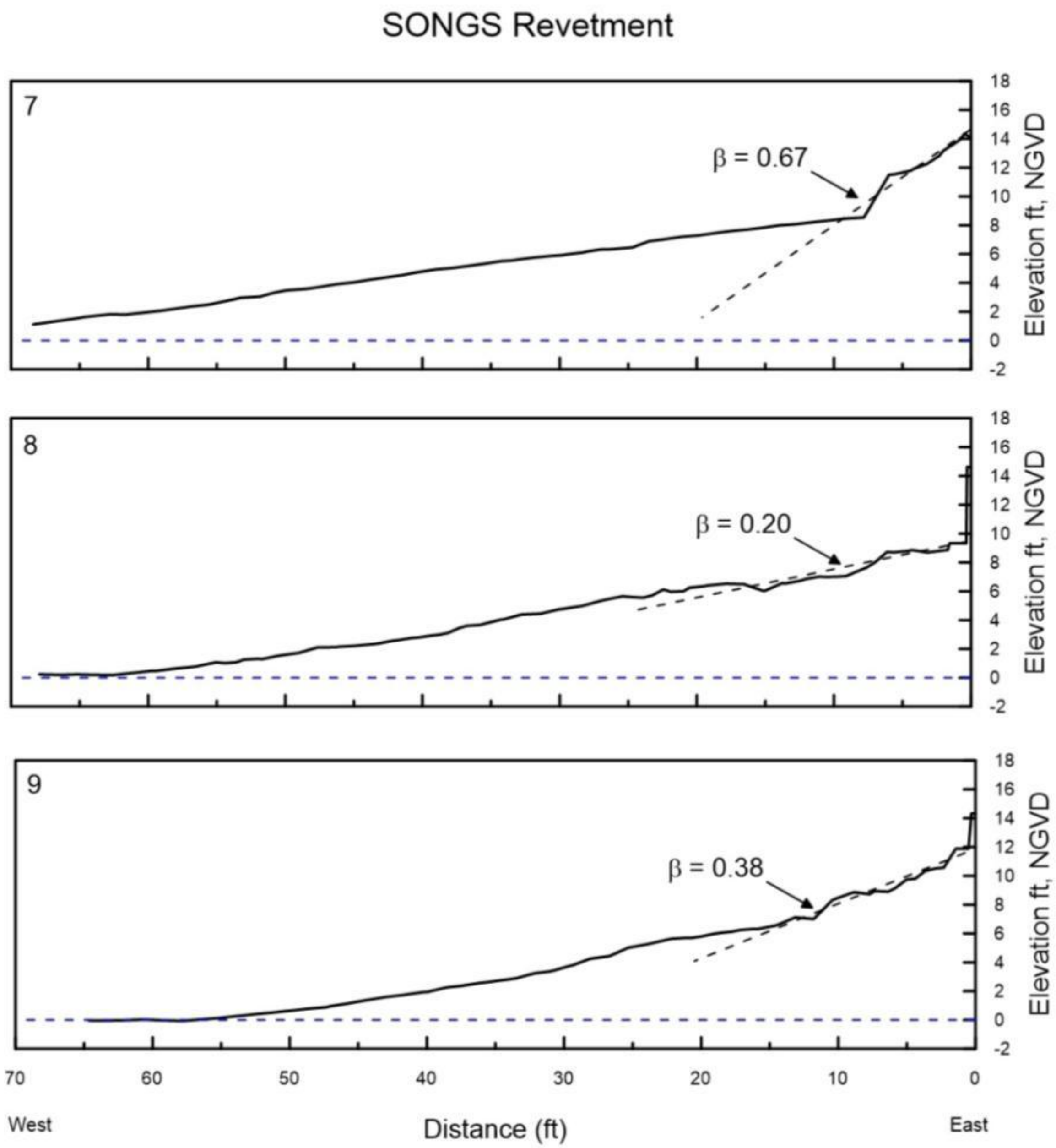

Figure B-3. Cross sections of SONGS revetment along ranges 7-9, surveyed on 5 March 2020. β represents the revetment slope.

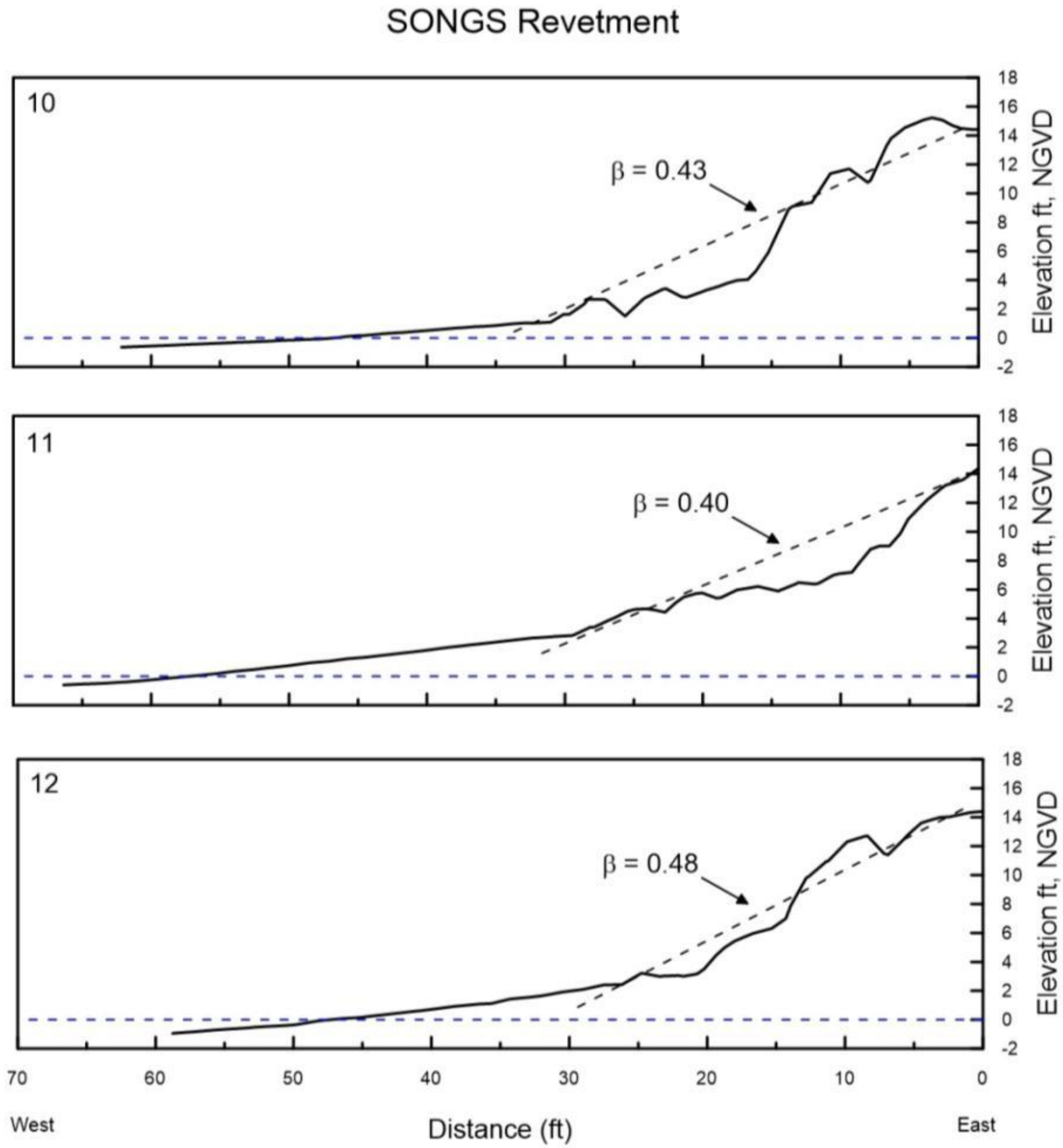

Figure B-4. Cross sections of SONGS revetment along ranges 10-12, surveyed on 5 March 2020. β represents the revetment slope.

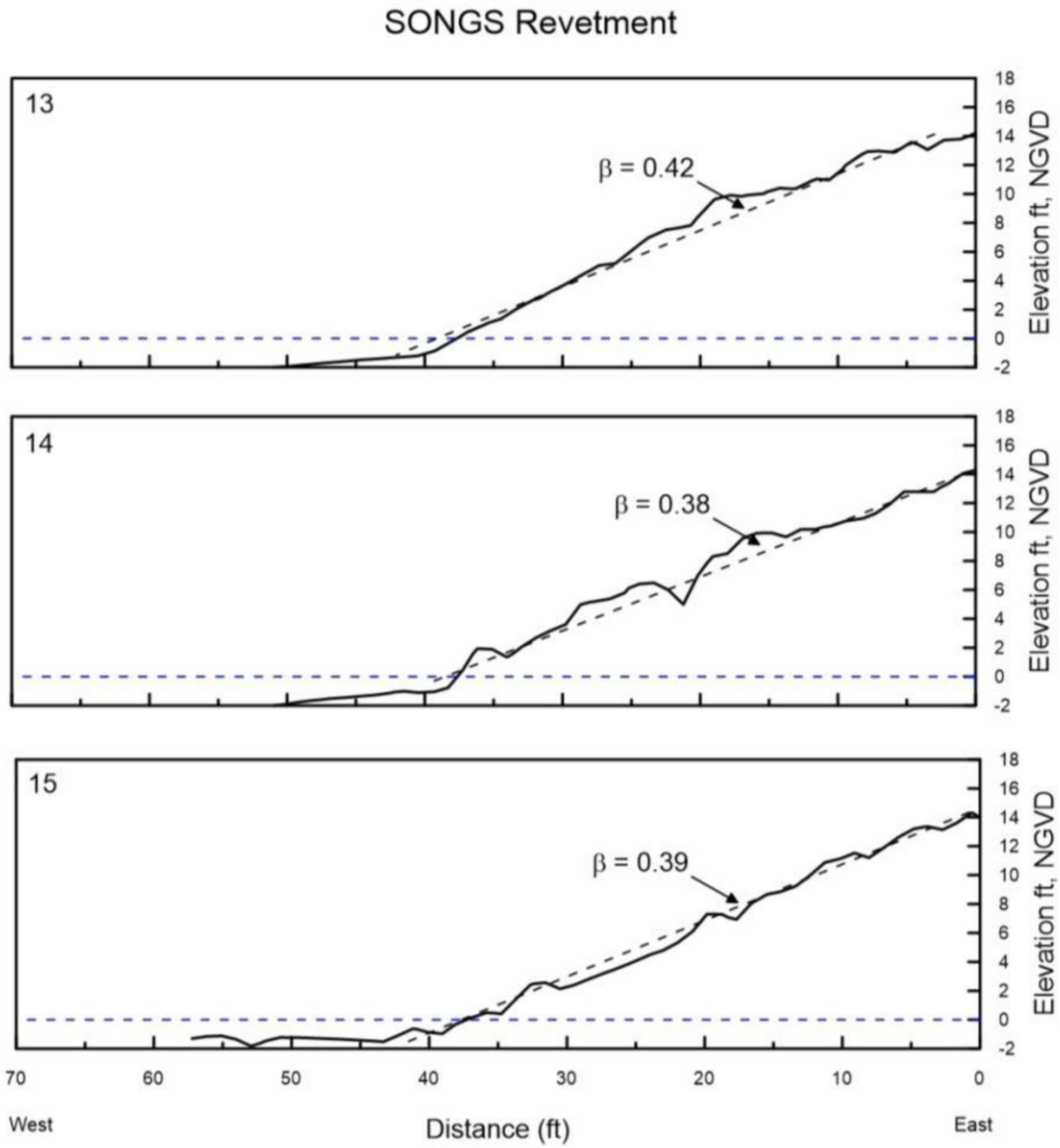

Figure B-5. Cross sections of SONGS revetment along ranges 13-15, surveyed on 5 March 2020. β represents the revetment slope.

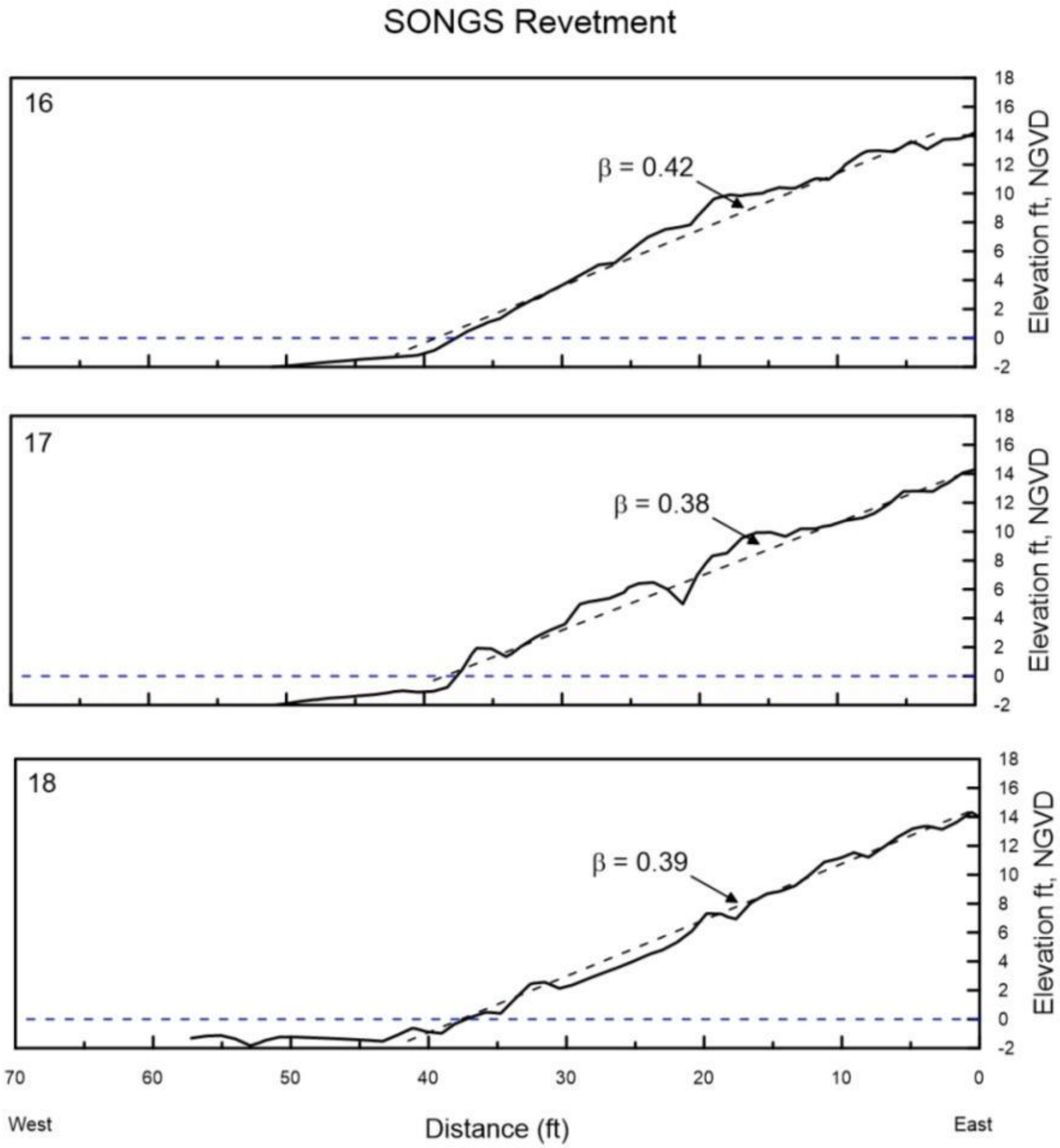

Figure B-6. Cross sections of SONGS revetment along ranges 16-18, surveyed on 5 March 2020. β represents the revetment slope.

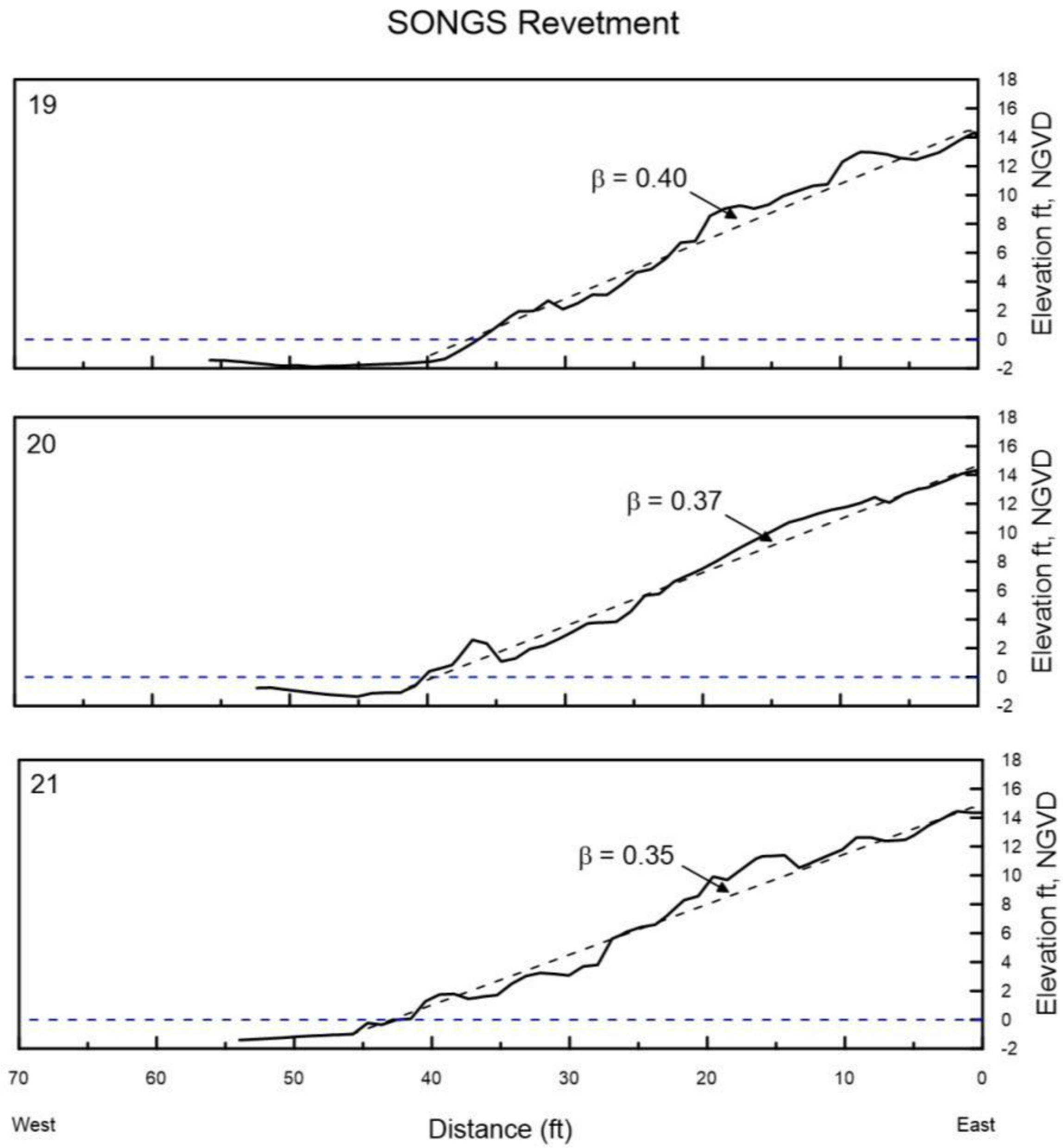

Figure B-7. Cross sections of SONGS revetment along ranges 19-21, surveyed on 5 March 2020. β represents the revetment slope.

APPENDIX C

HISTORICAL AERIAL PHOTOGRAPHS
NORTH AND SOUTH SONGS

Photo C-1. Photograph showing revetment covered by sand and fronted by a wide beach at the northern end of SONGS (10 March 2003).

Photo C-2. Photograph showing waves from north swell attacking SONGS revetment at the southern end of SONGS (10 March 2003).

Photo C-3. Photograph showing waves attacking the revetment and the presence of a sand beach at the northern end of SONGS (26 November 2003).

Photo C-4. Photograph showing waves attacking SONGS revetment at the southern end of SONGS (26 November 2003).

Photo C-5. **Photograph showing revetment covered by sand and fronted by a wide beach at the northern end of SONGS (2 August 2006).**

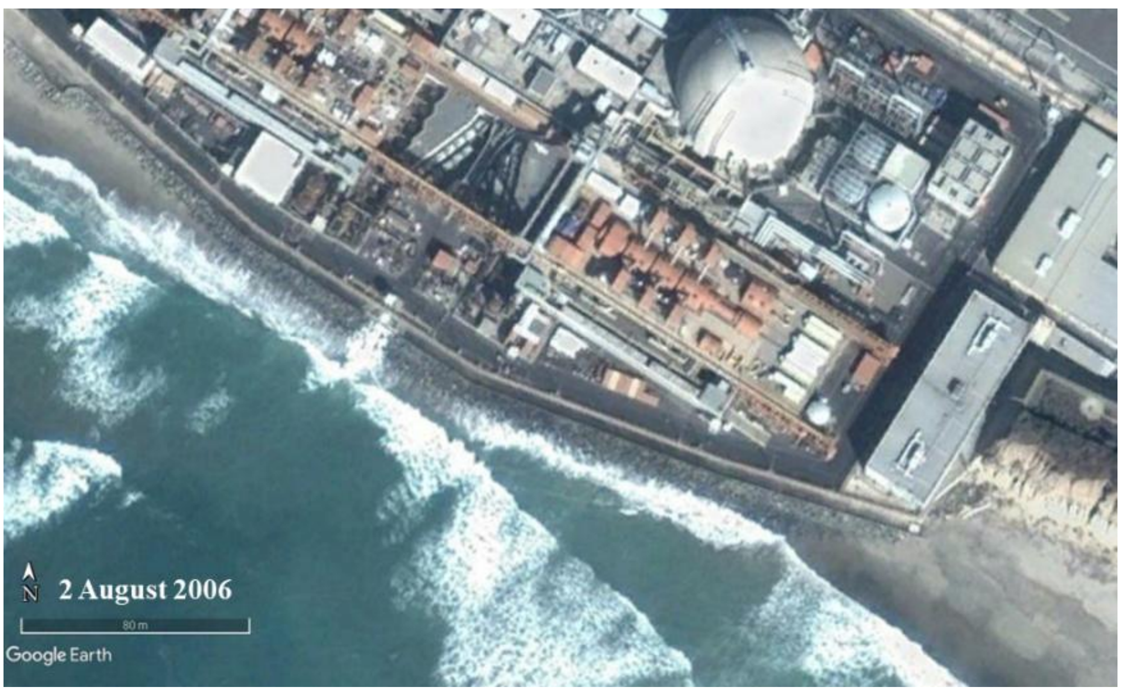

Photo C-6. **Photograph showing waves from north swell attacking SONGS revetment at the southern end of SONGS (2 August 2006).**

Photo C-7. **Photograph showing revetment covered by sand and fronted by a wide beach at the northern end of SONGS (31 January 2006).**

Photo C-8. **Photograph showing waves from north swell attacking SONGS revetment and refracting towards south at the southern end of SONGS (31 January 2006).**

Photo C-9. Photograph showing revetment covered by sand and fronted by a wide beach at the northern end of SONGS (31 January 2008).

Photo C-10. Photograph showing waves attacking SONGS revetment at the southern end of SONGS (31 January 2008).

Photo C-11. Photograph showing revetment covered by sand and fronted by a wide beach at the northern end of SONGS (12 November 2013).

Photo C-12. Photograph showing waves attacking SONGS revetment and refracting towards south at the southern end of SONGS (12 November 2013).

Photo C-13. Photograph showing revetment exposed and fronted by a wide beach at the northern end of SONGS (27 April 2014).

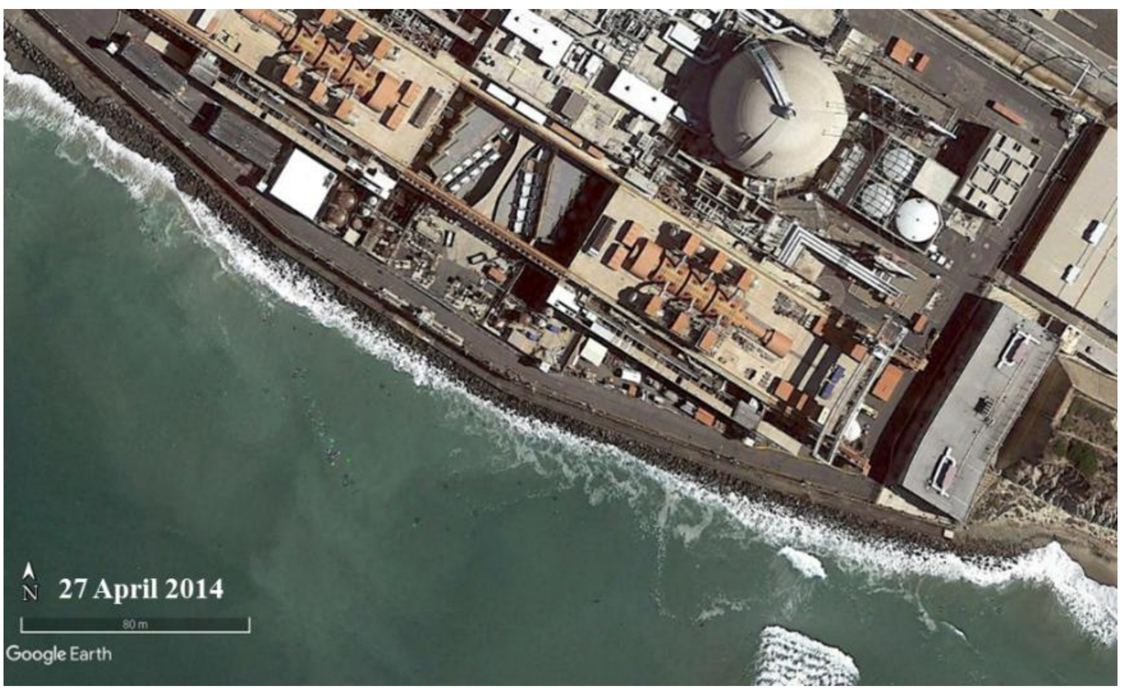

Photo C-14. Photograph showing waves attacking SONGS revetment and refracting towards south at the southern end of SONGS (12 November 2013).

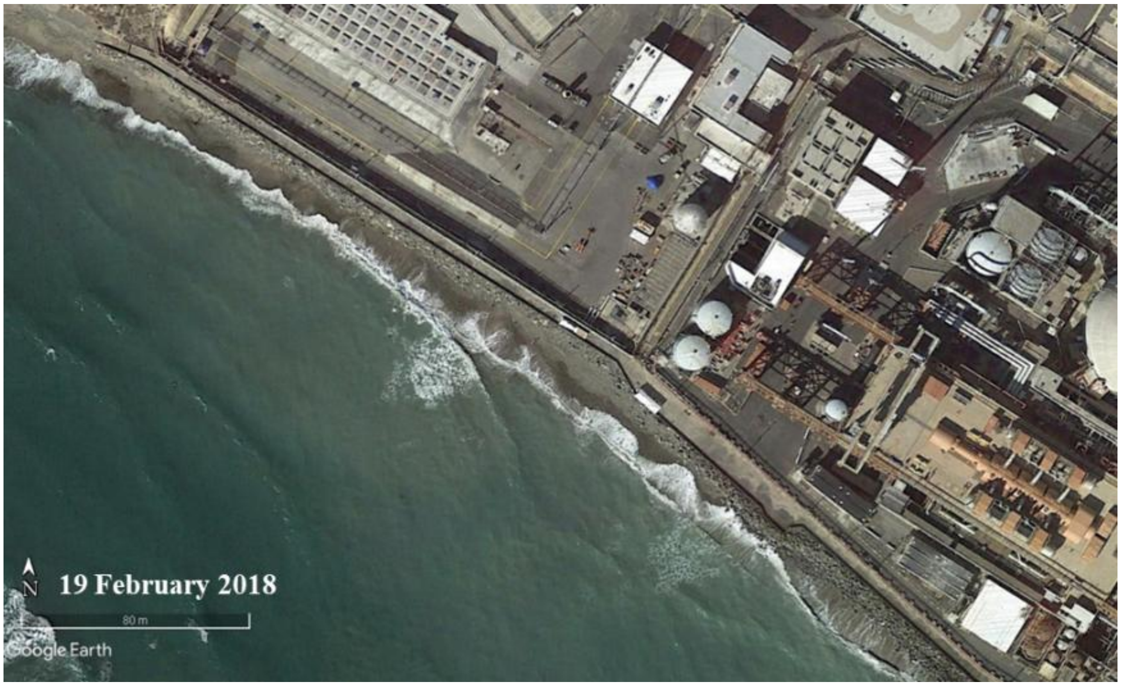

Photo C-15. Photograph showing revetment exposed and fronted by a sand beach at the northern end of SONGS (19 February 2018).

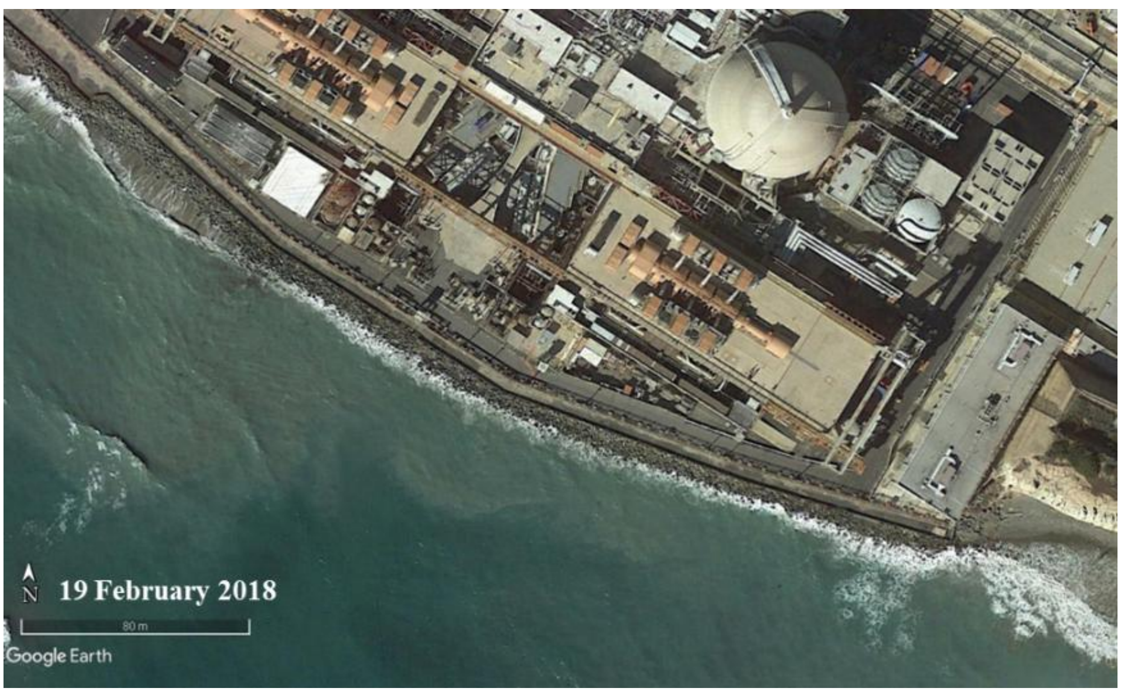

Photo C-16. Photograph showing waves from north swell attacking SONGS revetment and refracting towards south at the southern end of SONGS (19 February 2018).

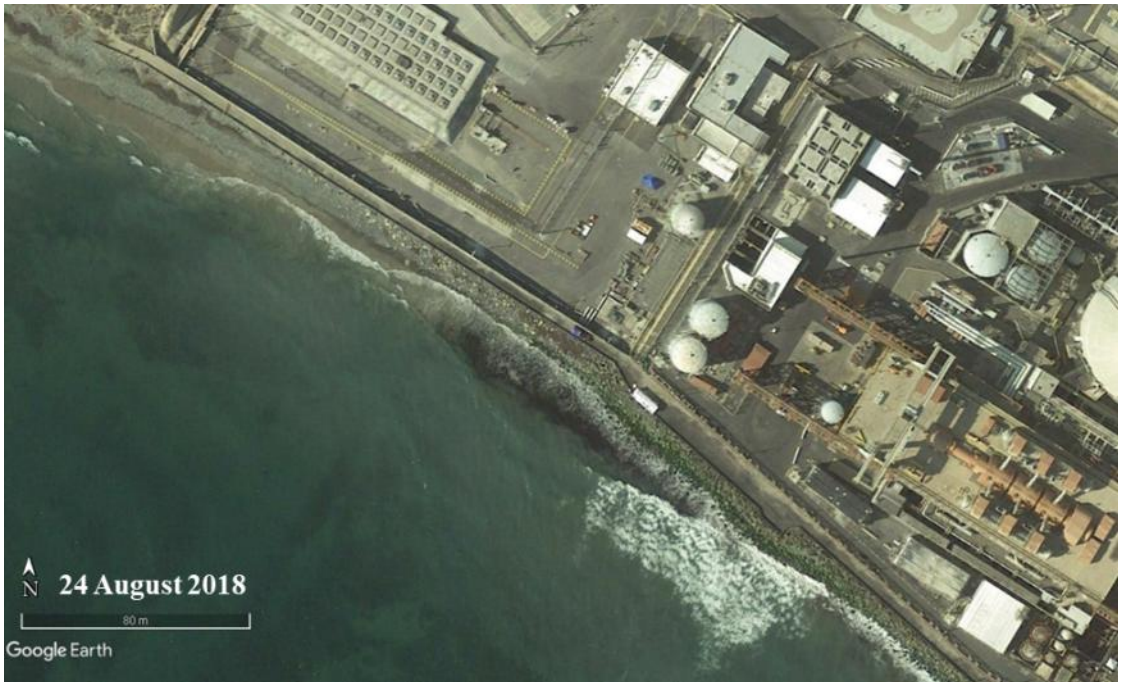

Photo C-17. Photograph showing revetment exposed and fronted by a wide beach at the northern end of SONGS (24 August 2018).

Photo C-18. Photograph showing waves from north swell attacking SONGS revetment and refracting towards south at the southern end of SONGS (24 August 2018).

APPENDIX D

PHOTOGRAPHS FROM SURVEY

Photo D-1. Photograph taken on 5 March 2020, showing range 1 partially covered with sand and cobbles.

Photo D-2. Photograph taken on 5 March 2020, showing range 2 partially covered with sand.

Photo D-3. Photograph taken on 5 March 2020, showing range 3 partially covered with sand.

Photo D-4. Photograph taken on 5 March 2020, showing range 4 mostly covered with sand.

Photo D-5. Photograph taken on 5 March 2020, showing range 5 mostly covered with sand and cobbles.

Photo D-6. Photograph taken on 5 March 2020, showing range 6 mostly covered with sand and cobbles.

Photo D-7. Photograph taken on 5 March 2020, showing range 7 partially covered with sand and cobbles.

Photo D-8. Photograph taken on 5 March 2020, showing range 8 mostly covered with cobbles.

Photo D-9. Photograph taken on 5 March 2020, showing range 9 mostly covered with cobbles.

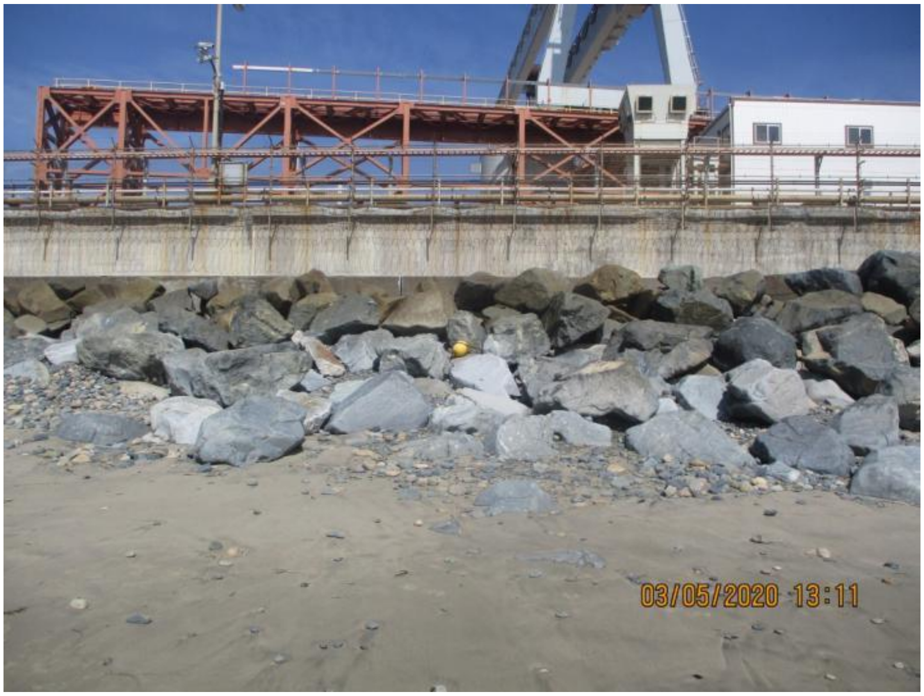

Photo D-10. Photograph taken on 5 March 2020, showing range 10 and the increase in riprap along seawall.

Photo D-11. Photograph taken on 5 March 2020, showing range 11 partially covered with sand and cobbles.

Photo D-12. Photograph taken on 5 March 2020, showing range 12 partially covered with sand and cobbles.

Photo D-13. Photograph taken on 5 March 2020, showing range 13. Seaward base of revetment partially covered with sand.

Photo D-14. Photograph taken on 5 March 2020, showing range 14. Seaward base of revetment partially covered with sand.

Photo D-15. Photograph taken on 5 March 2020, showing range 15 increasing in revetment volume with decreasing beach width.

Photo D-16. Photograph taken on 5 March 2020, showing range 16 with a high volume of rocks and minimal beach width along revetment.

Photo D-17. Photograph taken on 5 March 2020, showing range 17 with a high volume of rocks and minimal beach width along revetment.

Photo D-18. Photograph taken on 5 March 2020, showing range 18 with a high volume of rocks and minimal beach width along revetment.

Photo D-19. Photograph taken on 5 March 2020, showing range 19 with a high volume of rocks and minimal beach width along revetment.

Photo D-20. Photograph taken on 5 March 2020, showing range 20 with a high volume of rocks and minimal beach width along revetment.

Photo D-21. Photograph taken on 5 March 2020, showing range 21 with a high volume of rocks along revetment nearing the end of walkway.

Photo D-22. Photograph taken on 5 March 2020, showing the start of southern outcrop at end of walkway with continued high volume of rocks.

Photo D-23. Photograph taken on 5 March 2020, showing the southern outcrop slanting towards bluffs with increasing beach width.

Photo D-24. Photograph taken on 5 March 2020, showing the end of southern outcrop. south at the southern end of SONGS (24 August 2018).

APPENDIX E

2017-2019 BEACH PROFILE SURVEYS AT SAN ONOFRE

SAN ONOFRE NUCLEAR GENERATING STATION (SONGS) UNITS 2 & 3 DECOMMISSIONING PROJECT

2017-2019 BEACH PROFILE SURVEYS AT SAN ONOFRE

by

M. Hany S. Elwany, Ph.D.
Reinhard E. Flick, Ph.D.
Frederico Scarelli, Ph.D.

Submitted to:

SOUTHERN CALIFORNIA EDISON
2244 Walnut Grove Avenue
Rosemead, CA 91770

COASTAL ENVIRONMENTS, INC.
2166 Avenida de la Playa, Suite E
La Jolla, CA 92037

17 February 2020
Revised on 09 March 2020
CE Reference No. 20-03

TABLE OF CONTENTS

LIST OF APPENDICES

LIST OF TABLES

LIST OF FIGURES

SAN ONOFRE NUCLEAR GENERATING STATION (SONGS) UNITS 2 & 3 DECOMMISSIONING PROJECT

2017-2019 BEACH PROFILE SURVEYS AT SAN ONOFRE

1.0 INTRODUCTION

This report summarizes the beach profile survey data from the 12 surveys conducted at San Onofre from 2017 through 2019. The goals of this report are to address the recent characteristics of the beach nearby the San Onofre Nuclear Generating Station (SONGS), and to define the short- and long-term erosion and accretion patterns.

This report is submitted in response to Special Provision 14 in the California State Lands Commission's (CLSC) Lease No. PRC 6785.1 for the use, maintenance and decommissioning of existing offshore improvements associated with SONGS. Special Provision 14 provides, in relevant part, that Southern California Edison Co. (SCE), San Diego Gas & Electric Co. (SDG&E), and the City of Riverside (Riverside) collectively as "Lessee," "comply with applicable provisions or standards addressing sea-level rise that may be required or adopted by local, state, or federal agencies related to and affecting the Lease Premises. Lessee shall provide Lessor with an annual summary, to include information identified below, by the anniversary date of each year, beginning March 21, 2020 or a date to be mutually agreed to by Lessee and Lessor's staff. The summary shall include: ...beach profile assessments..."

Recent beach characteristics are defined by the 2017, 2018, and 2019 measurements carried out quarterly. These capture the beach configuration corresponding to the autumn, winter, spring, and summer seasons, as well as continuing erosion or accretion trends. Additionally, in each year, two surveys including the offshore portion of the beach were conducted at San Onofre. The results of each survey have been presented in reports by Coastal Environments, Inc. (CE, 2017, 2018, 2019). Longer-term beach change patterns are characterized by comparing beach widths from these recent surveys to comparable measurements from 1985-1993 sponsored by Southern California Edison (SCE). The earliest directly comparable data were taken in May 1985, just after the sand release of the SONGS Units 2 and 3 laydown pad (Flick and Wanetick, 1989), and from 1990-1993 (Elwany et al., 1994), 2000 (CE, 2000), and 2016 (Elwany et al., 2016).

Data for this study comes from the 12 surveys carried out from March 2017 through October 2019 (Table 1-1). Each survey covered seven profiles (Figure 1-1). Beach profile measurements generally extended to 12 ft below mean sea level (MSL). Two offshore profiles each year extended to 40 ft water depth using a boat-mounted fathometer. Profile elevations are plotted relative to the National Geodetic Vertical Datum 1929 (NGVD), which is 0.44 ft below MSL.

In Section 2 of this report, we present an overview of the data and how it was collected. In Section 3, we then discuss the characteristics of SONGS beach profiles and how these relate to typical Southern California beaches. Wave climate at San Onofre is presented in Section 4.

Beach width changes and shoreline trends are discussed in Sections 5 and 6. In Section 7, we utilized the available historical information to better understand beach width fluctuations over a long time scale and shoreline changes at San Onofre. Our conclusions are detailed in Section 8.

This study documents the complex and temporal changes of the beach widths and profiles in Southern California, especially at San Onofre Beach. Appendix A, B, and C show the beach profiles for 2017, 2018, and 2019, respectively. Appendix D shows the offshore beach profile surveys carried out between 2017 and 2019. Appendix E presents the aerial photographs north and south of SONGS for the period between 1994 and 2014, and Appendix F shows the photographs taken at San Onofre Beach in 2017, 2018, and 2019.

Table 1-1. Surveys at San Onofre, 2017-2019.

Survey Number	Date	Season	Number of Profiles
1	01Mar17	Winter	7
2	19May17	Spring	7
3	16Aug17	Summer	7
4	02Nov17	Autumn	7
5	23Jan18	Winter	7
6	29May18	Spring	7
7	22Aug18	Summer	7
8	18Nov18	Autumn	7
9	04Mar19	Winter	7
10	23Apr19	Spring	7
11	25Jun19	Summer	7
12	14Oct19	Autumn	7

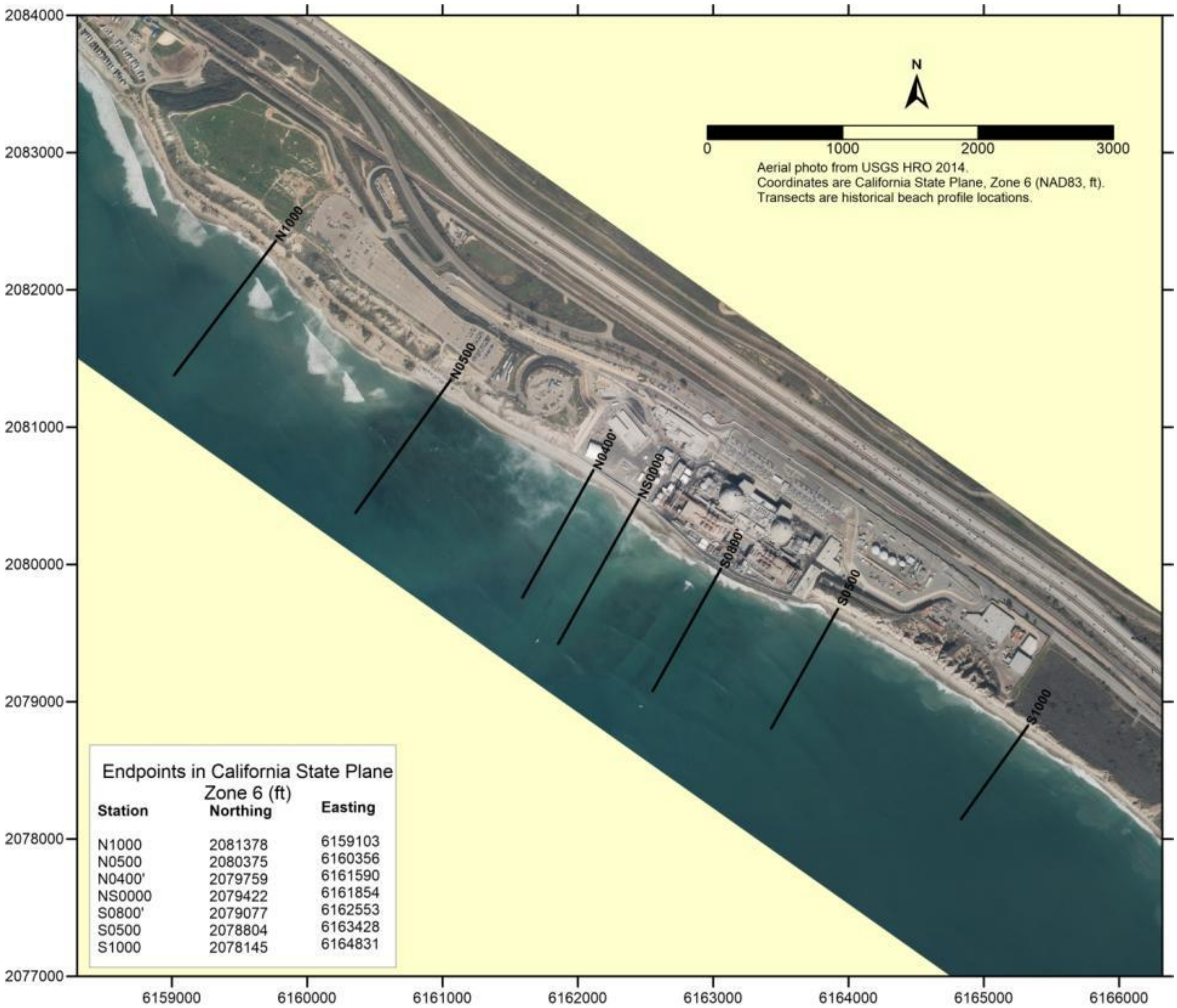

Figure 1-1. Locations of beach profiles surveyed at SONGS.

2.0 SURVEY METHOD

A total station (Sokkia SET-610), data logger (Spectra Precision Ranger), and a prism attached to a 16-ft rod held by a person were used for the beach profile surveys. The procedure using the total station is similar to the standard rod and level technique, but simpler, faster, and more accurate. The rod holder carries a prism target at the top of a fixed-length pole that reflects an infrared beam sent from the total station. The crosshairs in the station telescope are focused on the prism and the instrument measures the slant distance and horizontal and vertical angles to the target. A handheld electronic field book data logger especially designed for the task calculates the relative coordinates and elevation and stores the results. Figure 2-1 illustrates the survey method.

All measurements at a survey line are made relative to the first reading taken on the benchmark at that profile. Benchmarks were placed as close as practical to the edge or face of the sea cliff. Efforts were made to position the benchmarks used for recent surveys (2017 through 2019) at the same location as the benchmarks used for all surveys conducted from 1985 to 1993. This enables us to compare the results of the latest surveys with previous data (Flick and Wanetick, 1989; Waldorf, 1989; Elwany et al., 1992, and 1993). The recent survey lines are oriented perpendicular to the mean shoreline using approximately the same fixed bearings as before.

The offshore portions of the profiles were acquired with a digital acoustic echo sounder operated from a 27-ft shallow-draft survey vessel. A Differential Global Positioning System (DGPS) receiver was used to determine the position of each sounding. To improve the accuracy of each position, differential corrections transmitted in real time from U.S. Coast Guard (USCG) beacons were utilized. All systems were interfaced to a laptop computer using the Hypack survey package.

At each transect, the boat traveled from the offshore limit to the surf zone guided by a DGPS navigation system. Soundings were acquired on a near-continuous basis (approximately four to five per second). Vessel positions were recorded at 1-second intervals and merged with the soundings using Hypack bathymetric survey software. The calibration of the echo sounder was checked at the beginning and end of each survey session using a standard “bar check” procedure. The merged plots from the nearshore and offshore profile surveys are presented in Appendix D.

The horizontal coordinates of the profile starting points were determined by DGPS, and the elevations of these points were determined based on existing benchmarks near SONGS. Figure 2-2 shows these benchmarks, and their coordinates are presented in Table 2-1. Photographs corresponding to these benchmarks and the surveyed transects are shown in Appendix F. The locations of the beach profiles are shown in Figure 1-1. Table 2-2 gives the horizontal coordinates and elevations of the starting points and the alignment (degrees) of each profile.

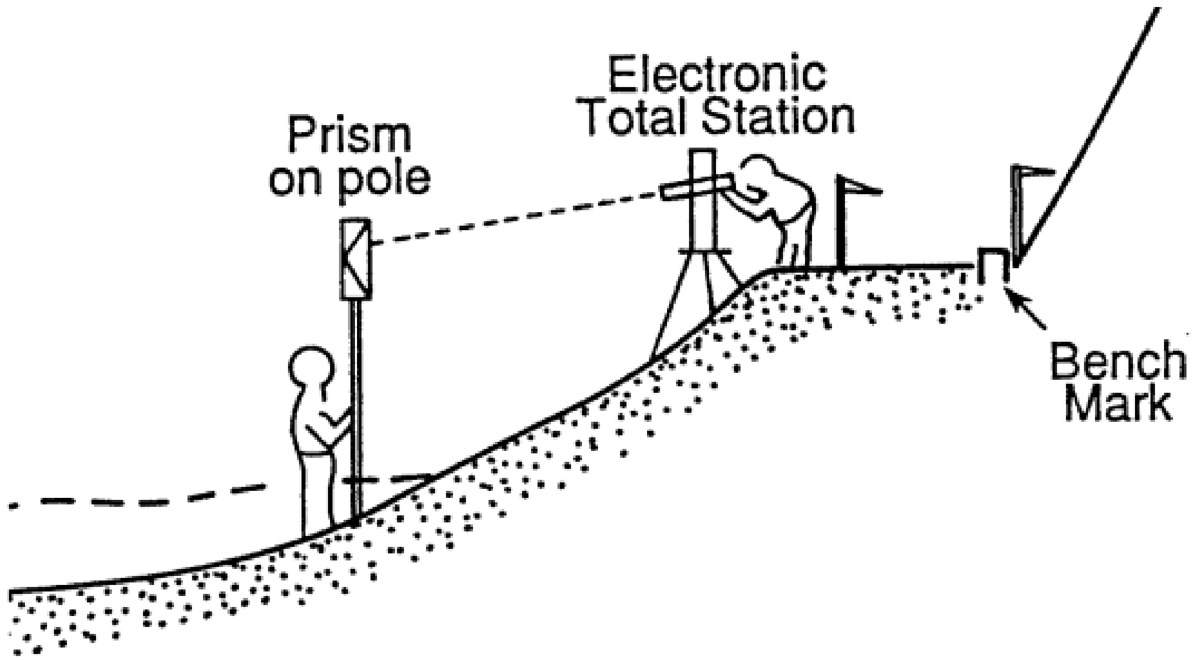

Figure 2-1. Schematic illustration of the beach profile survey method.

Figure 2-2. Locations of benchmarks at SONGS indicated by green triangular symbols (SO1530, 2051611, HV-07, 2051612, and 2051613).

Table 2-1. Locations and elevations of benchmarks.

Station	Easting US Survey Feet	Northing US Survey Feet	Elevation (ft) NGVD
SO1530	6158825.91[a]	2083254.09[a]	17.69
2051611	6161974.95	2080779.78	16.81
2051612	6162911.73	2080065.75	11.23
2051613	6163212.04	2079884.76	11.17
HV-07	6162550.71	2080377.00	11.47

[a] = Horizontal coordinates determined by GPS.

Table 2-2. Range start point coordinates, elevations, and alignments.

Range	California State Plane Coordinates, Zone 6 (ft), NAD 83		Elevation, NGVD (ft)	Magnetic Heading
	Northing	Easting		
N1000	2082359.92	6159761.45	17.69	205
N0500	2081339.99	6161050.00	15.87	203.5
N0400'	2080691.70	6162106.26	14.32	197
NS0000	2080473.91	6162441.66	14.42	197
S0800'	2079969.71	6163054.98	14.33	197
S0500	2079711.68	6163931.78	varies[a]	203
S1000	2078824.56	6165320.87	varies[a]	203.5

[a] = Start point elevations for S0500 and S1000 are not fixed. Unlike the other profiles which start on a fixed structure, these profiles are beginning at the back of the beach, below the cliffs, which varies in elevation from one survey to another.

3.0 BEACH PROFILE CHARACTERISTICS

The beach profiles at San Onofre have much in common with other typical Southern California beaches (Figure 3-1). The characteristics of San Onofre beaches are discussed in detail in Coastal Analysis for End-State Planning of SONGS, Phase 1 (Elwany et al., 2016). A brief description is given below.

The beaches at San Onofre consist of a relatively thin veneer of medium to coarse sand backed by a sea cliff of varying height. In most places, cobble and bedrock underlay the beach sands at various depths. These depths can go from zero, where the sand cover is stripped, to several meters where there is an adequate supply of sand to cover the bedrock or the cobble layer.

The subaerial portion of the beach profile extends from the cliff face (or sea wall) to the mean water line. It is distinguished by a narrow to medium width, relatively flat berm, and a moderately steep beach face slope. The berm height and beach face slope both depend on the sand grain size and the wave climate. The subaerial beach width is defined as the distance from the cliff face (or seawall) to the intersection of the profile with the NGVD elevation plane.

The beach berm may contain one or more storm scarps. These are erosional features resulting from large waves that remove sand from the beach face and transport it offshore. This represents the normal summer to winter erosion sequence that progressively narrows the berm width and flattens the beach slope. The sand moved offshore often forms into one or more bars, generally in depths less than about 10 ft (3 m), but seaward of the low tide terrace. The bars act as reservoirs for the sand that is returned to the shore face during the winter to summer accretion phase, coinciding with milder seasonal wave conditions.

Berm heights at San Onofre average about 10 ft (3 m), and foreshore slopes are about 1:7, vertical to horizontal, or about 8°. Both are fairly uniform longshore. The lack of a winter berm has been common at the sea wall in front of SONGS during the past few years. Lack of sand and occasional high wave activity have resulted in some displacement and settling of the rock riprap, which provides toe protection to the SONGS beach access walkway retaining wall.

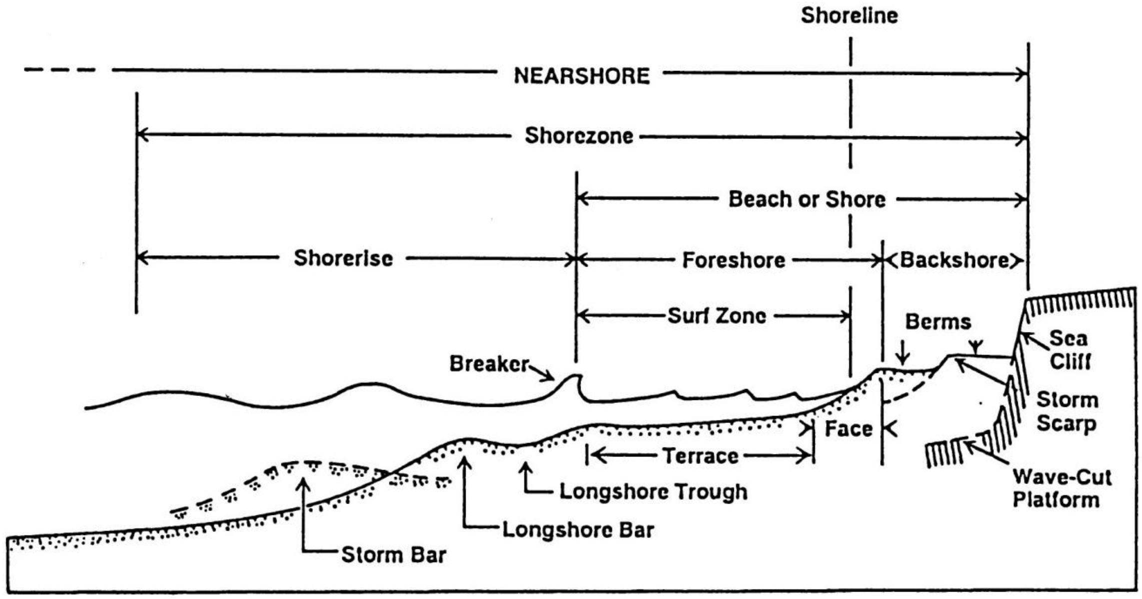

Figure 3-1. Typical Southern California beach profile (Inman, 1980).

4.0 WAVE CHARACTERISTICS

4.1 WAVES

Waves provide the largest source of energy to the coast of California and are a critical influence for sand transport and beach erosion, as well as coastal flooding and damage. This section reviews the relevant properties of waves at San Onofre with an emphasis on SONGS.

4.2 WAVE CLIMATE OVERVIEW

Ocean waves in southern California fall into three main categories (USACE, 1986):

1. Northern Hemisphere Swell: Relatively long waves generated in the North Pacific that propagate into Southern California waters;

2. Southern Hemisphere Swell: Similar waves generated south of the equator during the boreal winter; and

3. Local Seas: Relatively short-period waves generated within the Southern California Bight.

Southern California is sheltered from north Pacific swell[1] by numerous offshore islands and shoals (Figure 4-1), thus greatly complicating the coastal wave climate (Pawka, 1982 and 1983; Crosby et al., 2017). San Onofre and SONGS are located within an area of the Southern California Bight sheltered by Santa Cruz, Santa Rosa, Santa Catalina, and San Clemente islands. Consequently, much of the North Pacific swell wave energy is greatly reduced before reaching the mainland shore. The largest windows from which swell can reach San Onofre are from the south at angles of 155°-231° (relative to true north), and the southwest from 250°-265°. Northern Hemisphere winter storms produce larger waves than those in the summer months. However, the predominant northwest winter swell approach directions (270°-360°) are largely blocked by the California mainland at Point Conception, and the islands (Figure 4-1). Therefore, it is the shorter period seas (< 12 sec) generated by waves inside the Bight having approach angles of about 279°-295° that reach San Onofre.

Summer swells from distant Southern Hemisphere winter storms are frequent, but usually of low amplitude and therefore of little consequence, except for recreational surfing. However, San Onofre is exposed to several windows of Northern Hemisphere swell and waves, most notably from extra-tropical storm activity east of Hawaii with approach directions from 250°-265° (Figure 4-1).

Wave climate within the Southern California Bight varies on annual and inter-decadal time scales. This variation is largely due to the regional effects of El Niño and La Niña events, in which interspersed years-long periods of cooler or warmer Pacific Ocean water temperatures loosely correlate with storm frequency and intensity, and therefore with wave conditions.

[1] Swell is loosely defined as waves generated outside the area and having periods longer than about 12 sec.

Longer-period ocean temperature and atmospheric pressure variations also occur on longer time scales of decades that strengthen or weaken the El Niño-La Niña episodes.

For example, wave heights off California tended to be moderate from the mid-1940s to the mid-1970s when generally cooler and drier climate conditions prevailed. Starting in the late 1970s, a so-called “regime shift” occurred, which brought generally warmer and wetter conditions with more frequent and more intense storms and attendant coastal erosion, flooding, and damage. High-energy winter waves approached the coastline from the west or slightly south of west, and shorter-period swell were produced by hurricanes off Central America. Most notably, the winters of 1982-83, 1988, and 1997-98 had high waves and storm surges that coincided in some cases with extreme high tides, causing hundreds of millions of dollars in damages.

Long-term wave data gathered by the Coastal Data Information Program (CDIP, 1992) at Oceanside and San Clemente were also used here to describe wave conditions at San Onofre for this study. These measurements were made in 36 ft (11 m) water depth using a directional pressure-sensor array over a 16-year period from late 1978 to December 1994 (including some data gaps). Figure 4-2 shows the maximum monthly significant wave height (Hs) derived from the CDIP measurements. This shows that extreme wave conditions in Oceanside, and by extension at San Onofre, vary both seasonally and from year to year. On the seasonal time scale, the largest wave events occur between the months of November and March. In contrast, the months of April to October rarely have maxima exceeding 7 or 8 ft (2.1 to 2.4 m). The largest wave storm was recorded on 18 January 1988, with an Hs of 15.8 ft (4.7 m).

Figure 4-3 shows the histogram of wave period for those waves having Hs > 4 ft (1.2 m). Two distinct peaks at wave periods of 8-10 sec and 14-16 sec are evident. Figure 4-4 shows the relation between wave heights measured at San Onofre and Oceanside during the spring and early summer 2000. The linear relationship of Hs at the two sites is:

$$\text{San Onofre Hs} = 0.76 \text{ Oceanside Hs} + 0.44$$

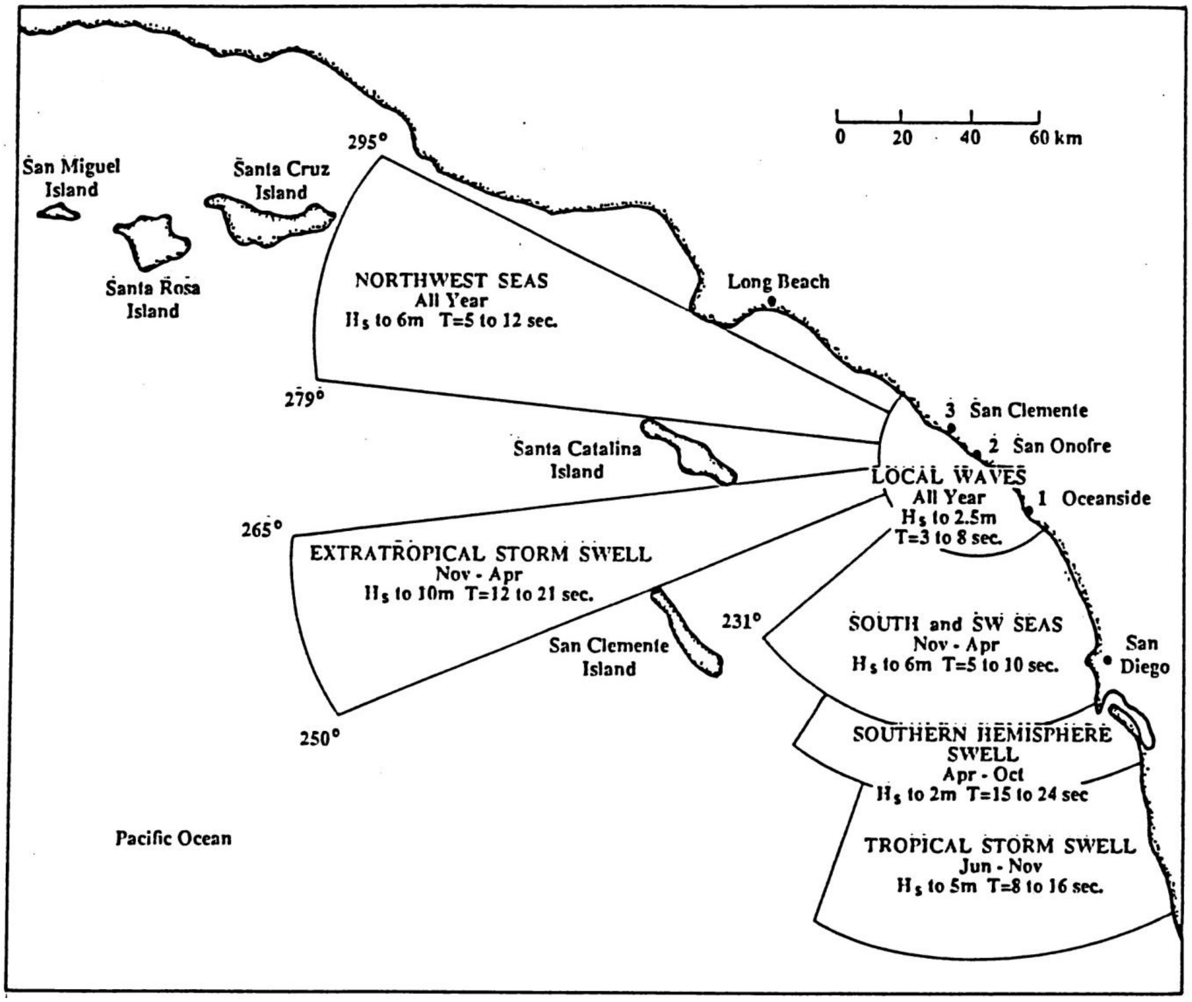

Figure 4-1. Wave exposure at San Onofre illustrating mainland and island-shadowing and resulting wave-exposure windows.

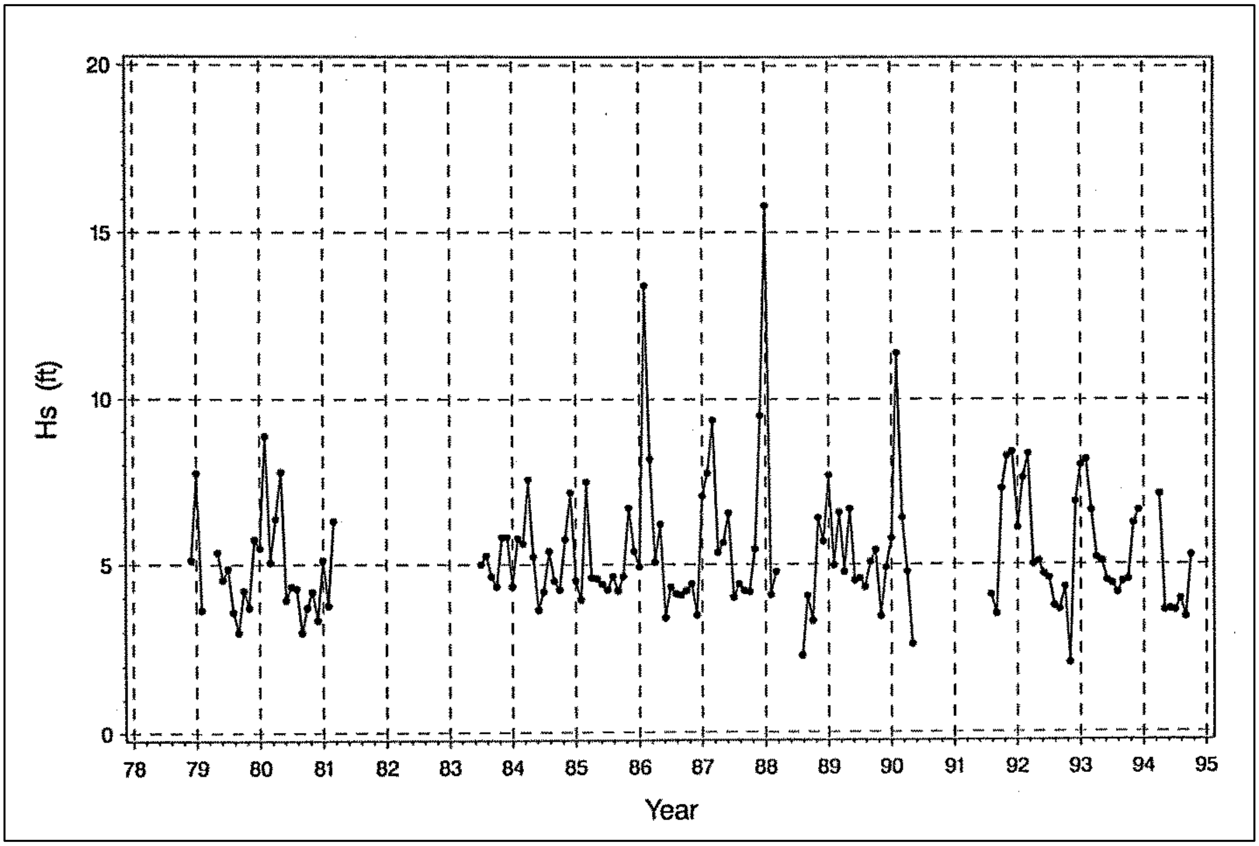

Figure 4-2. Maximum monthly significant wave height at Oceanside from the Coastal Data Information Program wave array, 1978-1994.

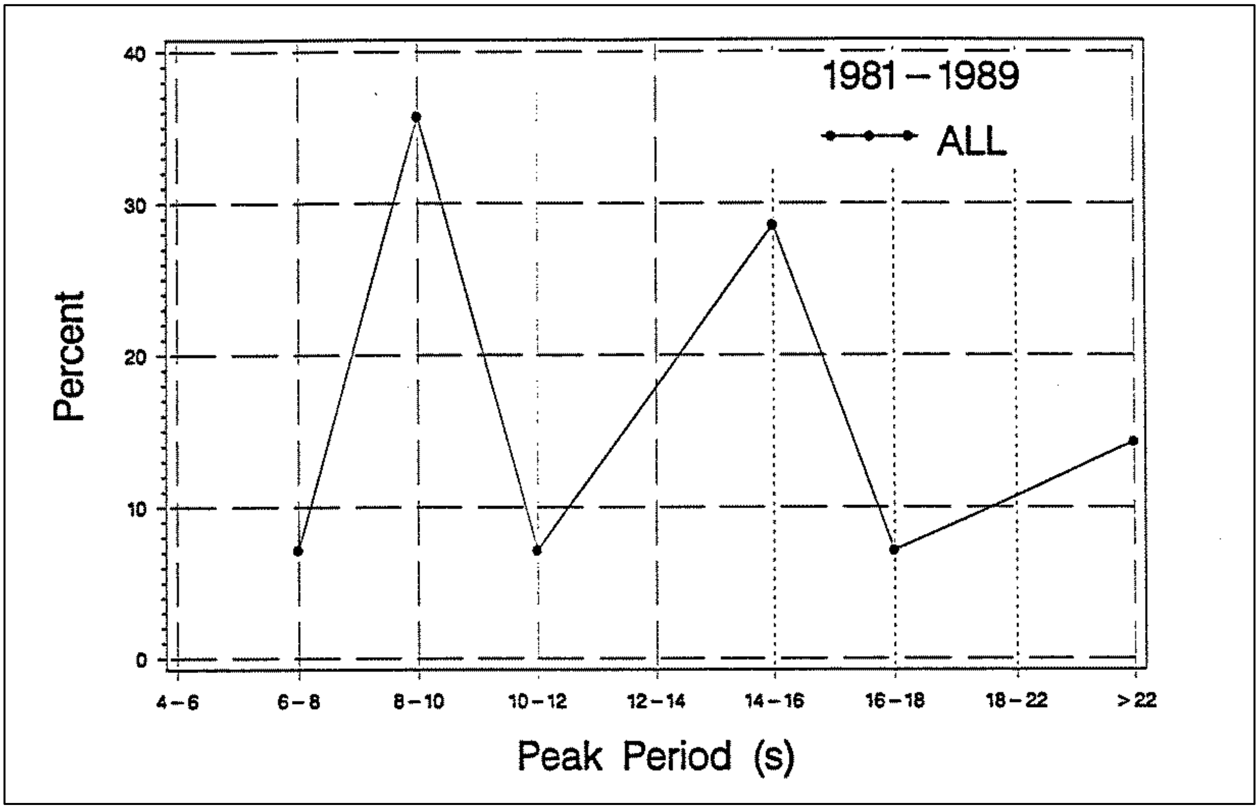

Figure 4-3. Percent occurrence of Oceanside daily mean peak period when Hs > 4ft (1.2 m), 1981-1989.

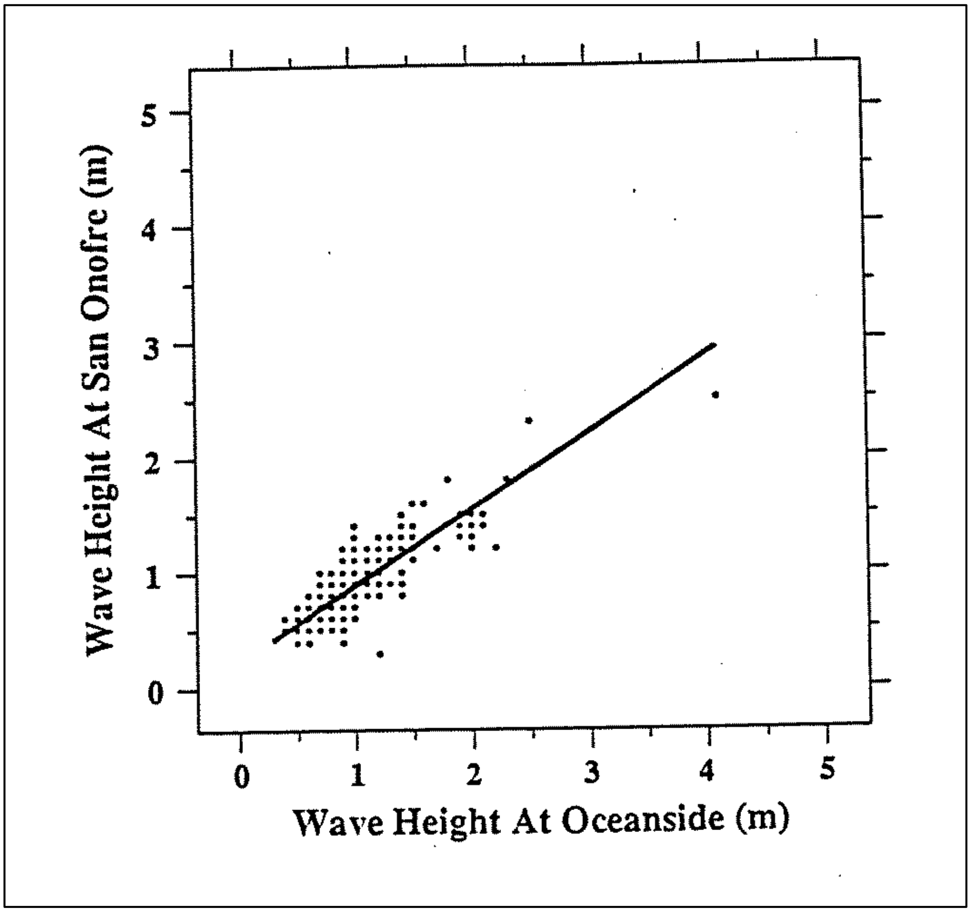

Figure 4-4. Scatter plot of significant wave heights (m) at San Onofre (y-axis) and Oceanside (x-axis), 1985-1986. From Elwany et al. (2016).

5.0 BEACH WIDTH CHANGES FROM 2017 THROUGH 2019

Massive beach widening at San Onofre was associated with SONGS construction activity that stretched over 20 years from 1964, when Unit 1 was started, to late 1984 when Units 2 and 3 were completed. Flick and Wanetick (1989) documented these changes using profile data and photographs gathered by SCE starting from the first Unit 1 excavations in 1964. Two temporary laydown pads were built, and over 1 million cubic meters of sand were placed on the beach during the course of construction. The first pad existed from 1964 to 1966 for Unit 1, and the second from 1975 to 1985 for Units 2 and 3.

The pads were formed of sand fill behind heavy sheet pile bulkheads, and provided equipment staging and workspace. The second pad extended about 70 m seaward of the present position of the seawall. Together with the sand nourishment, even this modest width sufficiently interrupted the longshore transport of sand to widen and stabilize the beaches for several kilometers up coast. Significantly, profile data and aerial photographs showed that no appreciable down-coast erosion occurred. This is most likely because the nourishment material satisfied the longshore transport potential until the upcoast beach was wide enough to establish natural sand bypassing around the structure. Design parameters valuable for future beach stabilization and nourishment projects can be gleaned from the SONGS construction experience. These parameters include the seaward dimension of the pad, the volumes of sand deposited on the beach, the wave climate, and the time spans involved in upcoast fillet accretion and bypassing.

Dramatic narrowing of the beaches has occurred since the Units 2 and 3 laydown pad was removed in early 1985, especially north and adjacent to SONGS. The rate of retreat and its present trend varies depending on location. It is most conspicuous from profile N1000, located north of the plant at San Onofre State Beach, to profile S1000, south of the plant. The retreat at the stage beach has become acute since 1992. At this range, most of the previously wide sandy beach has disappeared and the surf runup has occasionally breached several areas in the parking lot. The beaches from profile S1000 to the south initially widened as sand from the laydown pad was made available by wave induced transport. However, in the early 1990s, these too began slowly to retreat (Elwany et al., 1993).

Beach width changes from 2017 through 2019 at seven profiles from N1000 to S1000 are illustrated in Figures 5-1a and 5-1b. The beach width for each survey at each profile was computed as the distance from the respective benchmark to the intersection of the beach and the NGVD. Table 5-1 summarizes the beach width observations at each profile for the 12 surveys conducted between March 2017 and October 2019.

Beach width changes between October 2019 and the aforementioned previous surveys are given in Table 5-2. The data in Table 5-2 show that the profiles N1000, N0500, N0400', NS0000, and S0800' accreted, while profiles S0500, and S1000 eroded.

Interestingly, the seasonal cycle at these southern locations seems to be reversed, in that the beaches are narrower late in the year and widen by spring. This may be due to the presence of a large rock outcrop reef feature just down coast of S3500. Southward transport of sand prevalent during winter may pile up against this reef, which acts as a barrier to the longshore transport thus widening the beach. During summer, when northward transport of sand results from the dominant south swell, the area north of the reef would be relatively starved of sand, even as material is moved away to the north, leading to narrowing during this season. Similar observations have been made at other Southern California beaches that are bounded by headlands (Thompson, 1987). The yearly mean beach width for each range is presented for 2017, 2018 and 2019 in Table 5-3.

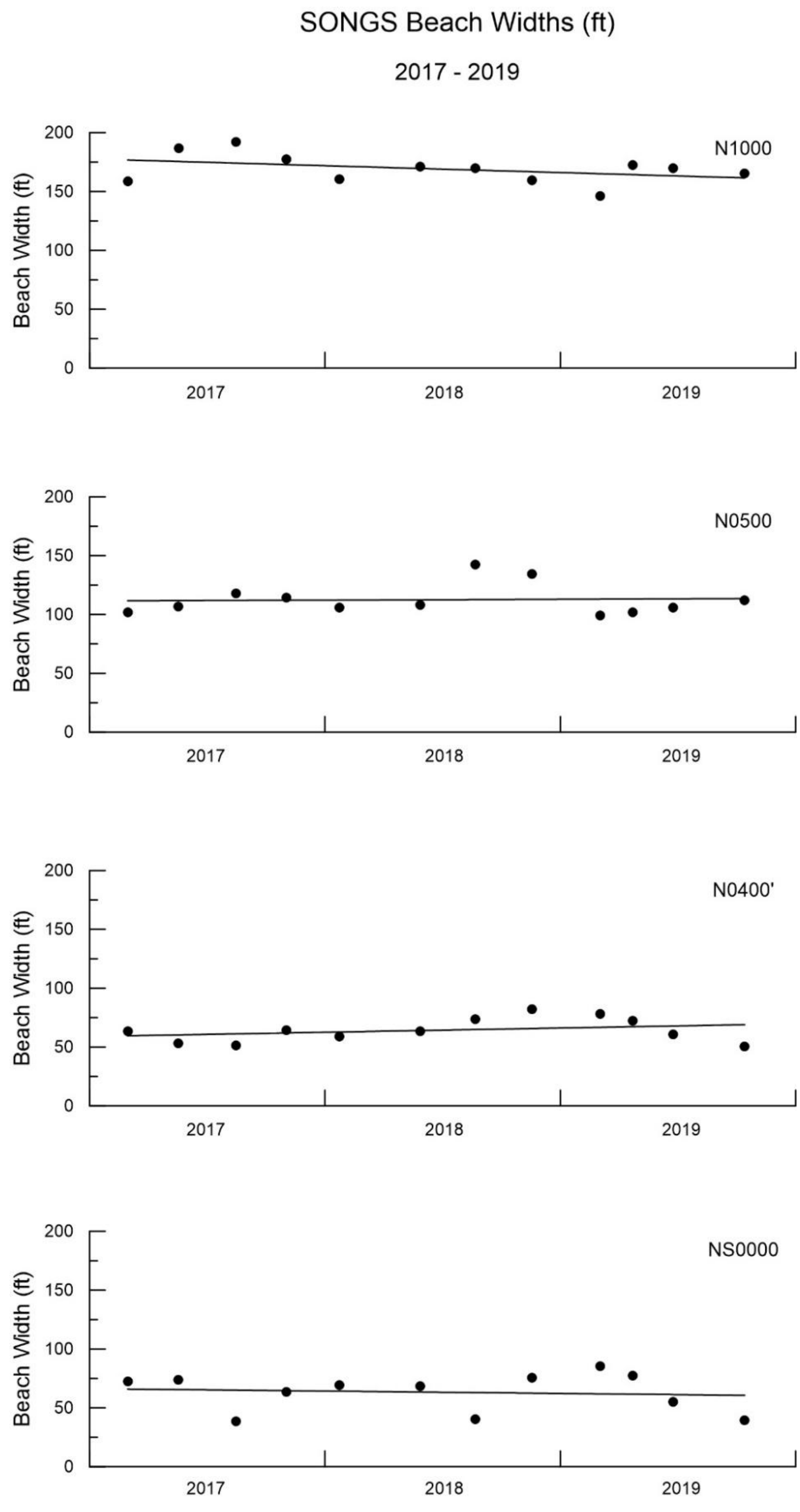

Figure 5-1a. Beach width changes at San Onofre at N1000 – NS0000.

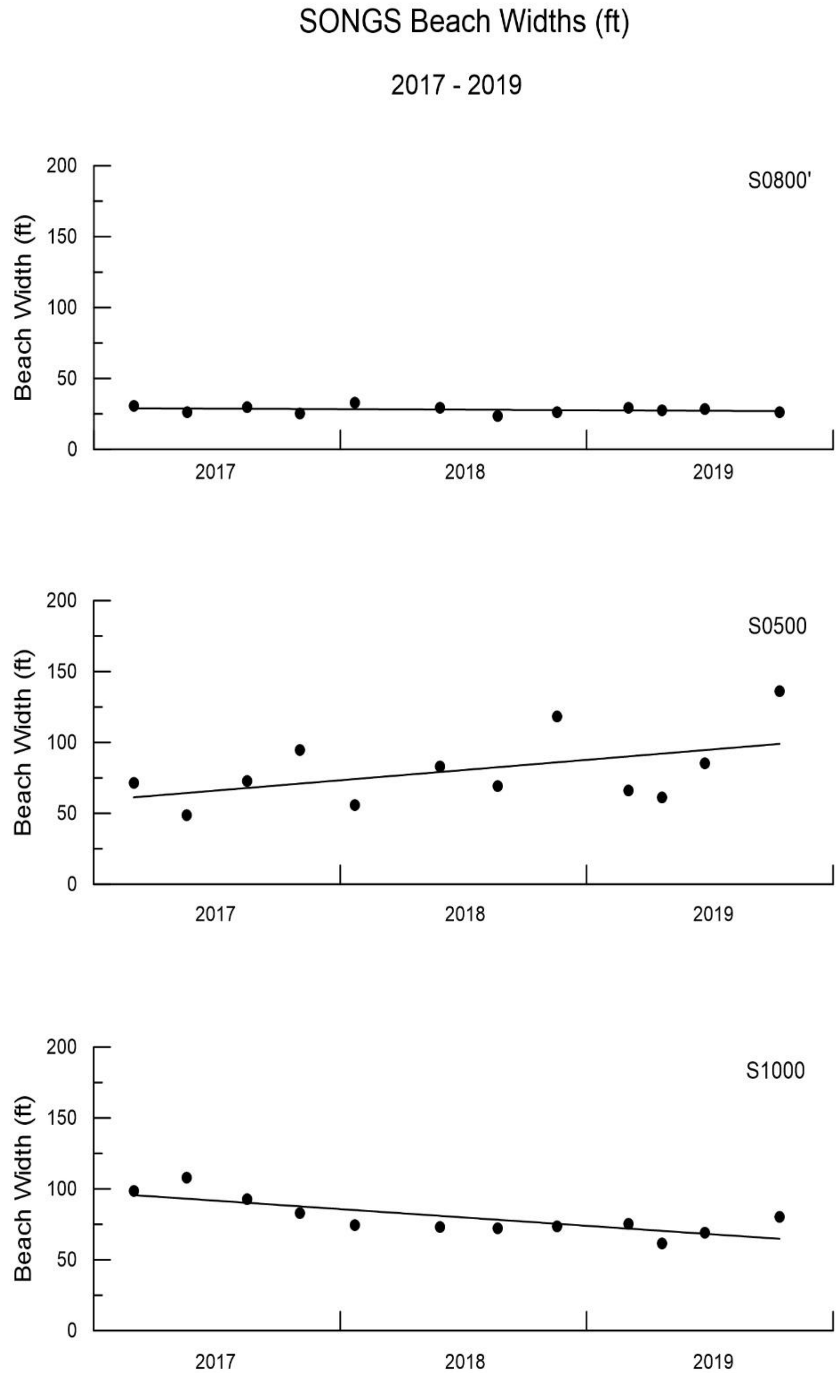

Figure 5-1b. Beach width changes at San Onofre at S0800' – S1000.

Table 5-1. Distance (ft) between shoreline and start point for profiles (2017-2019).

Survey Date	Profile						
	N1000	**N0500**	**N0400'**	**NS0000**	**S0800'**	**S0500**	**S1000**
01Mar17	158.6	102.0	63.4	72.4	30.8	71.4	98.6
19May17	187.0	106.5	53.0	74.0	26.1	48.6	107.8
16Aug17	192.1	117.7	51.2	38.4	29.9	72.7	92.7
02Nov17	177.4	114.3	64.4	63.6	25.5	94.6	82.8
23Jan18	160.4	106.1	58.8	69.5	33.0	55.7	74.6
29May18	171.4	108.3	63.5	68.4	29.3	83.1	73.3
22Aug18	169.8	142.6	73.6	40.6	23.4	69.2	72.1
18Nov18	159.3	134.4	82.0	75.5	26.0	118.2	73.4
04Mar19	146.3	99.2	78.1	85.5	29.5	66.3	75.5
23Apr19	172.3	101.8	72.3	77.4	27.5	61.0	61.6
25Jun19	169.9	105.7	60.6	54.9	28.4	85.4	69.0
14Oct19	165.3	112.0	50.4	39.5	26.5	136.2	80.3

Table 5-2. Beach widths differences from October 2019 survey.

Survey Date	Beach Width Change[a]						
	N1000	**N0500**	**N0400'**	**NS0000**	**S0800'**	**S0500**	**S1000**
01Mar17	6.7	10.0	-13.0	-33.0	-4.3	64.7	-18.3
19May17	-21.7	5.5	-2.6	-34.6	0.4	87.6	-27.5
16Aug17	-26.8	-5.7	-0.8	1.0	-3.4	63.5	-12.4
02Nov17	-12.1	-2.3	-14.0	-24.1	1.0	41.5	-2.6
23Jan18	4.9	5.9	-8.5	-30.0	-6.6	80.4	5.7
29May18	-6.1	3.7	-13.1	-29.0	-2.8	53.1	7.0
22Aug18	-4.4	-30.6	-23.2	-1.2	3.0	66.9	8.2
18Nov18	6.0	-22.4	-31.7	-36.0	0.5	18.0	6.9
04Mar19	19.0	12.8	-27.7	-46.0	-3.1	69.9	4.7
23Apr19	-7.0	10.2	-21.9	-37.9	-1.1	75.1	18.7
25Jun19	-4.6	6.3	-10.2	-15.5	-1.9	50.7	11.3
Average Change	-4.2	-0.6	-15.2	-26.0	-1.7	61.0	0.1

[a] = Distances are in feet. Positive values indicate accretion and negative values indicate erosion.

Table 5-3. Yearly mean beach widths (ft).

Survey Year	Profile						
	N1000	**N0500**	**N0400'**	**NS0000**	**S0800'**	**S0500**	**S1000**
2019	163.5	104.7	65.3	64.3	28.0	87.2	71.6
2018	165.2	122.8	69.5	63.5	27.9	81.5	73.3
2017	178.8	110.1	58.0	62.1	28.1	71.8	95.5
Mean	169.2	112.5	64.3	63.3	28.0	80.2	80.1

6.0 ESTIMATION OF SHORELINE TREND AND SEASONAL CYCLE

The observed shoreline changes at various profiles consist of two components. The first is the seasonal cycle, which is superimposed on the second component: the long-term trend in the beach width. The trend is due to the processes that affect beach width on longer time scales, such as wave climate or sand supply changes likely also play a role.

The beach profile data from March 2017 through October 2019 have been used to separate trends in shoreline changes from the yearly seasonal cycle in order to obtain quantitative estimates for the two parameters. The shoreline data from the 12 surveys were regressed against the total number of days during this time period, and a straight line was fitted to the entire data set (Figures 5-1a and 5-1b). The slope of this line gives the trend and rate (ft/year) of change of the beach width.

These regression values were then used to determine the seasonal shoreline changes. The expected beach width value obtained via linear regression was subtracted from the measured values for each survey date between March 2017 and October 2019. By removing this slope and "detrending" the measured data, the seasonal shoreline cycle for each SONGS profile was determined (Figures 6-1a and 6-1b). The estimate of yearly seasonal beach width changes at San Onofre are presented in Table 6-1. These values were determined by taking the difference between the minimum and maximum beach widths for each year. The average seasonal fluctuation is about 26.01 ft.

Table 6-2 gives the estimates of the observed trends in beach width for 2017, 2018, and 2019. Statistical tests were carried out on the trend, and p-values are presented in Table 6-2. The trend is significantly different from zero on those ranges with p-value < 0.05. The maximum trend observed is 14.39 ft/year and occurred at S0500.

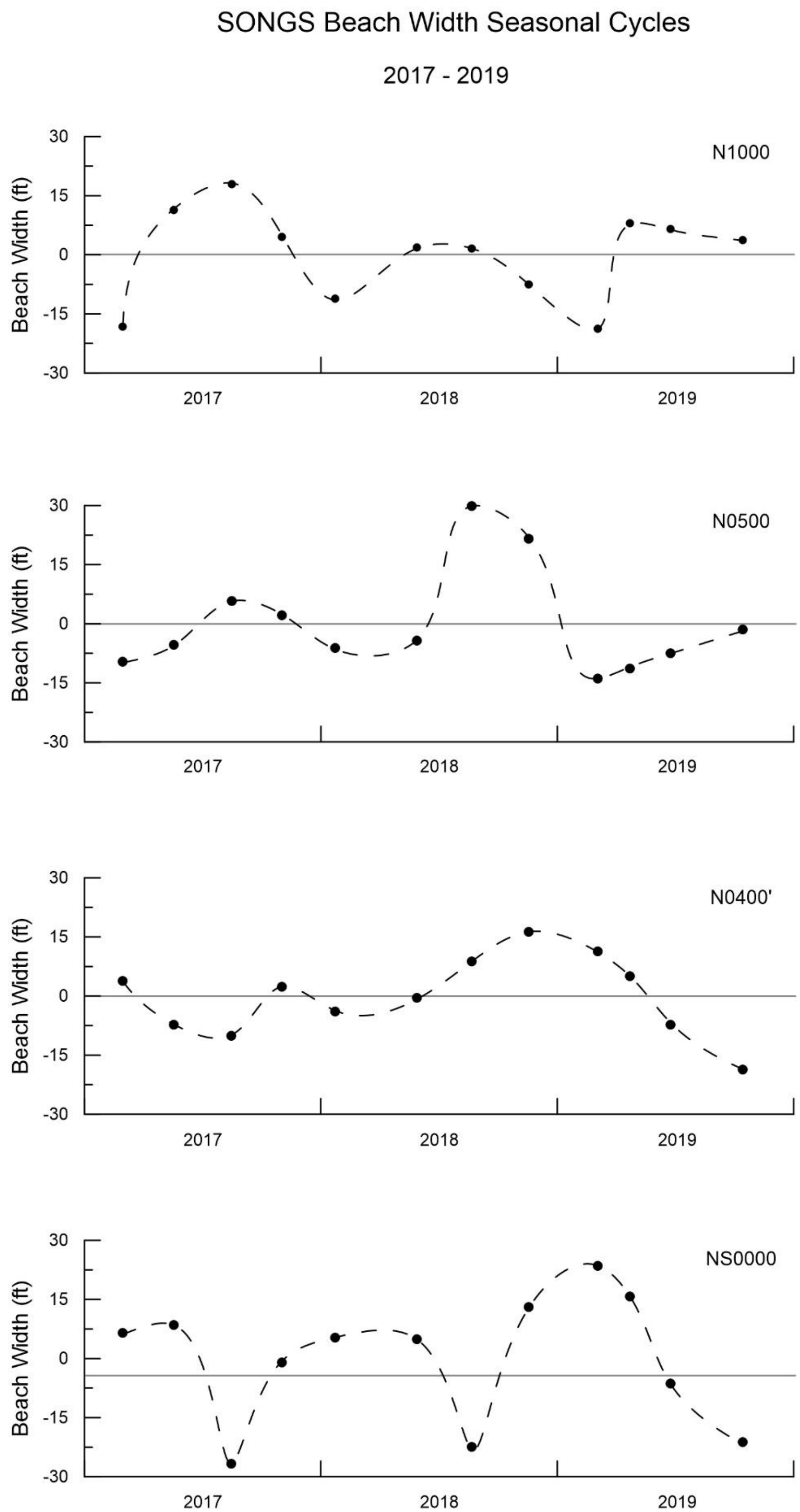

Figure 6-1a. SONGS beach width seasonal cycles at N1000 – NS0000 (2017-2019).

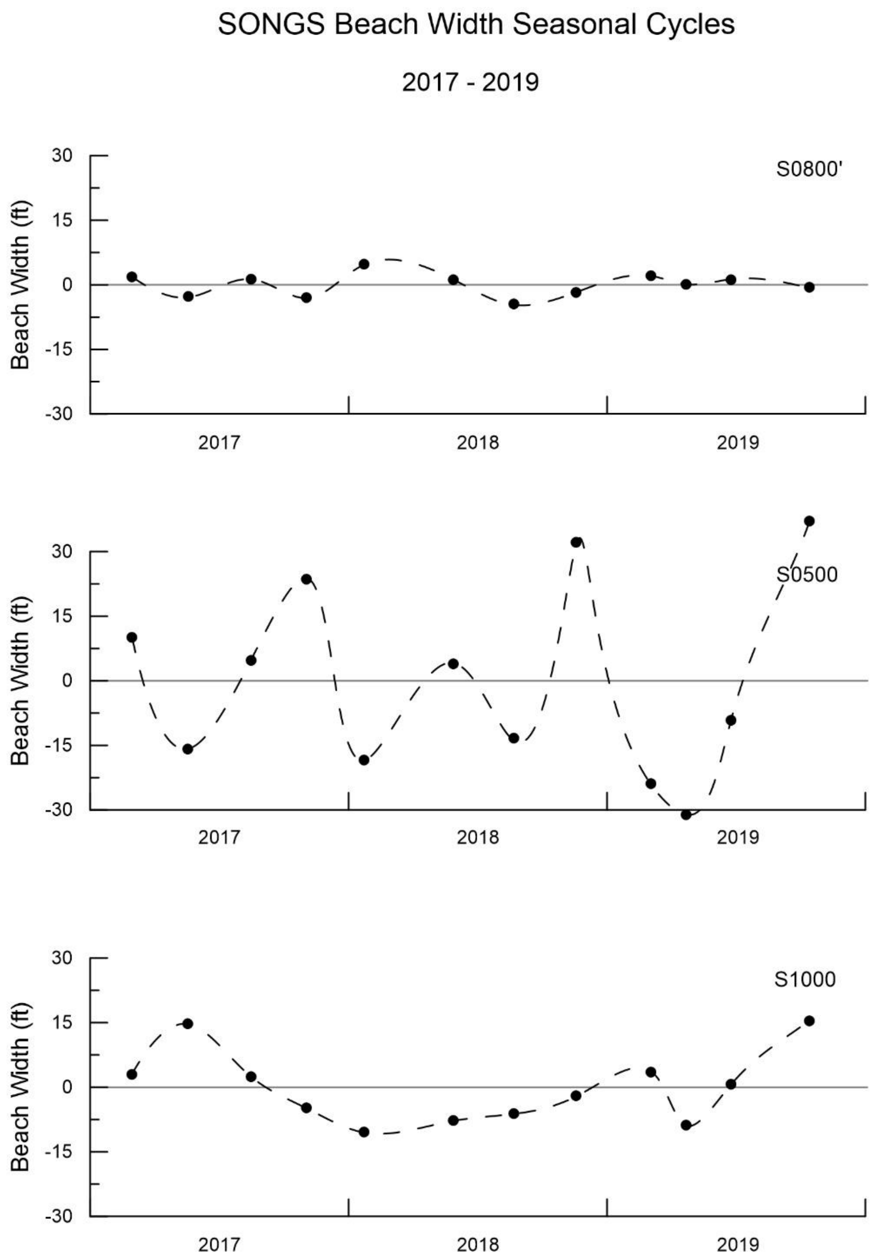

Figure 6-1b. SONGS beach width seasonal cycles at S0800' – S1000 (2017-2019).

Table 6-1. Seasonal beach width changes at San Onofre.

Profile	Seasonal Beach Width Change (ft)			Mean
	2017	2018	2019	
N1000	36.16	13.05	26.77	25.33
N0500	15.40	36.09	12.39	21.29
N0400’	13.90	20.24	29.93	21.36
NS0000	35.08	35.36	44.75	38.40
S0800’	4.55	9.18	2.63	5.45
S0500	39.49	50.64	68.25	52.79
S1000	19.60	8.42	24.28	17.43
Mean	23.45	24.71	29.86	26.01

Table 6-2. Linear regression analysis of beach width, March 2017 – October 2019.

Profile	Rate of Change (ft/yr)	Intercept (ft)	p-value[a]	Trend
N1000	-5.82	177.7	0.1958	Slight erosion[a]
N0500	0.71	111.5	0.8863	Slight accretion[a]
N0400'	3.60	59.0	0.3416	Slight accretion[a]
NS0000	-2.03	66.3	0.7351	Slight erosion[a]
S0800'	-0.75	29.1	0.4458	Slight erosion[a]
S0500	14.39	58.9	0.1072	Slight accretion[a]
S1000	-11.76	97.5	0.0035	Erosion[b]

[a] = p-values > 0.05 indicate a statistically not significant trend (i.e., trend is equal to zero).
[b] = p-values < 0.05 indicate a statistically significant trend (i.e., trend is not equal to zero).

7.0 BEACH PROFILES AND WIDTH FROM 1964 THROUGH 2019

The available beach profile data at San Onofre from 1945 through 1998 were used in evaluating the observed changes from 2017 through 2019. There are large gaps in the beach profile data sets where no beach surveys were carried out, but the available information is useful to better understand beach width fluctuations over a long time scale. Beach width is controlled by waves, sediment supply, beach site location and surroundings, and the beach nearshore and offshore bathymetry.

7.1 BEACH PROFILE HISTORY

The earliest beach profile data (1945-1949) for the area were collected by Shepard (1950a, b) at four range lines, three of which are shown in Figure 7-1. The benchmarks for these three surveys are noted as "Crescent" (farthest upcoast), "Fence" (about 4,000 ft [1,200 m] upcoast of Unit 1), and "Surf" (about 660 feet [200 m] upcoast of Unit 1). Shepard's original survey notes are available in the Scripps Institution of Oceanography (SIO) archives, but efforts to reconstruct the profiles were unsuccessful.

The first set of beach profiles associated with Unit 1 construction was taken on 15 May 1964 and represents the San Onofre State Beach area before the influence of any construction activity, which began in June 1964. A second set of profiles was taken on 13 July 1964, which would also have been before construction activity had any effect. Note that Figure 7-1 also shows the location of the Unit 1 laydown pad (the hatched area), which was in existence from 1964 through 1966. The last set of profiles recorded in this phase of beach measurement, taken on 29-30 October 1970, represents the beach well after the disappearance of the pad's influence.

The next beach profile study began in 1974 as part of the oceanographic monitoring program for the construction of Units 2 and 3. Benchmarks "B1," "B3," "B5," "B6," and the remote "B7" (the triangles in Figure 7-1) were established at the beginning of construction for Units 2 and 3. The 3 May 1974 set of profiles represents the "pre-construction beach" in this series. The "B1" line, which is nearest the 1964-1971 "A" line, is shown in Figure 7-1. SCE land survey teams performed these profile surveys, which extend to a depth of -2 to -6 ft (-0.6 to -1.8 m) mean lower low water (MLLW). These profile lines were monitored monthly from 1974 through early 1979.

The larger Units 2 and 3 laydown pad (shown in Figure 7-1, to the right [south] of the Unit 1 pad) was in existence from 1974 through early 1985. The beach profiling work started again in 1985 after the laydown pad had been removed and the sand behind it had been released. The first set of these measurements was taken in May 1985, and this phase of the beach measurement program concluded in September 1987, with nine sets of profiles recorded. An additional survey was carried out by Waldorf (1989) in January 1989. Wading depth profiles were measured every 500 m along the beach, from -6,600 ft (-2,000 m) (north) to +9,900 ft (+3,000 m) (south) (Figure 7-1). These survey lines reached to about -1.5 ft (-0.45 m) depth (MLLW) in the surf zone. The benchmarks for these surveys along the bottom of the cliff face are represented in Figure 7-1 as dots along the beach.

The beach profiling work carried out by CE was started in 1991 and continued through February 1994. Additional surveys were performed along the 1985-1989 range lines at 1650-ft (500 m) intervals (Elwany et al., 1992, 1993, 1994). Up to 14 profile lines were surveyed on a quarterly basis. The locations of these ranges are shown in Figure 7-2. Additional beach profile surveys were carried out by CE in 2000 and 2016 on the same ranges.

7.2 BEACH WIDTH DATA

Most pertinent to this study were the data that documented changes at San Onofre State Beach through the time of construction of Units 1, 2, and 3, and the data gathered after the 1985 removal of the Units 2 and 3 laydown pads. The SONGS beach surveys showed how the local beach responded to the massive input of sand from construction activities (1985-2000), and also provided pre-construction beach conditions. The pre-construction beach width is shown in Figure 7-3.

The post-1985 profile data shown in Figures 7-4 and 7-5 document the return to a narrower state of the beach over time since the completion of construction. The data provided documentation for the period of 1964 to 2000 of two complete sand pads, one for Unit 1 and the other for Units 2 and 3, of progressive beach widening due to placement of the sand pads and of the subsequent narrowing back to the natural configuration. A comparison of 2000 and 2016 profiles at profile NS0000 is shown in Figure 7-6.

Comparison between beach width at N1000, N0500, NS0000, S0500, S1000 during the period between 1993, 2000, 2016, and 2017 and 2019 are given in Table 7-1. The long-term average erosion rate of the beach erosion at San Onofre beach is 2-3 ft/year.

Figure 7-7 shows the beach width measured between 1991 through 1993 and between 2016 through 2019. The solid line is the mean of beach width for the referenced periods. The dotted lines cover the period where no long-term measurements were carried out.

The beach at San Onofre State Beach, which extends 1 km north and south from SONGS, has retreated considerably and subsequently has caused the cliffs to retreat by about 1.34 ft/year (Hapke & Reed, 2007) due to wave action. Table 7-2 gives the estimated average winter-summer seasonal cycle for the beach width data collected during 1990-1993 (34 ft) and 2017-2019 (31 ft).

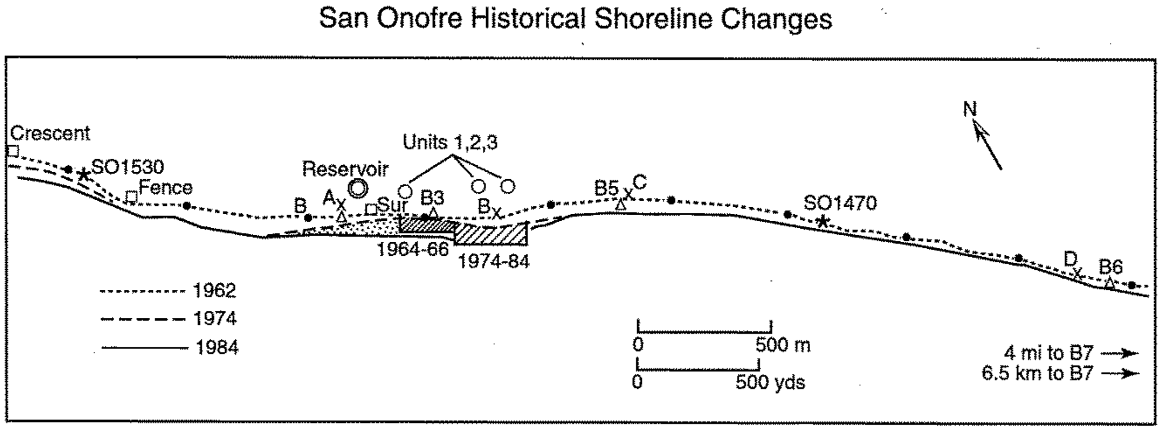

Figure 7-1. **SONGS area historical shoreline changes, laydown pad locations (bracketed hatch marks labeled 1964-66 are for Unit 1; those labeled 1974-84 are for Units 2 and 3), and fillet beach (stippled). The shorelines in this figure are an approximation of MHHW traced from photographs for 1962, 1974, 1984. The fillet beach is a salient, perimeter beach. Benchmark designations for early profiles: Crescent, Fence, and Surf, 1940s; A-D, 1984-86; B1-B7, 1974-85. Flick et al. (2010).**

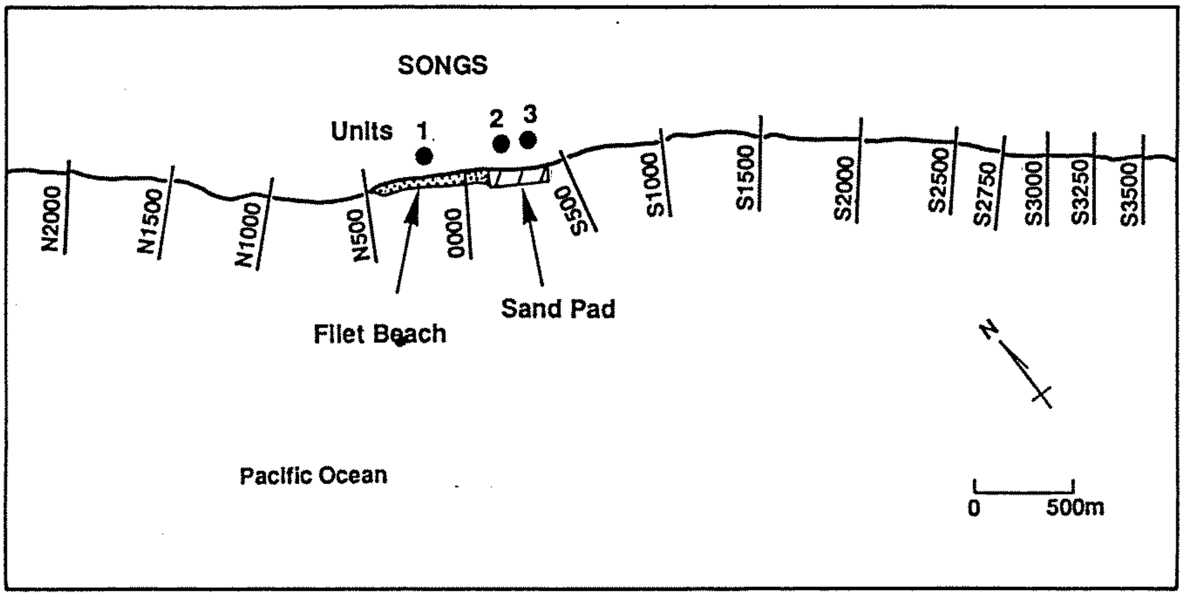

Figure 7-2. Beach profile range lines at San Onofre, 1990-1993.

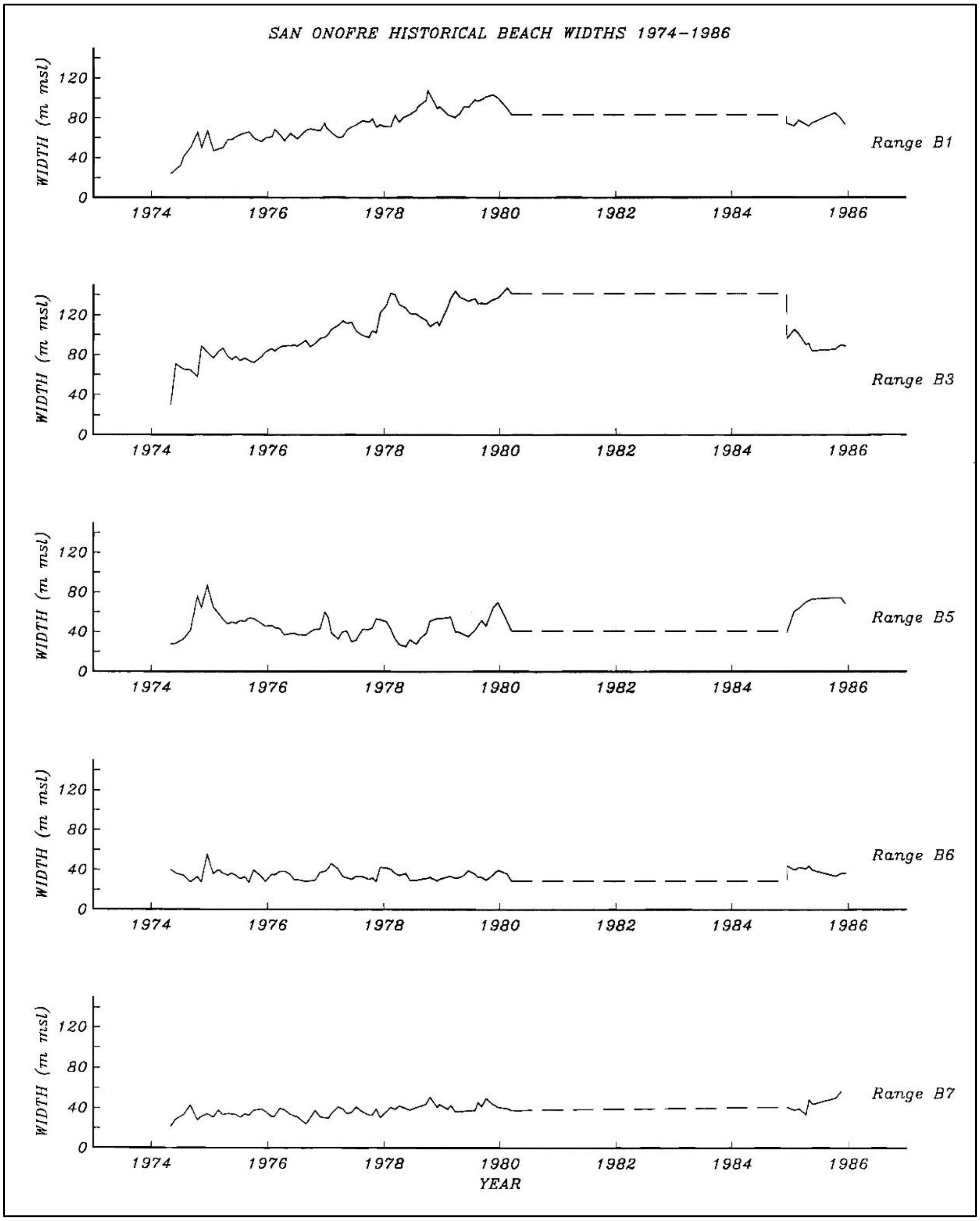

Figure 7-3. Beach-width time histories around the time of Units 2 and 3 construction. Broken lines show time of missing data.

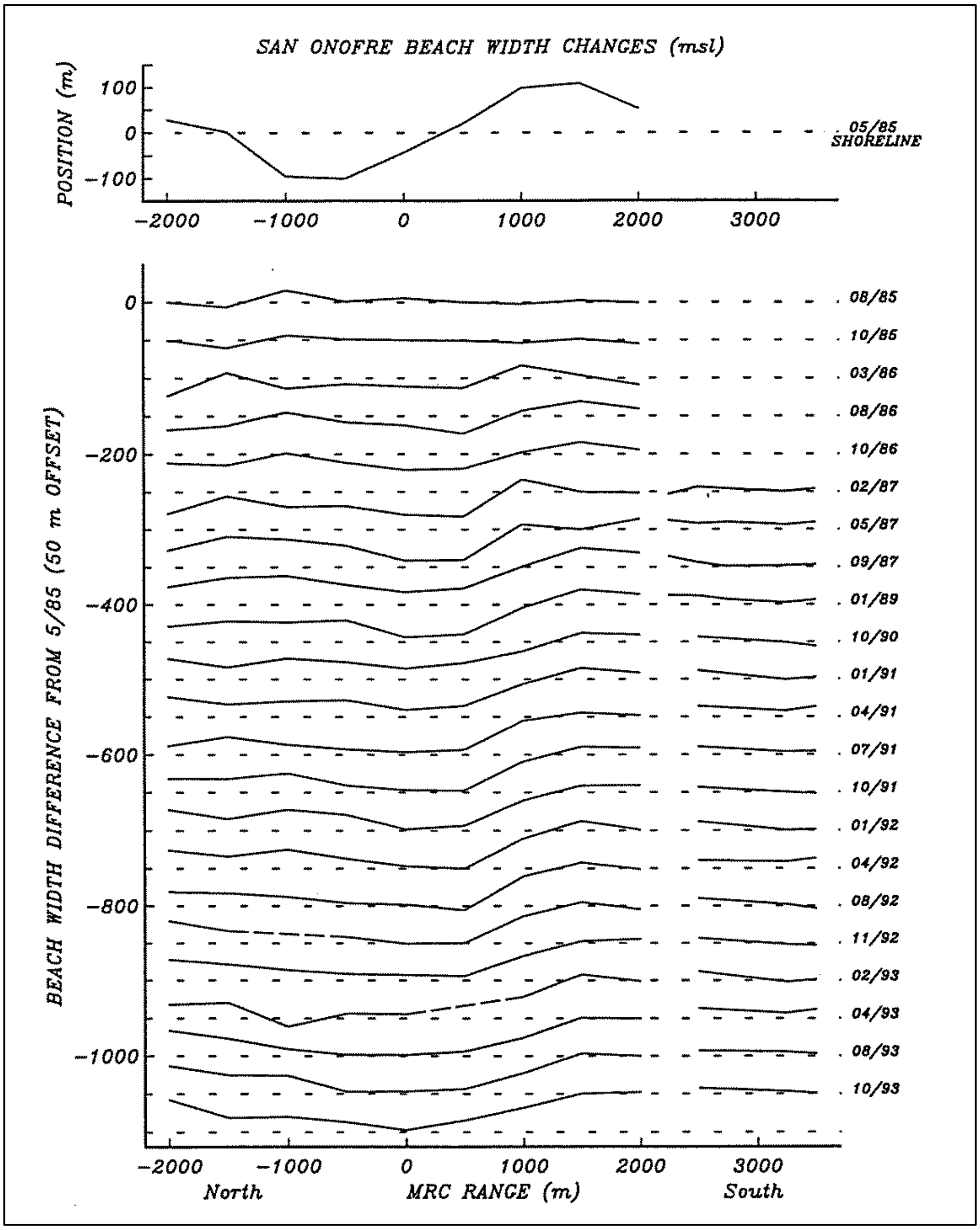

Figure 7-4. Time history of beach-width changes at San Onofre after removal of Units 2 and 3 laydown pad. Changes for dates (month/year) at right relative to May 1985 survey (top panel).

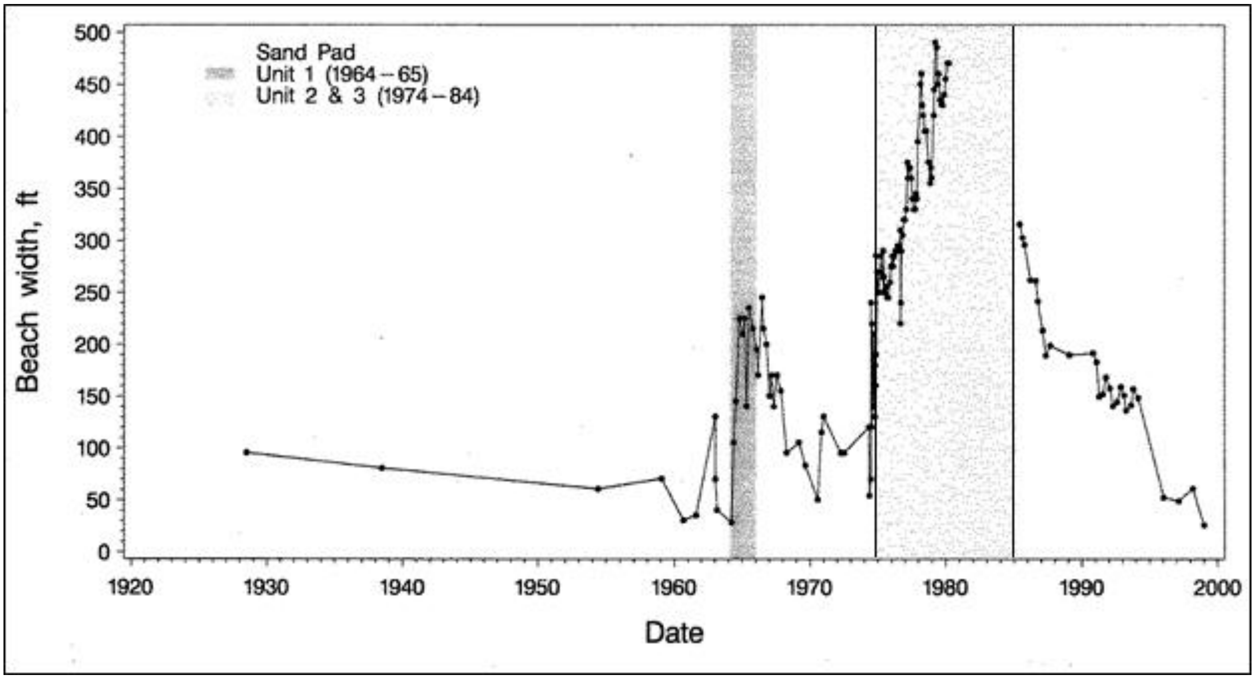

Figure 7-5. Historical beach width adjacent to Unit 1, 1928-2000. Vertical columns show periods when laydown pads were present.

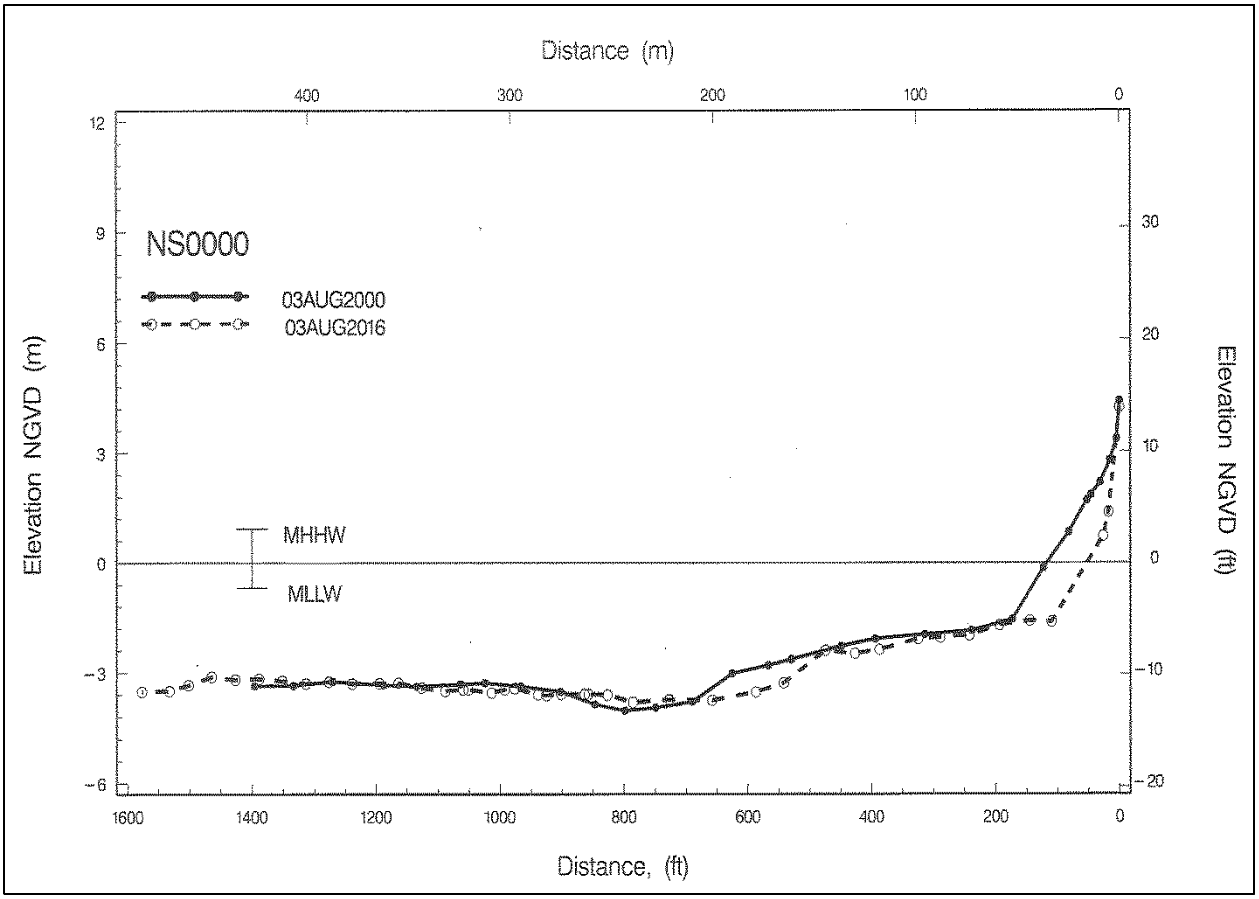

Figure 7-6. Beach profiles at NS0000, years 2000 and 2016.

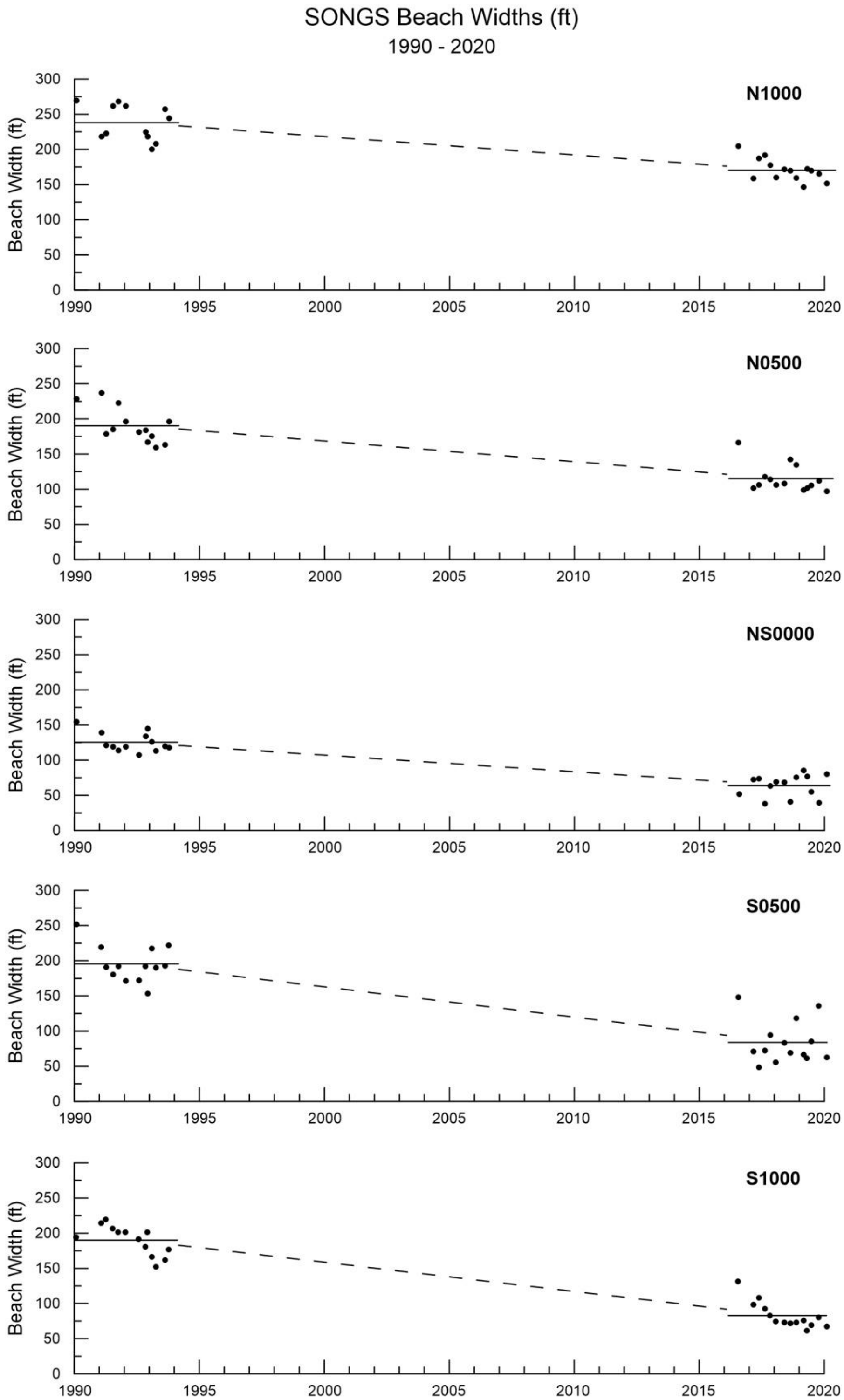

Figure 7-7. Beach width measured between 1991 through 1993 and between 2016 through 2019. Solid lines are the mean of beach width for the referenced periods and dotted lines cover the period where no long-term measurements were carried out.

Table 7-1. Mean beach widths (ft) at San Onofre.

Survey Period	Profiles				
	N1000[a]	N0500[a]	NS0000[b]	S0500[c]	S1000[c]
1990-1993	227.3	173.5	119.1	205.5	164.3
Aug 2000	275.8	183.2	106.6	362.8	220.86
July 2016	204.5	116.4	204.5	102.3	106.7
2017-2019	169.2	112.5	63.3	80.2	80.1

[a] Average beach profile width at North Beach in 1964 is 295 ft. from Figure 7-3.
[b] Average beach profile width Fronting SONGS in 1964 is 229 ft. from Figure 7-3.
[c] Average beach profile width at South Beach in 1964 is 196 ft. from Figure 7-3.

Table 7-2. Estimates of seasonal beach widths changes at San Onofre (ft).

Survey Period	Profiles					
	N1000	N0500	NS0000	S0500	S1000	Mean
1990-1993	50.76	40.7	20.43	38.7	18.5	33.8
2017-2019	25.33	21.29	38.4	52.79	17.43	31.1

8.0 CONCLUSIONS

Construction activities at SONGS over the 20-year period from 1965 to 1984 resulted in substantial increases in beach width adjacent to and north of the plant. These increases were primarily a result of the large quantities of excavated sand being placed on the beach and the Unit 1 and Units 2 and 3 laydown pad structures that served to retain the fill. Since the removal of the Units 2 and 3 laydown pad in 1985, the beaches adjacent to and north of SONGS have experienced dramatic narrowing and returned to their pre-construction configuration (Figures 7-4 and 7-5).

In the period between 2000 and 2019, this is due to limited sand supply from the surrounding creeks and rivers. Since the end of the last wet period in 1998, sediment flows from the surrounding waterways have been considerably reduced.

In the long term, the heavily used beach access and parking at San Onofre State Beach just north of SONGS is likely to continue slowly erroded as this area continues to return to its more natural, pre-construction beach width.

The amplitude of the seasonal cycles in beach width are distinguishable from the net advance or retreat. The average seasonal cycle varied from 31 to 33 ft (Section 7).

Table 7-1 presents the mean beach width for the periods 1990-1993, Aug 2000, and 2017-2019. It is noticeable that the mean beach width for Aug 2000 is larger than the beach width for the other periods in response to the natural sand supply from the cliffs and the adjacent rivers during 1993, 1995 and 1998 floods (Elwany et al., 1999),

The changes of the beach width are controlled by the sand supply, waves, topography of the site (presence of headland and coastal protection structures), and nearshore and offshore bathymetry. In Southern California, the presence of the offshore islands, the complex bathymetry offshore, and the presence of cropped bed rocks nearshore can cause a single, straight beach to experience various beach width changes along different stretches of the beach.

The beach profile surveys and photography programs sponsored by SCE since 1964 have provided valuable information and understanding of the response at San Onofre to beach filling and the construction of stabilizing structures. This insight will be valuable as sea level rise accelerates in the future.

9.0 REFERENCES

CDIP, 1992. *Coastal Data Information Program, Multi-Year Report: Vol. I, 1975-1991*. Scripps Institution of Oceanography, SIO Ref. No. 91-32. 295 pp. and 2 appendices.

Coastal Environments, 2000. *SONGS Unit 1 Deconstruction Marine Impacts Study, Phase I*. Unpublished report submitted to Southern California Edison Company, 24 January 2000, CE Ref. No. 2000-03, 44 pp. plus 2 appendices.

Coastal Environments, 2017. San Onofre Nuclear Generating Station, November 2-3, 2017 Beach Profiles, San Onofre, California, Data Report. Submitted to Southern California Edison, 7 November 2017. CE Ref. No. 17-22, 7 pp. + 2 appendices

Coastal Environments, 2018. San Onofre Nuclear Generating Station, November 18-21, 2018 Beach Profiles, San Onofre, California, Data Report. Submitted to Southern California Edison, 27 November 2018, CE Ref. No. 18-16, 29 pp. + 2 appendices.

Coastal Environments, 2019. San Onofre Nuclear Generating Station, October 14, 2019 Beach Profiles, San Onofre, California, Data Report. Submitted to Southern California Edison, 30 October 2019, CE Ref. No. 19-33, 29 pp. + 2 appendices.

Crosby, S.C., B. D. Cornuelle, W.C. O'Reilly, and R. T. Guza , 2017. Assimilating global wave model predictions and deep-water wave observations in nearshore swell predictions, *Jour. Atmos. and Oceanic Tech*., 34(8), 1823-1836.

Elwany, M. H. S., and R. E Flick, 1992. *1991 Beach Profile Survey at San Onofre*. Unpub. Report, Southern California Edison Co., CE Ref. No. 92-1. 24 pp. and 1 appendix.

Elwany, H., R. Flick, W. Waldorf, and J. Wanetick, 1993. *1992 Beach Profile Survey at San Onofre*. Report submitted to Southern California Edison Co., 20 April 1993, CE Ref. No. 93-7. 26 pp. and appendices.

Elwany, H., R. Flick, and Samia Aijaz,1994. *1993 Beach Profile Survey at San Onofre*. Final Report submitted to Southern California Edison Co., 1 July 1994, CE Ref. No. 94-7. 32 pp. and 2 appendices.

Elwany, M. H. S., A. Linquist, R. Flick, W. O;Reilly, J. Retizel, and W. Boyd, 1999. Study of Sediment Transport Conditions in the Vicinity of Agua Hedionda Lagoon. Technical Report, Volume I, Center For Coastal Studdies, Scripps Istitutionof Oceangraphy, 8 January 199, SIO Ref N. 00.07. 10 Chapters and 3 Appendiceis.

Elwany, H., R.E. Flick, and A.D. Young, 2016. *Coastal Analysis for End-State Planning of San Onofre Nuclear Generating Station*, *Phase 1*. Report prepared for Southern California Edison by Coastal Environments, La Jolla, CA, CE Reference No. 16-26, 151 pp.

Flick, R.E., and J.R. Wanetick, 1989. *San Onofre Beach Study*. Unpublished report submitted to Southern California Edison Co., Rosemead, CA, October 1989, SIO Ref. No 89-20. 26 pp. and 25 figures.

Flick, R., J.R. Wanetick, M.H. Elwany, R.S. Grove, and B.W. Waldorf, 2010. Beach changes from construction of San Onofre Nuclear Generating Station, 1964-1989. Shore & Beach, 78(4): 12-25.

Hapke, C.J. and D. Reid, 2007. *National Assessment of Shoreline Change, Part 4: Historical Coastal Cliff Retreat along the California Coast.* USGS Report 2007-1133.

Inman, D.L., 1980. Man's Impact on the California Coast Zone. Report submitted to State of California, The resources Agency, Department of Boating & Waterways, p. 18.

Pawka, S.S., 1982. *Wave directional characteristics on a partially sheltered coast*. Ph.D. dissertation, University of California, San Diego, 246 pp.

Thompson, W.C., 1987. Seasonal Orientation of California Beaches, *Shore and Beach*, Vol. 55, No. 3-4, p. 67-70.

U.S. Army Corps of Engineers, 1986. *Southern California Coastal Processes Data Summary*. CCSTWS 86-1, Corps of Engineers, Los Angeles District, Los Angeles, CA. 572 pp.

Waldorf, B.W., 1989. *Beach Profiles in the Vicinity of the San Onofre Nuclear Generating Station*. Unpublished data report submitted to Southern California Edison Company. 5 pp. and appendices.

APPENDIX A

2017 BEACH PROFILES

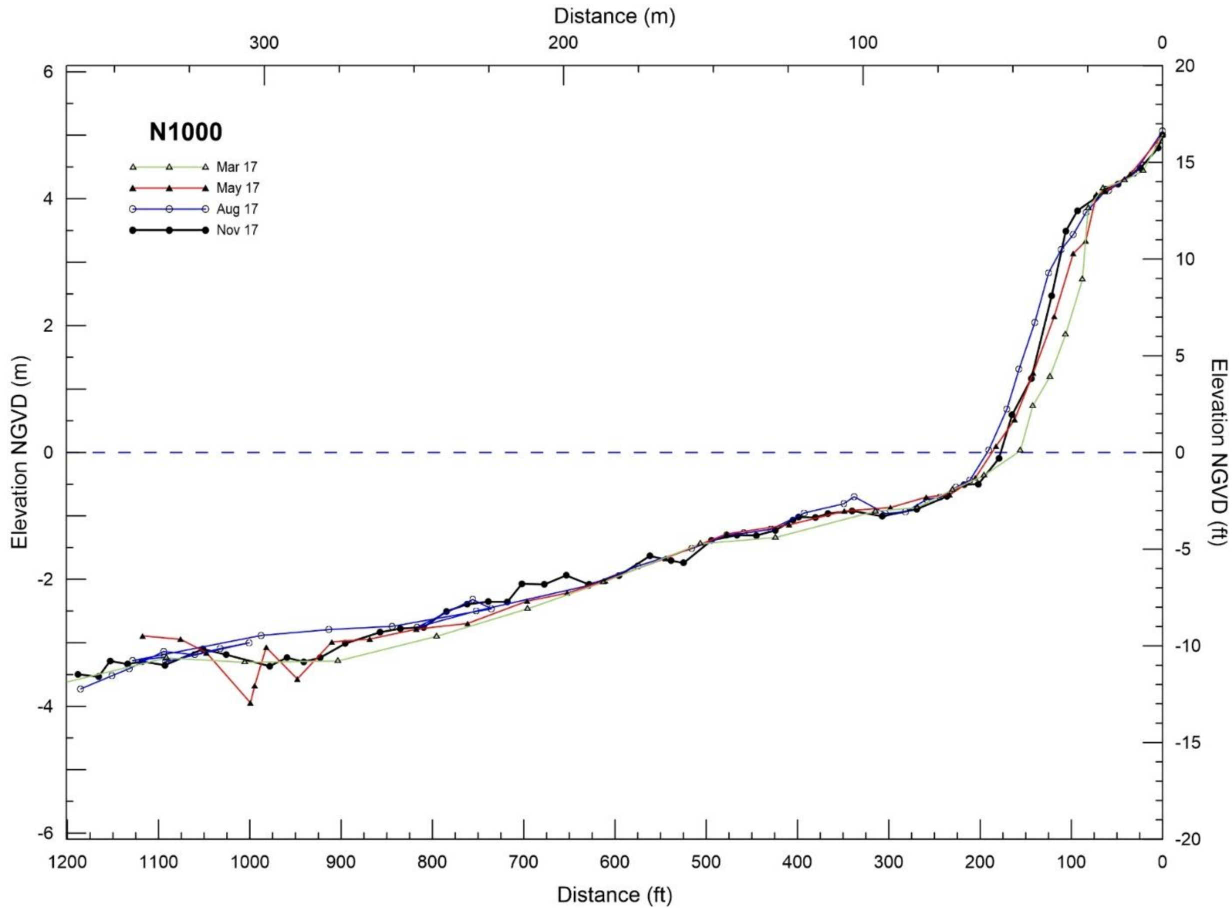

Figure A-1. 2017 Beach profile surveys of N1000.

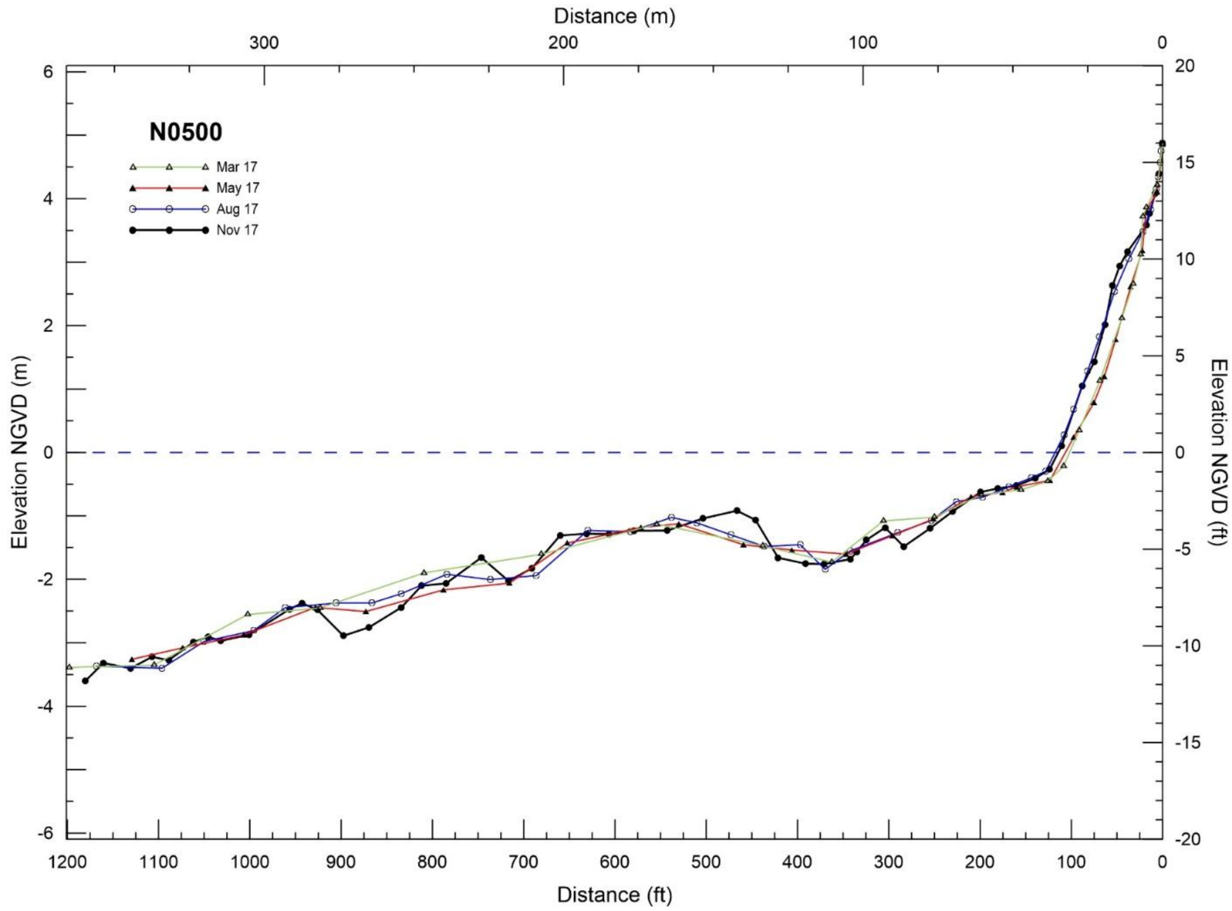

Figure A-2. 2017 Beach profile surveys of N0500.

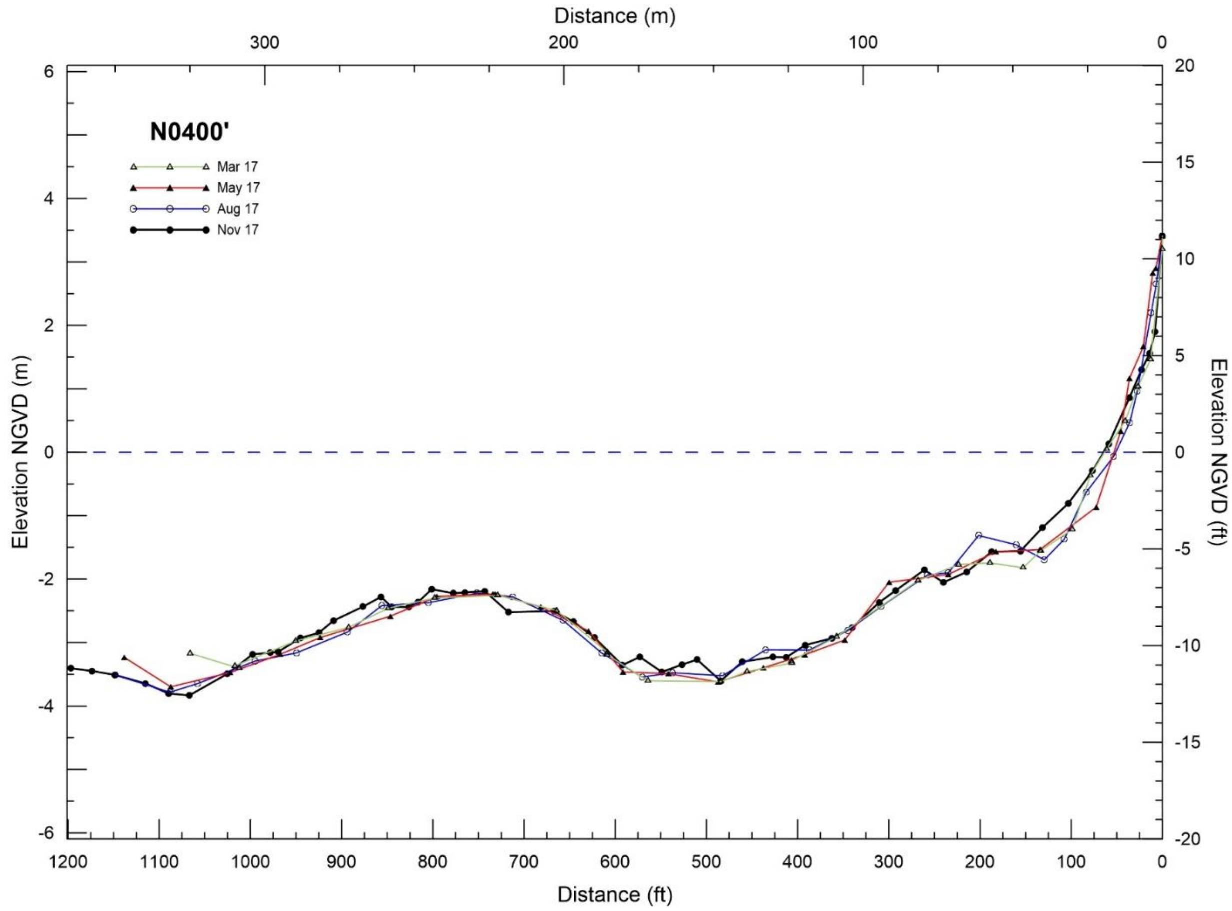

Figure A-3. 2017 Beach profile surveys of N0400'.

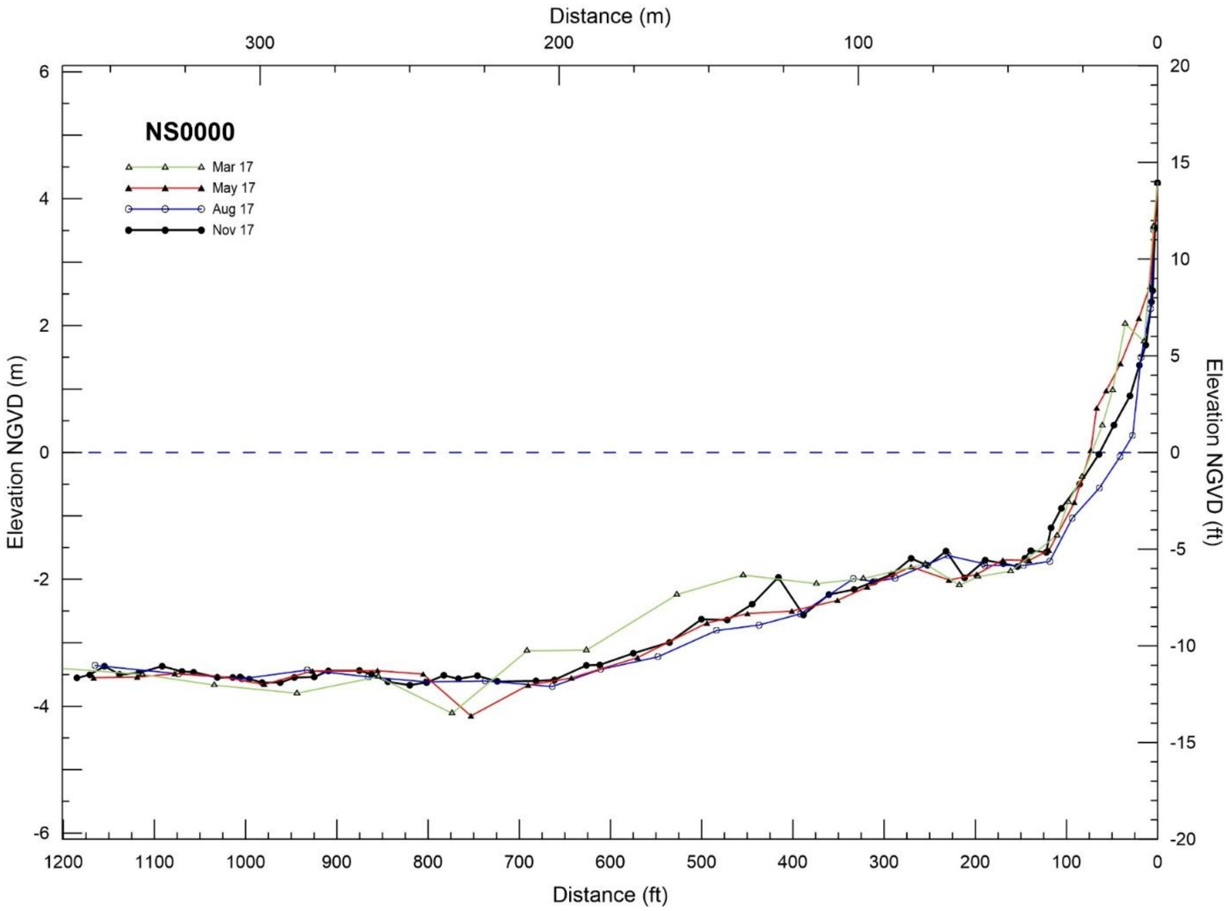

Figure A-4. 2017 Beach profile surveys of NS0000.

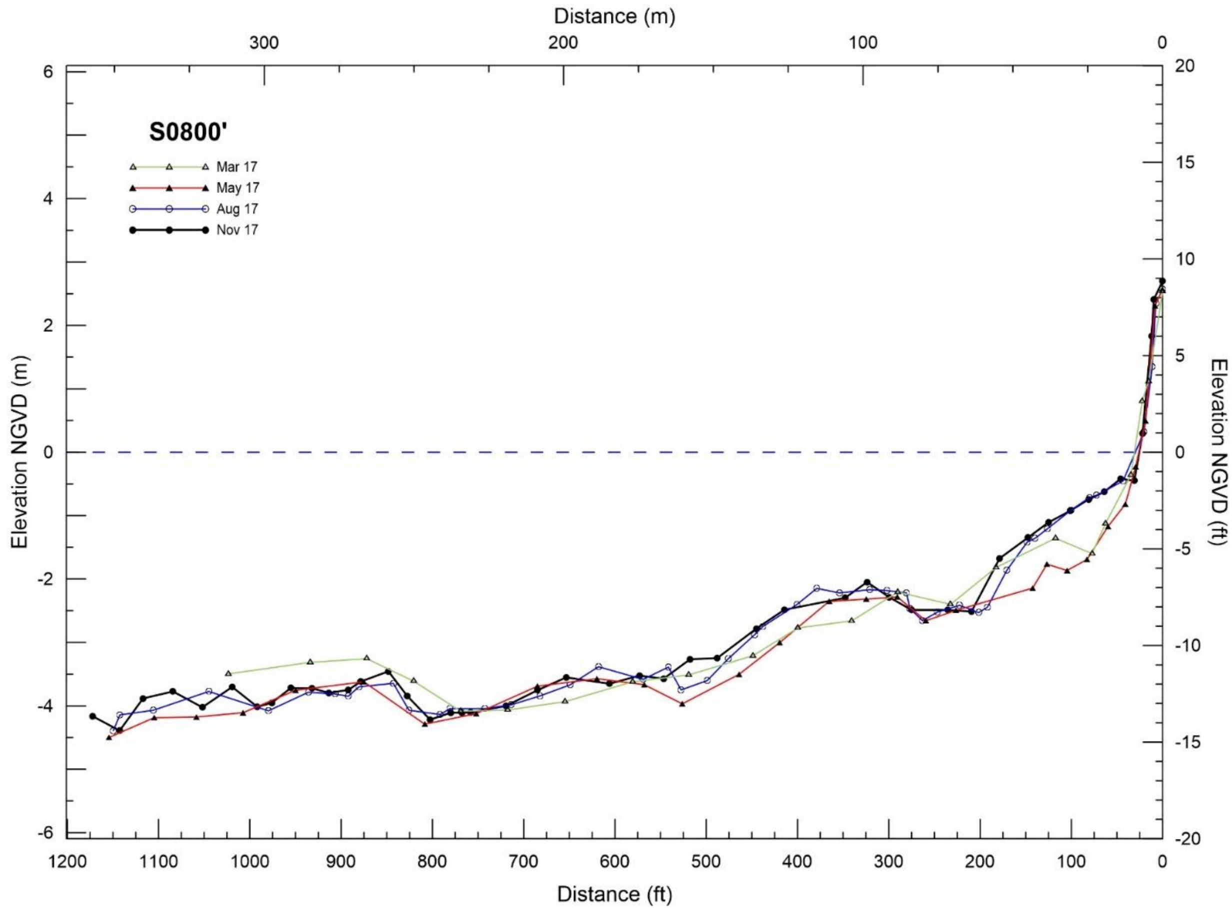

Figure A-5. 2017 Beach profile surveys of S0800'.

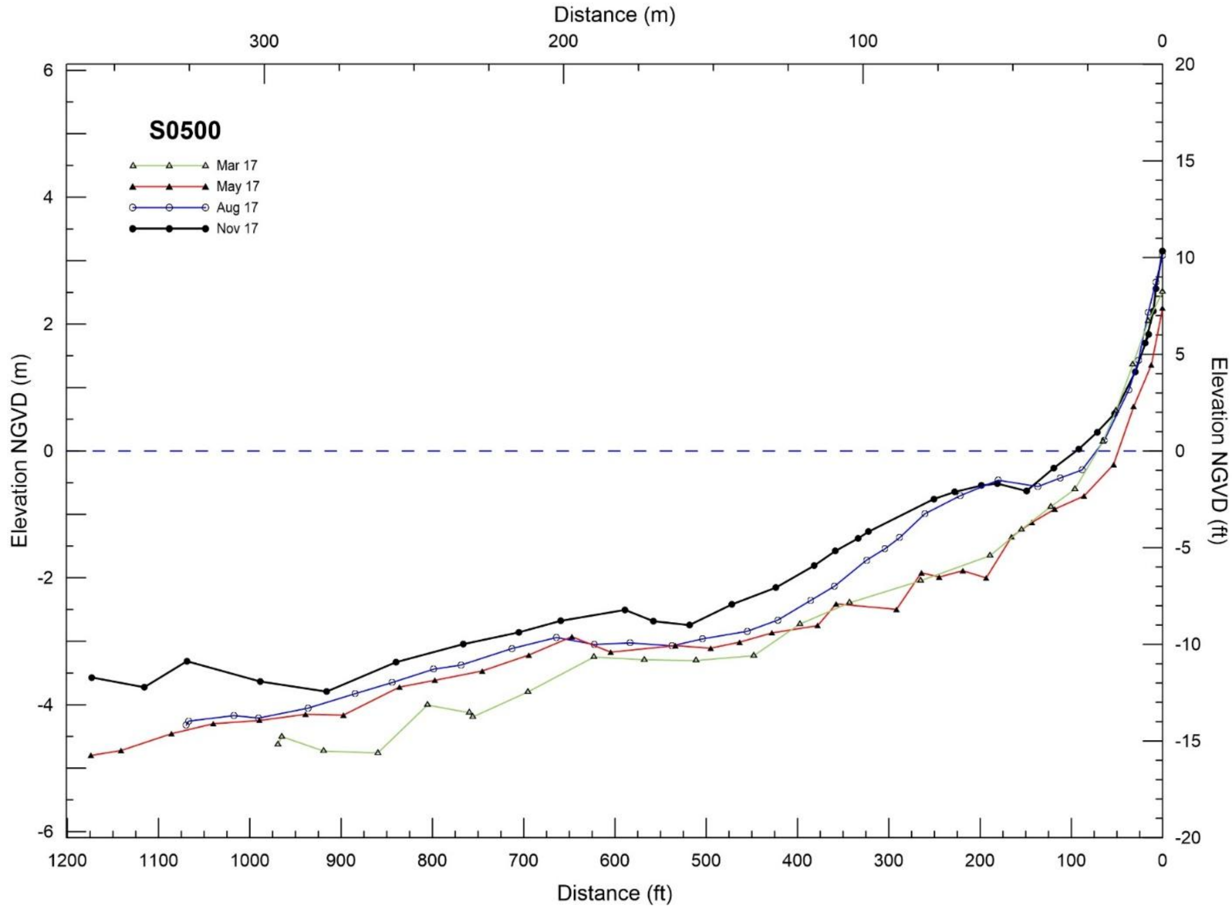

Figure A-6. 2017 Beach profile surveys of S0500.

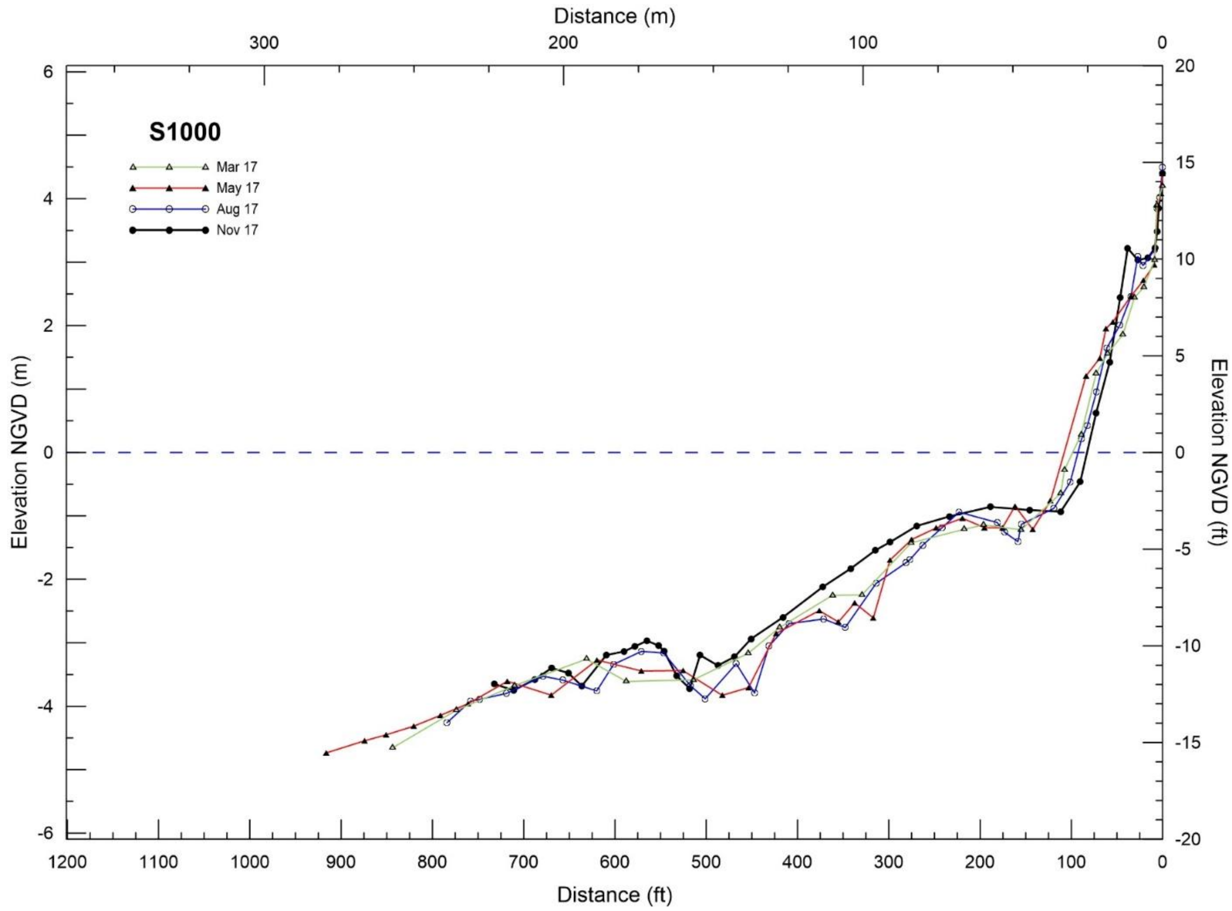

Figure A-7. 2017 Beach profile surveys of S1000.

APPENDIX B

2018 BEACH PROFILES

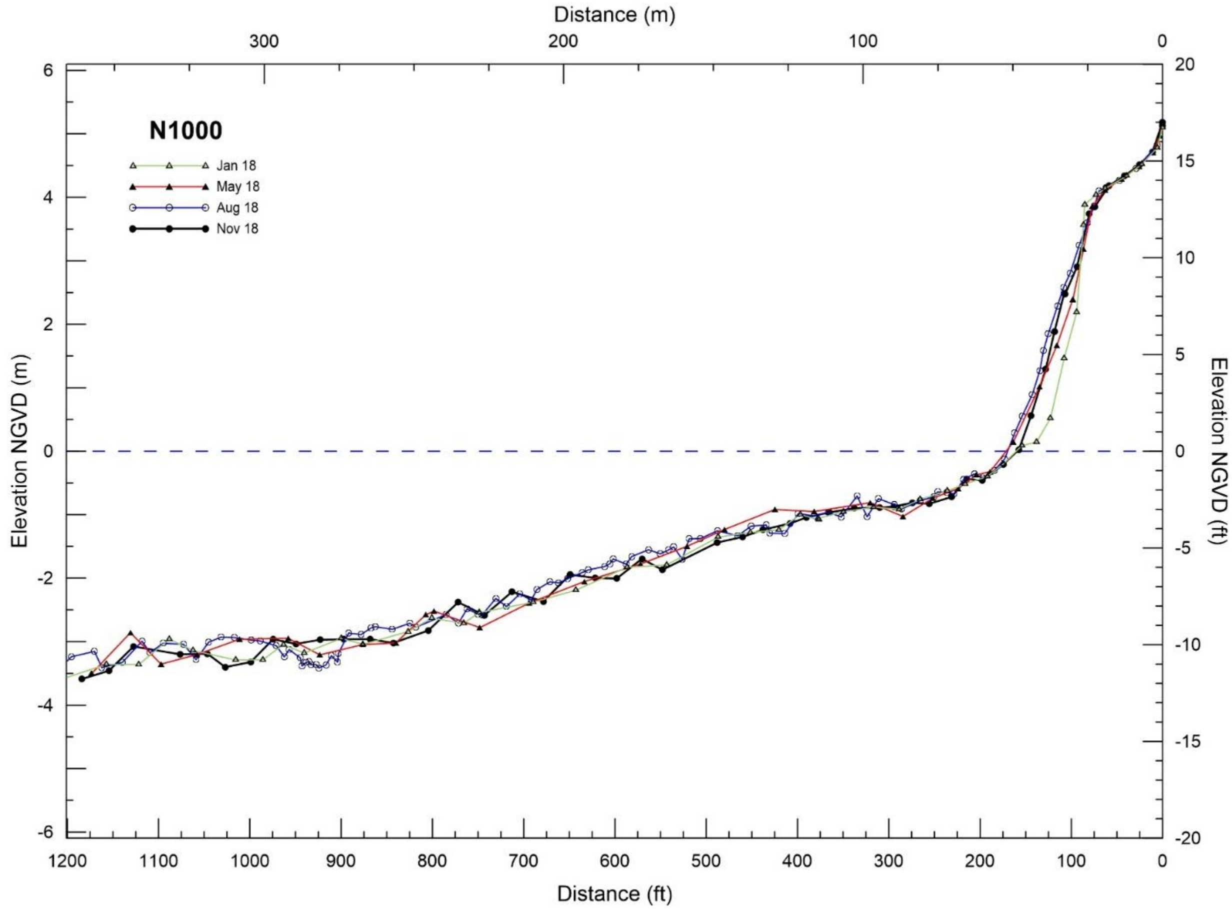

Figure B-1. 2018 Beach profile surveys of N1000.

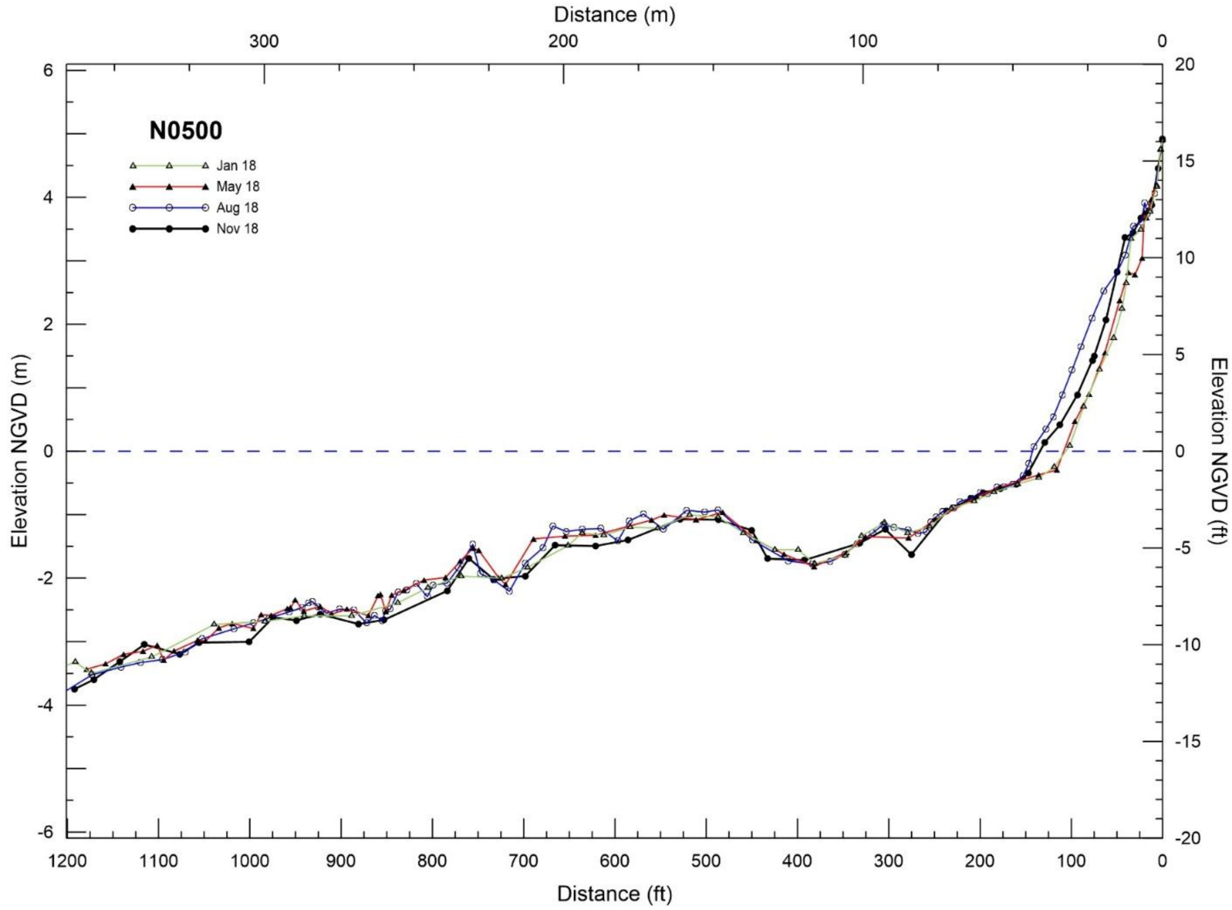

Figure B-2. 2018 Beach profile surveys of N0500.

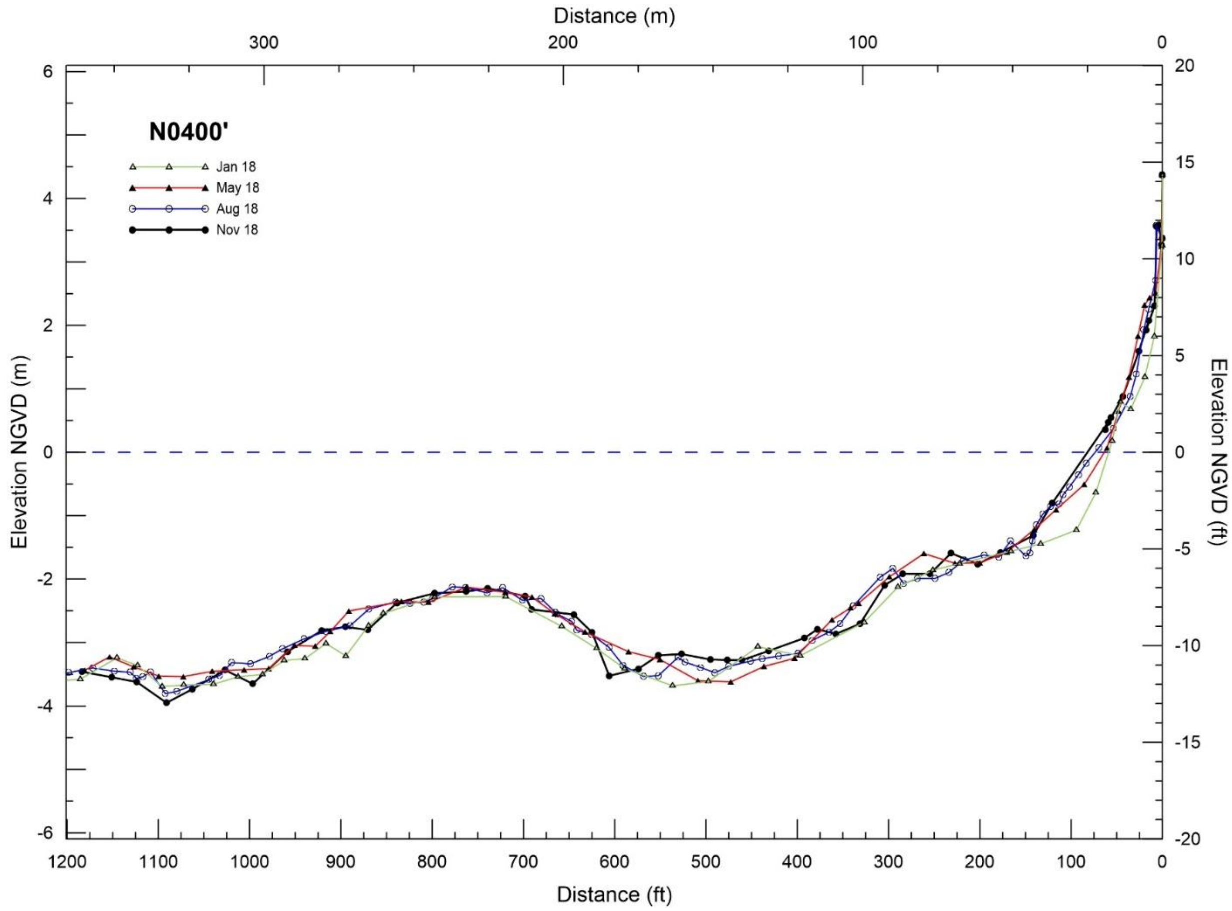

Figure B-3. 2018 Beach profile surveys of N0400'.

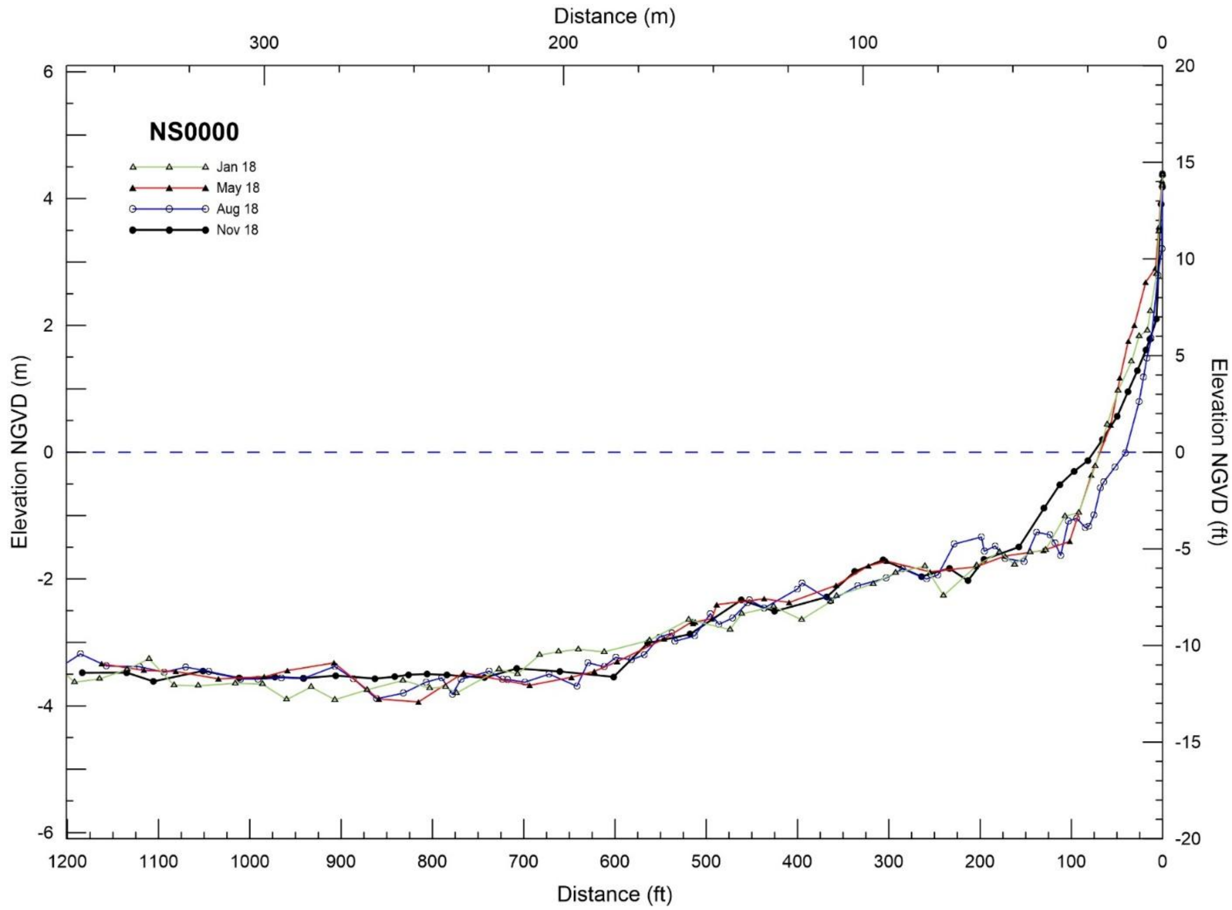

Figure B-4. 2018 Beach profile surveys of NS0000.

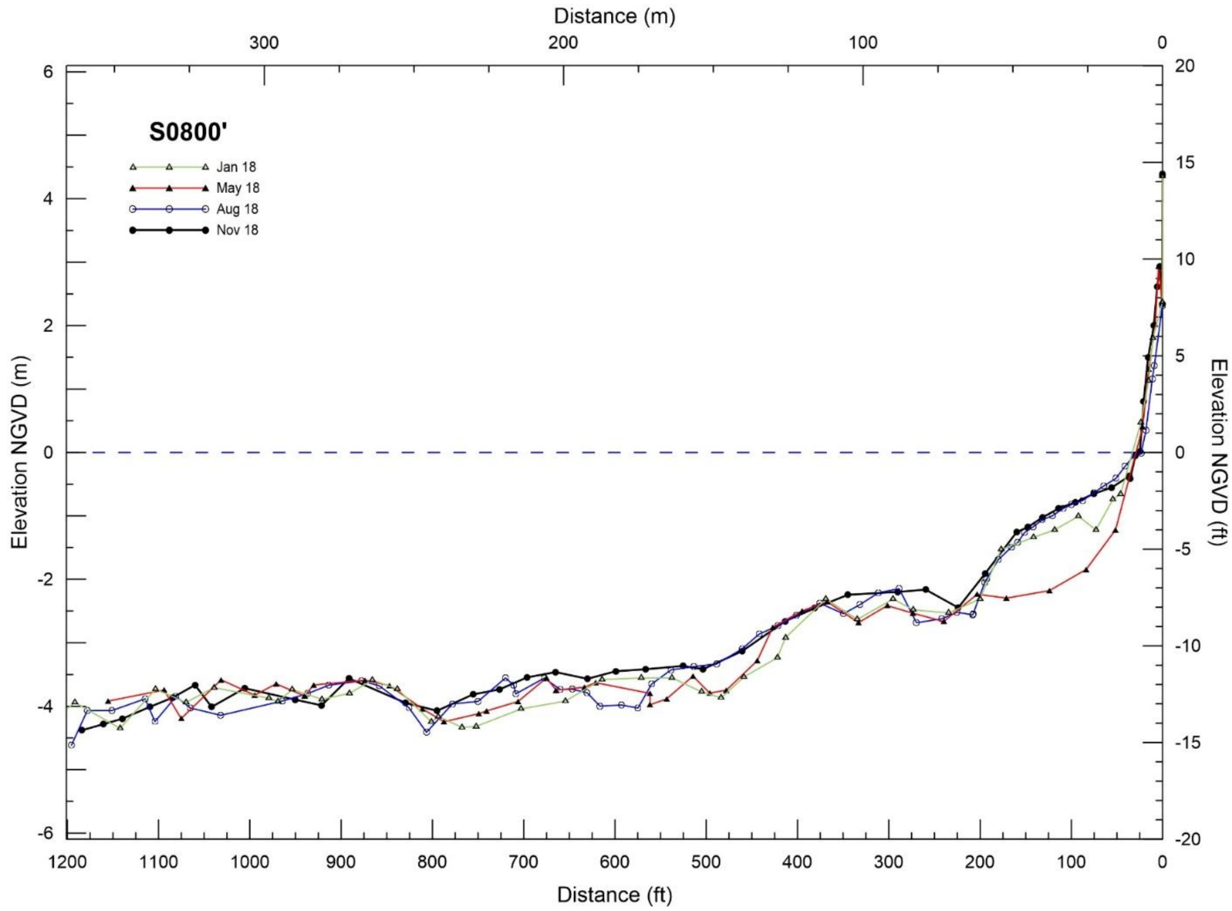

Figure B-5. 2018 Beach profile surveys of S0800'.

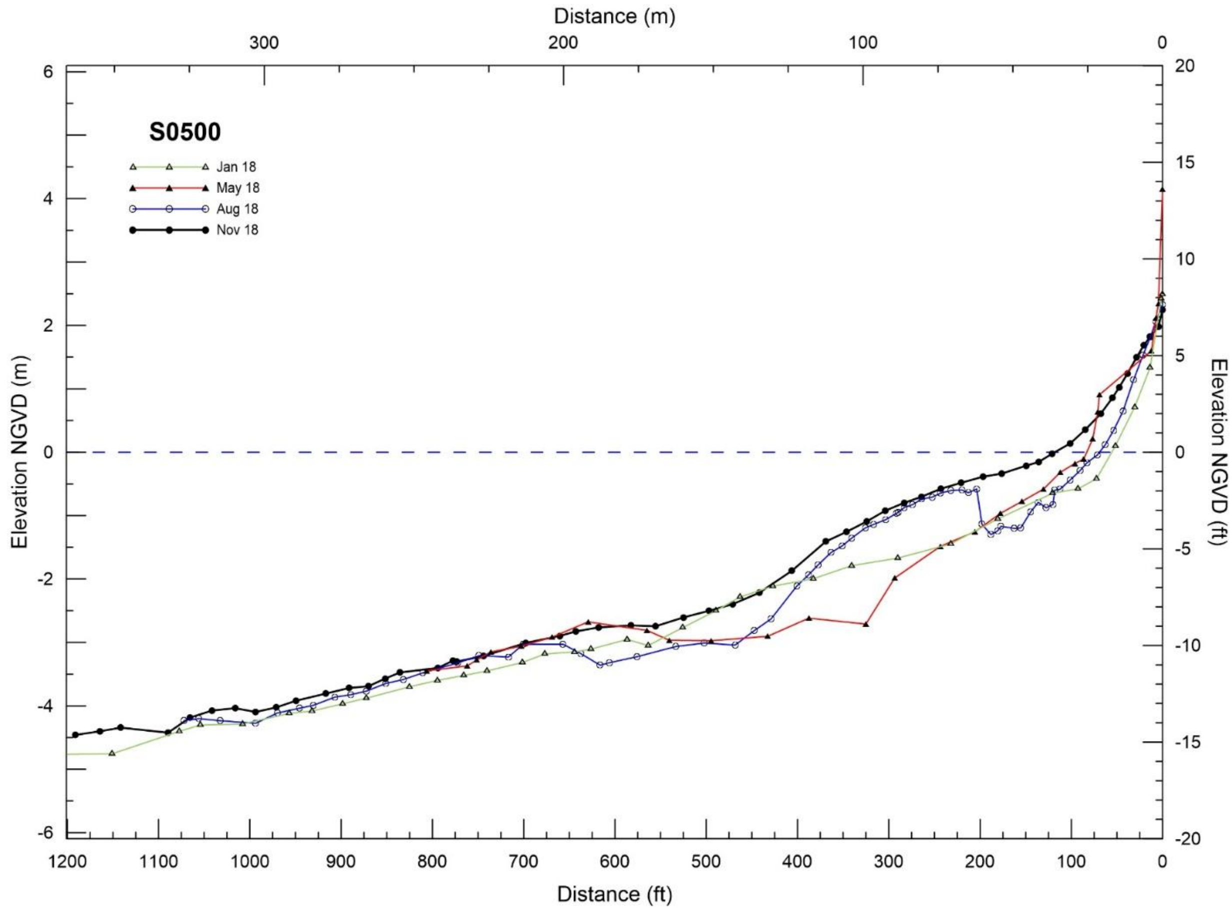

Figure B-6. 2018 Beach profile surveys of S0500.

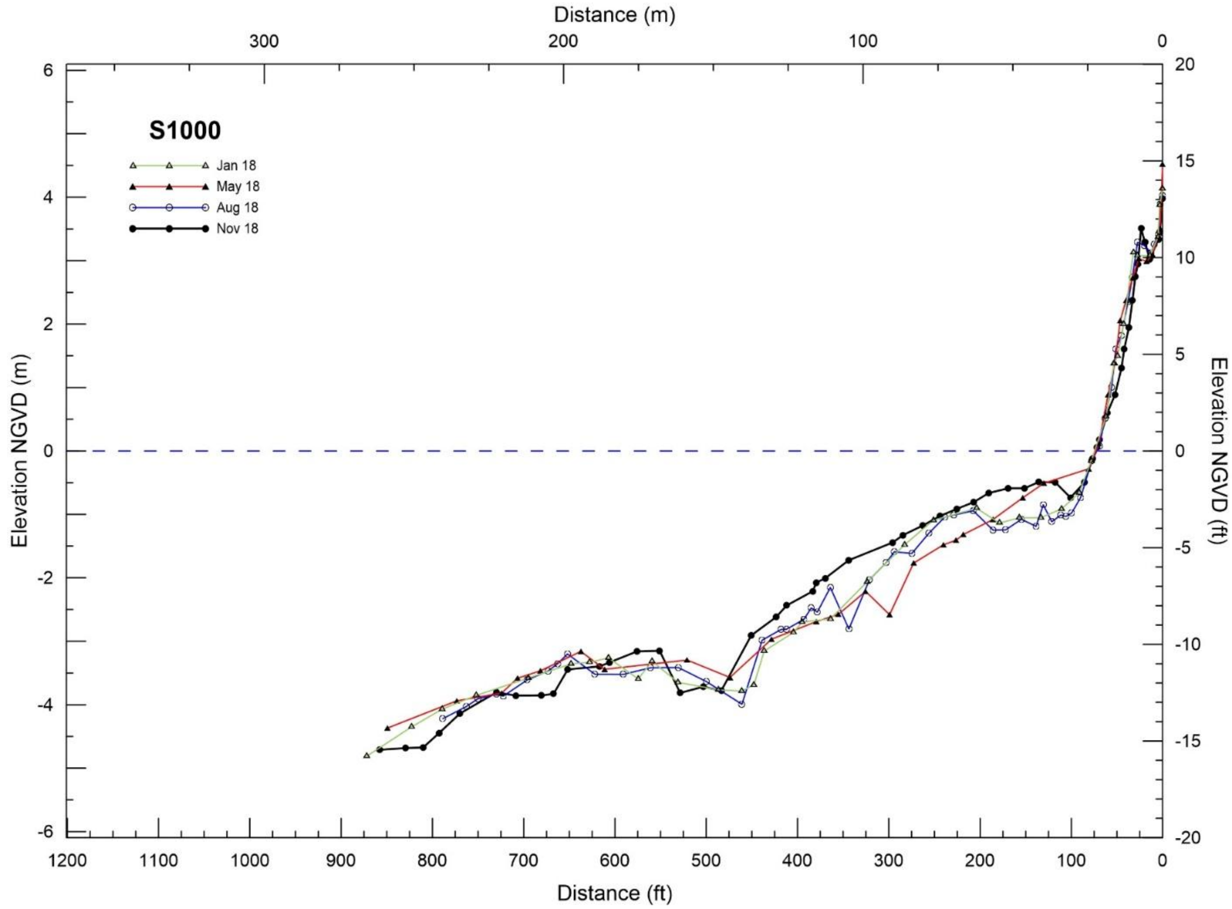

Figure B-7. 2018 Beach profile surveys of S1000.

APPENDIX C

2019 BEACH PROFILES

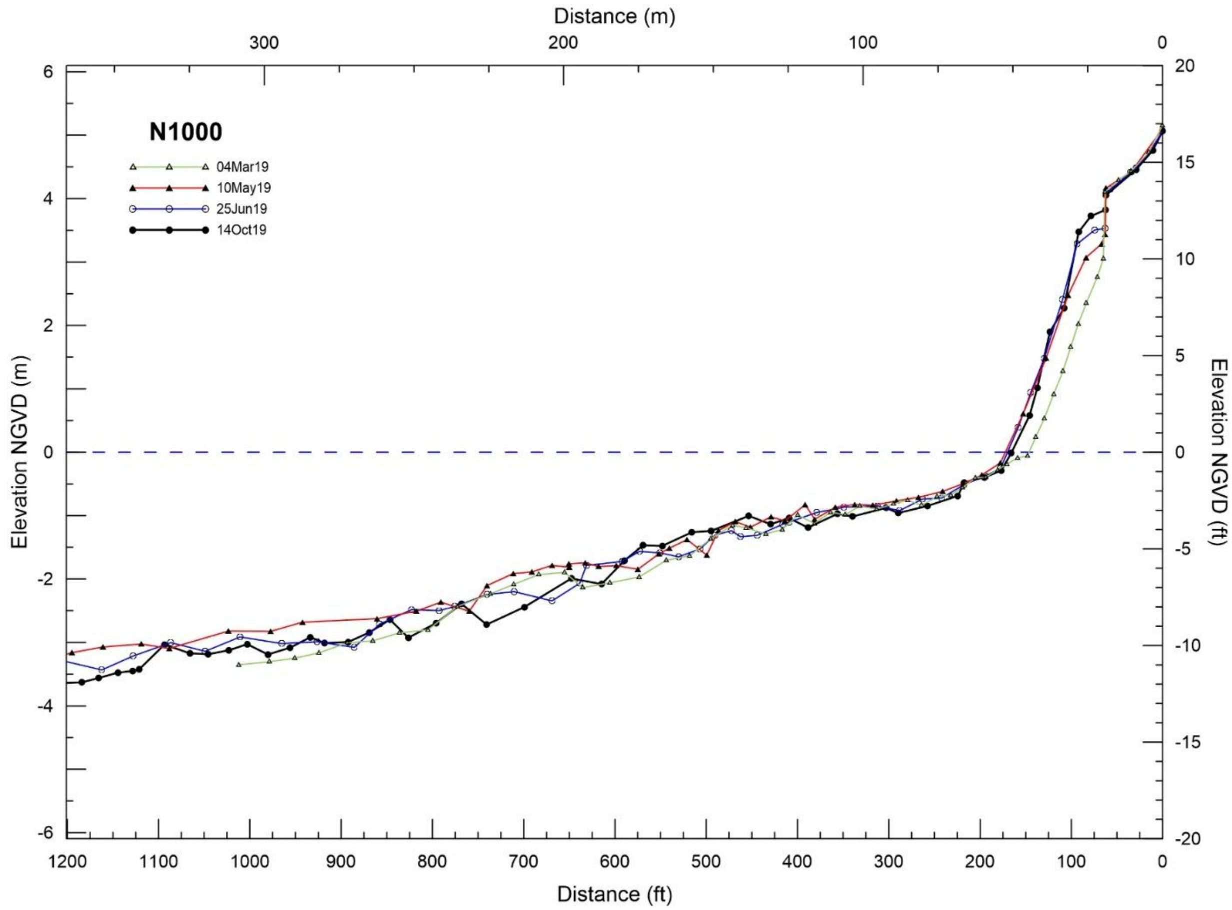

Figure C-1. 2019 Beach profile surveys of N1000.

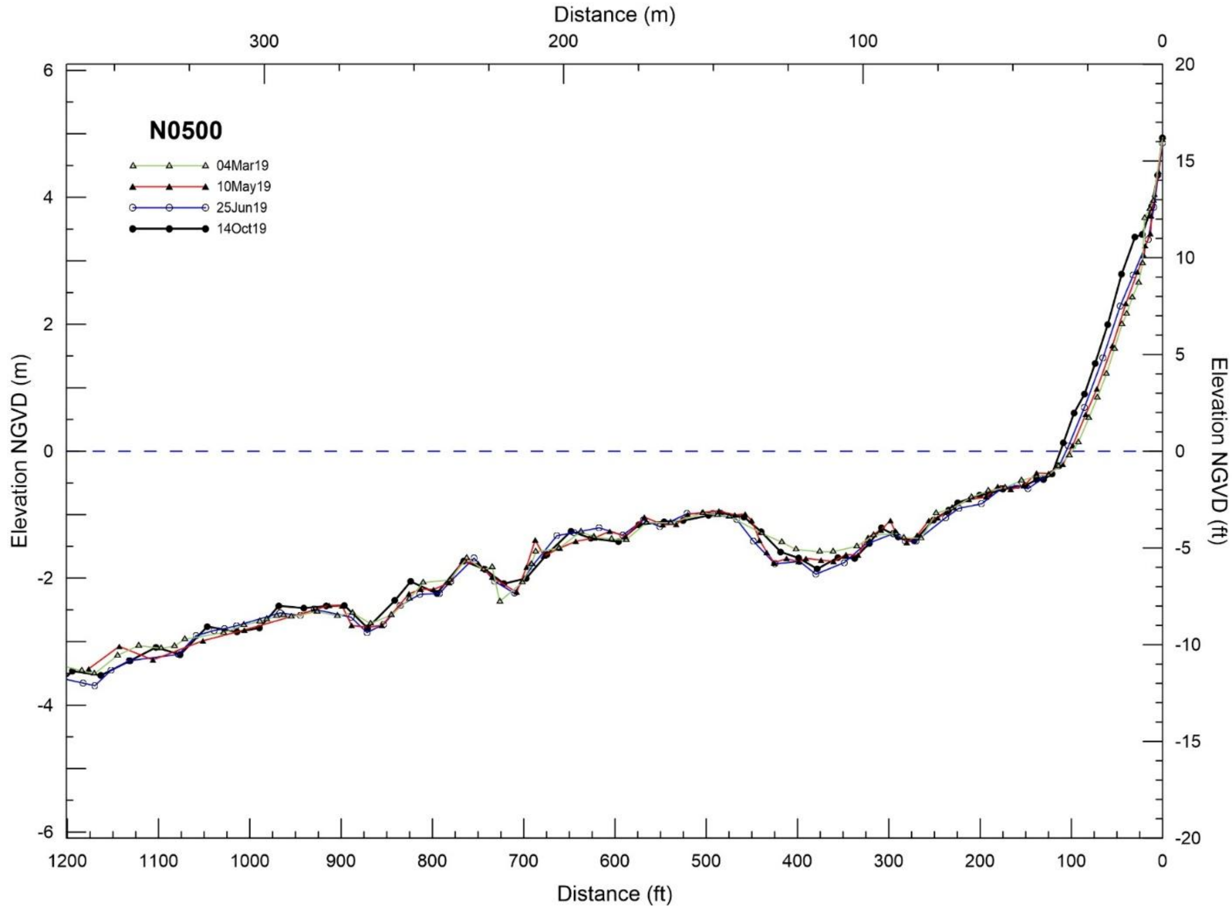

Figure C-2. 2019 Beach profile surveys of N0500.

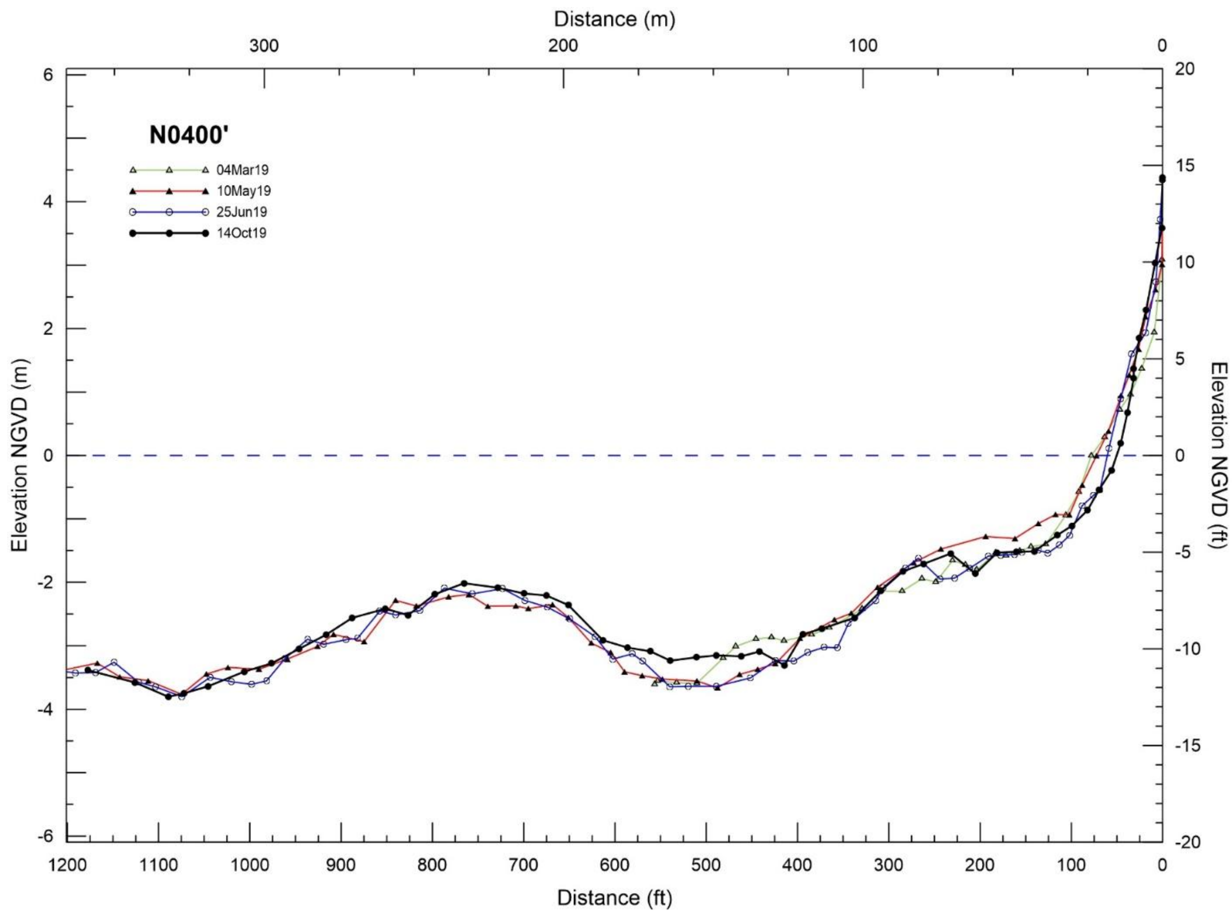

Figure C-3. 2019 Beach profile surveys of N0400'.

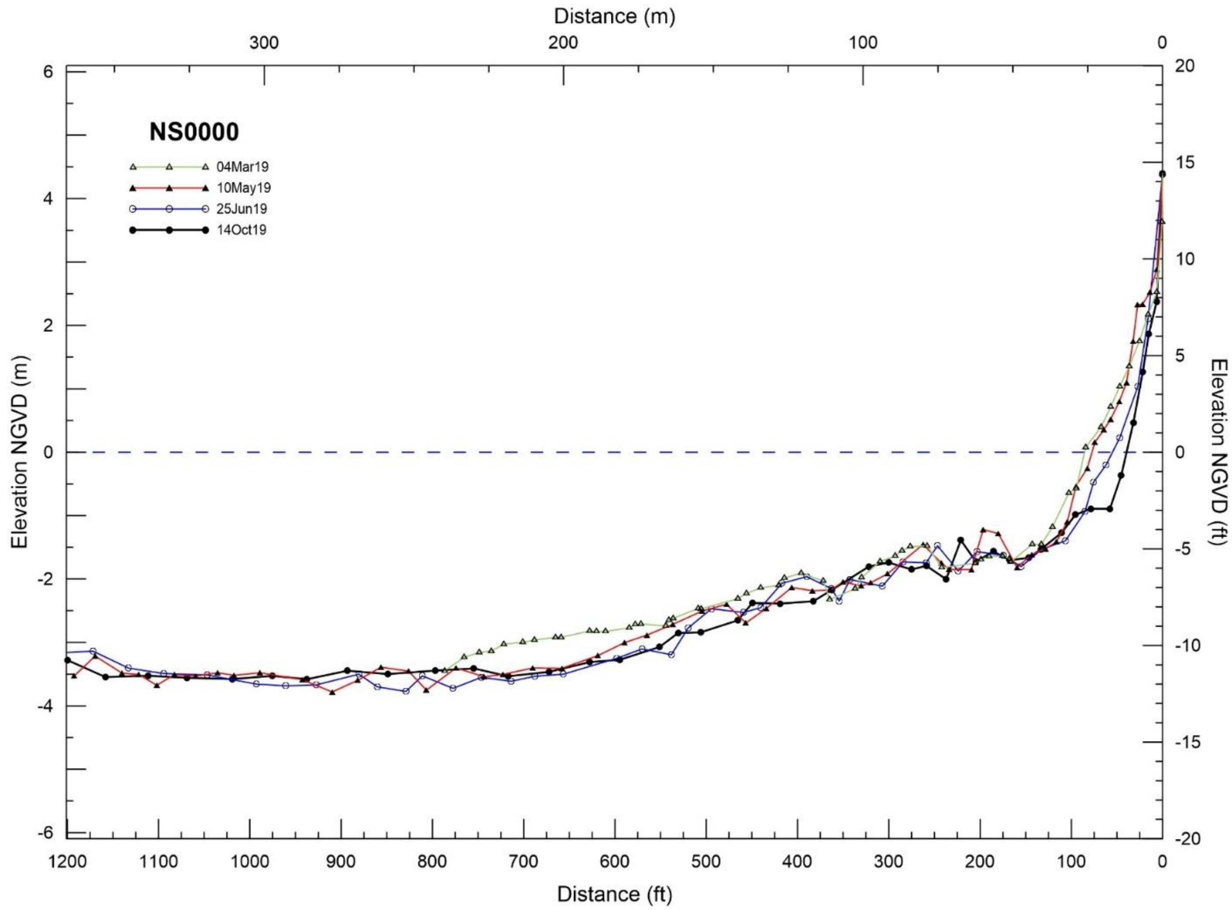

Figure C-4. 2019 Beach profile surveys of NS0000.

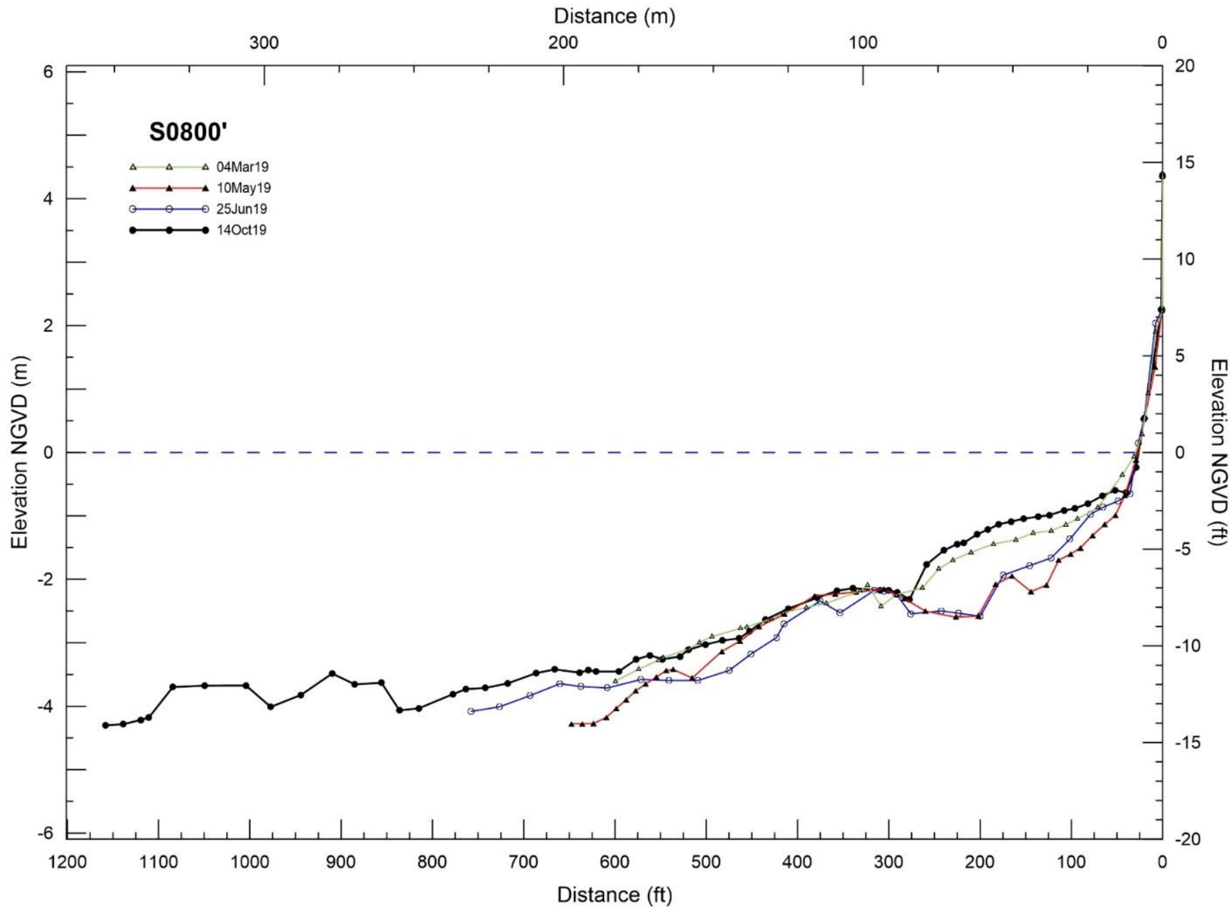

Figure C-5. 2019 Beach profile surveys of S0800'.

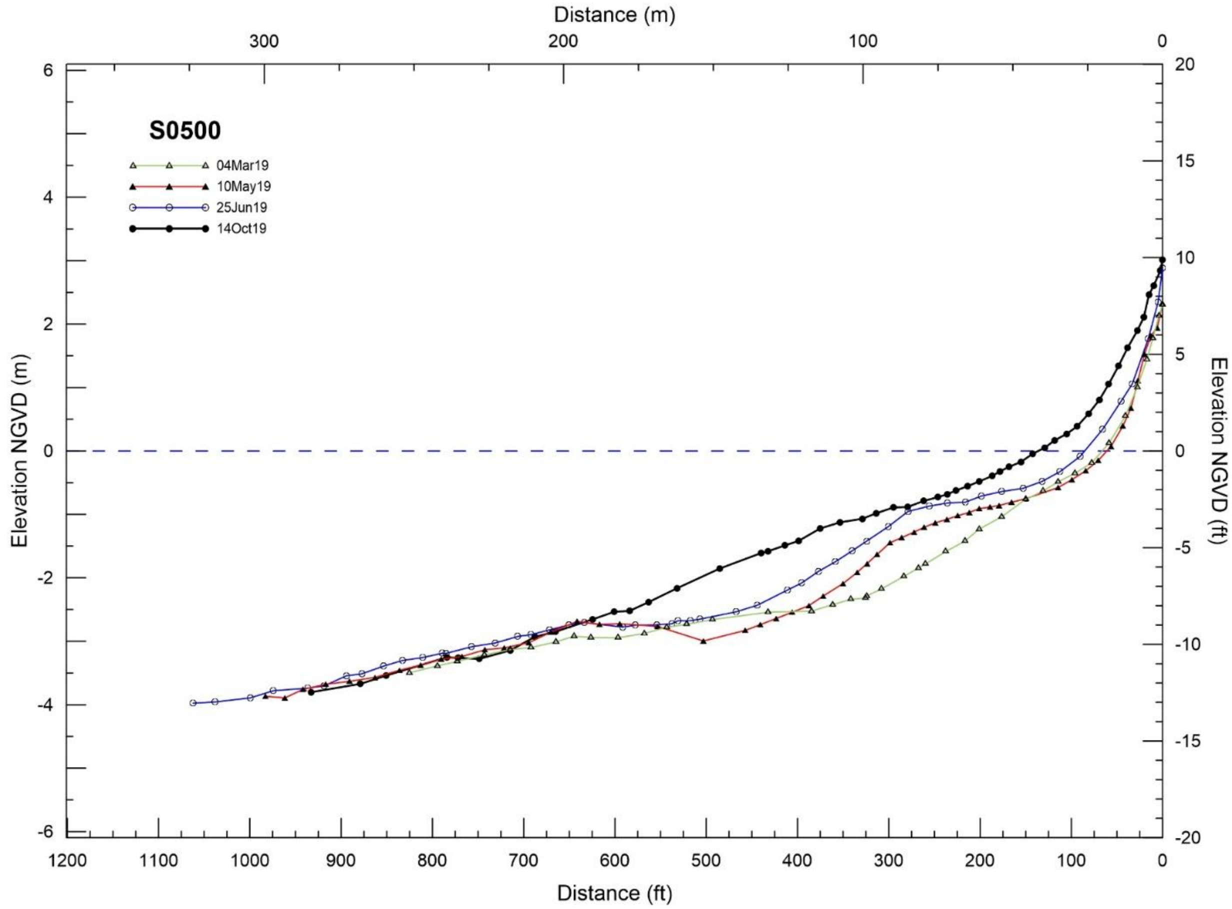

Figure C-6. 2019 Beach profile surveys of S0500.

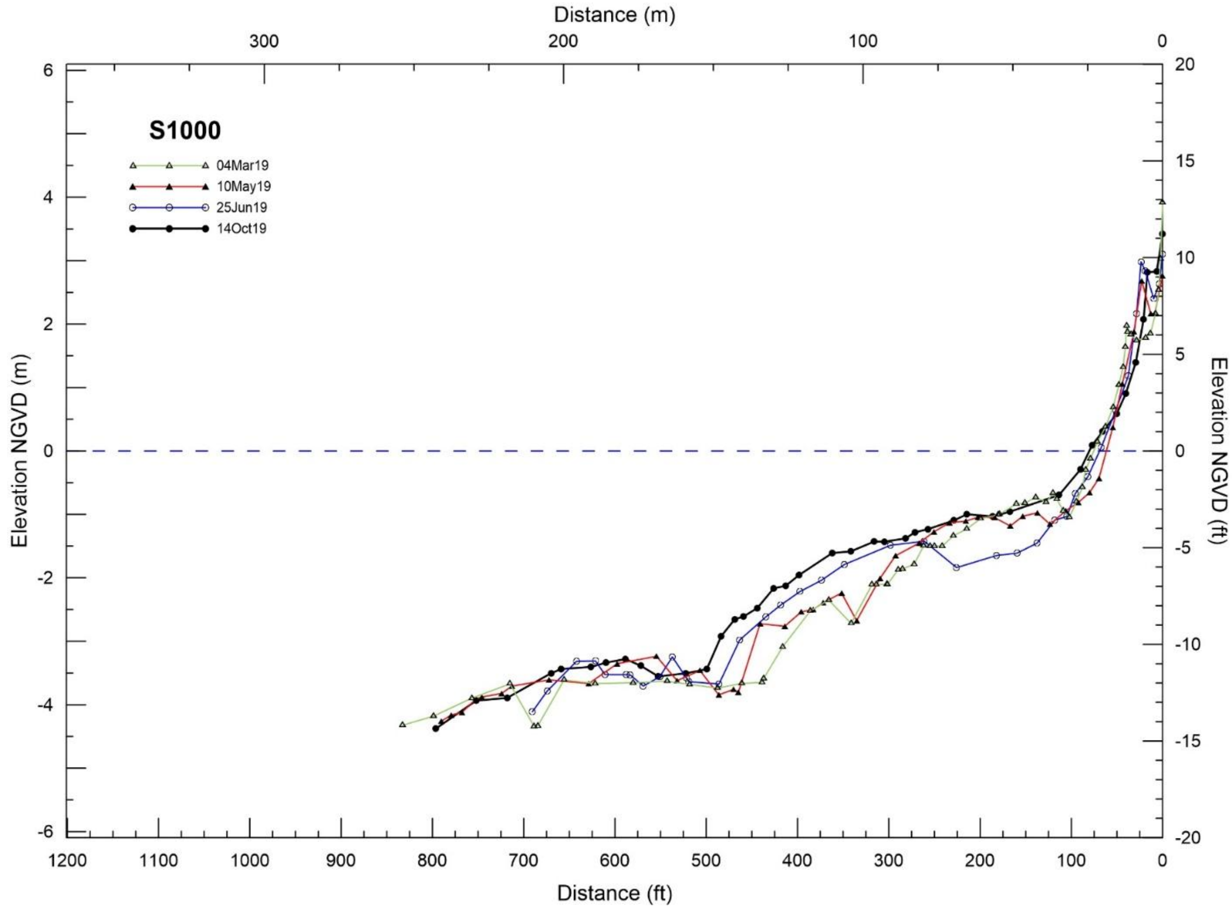

Figure C-7. 2019 Beach profile surveys of S1000.

APPENDIX D

OFFSHORE BEACH PROFILES

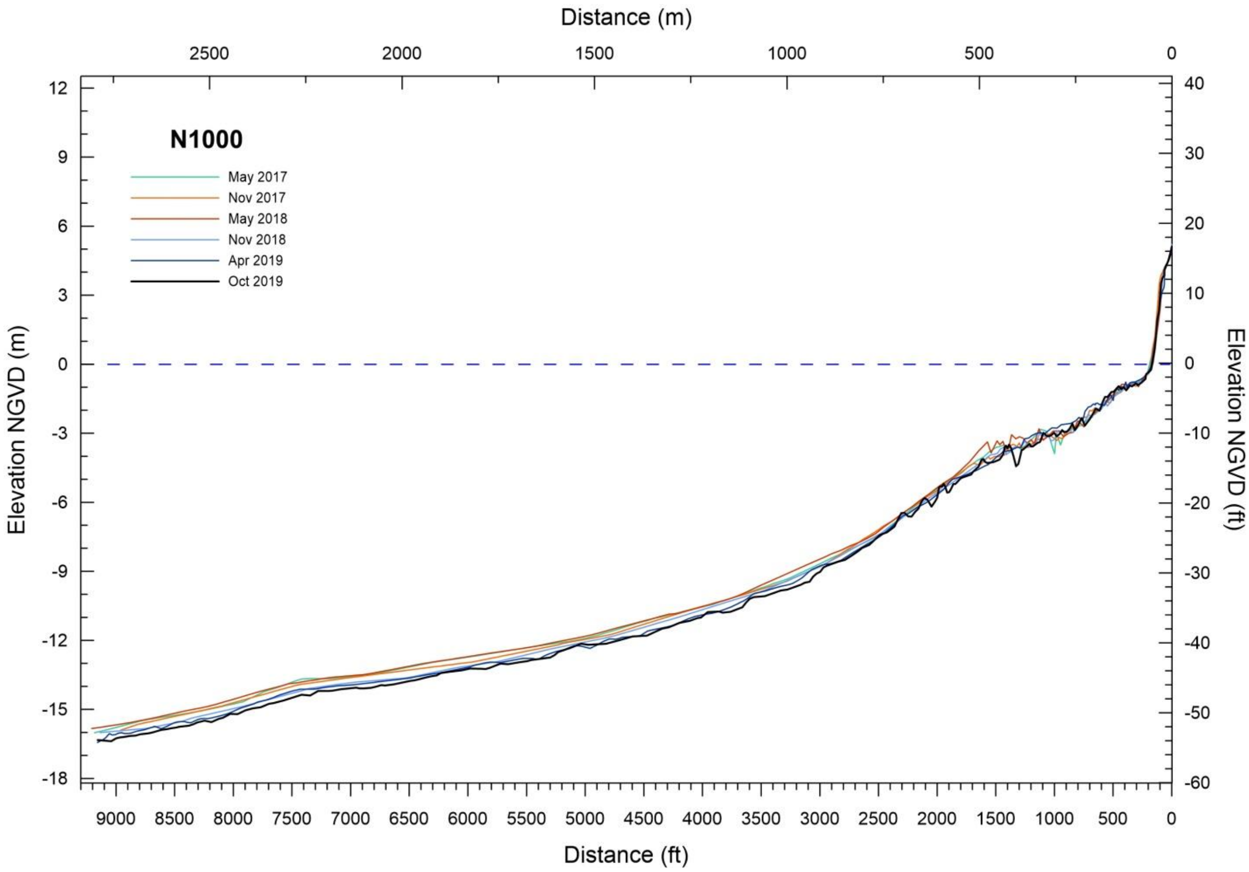

Figure D-1. Offshore Beach profile surveys of N1000.

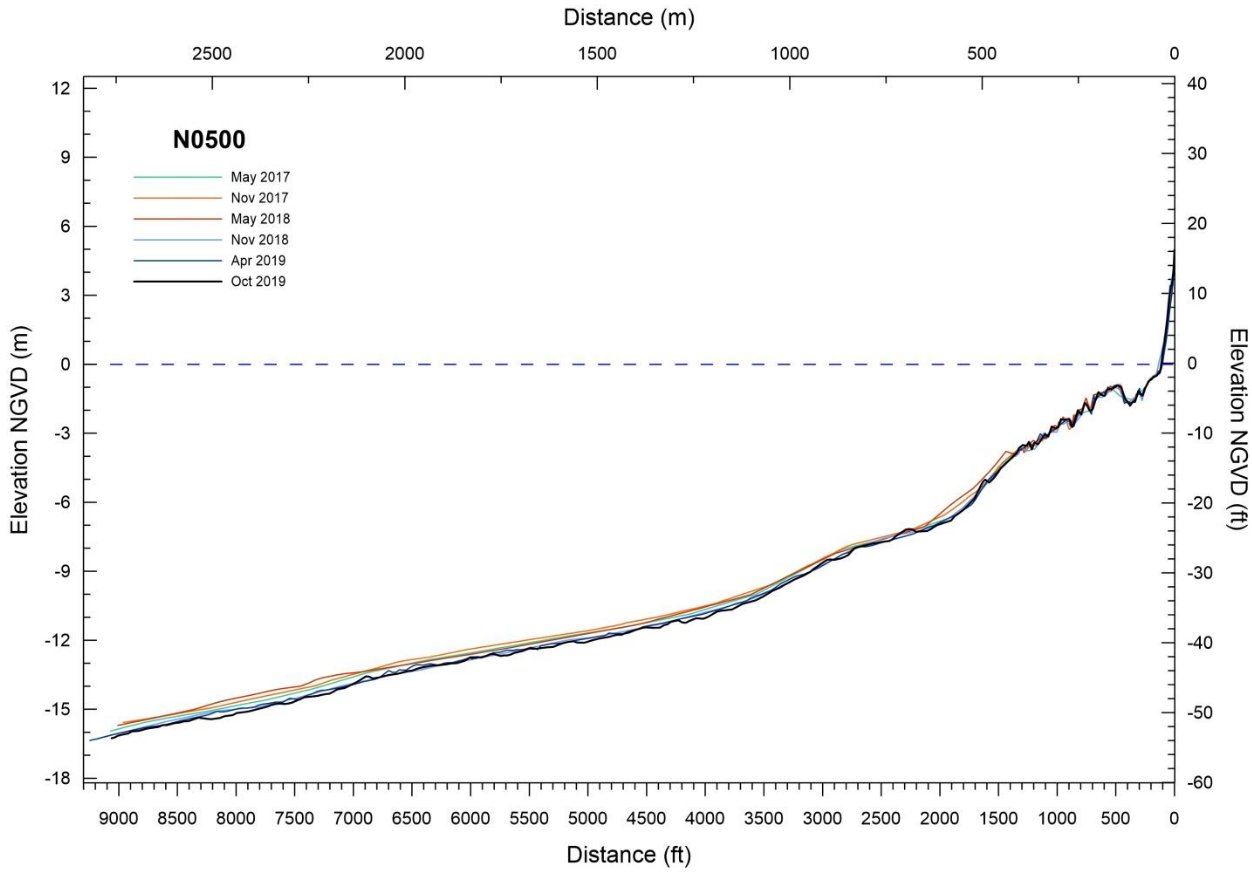

Figure D-2. Offshore Beach profile surveys of N0500.

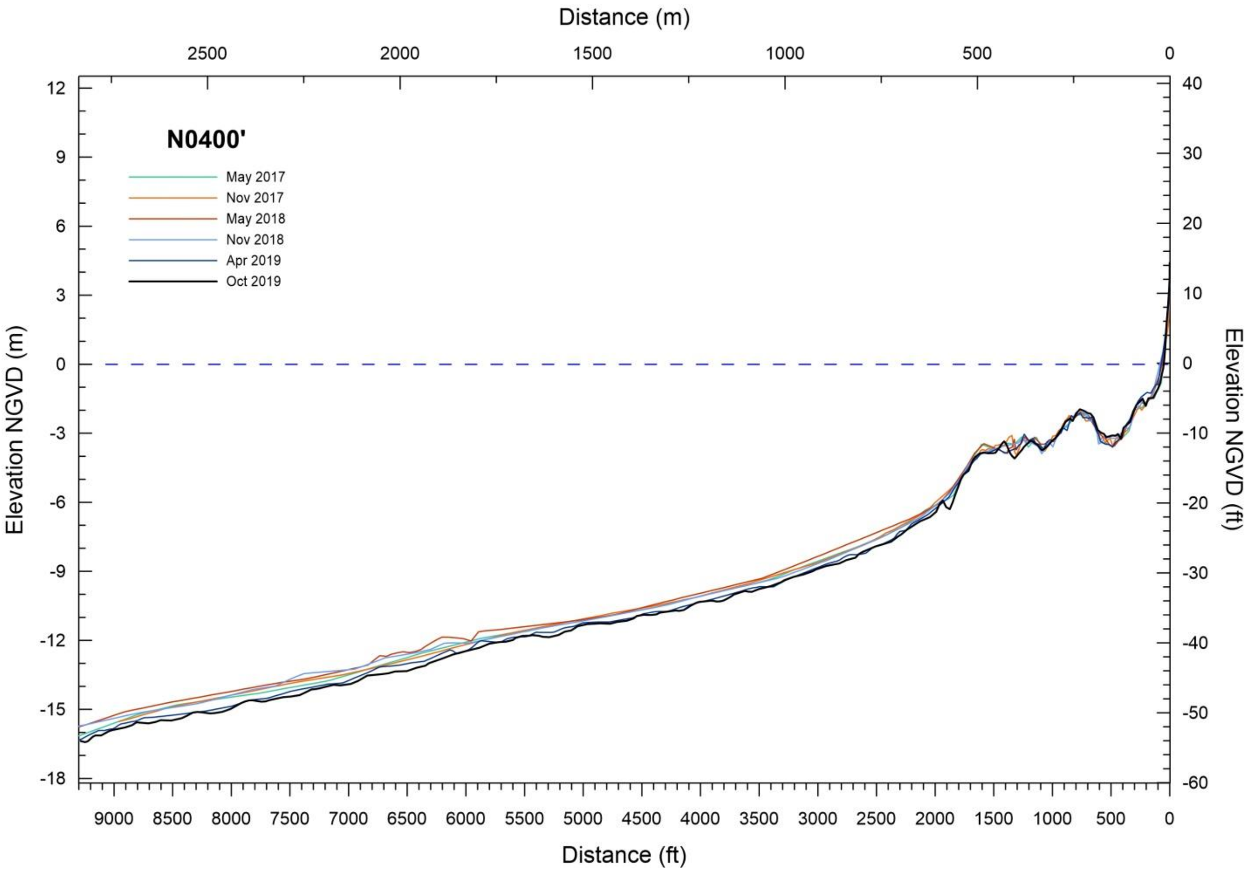

Figure D-3. Offshore Beach profile surveys of N0400'.

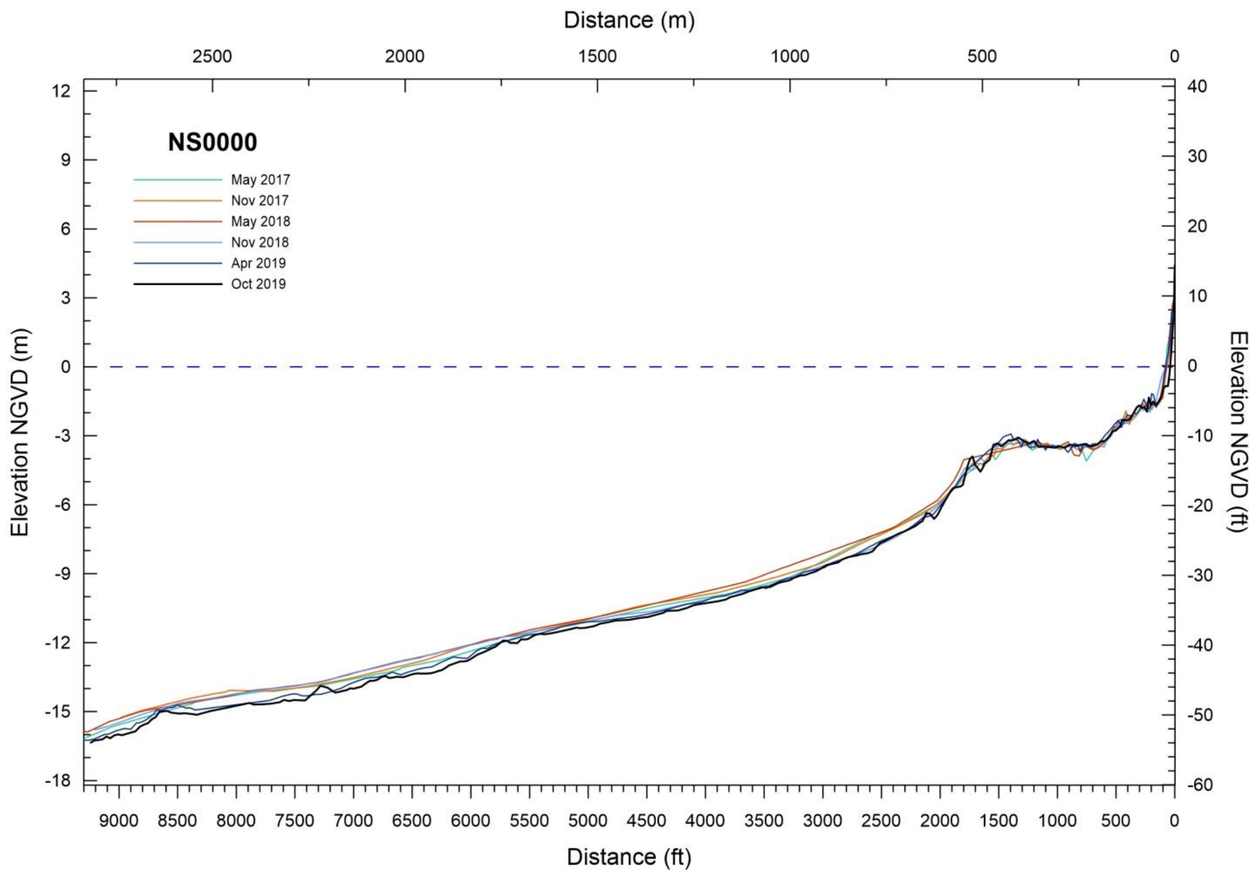

Figure D-4. Offshore Beach profile surveys of NS0000.

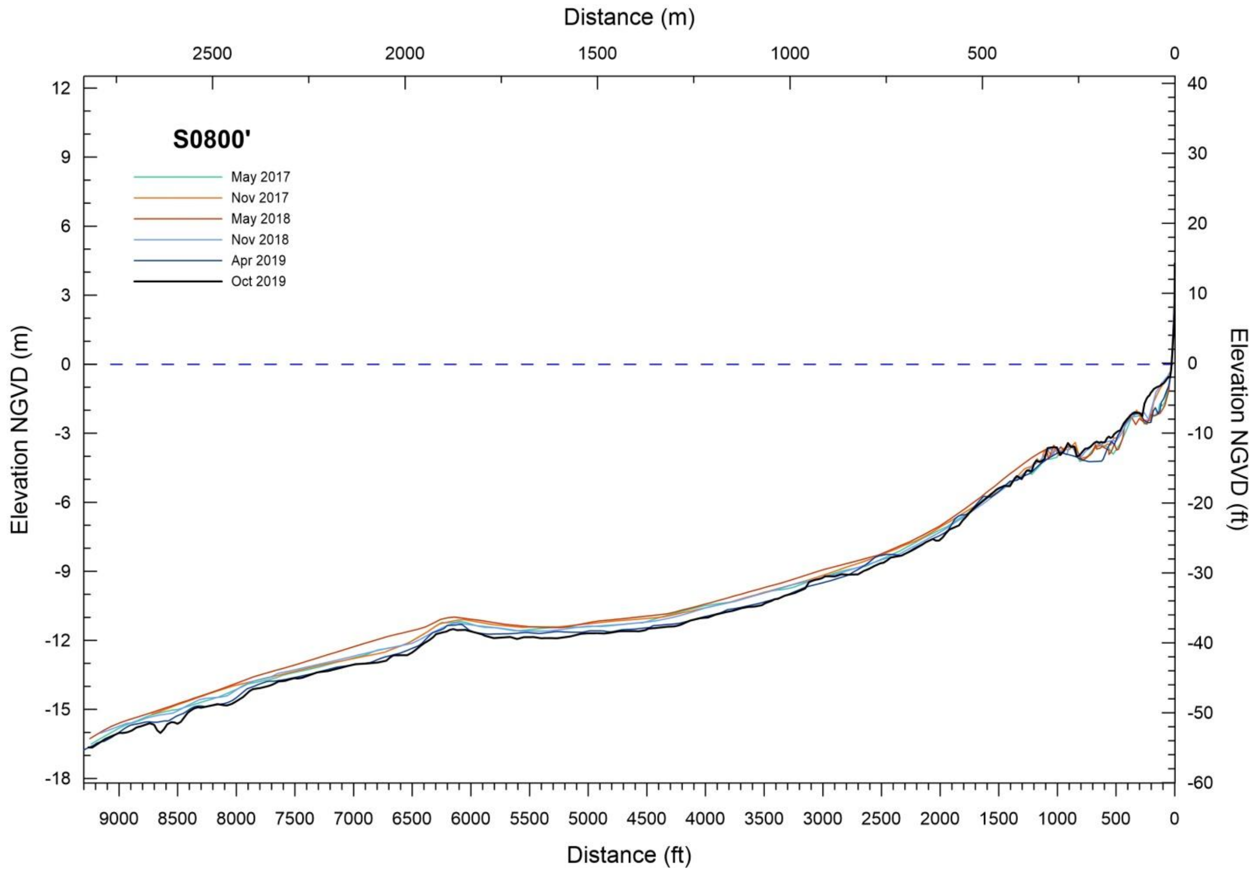

Figure D-5. Offshore Beach profile surveys of S0800'.

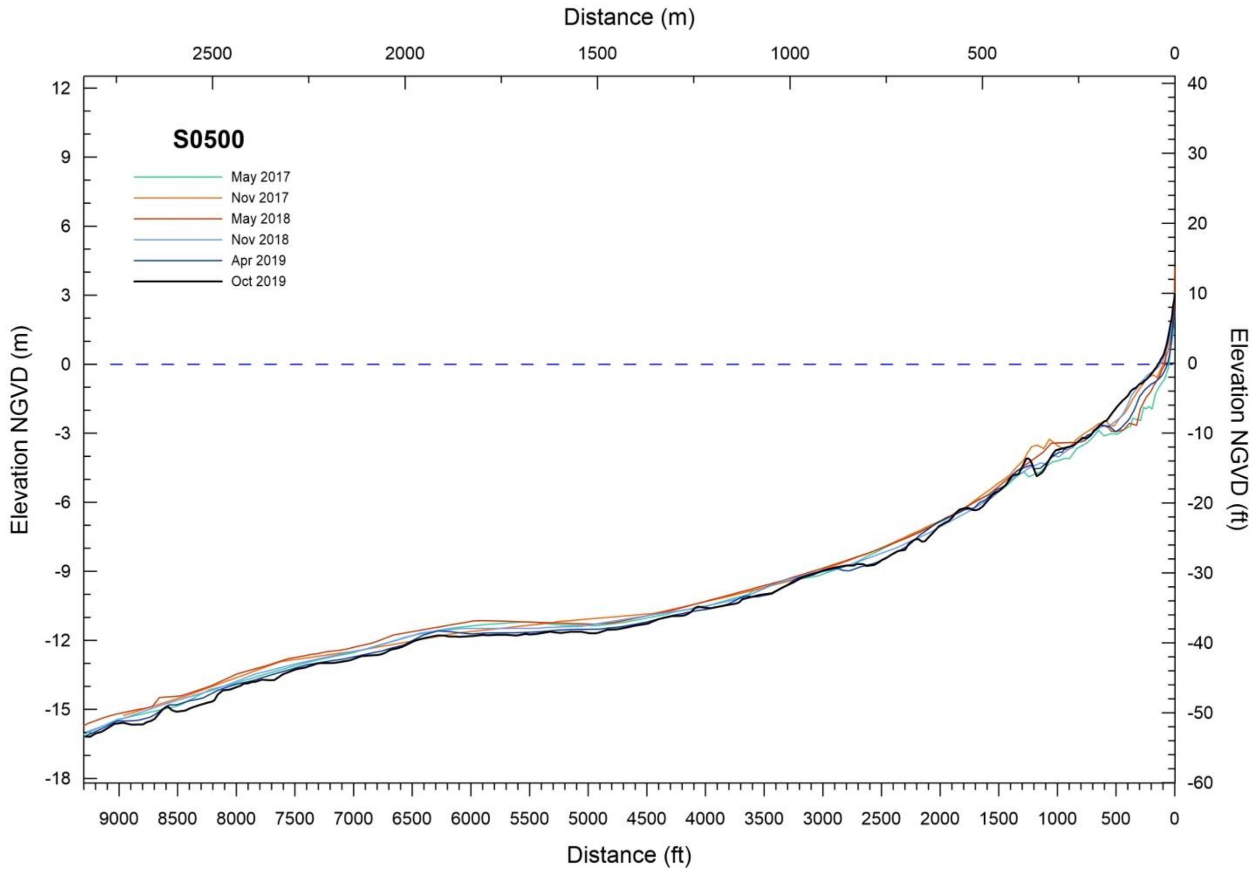

Figure D-6. Offshore Beach profile surveys of S0500.

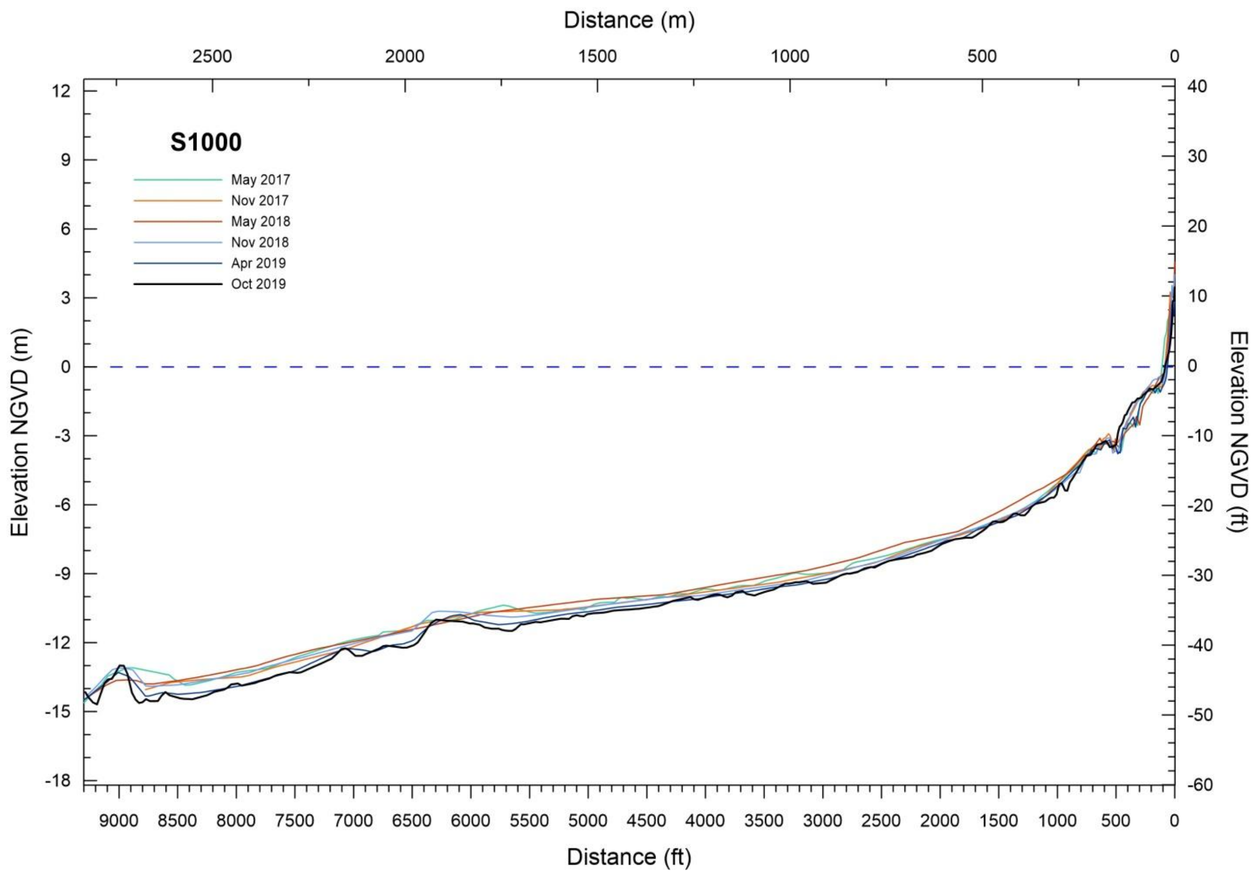

Figure D-7. Offshore Beach profile surveys of S1000.

APPENDIX E

AERIAL PHOTOGRAPHS
NORTH AND SOUTH SONGS

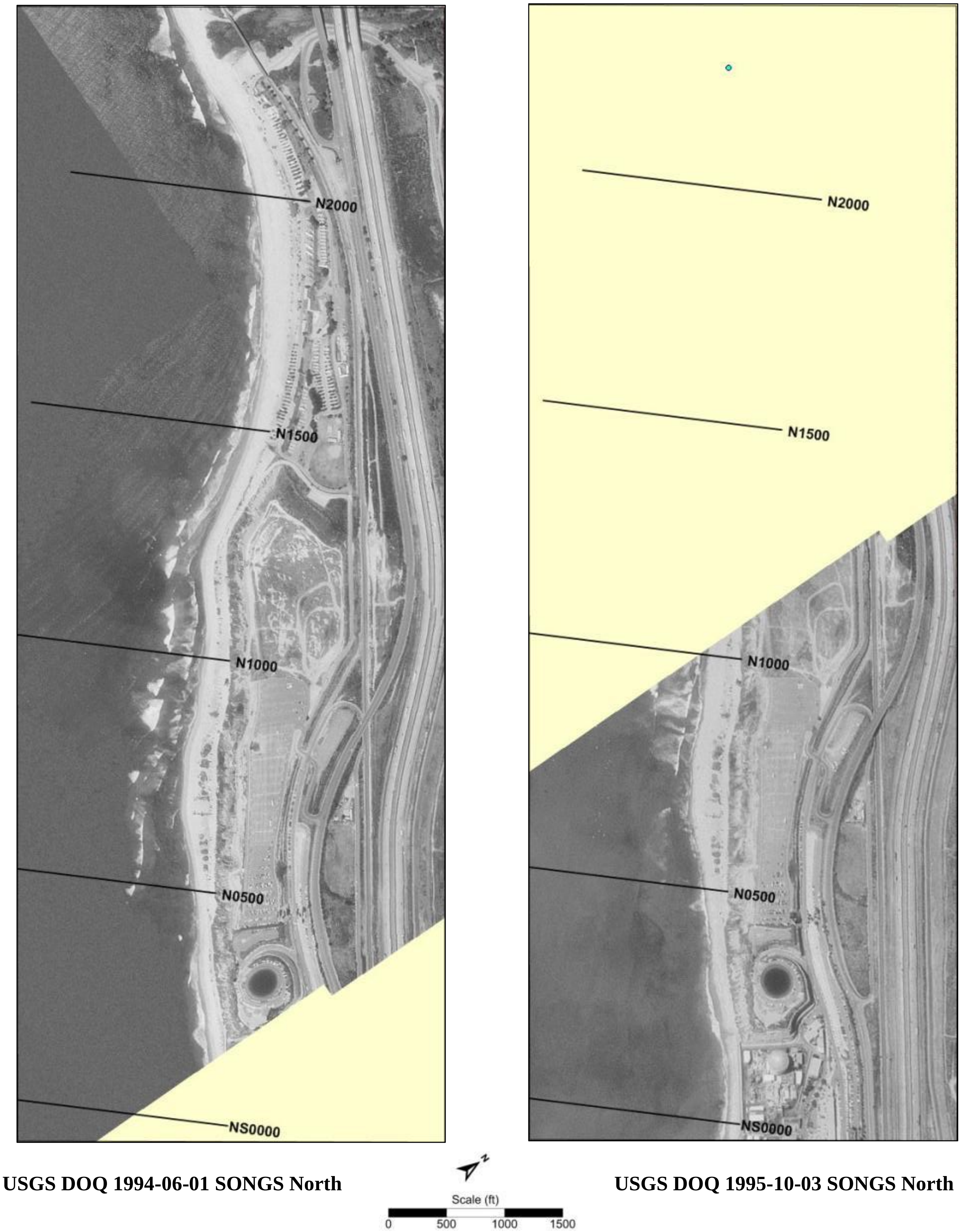

Figure E-1. Photographs taken in 1994 (left) and 1995 (right), showing an aerial perspective of the beach North of SONGS.

USGS DOQ 1994-06-01 SONGS South

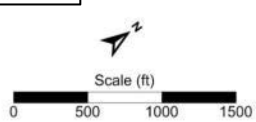

USGS DOQ 1995-10-03 SONGS South

Figure E-2. Photographs taken in 1994 (left unavailable) and 1995 (right), showing an aerial perspective of the beach South of SONGS.

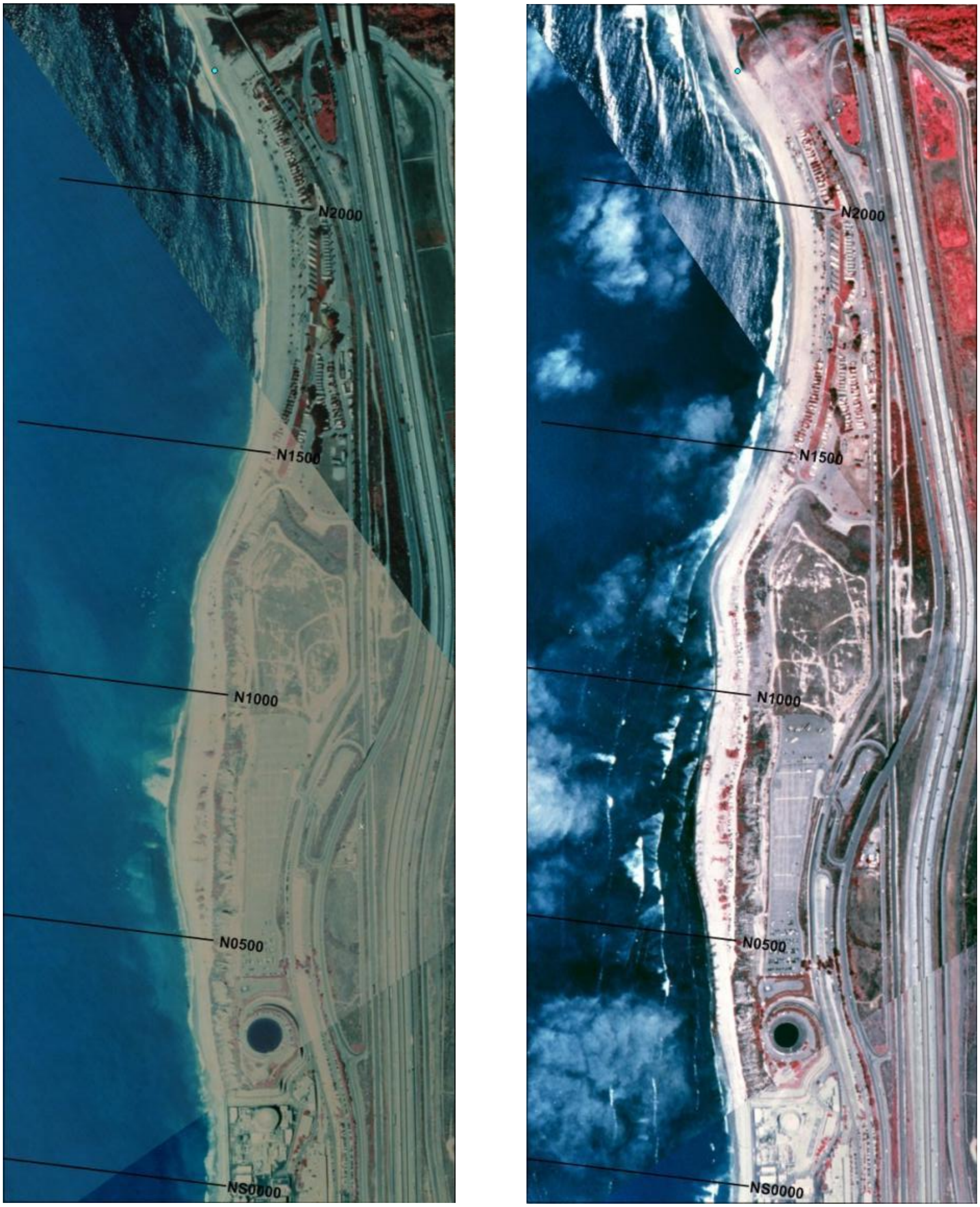

USGS DOQ 1997-10-16 SONGS North **USGS DOQ 2002-06-15 SONGS North**

N

Scale (ft)

0 500 1000 1500

Figure E-3. Photographs taken in 1997 (left) and 2002 (right), showing an aerial perspective of the beach North of SONGS.

USGS DOQ 1997-10-16 SONGS South

Scale (ft)
0 500 1000 1500

USGS DOQ 2002-06-15 SONGS South

Figure E-4. Photographs taken in 1997 (left) and 2002 (right), showing an aerial perspective of the beach South of SONGS.

USGS HRO 2003-03-01 SONGS North

USGS HRO 2003-11-18 SONGS North

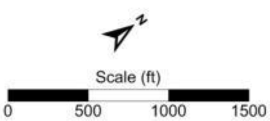

Figure E-5. Photographs taken in 2003, showing an aerial perspective of the beach North of SONGS.

USGS HRO 2003-03-01 SONGS South

USGS HRO 2003-11-18 SONGS South

Scale (ft)
0 500 1000 1500

Figure E-6. Photographs taken in 2003, showing an aerial perspective of the beach South of SONGS.

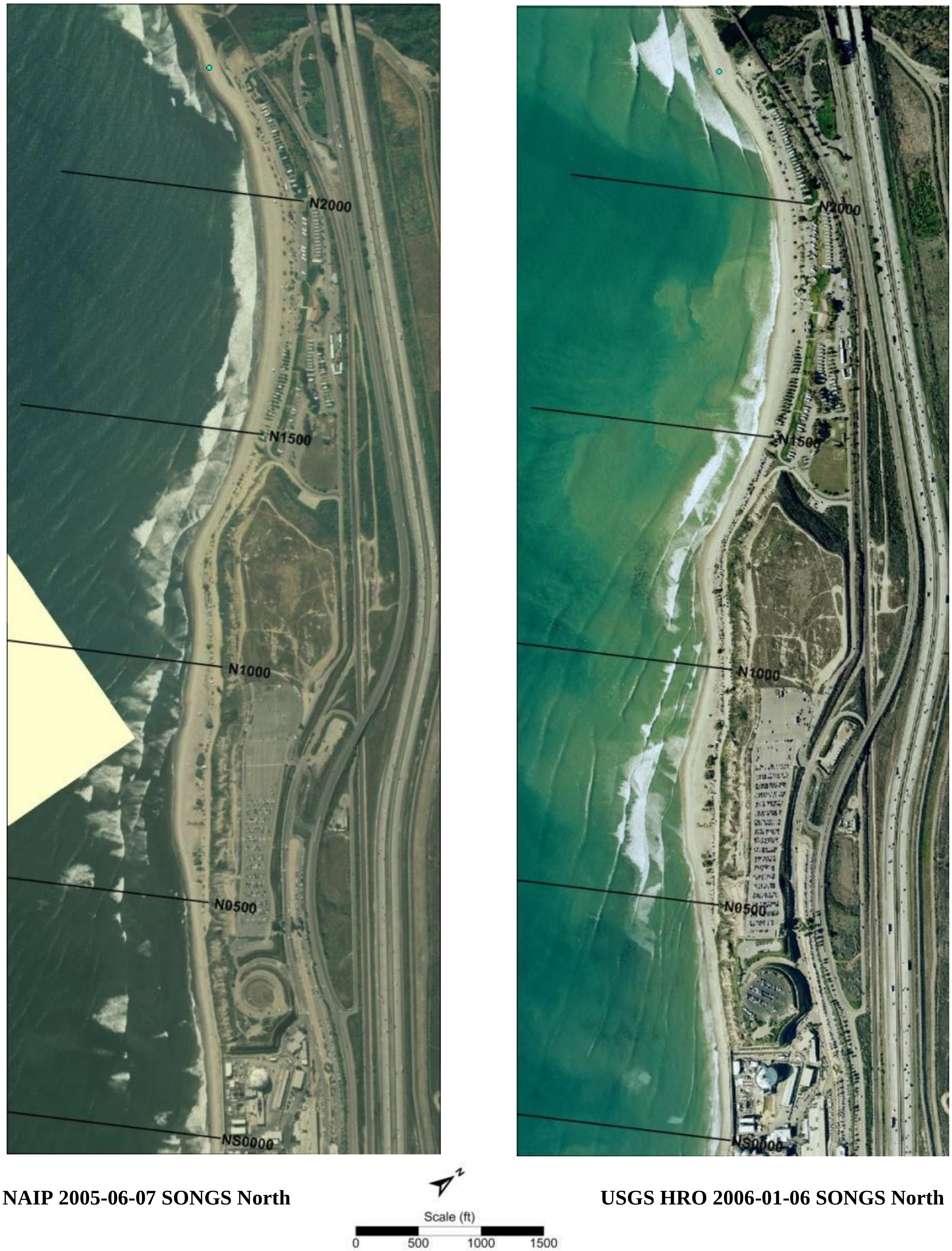

Figure E-7. Photographs taken in 2005 (left) and 2006 (right), showing an aerial perspective of the beach North of SONGS.

NAIP 2005-06-07 SONGS South

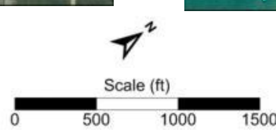

USGS HRO 2006-01-06 SONGS South

Figure E-8. Photographs taken in 2005 (left) and 2006 (right), showing an aerial perspective of the beach South of SONGS.

NAIP 2009-06-26 SONGS North **NAIP 2010-05-01 SONGS North**

Figure E-9. Photographs taken in 2009 (left) and 2010 (right), showing an aerial perspective of the beach North of SONGS.

NAIP 2009-06-26 SONGS South

NAIP 2010-05-01 SONGS South

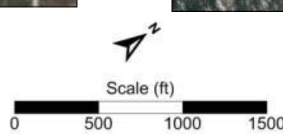

Figure E-10. Photographs taken in 2009 (left) and 2010 (right), showing an aerial perspective of the beach South of SONGS.

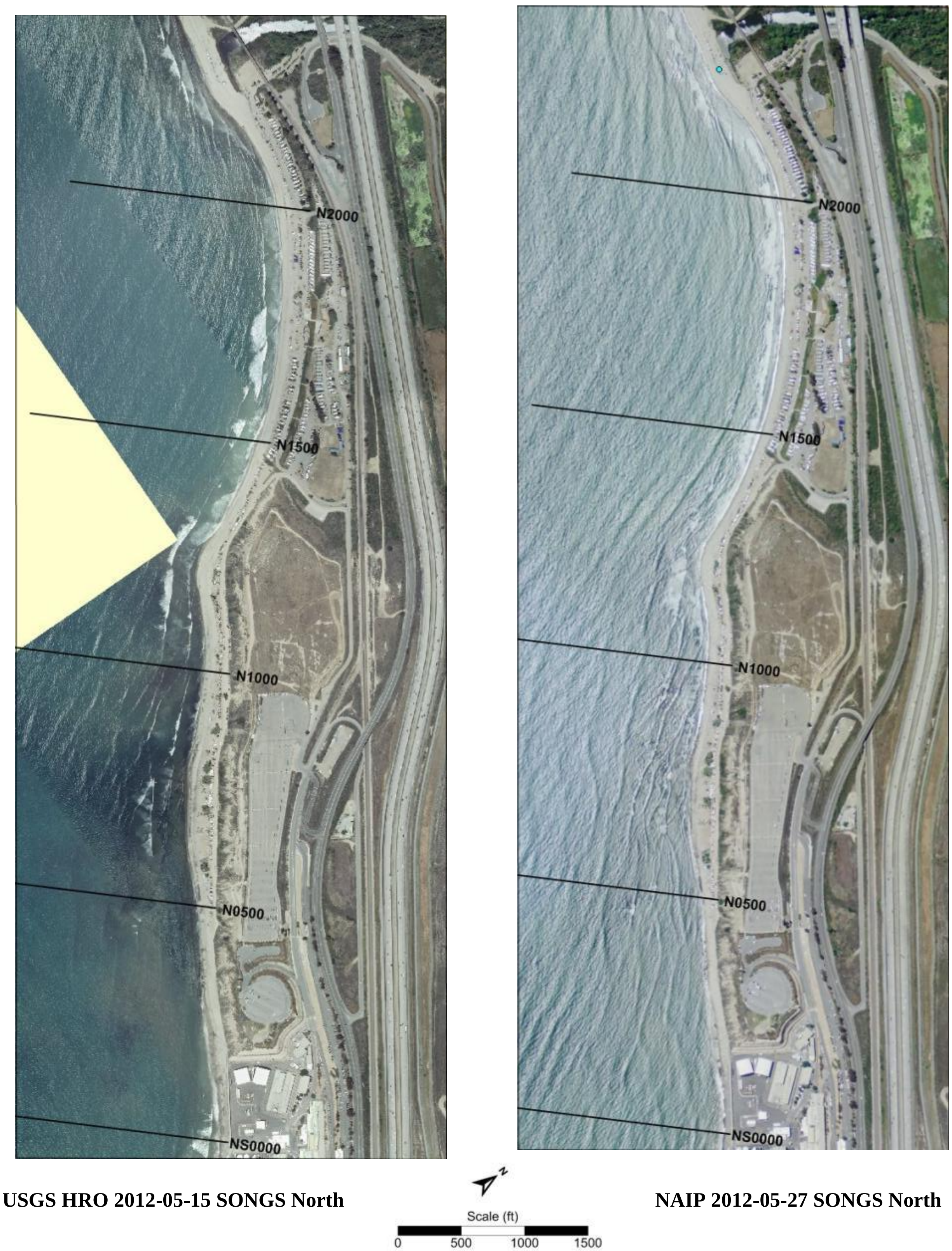

Figure E-11. Photographs taken in 2012, showing an aerial perspective of the beach North of SONGS.

Figure E-12. Photographs taken in 2012, showing an aerial perspective of the beach South of SONGS.

Figure E-13. Photographs taken in 2014, showing an aerial perspective of the beach North of SONGS.

NAIP 2014-06-03 SONGS South **USGS-HRO 2014-10-27 SONGS South**

Scale (ft)
0 500 1000 1500

Figure E-14. Photographs taken in 2014, showing an aerial perspective of the beach South of SONGS.

APPENDIX F

PHOTOGRAPHS OF SAN ONOFRE BEACH TAKEN IN 2017, 2018, AND 2019

Figure F-1. Looking south (left) and north (right) from range N1000 in June 2017.

Figure F-2. Looking south (left) and north (right) from range N1000 in January 2018.

Figure F-3. Looking south (left) and north (right) from range N1000 in October 2019.

Figure F-4. Looking south (left) and north (right) from range N0500 in August 2017.

Figure F-5. Looking south (left) and north (right) from range N0500 in January 2018.

Figure F-6. Looking south (left) and north (right) from range N0500 in October 2019.

Figure F-7. Looking south (left) and north (right) from range N0400' in June 2017.

Figure F-8. Looking south (left) and north (right) from range N0400' in January 2018.

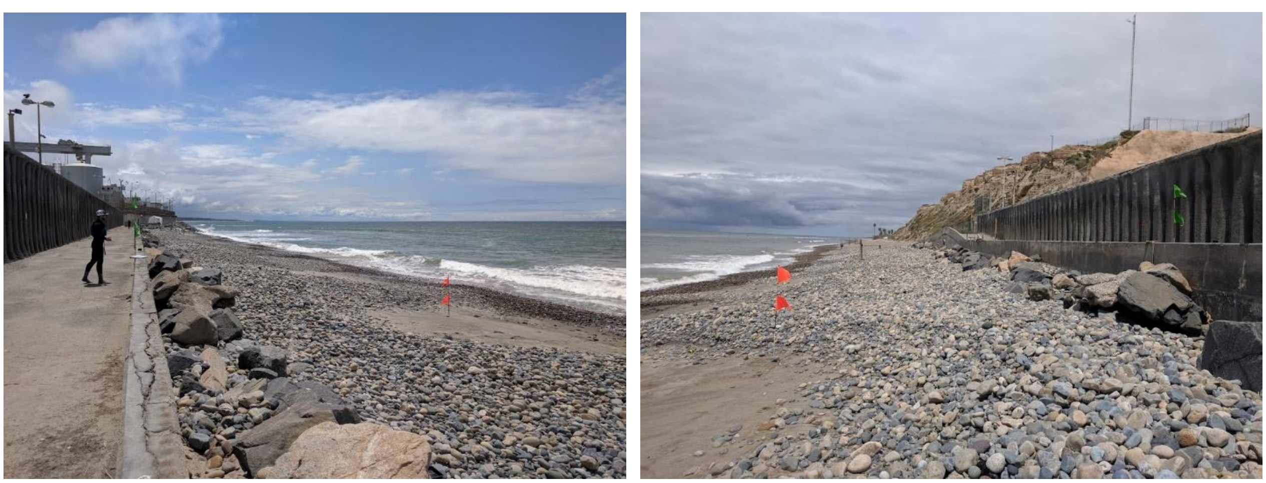

Figure F-9. Looking south (left) and north (right) from range N0400' in May 2019.

Figure F-10. Looking south (left) and north (right) from range NS0000 in May 2017.

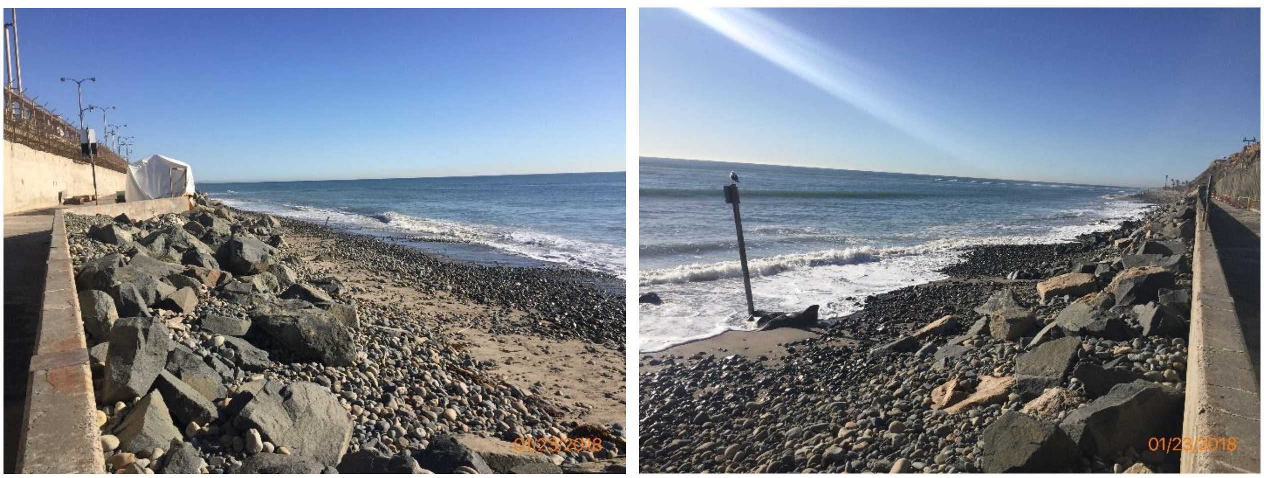

Figure F-11. Looking south (left) and north (right) from range NS0000 in January 2018.

Figure F-12. Looking south (left) and north (right) from range NS0000 in October 2019.

Figure F-13. Looking south (left) and north (right) from range S0800' in November 2017

Figure F-14. Looking south (left) and north (right) from range S0800' in November 2018.

Figure F-15. Looking south (left) and north (right) from range S0800' in November 2019.

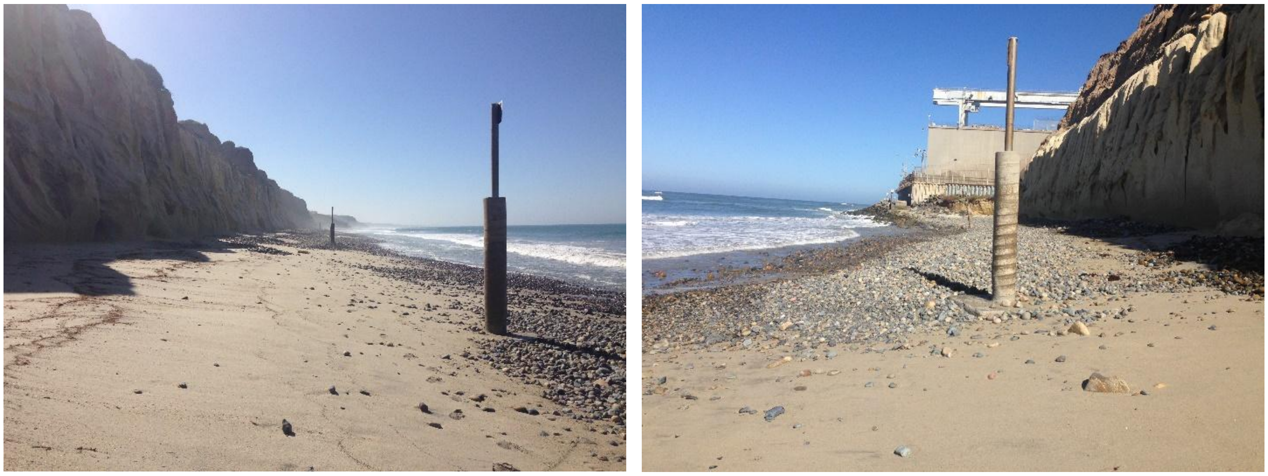

Figure F-16. Looking south (left) and north (right) from range S0500 in May 2017.

Figure F-17. Looking south (left) and north (right) from range S0500 in November 2018.

Figure F-18. Looking south (left) and north (right) from range S0500 in October 2019.

Figure F-19. Looking south (left) and north (right) from range S1000 in November 2017.

Figure F-20. Looking south (left) and north (right) from range S1000 in November 2018.

Figure F-21. Looking south (left) and north (right) from range S1000 in October 2019.

APPENDIX F

2019 GROUNDWATER LEVEL AT SAN ONOFRE GENERATING STATION

2019 GROUNDWATER LEVELS AT
SAN ONOFRE NUCLEAR GENERATING STATION,
SAN ONOFRE, CALIFORNIA

Prepared by

Coastal Environments, Inc.
2166 Avenida de la Playa, Suite E
La Jolla, CA 92037

Prepared for

Southern California Edison Company
2244 Walnut Grove Avenue
Rosemead, CA 91770

04 March 2020
Revised 18 March 2020
CE Reference No. 20-05

TABLE OF CONTENTS

LIST OF APPENDICES

LIST OF FIGURES

LIST OF TABLES

2019 GROUNDWATER LEVELS AT SAN ONOFRE NUCLEAR GENERATING STATION,

SAN ONOFRE, CALIFORNIA

1.0 INTRODUCTION

This report has been compiled per Special Provision 14 (b) in the California State Lands Commission Lease No. PRC 6785.1 for the use, maintenance, and decommissioning of exiting offshore improvements associated with the San Onofre Nuclear Generating Station (SONGS). Lease Provision 14 (b) requires, as part of compliance with applicable provisions or standards addressing sea-level rise that may be required or adopted by local, state or federal agencies related to and affecting the lease premises, that the Lessee provide an annual summary including quarterly groundwater elevation data collected from onsite monitoring wells.

In accordance with this requirement, this report compares the quarterly groundwater elevation data from the 16 wells located within SONGS against coastal tide data to observe any correlation between elevation values. Data for both groundwater and tidal elevations span from January to December 2019.

At coastal discharge boundaries, freshwater and saltwater are typically slow to mix; the less-dense freshwater remains at the top of the water table, riding above the denser saltwater wedge which extends below the land. Closer to the shoreline, however, daily tidal changes can result in a short-term mixing of water sources and can directly raise or lower the water table. San Onofre exemplifies one of these shallow coastal aquifers where tidal effects on groundwater levels have been noted in 2019 groundwater measurements.

Section 2 of this report describes the sources and uses of the SONGS groundwater well and tidal data, as well as how this data was organized to obtain discernable results. Section 3 presents these results both graphically and in table format, while Section 4 discusses these results and the relationship between groundwater elevation, daily tides, and SLR at SONGS. Ultimately, this report finds that projected groundwater elevations in 2050 are lower than the Independent Spent Fuel Storage Installation (ISFSI) support foundation by 1.35 and 0.55 ft. for a medium-high and extreme risk aversion scenario, respectively (Section 3).

2.0 ANALYSIS METHODS

Groundwater and well data for the year 2019 was provided by Southern California Edison (SCE) and compared against tidal data gathered by Coastal Environments (CE). These include quarterly data from SCE Ground Water protection Initiative (GPI) wells and other wells where data is collected semiannually or annually. A small number of observations were not transmitted to CE because SCE did not have associated location and ground surface elevation information needed to compute groundwater elevation relative to a known datum. ISFSI pad cross-sections were also provided by SCE. Figures 2-1 and 2-2 show the locations of the sampled wells at SONGS. Individual wells were measured 1, 2, or 4 times within the calendar year. Data provided for the 16 wells located within SONGS included: date and time of sample, ground surface elevation of well, measured water depth, and groundwater elevation.

Groundwater elevations were determined by measuring the wells' water depth, defined as the distance from a well's ground surface to its water level. This value was then subtracted from the known ground surface elevation of each well to determine groundwater elevations. Elevation data are presented in NGVD29 (National Geodetic Vertical Datum, 1929) for this report. Unlike MLLW (Mean Lower Low Water) datum values which vary between tidal epochs, NGVD29 datum values remains fixed. Additionally, NGVD29 lies closer to Mean High Water (MHW) than MLLW, making NGVD29 more useful for representing current sea levels and SLR. Elevation values can be converted between datums by subtracting 2.60 ft. from MLLW (Epoch 1941-1959) to get the elevation in NGVD29. Appendix A presents the groundwater measurements for the 16 wells in both datums.

To better examine groundwater trends, each of the 16 wells was assigned to one of three groups based on their elevation and location within SONGS. Group 1 includes wells NIA-1, NIA-2, NIA-3, NIA-4, NIA-5, NIA-6, NIA-7, NIA-10, and NIA-11. This clustered group of wells occupies the lowest ground surface elevation and is located between the shoreline and North Industrial Area (Unit 1 remnants and ISFSI). Group 2 includes wells PA-1, PA-2, PA-3, and PA-4, which are at middling ground surface elevations and located between Unit 2/3 structures and the shoreline. Group 3 includes the remaining wells OCA-1, OCA-2, and OCA-3, which have the highest ground surface elevations and lie farthest from the shoreline.

Figure 2-1. Locations of SONGS groundwater wells.

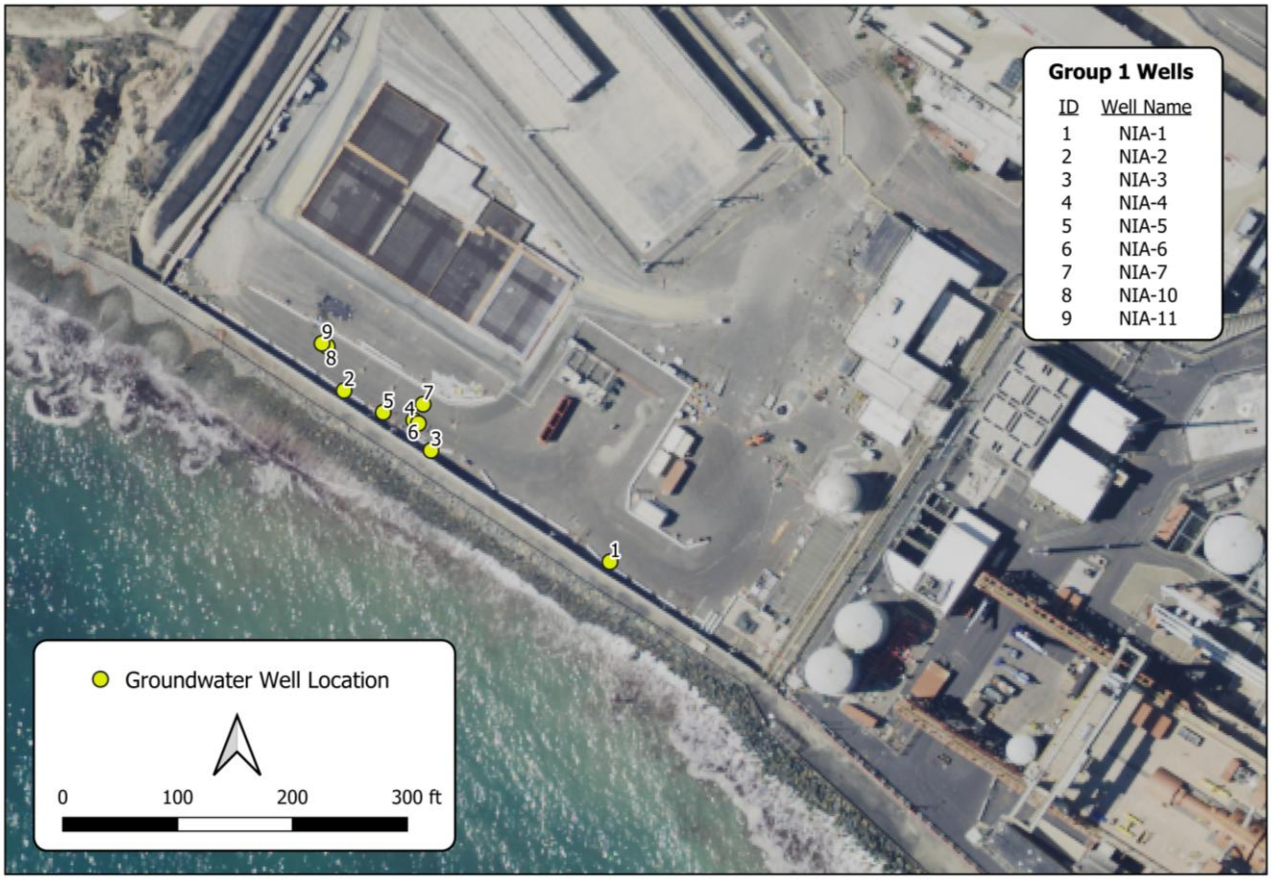

Figure 2-2. Locations of Group 1 SONGS groundwater wells.

3.0 RESULTS

Table 3-1 displays the pertinent groundwater well elevation data for all measured samples, as well as the corresponding tidal data. Table 3-2 shows the mean groundwater elevations for each well group. Mean elevations were also calculated for individual wells that were measured more than once in 2019. Standard deviation values were not calculated for wells measured once during 2019.

Figures 3-1 through 3-3 graphically show the groundwater elevations for each well plotted against the measured daily maximum and minimum tide elevations for 2019. Each figure displays well measurements from one of the three well groups; this allows for a visual comparison of groundwater elevations for wells within similar areas of SONGS.

The Group 1 wells are located just west of the Unit 1 remnants and ISFSI pads and their ground elevations vary from 11.19 to 13.46 ft. The groundwater at these wells varies from 1.73 to 3.50 ft. (Table 3-1) and the mean groundwater elevation for these 9 wells is 2.62 ft. (Table 3-2). Due to their location within SONGS, Group 1 data were used to determine the distance between groundwater levels and the Holtec UMAX ISFSI support foundation in 2050, where the projections of SLR according to the Ocean Protection Council (OPC) is 2 ft. for a medium-high risk aversion scenario and 2.8 ft. for the H++ extreme risk scenario. Figure 3-4 shows these 2050 sea level projections, along with the 2019 groundwater elevations, in comparison to the ISFSI pad. The H++ scenario ground water elevation for 2050 is 5.42 ft. and is lower than the bottom of the Holtec UMAX ISFSI support foundation (5.97 ft., NGVD) by 0.55 ft. The CCC scenario ground water elevation for 2050 is 4.62 ft., NGVD and is 1.35 ft. lower than the bottom of the ISFSI support foundation. Figure 3-5 is similar to Figure 3-4 but the elevation values are referenced to MLLW (Epoch 1941-1959).

Table 3-1. SONGS groundwater well sample data.

Well Group	Well Description	Sample Date	Sample Time	Ground Surface Elevation (NGVD29, ft.)	Groundwater Elevation (NGVD29, ft.)	Ocean Tide Level (NGVD29, ft.)
Group 1	NIA-1	7-Feb-19	10:46	11.19	3.50	2.22
		3-Jun-19	8:38	11.19	2.26	0.92
		15-Aug-19	8:48	11.19	2.04	1.32
		7-Nov-19	8:30	11.19	2.70	1.52
	NIA-2	6-Feb-19	13:29	12.80	3.25	-0.83
		3-Jun-19	10:52	12.80	2.77	0.69
		19-Aug-19	9:09	12.80	1.73	0.68
		6-Nov-19	8:51	12.80	2.58	0.94
	NIA-3	28-Aug-19	9:14	11.25	2.76	1.50
	NIA-4	28-Aug-19	14:17	11.58	2.09	-0.23
	NIA-5	18-Sep-19	8:44	12.08	2.33	1.80
	NIA-6	25-Mar-19	11:00	11.59	2.13	0.17
		28-Aug-19	11:21	11.59	2.78	0.00
	NIA-7	18-Sep-19	10:54	12.14	3.15	2.51
	NIA-10	16-Sep-19	9:53	13.46	2.94	2.40
	NIA-11	25-Mar-19	13:05	13.46	2.46	0.54
		16-Sep-19	13:13	13.46	3.16	0.30
Group 2	PA-1	11-Feb-19	10:13	26.21	1.87	2.36
		5-Jun-19	9:27	26.21	1.12	2.90
		22-Aug-19	8:09	26.21	1.69	2.46
		14-Nov-19	8:37	26.21	2.37	5.92
	PA-2	27-Feb-19	10:02	26.91	0.96	0.68
		5-Jun-19	12:08	26.91	0.61	3.48
		22-Aug-19	10:49	26.91	1.06	3.92
		18-Nov-19	8:56	26.91	1.53	4.06
	PA-3	28-Feb-19	9:44	26.72	1.1	1.16
		6-Jun-19	8:07	26.72	1.46	0.96
		26-Aug-19	8:24	26.72	1.35	3.58
		11-Dec-19	8:50	26.72	1.28	5.88
	PA-4	4-Mar-19	9:24	26.34	2.41	4.31
		6-Jun-19	11:21	26.34	0.79	3.50
		26-Aug-19	11:09	26.34	1.51	2.81
		9-Dec-19	9:39	26.34	2.41	3.71

Table 3-1 (cont). SONGS groundwater well sample data.

Well Group	Well Description	Sample Date	Sample Time	Ground Surface Elevation (NGVD29, ft.)	Groundwater Elevation (NGVD 29, ft.)	Ocean Tide Level (NGVD29, ft.)
Group 3	OCA-1	24-Jan-19	9:25	45.09	3.51	2.34
		17-Apr-19	8:51	45.09	3.46	1.89
		14-Aug-19	9:20	45.09	3.48	1.34
		31-Oct-19	10:10	45.09	3.64	3.41
	OCA-2	23-Jan-19	10:15	113.79	3.55	3.58
		10-Apr-19	9:41	113.79	3.37	-1.34
		12-Aug-19	10:42	113.79	3.64	0.23
		30-Oct-19	10:00	113.79	3.84	3.74
	OCA-3	30-Jan-19	9:02	103.1	2.73	0.54
		29-May-19	9:03	103.1	2.29	-0.63
		14-Aug-19	13:23	103.1	2.55	-0.59
		28-Oct-19	12:30	103.1	3.3	-0.62

Table 3-2. Mean SONGS groundwater elevations.

Well Group	Well Description	Ground Surface Elevation (NGVD29, ft.)	Mean Groundwater Level (NGVD29, ft.)		Standard Deviation (ft.)	
			Well	Group	Well	Group
Group 1	NIA-1	11.19	2.63	2.62	0.64	0.49
	NIA-2	12.80	2.58		0.63	
	NIA-3	11.25	2.76		N/A	
	NIA-4	11.58	2.09		N/A	
	NIA-5	12.08	2.33		N/A	
	NIA-6	11.59	2.45		0.46	
	NIA-7	12.14	3.15		N/A	
	NIA-10	13.46	2.94		N/A	
	NIA-11	13.46	2.81		0.49	
Group 2	PA-1	26.21	1.75	1.47	0.52	0.56
	PA-2	26.91	1.04		0.38	
	PA-3	26.72	1.30		0.15	
	PA-4	26.34	1.78		0.78	
Group 3	OCA-1	45.09	3.52	3.28	0.08	0.49
	OCA-2	113.79	3.60		0.20	
	OCA-3	103.10	2.72		0.43	

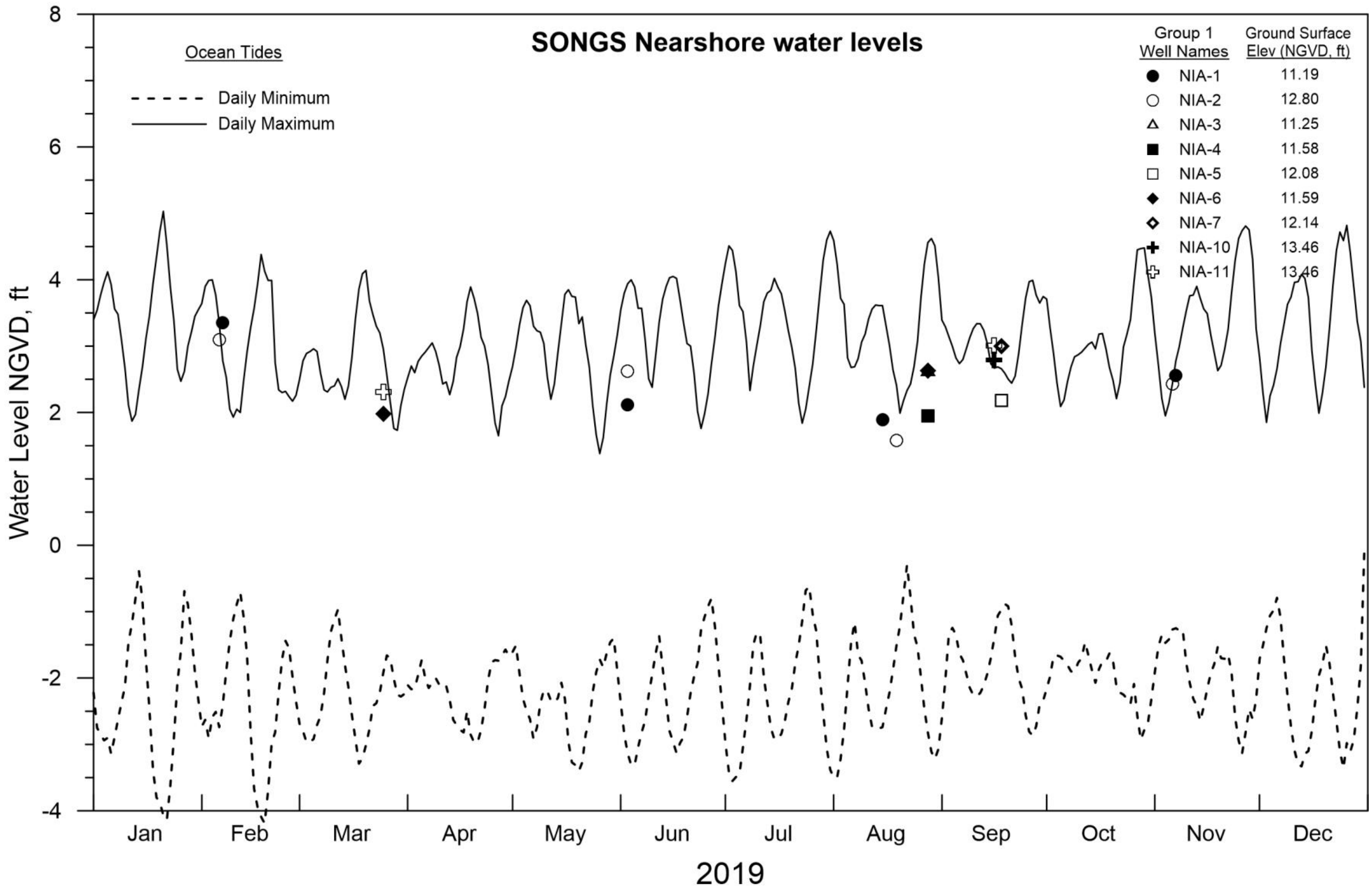

Figure 3-1. Groundwater elevation of Group 1 SONGS wells and daily tides for 2019.

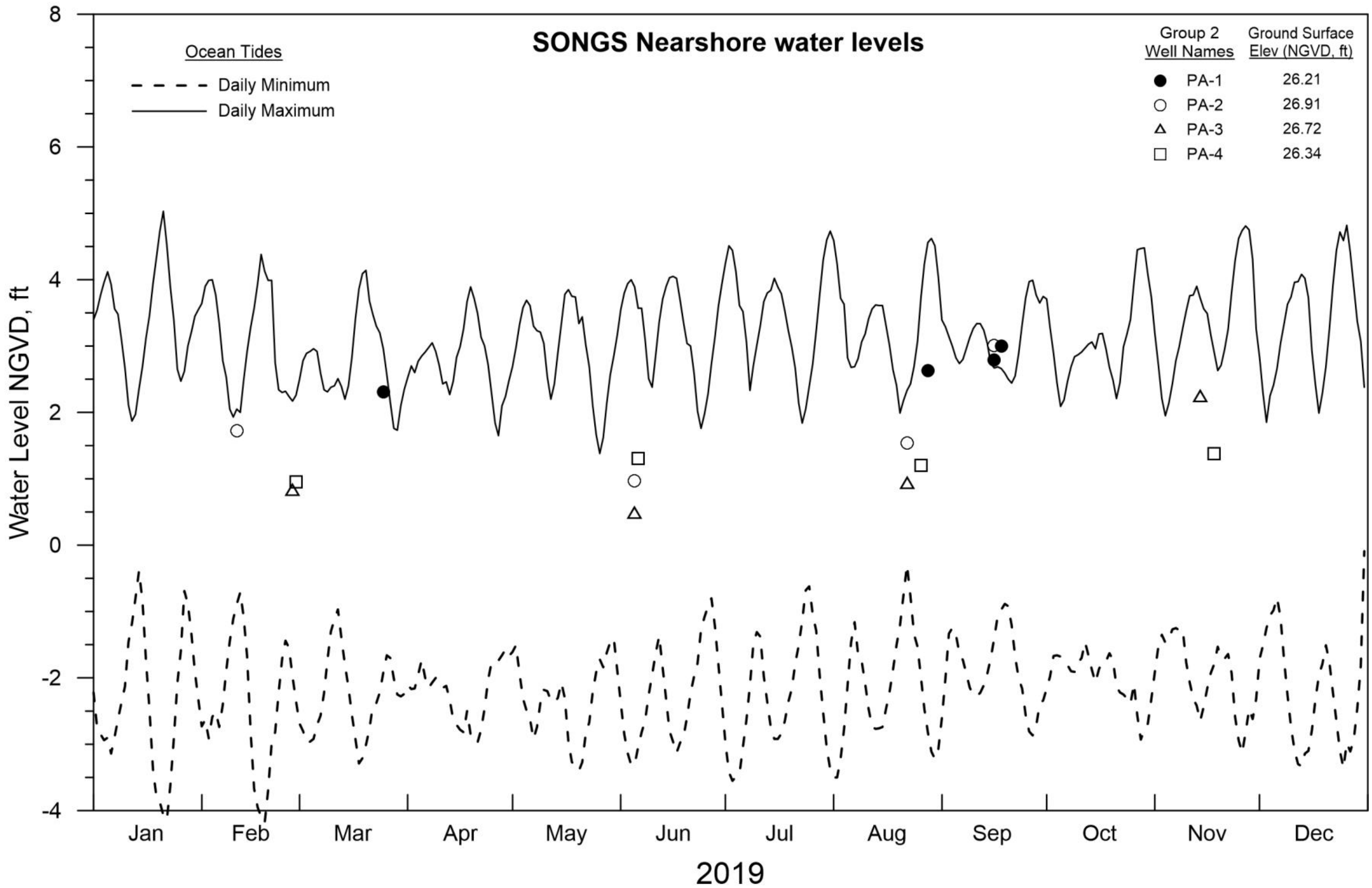

Figure 3-2. Groundwater elevation of Group 2 SONGS wells and daily tides for 2019.

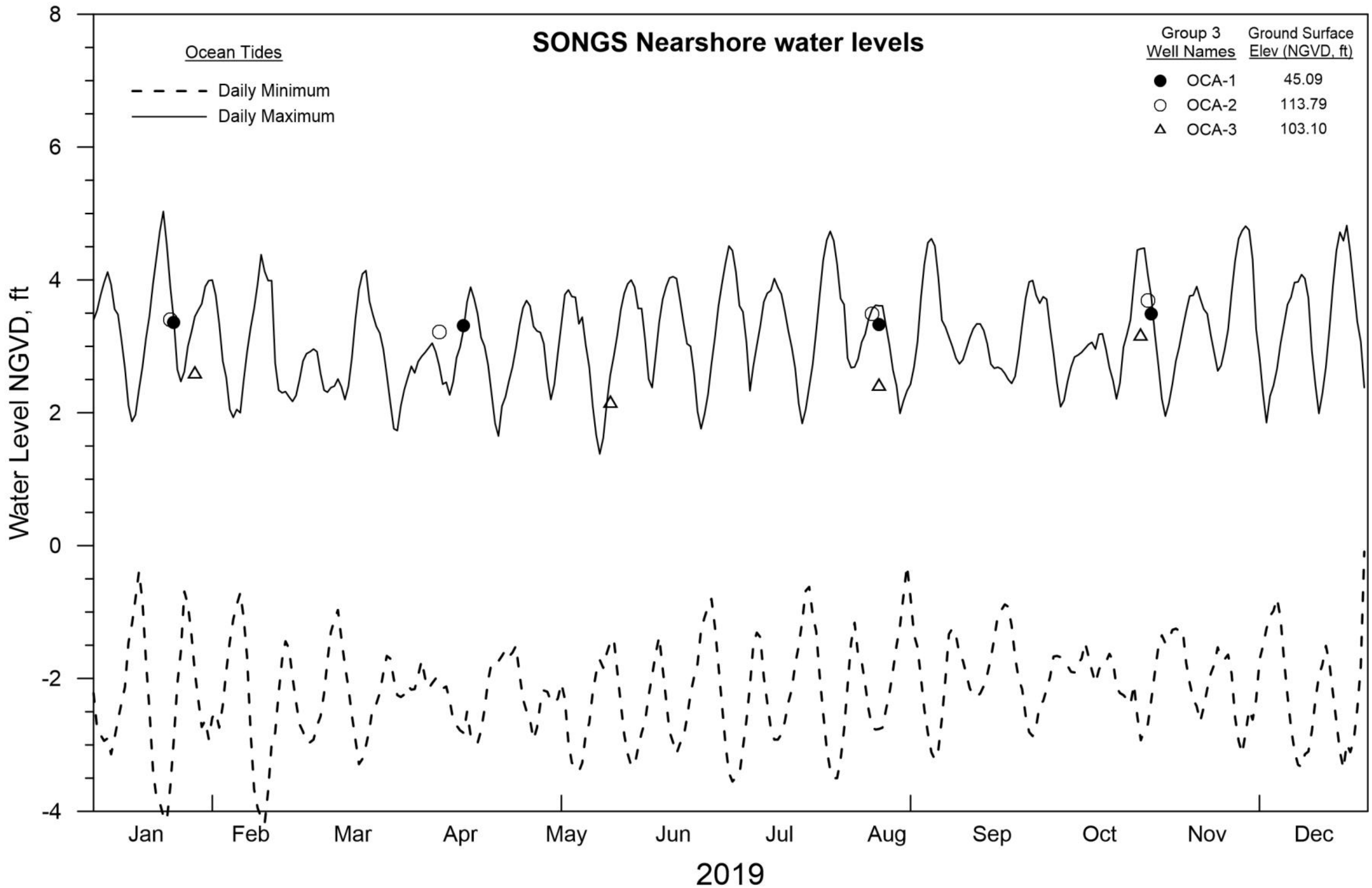

Figure 3-3. Groundwater elevation of Group 3 SONGS wells and daily tides for 2019.

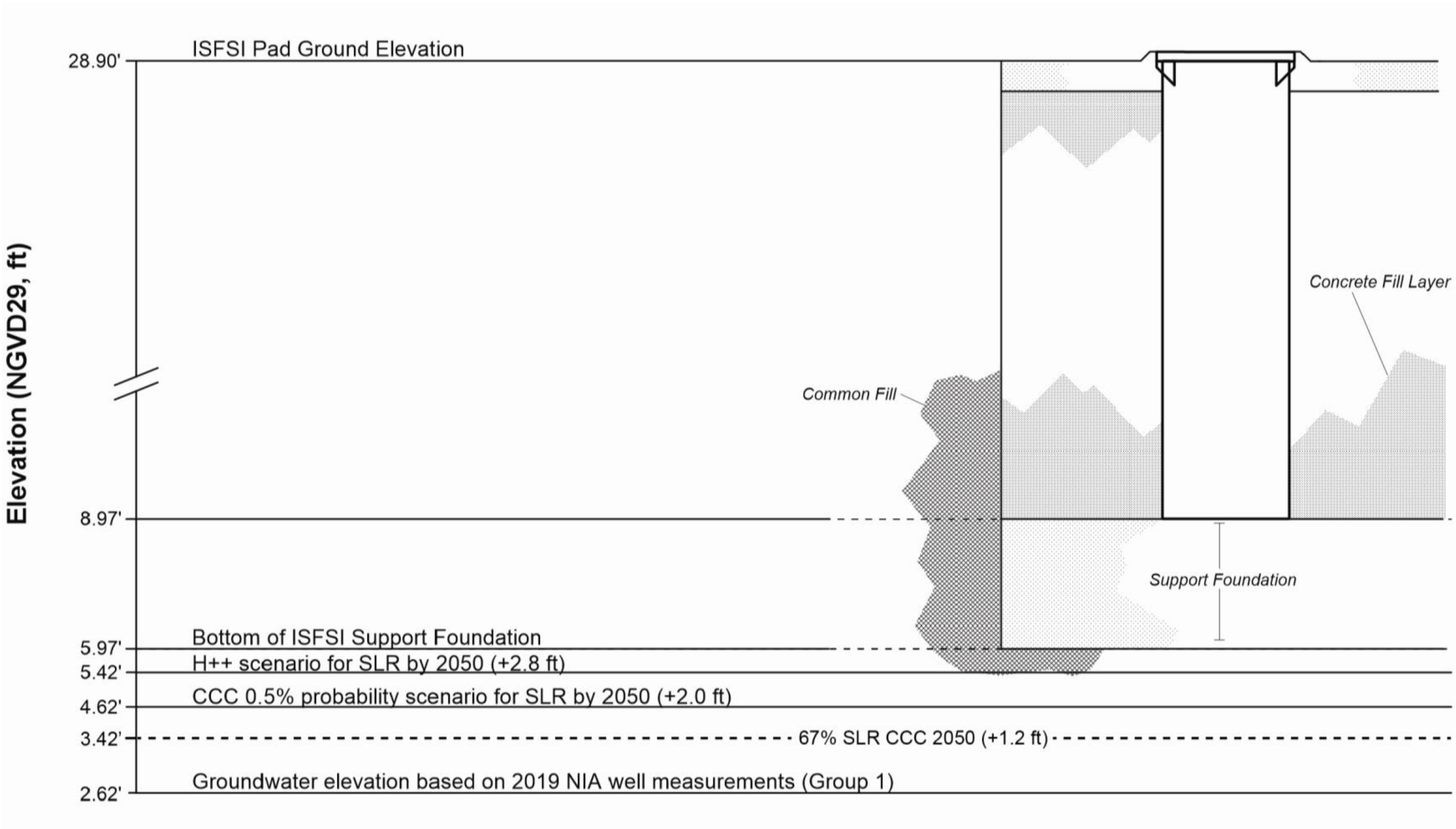

Figure 3-4. Groundwater elevations (NGVD29) for 2019 and for the OPC projections in 2050. The CCC projections (2018) for sea level rise are based on OPC projections.

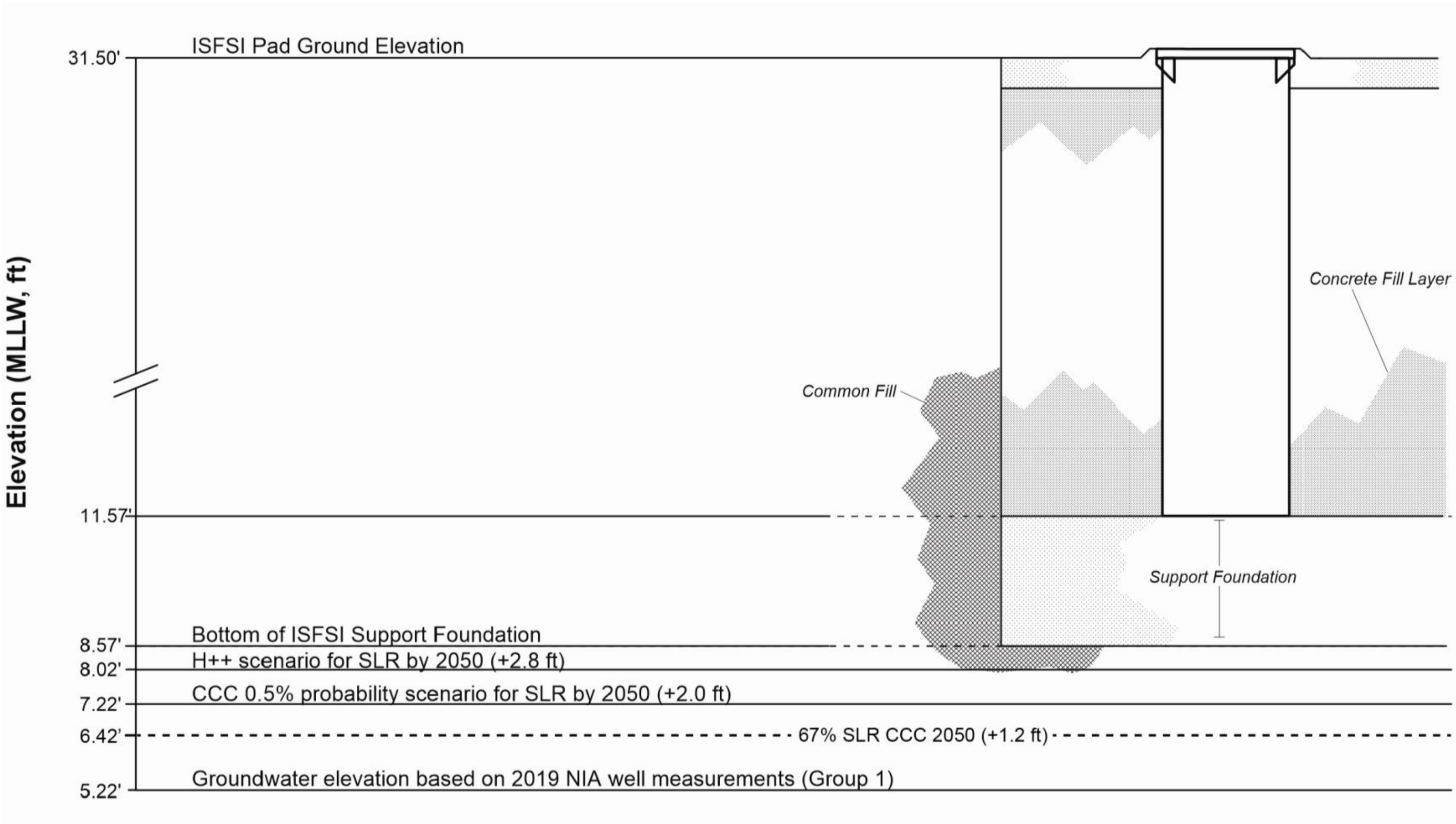

Figure 3-5. Groundwater elevations for 2019 referenced to MLLW (Epoch 1941-1959). Ground water elevations for 2050 are also shown based on sea level rise projections of OPC (2018) and CCC (2018).

4.0 CONCLUSIONS

Overall, the data shows that wells located closer to the shoreline (Groups 1 and 2) experience a larger tidal influence on their groundwater levels. On average, these wells have lower mean groundwater levels closely match the mean high water level at the ocean (approximately 2.31 ft., NGVD29). Group 3 is located at higher elevations and its ground water elevations are higher than Groups 1 and 2.

Group 1 wells were selected to estimate groundwater elevations underneath the ISFSI pads. Because Group 1 wells are located closest to the ISFSI pads, their mean groundwater elevation provides a good estimate for groundwater elevations at the ISFSI. The OPC has several scenarios for how high sea levels will rise by 2050 (OPC, 2018). As sea levels rise, groundwater levels will increase in about or less the same value. Therefore, 2 ft. rise in sea level by 2050 correlates to 2 ft. or less rises in groundwater elevation by 2050 at SONGS.

As shown in Figure 3-4, the highest H++ projected groundwater elevation scenario is 5.42 ft., NGVD and rests 0.55 ft. below the Holtec UMAX ISFSI (ISFSI) support foundation in 2050. The medium-high risk aversion CCC scenario has a 0.5% probability of SLR meeting or exceeding a +2 ft. projection; this scenario puts groundwater elevations at SONGS 1.35 ft. below the Holtec UMAX ISFSI support foundation in 2050. It should also be pointed out that the upper surface support foundation is 3 ft. above the bottom surface of the ISFSI support foundation (i.e., the support foundation pad is 3 ft. thick), minimizing any chance that the ground water will contact the Cavity Enclosure Containers (CECs) in which the spent nuclear fuel is stored.

5.0 REFERENCES

California Coastal Commission, 2015, updated 2018. *California Coastal Commission Sea Level Rise Policy Guidance, Interpretive Guidelines for Addressing Sea Level Rise in Local Coastal Programs and Coastal Development Permits,* California Coastal Commission, San Francisco, CA, 307 pp.

Ocean Protection Council, 2018. *State of California Sea-Level Rise Guidance, 2018 Update*, Sacramento, CA: California Natural Resources Agency, 84 pp. http://www.opc.ca.gov/updating-californias-sea-level-rise-guidance/

APPENDIX A

GROUNDWATER AND TIDAL DATA
2019

Table A-1. SONGS groundwater well and ocean tide elevation data.

Well Group	Well Description	Sample Date	Quarter	Sample Time	Measured Water Depth (ft.)	Ground Surface Elevation (MLLW, ft.)	Groundwater Elevation (MLLW, ft.)	Ground Surface Elevation (NGVD29, ft.)	Groundwater Elevation (NGVD29, ft.)	Ocean Tide Level (MLLW, ft.)	Ocean Tide Level (NGVD29, ft.)	Tide
Group 1	NIA-1	7-Feb-19	Q1	10:46	7.69	13.79	6.10	11.19	3.50	4.82	2.22	spring, falling
		3-Jun-19	Q2	8:38	8.93	13.79	4.86	11.19	2.26	3.52	0.92	spring, rising
		15-Aug-19	Q3	8:48	9.15	13.79	4.64	11.19	2.04	3.92	1.32	spring, rising
		7-Nov-19	Q4	8:30	8.49	13.79	5.30	11.19	2.70	4.12	1.52	mean, falling
	NIA-2	6-Feb-19	Q1	13:29	9.55	15.40	5.85	12.80	3.25	1.77	-0.83	spring, falling
		3-Jun-19	Q2	10:52	10.03	15.40	5.37	12.80	2.77	3.29	0.69	spring, falling
		19-Aug-19	Q3	9:09	11.07	15.40	4.33	12.80	1.73	3.28	0.68	mean, rising
		6-Nov-19	Q4	8:51	10.22	15.40	5.18	12.80	2.58	3.54	0.94	mean, falling
	NIA-3	28-Aug-19	Q3	9:14	8.49	13.85	5.36	11.25	2.76	4.10	1.50	spring, falling
	NIA-4	28-Aug-19	Q3	14:17	9.49	14.18	4.69	11.58	2.09	2.37	-0.23	spring, rising
	NIA-5	18-Sep-19	Q3	8:44	9.75	14.68	4.93	12.08	2.33	4.40	1.80	mean, rising
	NIA-6	25-Mar-19	Q2	11:00	9.46	14.19	4.73	11.59	2.13	2.77	0.17	mean, rising
		28-Aug-19	Q3	11:21	8.81	14.19	5.38	11.59	2.78	2.60	0.00	spring, falling
	NIA-7	18-Sep-19	Q3	10:54	8.99	14.74	5.75	12.14	3.15	5.11	2.51	mean, falling
	NIA-10	16-Sep-19	Q3	9:53	10.52	16.06	5.54	13.46	2.94	5.00	2.40	mean, falling
	NIA-11	25-Mar-19	Q2	13:05	11.00	16.06	5.06	13.46	2.46	3.14	0.54	mean, falling
		16-Sep-19	Q3	13:13	10.30	16.06	5.76	13.46	3.16	2.90	0.30	mean, falling
Group 2	PA-1	11-Feb-19	Q1	10:13	24.34	28.81	4.47	26.21	1.87	2.36	-0.24	neap, rising
		5-Jun-19	Q2	9:27	25.09	28.81	3.72	26.21	1.12	2.90	0.30	spring, rising
		22-Aug-19	Q3	8:09	24.52	28.81	4.29	26.21	1.69	2.46	-0.14	neap, rising
		14-Nov-19	Q4	8:37	23.84	28.81	4.97	26.21	2.37	5.92	3.32	spring, rising
	PA-2	27-Feb-19	Q1	10:02	25.95	29.51	3.56	26.91	0.96	0.68	-1.92	neap, falling
		5-Jun-19	Q2	12:08	26.30	29.51	3.21	26.91	0.61	3.48	0.88	spring, falling
		22-Aug-19	Q3	10:49	25.85	29.51	3.66	26.91	1.06	3.92	1.32	neap, rising
		18-Nov-19	Q4	8:56	25.38	29.51	4.13	26.91	1.53	4.06	1.46	mean, rising
	PA-3	28-Feb-19	Q1	9:44	25.62	29.32	3.70	26.72	1.1	1.16	-1.44	mean, falling
		6-Jun-19	Q2	8:07	25.26	29.32	4.06	26.72	1.46	0.96	-1.64	spring, rising
		26-Aug-19	Q3	8:24	25.37	29.32	3.95	26.72	1.35	3.58	0.98	mean, falling
		11-Dec-19	Q4	8:50	25.44	29.32	3.88	26.72	1.28	5.88	3.28	spring, falling
	PA-4	4-Mar-19	Q1	9:24	23.93	28.94	5.01	26.34	2.41	4.31	1.71	spring, falling
		6-Jun-19	Q2	11:21	25.55	28.94	3.39	26.34	0.79	3.50	0.90	spring, rising
		26-Aug-19	Q3	11:09	24.83	28.94	4.11	26.34	1.51	2.81	0.21	mean, falling
		9-Dec-19	Q4	9:39	23.93	28.94	5.01	26.34	2.41	3.71	1.11	spring, falling

Table A-1 (cont). SONGS groundwater well and ocean tide elevation data.

Well Group	Well Description	Sample Date	Quarter	Sample Time	Measured Water Depth (ft.)	Ground Surface Elevation (MLLW, ft.)	Groundwater Elevation (MLLW, ft.)	Ground Surface Elevation (NGVD29, ft.)	Groundwater Elevation (NGVD29, ft.)	Ocean Tide Level (MLLW, ft.)	Ocean Tide Level (NGVD29, ft.)	Tide
Group 3	OCA-1	24-Jan-19	Q1	9:25	41.58	47.69	6.11	45.09	3.51	4.94	2.34	spring, rising
		17-Apr-19	Q2	8:51	41.63	47.69	6.06	45.09	3.46	4.49	1.89	spring, falling
		14-Aug-19	Q3	9:20	41.61	47.69	6.08	45.09	3.48	3.94	1.34	spring, falling
		31-Oct-19	Q4	10:10	41.45	47.69	6.24	45.09	3.64	6.01	3.41	spring, falling
	OCA-2	23-Jan-19	Q1	10:15	110.24	116.39	6.15	113.79	3.55	6.18	3.58	spring, falling
		10-Apr-19	Q2	9:41	110.42	116.39	5.97	113.79	3.37	1.26	-1.34	neap, rising
		12-Aug-19	Q3	10:42	110.15	116.39	6.24	113.79	3.64	2.83	0.23	spring, falling
		30-Oct-19	Q4	10:00	109.95	116.39	6.44	113.79	3.84	6.34	3.74	spring, falling
	OCA-3	30-Jan-19	Q1	9:02	100.37	105.7	5.33	103.1	2.73	3.14	0.54	mean, falling
		29-May-19	Q2	9:03	100.81	105.7	4.89	103.1	2.29	1.97	-0.63	mean, falling
		14-Aug-19	Q3	13:23	100.55	105.7	5.15	103.1	2.55	2.01	-0.59	spring, falling
		28-Oct-19	Q4	12:30	99.80	105.7	5.90	103.1	3.3	1.98	-0.62	spring, falling